PLACE IN RETURN BOX to remove this checkout from your record.
TO AVOID FINES return on or before date due.
MAY BE RECALLED with earlier due date if requested.

DATE DUE	DATE DUE	DATE DUE

5/08 K:/Proj/Acc&Pres/CIRC/DateDue.indd

CHARACTERIZATION OF THE DIFFERENTIAL SUSCEPTIBILITY OF DOPAMINE NEURONAL POPULATIONS IN A MOUSE MODEL OF PARKINSON'S DISEASE

BY

Bahareh Behrouz

A DISSERTATION

Submitted to
Michigan State University
in partial fulfillment of the requirements
for the degree of

DOCTOR OF PHILOSOPHY

Neuroscience

2008

ABSTRACT

CHARACTERIZATION OF THE DIFFERENTIAL SUSCEPTIBILITY OF DOPAMINE NEURONAL POPULATIONS IN A MOUSE MODEL OF PARKINSON'S DISEASE

BY

Bahareh Behrouz

Parkinson's disease (PD) is a neurodegenerative disorder that causes severe motor impairments due to progressive loss of nigrostriatal (NS) dopamine (DA) neurons. Abnormal DA metabolism has been proposed to underlie the degeneration of these neurons, but not all DA neurons are affected to the same extent in PD. There is severe loss of NSDA neurons, adjacent mesolimbic (ML) DA neurons are less severely affected and tuberoinfundibular (TI) DA neurons remain intact. The reason for this differential susceptibility amongst DA neurons is unknown. Elucidating mechanisms by which some neurons are preferentially lost while others are protected should lead to discovery of protective factors that can be translated into therapies for PD.

The experiments in this dissertation characterize a model for PD using the toxin 1-methyl,4-phenyl-1,2,3,6-tetrahydropyridine (MPTP) that mimics the differential susceptibility of DA neuronal populations seen in PD. In the MPTP mouse model, NSDA neurons are highly susceptible, while MLDA neurons are less damaged and TIDA neurons remain fully protected. Furthermore, the immediate response of these neuronal populations suggests that MLDA neurons don't lose as much DA as NSDA neurons immediately following treatment with MPTP, suggesting there might be

heterogeneous populations of MLDA neurons, i.e. one that is susceptible and one that is resistant. On the other hand, TIDA neurons initially respond to MPTP treatment in a similar fashion to NSDA neurons, but rapidly recover. The recovery of these neurons from MPTP-induced DA loss is dependent on synthesis of new proteins following MPTP treatment. It is therefore likely that TIDA neurons upregulate the expression of proteins that allow for this recovery.

Microarray analysis of mRNA expression in NSDA and TIDA neurons reveal several important pathways and factors that may protect TIDA neurons after exposure to MPTP. One of the genes upregulated in TIDA neurons following MPTP treatment is the protective protein parkin. Mutations in this gene cause autosomal recessive PD and increased expression of this protein infers protection to cells in a variety of models, leading to the hypothesis that parkin upregulation may contribute to the recovery of TIDA neurons following MPTP treatment.

This hypothesis is tested by two separate approaches: exposing parkin knock out (KO) mice and wild type (WT) littermates to MPTP and stereotaxically injecting WT C57bl/6 mice with lentiviral particles expressing parkin shRNA in order to transiently knock down (KD) the expression of parkin. Animals receiving parkin shRNA lentivirus, but not parkin KO show stunted recovery of DA in response to MPTP treatment, suggesting parkin may be essential for the recovery of these neurons. Elucidating factors that are responsible for differential susceptibility to mitochondrial Complex I inhibition may be further translated into neuroprotective strategies that can prevent the ongoing degeneration of DA neurons in PD.

This dissertation is dedicated to the love of my life, Andy.

Thank you for inspiring, guiding and encouraging me to be the best I can be.

And to my parents,

All your sacrifices, love and support have made it possible for me to pursue my dreams.

ACKNOWLEDGEMENTS

I sincerely thank Andy, my parents, and Andy's parents for all their love, encouragement, and support and my aunt Mariam for her continued guidance. I thank my sister, Rozina, for motivating me to pursue higher education and for raising such a fantastic son, Pouya, to be the pride and joy of my life.

Drs. Lookingland and Goudreau, words alone cannot describe my gratitude for the exceptional training and guidance that I have received in your lab. I have been truly fortunate to have the opportunity to learn from you both.

I would like to thank my committee members Drs. MohanKumar, Gallo and Amalfitano for their guidance and advice, Dr. Sisk for her continued support throughout the years and for being a phenomenal role model and Dr. Wade for sparking my interest in Neuroscience.

I wish to thank the faculty, staff and students of the Neuroscience, Pharmacology/Toxicology and Neurology Programs. I also thank the members of the Goudreau/Lookingland laboratory who have made this experience fun and exciting. I will miss you.

TABLE OF CONTENTS

List of Tables xi

List of Figures xiii

List of Abbreviations Xviii

Chapter 1. General Introduction 1

A. Statement of Purpose 1

B. Parkinson's Disease 2

C. Degeneration of NSDA Neurons and Motor Abnormalities in PD 3

Normal NSDA Neuronal Function 3

NSDA Control of Basal Ganglia 6

NSDA Neurons and Control of Basal Ganglia in PD 8

D. Environmental and Genetic Factors and PD 8

E. Pathways Implicated in PD 11

Mitochondrial Function and Reactive Oxygen Species 11

Protein Degradation 15

Abnormal DA Metabolism 19

F. Differential susceptibility of DA neurons in PD 23

MLDA Neurons 26

TIDA Neurons 28

G. Animal models of PD 32

Neurotoxin-Based Models 32

MPTP 33

Rotenone 36

6-OHDA 38

Paraquat 39

Genetic and Gene Transfer Models 39

α-Synuclein 40

α-Synuclein KO or KD 41

Overexpression of WT or Mutant α-Synuclein 41

LRRK2 44

Parkin 45

Parkin KO 45

Overexpression of Parkin 46

Pink1 46

DJ1 47

H. Dissertation Objective 48

Chapter 2. Materials and Methods 50

A. Animals 50
Generation of Parkin Knock-Out Mice 50
Genotyping 50
B. Drugs 54
Chronic MPTP 54
Single Injection MPTP 54
Cycloheximide 55
GBR-12909 55
Lentiviral shRNA Against Mouse Parkin 55
C. Tissue Preparation 57
D. Neurochemical Analyses 60
E. Western Blot Analyses 61
Protein Extraction 61
Electrophoresis/Transfer Conditions 62
Protein Detection and Quantification 62
F. Immunohistochemistry 66
G. Unbiased Stereological Cell Counting 66
H. Rapid Immunofluorescent Staining 68
I. Laser Capture Microscopy (LCM) 70
J. RNA Isolation from LCM Samples 72
K. RNA Amplification 73
L. Microarray Hybridization and Initial Analysis 74
M. Microarray Data Analysis and Statistics 79
Normalization, Background Correction and
Data Summarization 79
The Use of Updated Annotation Files 82
Statistical Analyses 83
Cluster Analysis 83
Pathway Analysis with DAVID 86
Analysis of Candidate KEGG Pathways 86
N. RNA Isolation from Microdissected Tissue Punches 87
O. Reverse Transcription 88
P. Real Time Quantitative PCR 88
Q. Stereotaxic Lentiviral Injections 92
R. Statistical Analysis 96

Chapter 3: Characterization of Differential Susceptibility of TIDA, NSDA and MLDA Neurons in the Chronic MPTP Mouse Model 97
A. Introduction 97
B. Hypothesis 98
C. Experimental Design 98
D. Results 103
E. Discussion 113

Chapter 4: Characterization of the Immediate Neurochemical Responses of TIDA, NSDA and MLDA Neurons to a Single Injection of MPTP **119**
A. Introduction 119
B. Hypothesis 121
C. Experimental Design 121
Time Couse of Responses of TIDA, NSDA and MLDA Neurons to a Single Injection of MPTP 121
Effects of Blockade of DAT on the Response of TIDA, NSDA and MLDA Neurons to a Single Injection of MPTP 125
Effects of Protein Synthesis Inhibition on the Responses of TIDA, NSDA and MLDA Neurons to a Single Injection of MPTP 127
Effects of Immediate vs. Delayed Protein Synthesis Inhibition on the Response of TIDA, NSDA and MLDA Neurons to a Single Injection of MPTP 129
D. Results 131
Time Course of Responses of TIDA, NSDA and MLDA Neurons to a Single Injection of MPTP 131
Effects of Blockade of DAT on the Responses of TIDA, NSDA and MLDA Neurons to a Single Injection of MPTP 137
The Impact of Protein Synthesis Inhibition on the Neurochemical Responses of NSDA, MLDA and TIDA Neurons to a Single Injection of MPTP 144
The Impact of Immediate vs. Delayed Protein Synthesis Inhibition on the Neurochemical Responses of NSDA, MLDA and TIDA Neurons to a Single Injection of MPTP 149
E. Discussion 154
Differential Response of TIDA, NSDA and MLDA Neurons After a Single Injection of MPTP 154
Mechanism of MPP+ Uptake is Different in TIDA Neurons vs. NSDA and MLDA Neurons 157
Recovery of TIDA Neurons is Dependent on Synthesis of New Proteins after MPTP Treatment 159
F. General Conclusions 160

Chapter 5: Characterization of the Genomic Responses of TIDA and NSDA Neurons to a Single Injection of MPTP **162**
A. Introduction 162
B. Hypothesis 162
C. Experimental Procedures 163

D. Results 164
Genes with Differential Expression in ARC and SNpc in Control and MPTP Treated Mice 164
Unbiased Pathway Analysis of Microarray Data with DAVID 167
Cluster Analysis of Genes Significantly Higher in ARC than SNpc in MPTP-Treated Mice 176
Analysis of Candidate Genes 179
Real Time PCR Analysis of Candidate Genes 181
E. Discussion 185
Analysis of Pathways using DAVID Annotation Tools 185
Identification of Candidate Clusters 187
Analysis of Candidate Genes 189
Genes and Pathways that Potentially Protect TIDA Neurons from Toxicity 191

Chapter 6: The Involvement of Parkin in the Recovery of TIDA Neurons from MPTP-Induced DA Loss 191
A. Introduction 191
B. Hypothesis 198
C. Experimental Design 198
Parkin Protein Levels Following a Single Injection of MPTP 198
Neurochemical Response of TIDA Neurons to MPTP in Parkin KO mice and WT Littermates 198
Neurochemical Response of TIDA Neurons to MPTP Following Lentiviral Knock Down of Parkin 199
D. Results 199
Parkin Protein Levels Following a Single Injection of MPTP 199
Neurochemical Responses of TIDA Neurons to MPTP in Parkin KO and WT Mice 201
Neurochemical Responses of TIDA Neurons to MPTP Following Lentiviral Knock Down of Parkin 204
E. Discussion 209

Chapter 7. Concluding Remarks 214
DA Theory for Selective Vulnerability of NSDA Neurons in PD 214
Basal Differences Between NSDA and TIDA Neuronal Populations 215
Response of TIDA Neurons to MPTP 217
Hypotheses Regarding the involvement of Parkin in Recovery of TIDA Neurons 218
Protection of NSDA Neurons in PD 224

Appendix..... 226

References..... 270

LIST OF TABLES

1-1 Genes involved in Mendelian inheritable forms of Parkinson's disease..... 10

2-1 Sequence and catalog information for parkin and non-target shRNA lentiviral particles purchased from Sigma..... 56

2-2 Description of primary antibodies used in the experiments in this dissertation..... 63

2-3 Forward and reverse primers used for real time PCR analysis..... 89

3-1 The experimental endpoints used for indices of neuronal function in the chronic MPTP mouse model..... 102

3-2 Norepinephrine (NE) concentrations in median eminence (ME), striatum (ST) and nucleus accumbens (NA) of control and MPTP treated mice..... 107

3-3 Serotonin (5-HT; A) and 5-hydroxyindoleacetic acid (5-HIAA; B) concentrations in median eminence (ME), striatum (ST) and nucleus accumbens (NA) of control and MPTP treated mice..... 108

4-1 The experimental endpoints used for neuronal function following treatment with a single injection of MPTP..... 124

4-2 Norepinephrine (NE) concentrations in median eminence (ME), striatum (ST) and nucleus accumbens (NA) of saline control and MPTP treated mice..... 134

4-3 DOPAC concentrations (ng/mg protein) in ME, ST and NA after a single injection MPTP with protein synthesis inhibition using cycloheximide..... 148

4-4 DOPAC concentrations (ng/mg protein) in ST, NA and ME after a single injection MPTP with protein synthesis inhibition using cycloheximide..... 153

5-1 DAVID Pathway analysis of genes expressed higher in ARC than SNpc after treatment with MPTP..... 169

5-2 Relative expression levels of genes that regulate apoptosis in ARC vs. SNpc of saline and MPTP treated mice..... 171

5-3 DAVID Pathway analysis of genes higher in SNpc than ARC only after treatment with MPTP..... 178

5-4 Normalized mRNA expression levels of LRRK2, synuclein, DJ1, and Pink1 in ARC and SNpc of mice injected with saline or MPTP.... 184

6-1 The effects of parkin shRNA administration and a single injection of MPTP on norepinephrine (NE), serotonin (5-HT) and (5-HIAA) concentrations in the median eminence (ME)..... 207

A-1 Genes with statistically higher expression in ARC than SNpc of saline treated controls..... 227

A-2 Genes with statistically higher expression in SNpc than ARC of saline treated controls..... 237

A-3 Genes with statistically higher expression in ARC than SNpc of animals treated with MPTP..... 246

A-4 Genes with statistically higher expression in SNpc than ARC of animals treated with MPTP..... 258

LIST OF FIGURES

Images in this dissertation are presented in color.

1-1 Schematic diagram depicting the neurochemical events in a NSDA axon terminal 5

1-2 Function of the basal ganglia via the direct and indirect pathways in normal (left) and PD patients (right) 7

1-3 The mitochondrial electron transport chain 13

1-4 The Ubiquitin Proteasome System (UPS) 17

1-5 DA non-enzymatic (left) and enzymatic (right) metabolic pathways 22

1-6 Distribution of dopamine and norepinephrine neuronal populations in a sagittal view of the rat brain 25

1-7 Differences in the DA transmission, uptake and feedback inhibition in NSDA or MLDA neurons (top) and TIDA neurons (bottom) 30

1-8 Diagram describing distribution, bioactivation and site of action of MPTP 34

2-1 Genotyping of wild-type (WT), homozygous parkin knock-out (KO), heterozygous (HT) mice 53

2-2 Diagrams of coronal brain sections illustrating the location of micropunches used to dissect NA and ST 58

2-3 Diagrams of coronal brain sections illustrating the sections used to dissect ARC (top), VTA and SNpc bottom) 59

2-4 GAPDH levels in ARC and SNpc of control and MPTP treated mice 65

2-5 Time course of RNA degradation during rapid immunofluorescent staining for TH 69

2-6 Laser capture of tyrosine hydroxylase-immunoreactive (TH-IR) cells of SNpc 71

2-7 Visualization of individual arrays hybridized with amplified mRNA from ARC and SNpc of control animals..... 76

2-8 Visualization of individual arrays hybridized with amplified mRNA from ARC and SNpc of MPTP treated animals..... 77

2-9 Assessment of RNA quality in individual arrays..... 78

2-10 Mean expression levels (Y-axis) of all genes in each array (X-axis) before (top) and after (bottom) normalization with GCRMA..... 81

2-11 Cluster analysis of genes significantly higher in ARC than SNpc after treatment with a single injection of MPTP..... 85

2-12 GAPDH mRNA levels in ARC and SNpc of control and MPTP-treated mice..... 90

2-13 Bilateral stereotaxic injection of lentiviral vectors into ARC of control and MPTP-treated mice..... 93

2-14 Stereotaxic injection of lentiviral vector encoding for green fluorescent protein (GFP) into ARC of mice..... 94

2-15 IBA1 staining for brain sections from mice that received stereotaxic injection of lentiviral vector encoding for green fluorescent protein into ARC..... 95

3-1 Time course of chronic MPTP administration..... 99

3-2 The effects of chronic MPTP administration on DA levels in median eminence (ME), striatum (ST) and nucleus accumbens (NA)..... 104

3-3 The effects of chronic MPTP administration on DOPAC levels in median eminence (ME), striatum (ST) and nucleus accumbens (NA)..... 105

3-4 The effects of chronic MPTP administration on the ratio of DOPAC/DA in median eminence (ME), striatum (ST) and nucleus accumbens (NA)..... 106

3-5 Tyrosine hydroxylase immunoreactive (TH-IR) cells in the substantia nigra pars compacta (SNpc), ventral tegmental area (VTA) and arcuate nucleus (ARC) of control and MPTP treated mice..... 110

3-6 The effects of chronic MPTP administration on tyrosine hydroxylase immunoreactive (TH-IR) cell numbers in the arcuate nucleus (ARC), substantia nigra pars compacta (SNpc) and ventral tegmental area (VTA) 111

3-7 The effects of chronic MPTP administration on Nissl positive cell numbers in the arcuate nucleus (ARC), substantia nigra pars compacta (SNpc) and ventral tegmental area (VTA)..... 112

4-1 Paradigm for the single injection MPTP time course experiment.....122

4-2 Experimental paradigm for the combination of GBR pretreatment with a single injection MPTP..... 124

4-3 Experimental paradigm for the combination of cycloheximide pretreatment with a single injection of MPTP..... 128

4-4 Experimental paradigm for the combination of cycloheximide treatment with a single injection MPTP..... 130

4-5 The time course of effects of a single injection of MPTP on DA levels in median eminence (ME), striatum (ST) and nucleus accumbens (NA)..... 132

4-6 The time course of effects of a single injection of MPTP on DOPAC levels in median eminence (ME), striatum (ST) and nucleus accumbens (NA)..... 133

4-7 The time course of effects of a single injection of MPTP on 5-HT levels in median eminence (ME), striatum (ST) and nucleus accumbens (NA)..... 135

4-8 The time course of effects of a single injection of MPTP on 5HIAA levels in median eminence (ME), striatum (ST) and nucleus accumbens (NA)..... 136

4-9 The effects of GBR pre-treatment and single injection MPTP administration on DA levels in median eminence (ME)..... 138

4-10 The effects of GBR pre-treatment and single injection MPTP administration on DA levels in striatum (ST)..... 139

4-11 The effects of GBR pre-treatment and single injection MPTP administration on DA levels in nucleus accumbens (NA)..... 140

4-12 The effects of GBR pre-treatment and single injection MPTP administration on DOPAC levels in median eminence (ME)..... 141

4-13 The effects of GBR pre-treatment and single injection MPTP administration on DOPAC levels in striatum (ST)..... 142

4-14 The effects of GBR pre-treatment and single injection MPTP administration on DOPAC levels in nucleus accumbens (NA)..... 143

4-15 The effects of cycloheximide and MPTP administration on DA levels in median eminence (ME)..... 145

4-16 The effects of cycloheximide and MPTP administration on DA levels in striatum (ST)..... 146

4-17 The effects of cycloheximide and MPTP administration on DA levels in nucleus accumbens (NA)..... 147

4-18 The effects of immediate and delayed cycloheximide and single Injection MPTP on DA levels in ME..... 150

4-19 The effects of immediate and delayed cycloheximide and single Injection MPTP on DA levels in ST..... 151

4-20 The effects of immediate and delayed cycloheximide and single Injection MPTP on DA levels in NA..... 152

5-1 The pattern of expression of genes differentially expressed among regions in the control (top) and MPTP treated (bottom) animals... 165

5-2 The number of genes with statistically higher expression in ARC (top) and SNpc (bottom) under control and MPTP treated conditions..... 166

5-3 Relative expression levels of genes that regulate apoptosis in ARC vs. SNpc of saline and MPTP treated mice..... 170

5-4 Expression levels of genes related to DA metabolism, transport and secretion in ARC vs. SNpc of saline and MPTP treated Mice..... 175

5-5 Cluster Analysis of genes up-regulated in ARC but not SNpc after treatment with MPTP.....177

5-6 Expression levels of Parkinson's disease related genes in ARC vs. SNpc of saline and MPTP treated Mice..... 180

5-7 RT-PCR analysis of normalized parkin expression levels in ARC and SNpc in controls and MPTP treated mice..... 182

5-8 RT-PCR analysis of normalized UCH-L1 expression levels in ARC and SNpc in controls and MPTP treated mice..... 183

6-1 Structure and E3 ligase activity of parkin..... 194

6-2 The proposed role of parkin in selective degeneration of DA neurons..... 197

6-3 The effects of a single injection of MPTP on parkin levels in median eminence (ME) and striatum (ST)..... 200

6-4 The effects of a single injection of MPTP on DA levels in the median eminence (ME) of parkin knock out (KO) and wild type (WT) littermates..... 202

6-5 The effects of a single injection of MPTP on DA levels in the median eminence (ME) of parkin knock out (KO) and wild type (WT) littermates..... 203

6-6 The effects of parkin shRNA administration and a single injection of MPTP on DA levels in the median eminence (ME)..... 205

6-7 The relationship between DA concentration and parkin levels in ARC of mice that received both parkin shRNA (143, 145 or 147 sequences) and MPTP.....206

6-8 The effects of parkin shRNA administration and a single injection of MPTP on DA levels in the striatum (ST).....208

7-1 The proposed involvement of parkin in pathways that lead to cell death in Parkinson's disease..... 223

LIST OF ABBREVIATIONS

5-HIAA	5-hydroxyindoleacetic acid
5-HT	Serotonin
6-OHDA	6-hydroxydopamine
AADC	L-Aromatic amino acid decarboxylase
AD	Aldehyde dehydrogenase
ANOVA	Analysis of variance
ARC	Arcuate Nucleus
Complex I	Nicotinamide adenine dinucleotide (NADH)-ubiquinone reductase
DA	Dopamine
DAT	Dopamine transporter
DAVID	Database for Annotation, Visualization and Integrated Discovery
DJ1	Oncogene DJ1
DOPA	Dihydroxyphenylalanine
DOPAC	Dihydroxyphenylacetic acid
DOPAL	Dihydroxyphenylacetaldehyde
E1	Ubiquitin activating enzyme
E2	Ubiquitin conjugating enzyme
E3	Ubiquitin ligating enzyme
FDR	False discovery rate

GAPDH	Glyceraldehyde-3-phosphate dehydrogenase
GBR	GBR-12909
GO	Gene Ontology
GPe	Globus pallidus external segment
GPi	Globus pallidus internal segment
GSH	Glutathione
H2O2	Hydrogen peroxide
HPLC-EC	High performance liquid chromatography with electrochemical detection
IBR	In between ring
IR	Immunoreactive
KO	Knock out
KD	Knock down
LCM	Laser capture microscopy
LNAA	Large neutral amino-acid transporter
LRRK2	Leucine-rich repeat kinase 2
MAO	Monoamine oxidase
ME	Median eminence
Mito	Mitochondria
MLDA	Mesolimbic dopamine
MPDP	1-Methyl-4-phenyl-2,3-dihydropyridinium
MPP^+	1-Methyl-4-phenyl-pyridinium
MPTP	1-Methyl-4 phenyl-1,2,3,6-tetrahydropyridine

NA	Nucleus accumbens
NADH	Nicotinamide adenine dinucleotide
NE	Norepinephrine
NorBNI	nor-binaltorphimine
NSDA	Nigrostriatal dopamine
O2-	Superoxide
OH-	Hydroxyl radical
OONO-	Peroxynitrate
PD	Parkinson's disease
Pink1	PTEN induced putative kinase 1
PKC	Ca2+–calmodulin-dependent protein kinase
PM	Perfect-match
Probenecid	Dipropylsulfamoyl-benzoic acid
RDU	Relative density unit
RING	Really interesting new gene
ROS	Reactive oxygen species
SEM	Standard error of the mean
SNpc	Substantia nigra pars compacta
ST	Striatum
SOD	Superoxide dismutase
TH	Tyrosine hydroxylase
TIDA	Tuberoinfundibular dopamine

UPS	Ubiquitin proteosome system
U50488	Trans-3,4-dichloro-N-methyl-N-[2-(1-pyrrolindinyl)cyclohexyl]-benzene-acetanide methanesulfonate hydrate
UCH-L1	Ubiquitin carboxy-terminal hydrolase L1
VL	Ventral lateral thalamic nucleus
VMAT-2	Vesicular monoamine transporter
VTA	Ventral tegmental area
WT	Wild type

Chapter 1. General Introduction

A. Statement of Purpose

Parkinson's disease (PD) is a debilitating neurodegenerative disorder that causes severe motor impairment with underlying progressive degeneration of nigrostriatal (NS) dopamine (DA) neurons. While symptomatic therapies exist, there is currently no way to retard or halt the degenerative process. Abnormal DA metabolism has been proposed as a mechanism for the specific degeneration of NSDA neurons. However, all DA neurons are not affected to the same extent in PD. In fact, while there is severe loss of midbrain NSDA neurons, the adjacent mesolimbic (ML) DA neurons are affected to a much lesser degree than NSDA neurons and hypothalamic tuberoinfundibular (TI) DA neurons remain unaffected in PD. Other pathways implicated in the pathogenesis of the disease (e.g. mitochondrial dysfunction, protein degradation and oxidative stress) are central pathways that should be essential to all cells and do not explain this differential susceptibility.

The overall aim of the research discussed in this dissertation is to characterize the differential susceptibility of DA neuronal populations in an animal model of PD using pharmacological, neurochemical, molecular and biochemical approaches. The underlying hypothesis is that mechanisms intrinsic to TIDA neurons, which are unaffected in the disease process, protect these neurons from neurodegeneration that occurs in susceptible NSDA neurons. If this hypothesis is correct, elucidation of these factors could lead to development of therapies to protect NSDA neurons in PD, and

thereby prevent the progressive motor deficits associated with this devastating disease.

B. Parkinson's Disease

PD is a complex, multifactorial disorder that affects more than a million people in North America alone (Cookson et al, 2007). The disorder is characterized in the clinic by its debilitating motor symptoms, which include resting tremor, rigidity, bradykinesia (slowness of movement) and postural instability (Fahn, 2003). A definite diagnosis of PD requires post-mortem observation of NSDA neuronal loss, which underlies the motor symptoms of PD, as well as the presence of proteinaceous intracellular inclusions called Lewy bodies. The reason for selective vulnerability of NSDA neurons and the formation of Lewy bodies is not known, and there is currently no therapy to slow or stop the progressive nature of these pathological abnormalities in PD.

Current therapeutics for PD focus primarily on reducing the severity of motor symptoms using medications that replace DA activity at post-synaptic receptors. The most common treatment for PD is the precursor L-DOPA, which is decarboxylated predominantly by glial cells in the brain to form DA and reinstate DA transmission lost due to degeneration of substantial numbers of NSDA neurons. Coadministration with carbidopa blocks decarboxylation of L-DOPA in the periphery, allowing for fewer side effects. Other treatments include DA agonists, monoamine oxidase B inhibitors, and catechol-O-methyltransferase inhibitors. While these medications provide some relief

to patients, they only alleviate the symptoms and are unable to slow or stop the progressive degeneration of NSDA neurons in PD.

C. Degeneration of NSDA Neurons and Motor Abnormalities in PD

NSDA neurons, emanating from substantia nigra pars compacta (SNpc) and projecting to the striatum (ST), are key components of the extrapyramidal motor system and their degeneration underlies the motor deficits of PD. These motor deficits can be alleviated by mechanisms that restore striatal DA concentrations (Dauer and Przedborski, 2003). Understanding normal NSDA neuronal function is essential to discovering mechanisms that may underlie their degeneration in PD.

Normal NSDA Neuronal Function:

NSDA neurons have long projecting axons and form classic synapses with target medium spiny neurons in ST. The tightly controlled synthesis, storage, release and metabolism of DA in these neurons (**Figure 1-1**) allows for regulation of the activity of the basal ganglia that ultimately control voluntary movement. Synthesis of DA begins when dietary tyrosine is transported into DA axon terminals via the large neutral amino-acid transporter (Oxender and Christensen, 1963; Oldendorf and Szabo, 1976; Palacin et al., 1998), where it is hydroxylated to 3,4-dihydroxyphenylalanine (DOPA) by the rate limiting enzyme tyrosine hydroxylase (TH) (Levitt et al., 1965; Kumer and Vrana, 1996). In the cytoplasm, the enzyme L-aromatic amino acid decarboxylase (AADC) quickly decarboxylates DOPA into DA (Kumer and Vrana, 1996). The vesicular

monoamine transporter-2 (VMAT-2) rapidly and efficiently packages newly made DA into synaptic vesicles. Any newly synthesized cytosolic DA that is not packaged is degraded into 3,4-dihydroxyphenylacetic acid (DOPAC) through a two-step process catalyzed by mitochondrial monoamine oxidase (MAO) and aldehyde dehydrogenase (AD). Cytoplasmic DA regulates its own synthesis by inhibiting the activity of TH via end-product inhibition (Okuno and Fujisawa, 1985; Andersson et al., 1988; Haavik et al., 1990).

Vesicular DA is released into the synaptic cleft upon propagation of an action potential where it can bind to post-synaptic D1 or D2 receptors, thereby enhancing or inhibiting the firing of post-synaptic neurons by cAMP-dependent mechanisms (Onali et al., 1985; Monsma et al., 1990). DA released into the synapse can also activate pre-synaptic D2 autoreceptors and thereby inhibit further synthesis or release of DA (Christiansen and Squires, 1974; Roth, 1975). Excess DA is removed from the synapse by the high-affinity reuptake DA transporter (DAT) and is either repackaged into vesicles or rapidly metabolized to DOPAC (Kilty et al., 1991).

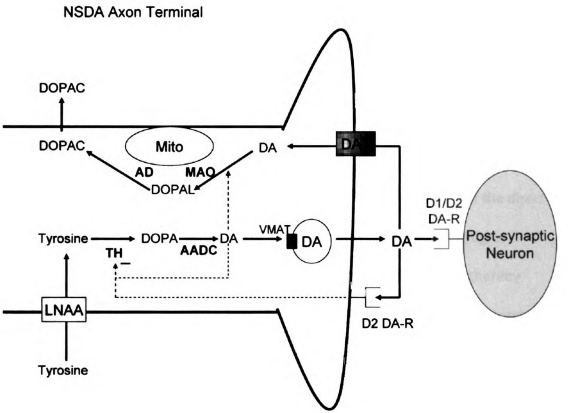

Figure 1-1. Schematic diagram depicting the neurochemical events in a NSDA axon terminal. Tyrosine is taken up into the axon terminal by the large neutral amino-acid (LNAA) transporter. Tyrosine is converted to DOPA by the rate limiting enzyme tyrosine hydroxylase (TH). DOPA is decarboxylated to DA by L-aromatic amino-acid decarboxylase (AADC) in the cytoplasm. Newly synthesized DA is transported by vesicular monoamine transporter-2 (VMAT) into synaptic vesicles for release. Newly synthesized DA can also be degraded by mitochondrial (Mito) MAO. DA released into the synapse can bind to post-synaptic D1 or D2 receptors (D1/D2 DA-R) or D2 autoreceptors (D2 DA-R). DA released into the synapse is removed via the DA transporter (DAT). Recaptured DA can be either repackaged into synaptic vesicles or degraded by MAO and aldehyde dehydrogenase (AD) to DOPAC. DOPAC is removed from the axon terminal through diffusion. (Drolet, 2006)

NSDA Control of Basal Ganglia

The release of DA from NSDA neurons in the ST regulates the activity of the basal ganglia which collectively refers to the SNpc, ST, globus pallidus and the subthalamic nucleus (Bergman, 1998). The interplay amongst these nuclei determines the control of voluntary motor behavior. As depicted in **Figure 1-2**, DA released by NSDA neurons in ST acts on excitatory D1 and inhibitory D2 receptors to activate the direct pathway and inhibit the indirect pathway, respectively. Activation of the direct pathway leads to inhibition of areas of the globus pallidus and substantia nigra reticulata, which in turn removes their tonic inhibition from the thalamus thereby promoting voluntary movement (Jackson et. al. 1994). The indirect pathway normally serves to inhibit the voluntary movement. Therefore, inhibition of the indirect pathway also promotes voluntary movement (Jackson and Westlind-Danielson 1994). As a simple analogy, D1 mediated activation of the direct pathway is akin to pressing the gas pedal in a car, whereas, D2 mediated inhibition of indirect pathway is similar to letting off the brake; both promote forward motion or in this case voluntary movement.

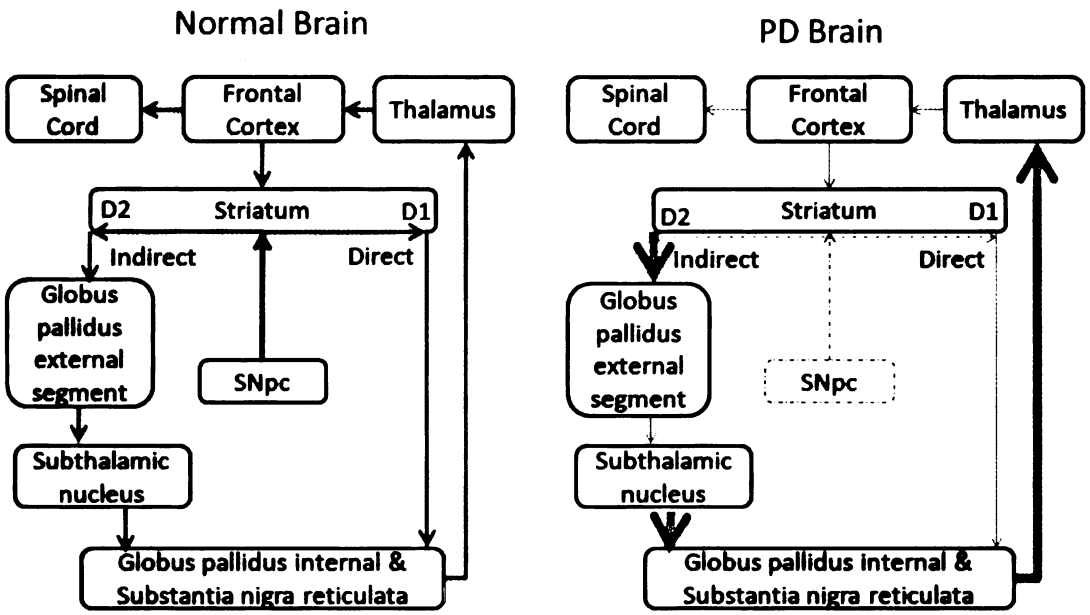

Figure 1-2. Function of the basal ganglia via the direct and indirect pathways in normal (left) and PD patients (right). In normal basal ganglia DA released from the SN activates the direct pathway, thereby inhibiting the globus pallidus internal segment and substantia nigra reticulata and disinhibiting the thalamus. DA released in the ST also inhibits the indirect pathway which leads to disinhibition of the globus pallidus external segment and inhibition of the subthalamic nucleus, which in turn causes less excitation of the globus pallidus internal segment and substantia nigra reticulata allowing for the thalamus to be disinhibited. Increased activity of the thalamus leads to excitation of the frontal cortex, which leads to activation of the spinal cord and increased voluntary movement. In PD patients (left) significantly less DA is released into the ST thereby less activation of the direct pathway and inhibition of the direct pathway can occur. This causes increased inhibition of the thalamus and complicates voluntary motor movement. Blue lines represent inhibitory and red lines represent excitatory synapses.

NSDA Neurons and Control of Basal Ganglia in PD

The loss of NSDA neurons leads to alterations in the activity of the neural circuits within the basal ganglia that regulate movement (**Figure 1-2**). The loss of DA in ST leads to an inhibition of the direct pathway and excitation of the indirect pathway, which results in lower firing rates of neurons in the motor cortex. The loss of motor cortex activity leads to lower activation of spinal cord motor neurons that activate peripheral muscle movement and a hypokinetic movement disorder. Since the loss of NSDA neurons underlies the cardinal motor symptoms of PD, halting the ongoing degeneration of these neurons will prevent the continued worsening of motor deficits in PD.

D. Environmental and Genetic Factors and PD

Most cases of PD are considered sporadic and of unknown source. While environmental factors have been implicated in the pathogenesis of the disease, no specific factor has been identified. Epidemiological studies have revealed that rural living, well-water consumption, pesticide use and occupations such as mining and welding are all associated with an increase risk for PD (Priyadarshi et al., 2000; Priyadarshi et al., 2001; Firestone et al., 2005; Jankovic, 2005). Other environmental factors such as coffee and alcohol consumption and cigarette smoking have been associated with reduced risk for the disease (Honig, 2000; Allam et al., 2002; Checkoway et al., 2002; Allam et al., 2004). However, the mechanisms by which these factors may influence disease risk remain unclear.

While most cases of PD are not inherited, several genetic mutations in families with a Mendelian pattern of inheritance have been identified and are listed in **Table 1-1**. These genetic mutations have shed some light on disease pathogenesis by implicating a number of interconnected molecular pathways (Hofer and Gasser, 2004). These studies also demonstrate that multiple mechanisms can lead to the degeneration of NSDA neurons and result in PD symptoms. Understanding the overlap in molecular mechanisms between these heritable and sporadic cases of PD may elucidate the complex pathways that underlie this disease. These pathways are described in detail below.

Gene	Chromosomal Position	Mutations	Pathology
SNCA	4q21	Dominant	Lewy bodies, NSDA and hippocampal neuronal loss
LRRK2	12p12	Dominant	Lewy bodies and NSDA loss
PARK2	6q25.2-q27	Recessive	Primarily NSDA loss
PINK1	1p35-p36	Recessive	Undetermined
DJ1	1p36	Recessive	Undetermined

Table 1-1. Genes involved in Mendelian inheritable forms of Parkinson's Disease. SNCA = α-synuclein, LRRK2 = Leucine rich repeat kinase 2, park2 = parkin, pink1 = PTEN induced putative kinase 1, and DJ1 = oncogene DJ-1.

E. Pathways Implicated in PD

Several molecular pathways have been proposed to play a role in the etiology of PD. There is consistent evidence for a role of mitochondrial dysfunction, malfunctions in the proteasome and other protein degradation pathways, as well as DA synthesis and metabolism. These pathways are explained below and evidence for the involvement of each, as well as interplay amongst these pathways is presented.

Mitochondrial Function and Reactive Oxygen Species

The mitochondrial electron transport chain has five complexes located in its inner membrane (**Figure 1-3**). Complexes I, III and IV use energy from the transfer of electrons down the transport chain to move protons from the mitochondrial matrix to the inner-membrane space and create a proton gradient across the inner membrane. Complex V can use the energy from this proton gradient to convert ADP to ATP. Disruptions in the electron transport chain can reduce ATP levels, and thereby decrease the supply of energy in the cell. Furthermore, under normal conditions oxygen can interact with electrons in the transport chain to form reactive oxygen species (ROS). All aerobic organisms are constantly exposed to ROS (Halliwell, 1992) but ROS can be scavenged primarily by glutathione under basal conditions. ROS that are not scavenged can cause damage to a variety of critical biological constituents including DNA, proteins and lipids. Mitochondria are thought to be the most important source of cellular free radicals, producing superoxide radicals at ubiquinone and NADH dehydrogenase (Turrens et al., 1985). Superoxide dismutase (SOD) normally converts superoxide to

H_2O_2, which reacts with transition metals to generate the prime mediator of cellular damage, the hydroxyl radical. Alternatively, superoxide can also react with nitric oxide to produce peroxynitrile (Beckman and Crow, 1993). Under physiological circumstances, approximately 2% of the oxygen consumed by mitochondria is converted to superoxide and this percentage is much higher in dysfunctional mitochondria.

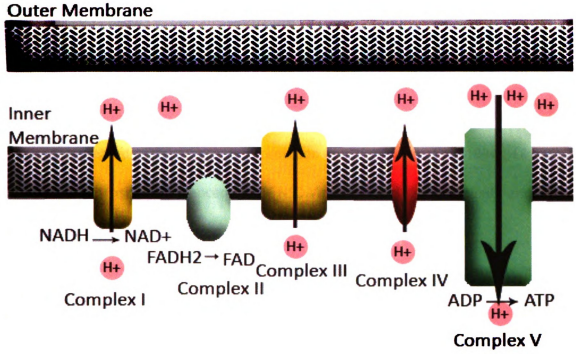

Figure 1-3. The mitochondrial electron transport chain. A hydrogen gradient is created in the inner membrane space utilizing enzymes on the inner mitochondrial membrane to oxidize NADH2+ to NAD+ (Complex I), and FADH2 to FAD (Complex II). Electrons are passed from Complex to Complex in the inner membrane of the mitochondrion, losing some of their energy at each step. These electrons provide energy to "pump" hydrogen protons (Complex V) across the inner mitochondrial membrane. The hydrogen protons tend to move down their concentration gradient providing energy to phosphorylate ADP into ATP.

The first clue that pointed to mitochondria as an important pathway in PD came when a group of individuals who injected themselves with synthetic heroin contaminated with 1-methyl,4-phenyl,1,2,3,6-tetrahyropiridine (MPTP) developed motor symptoms that closely matched symptoms of PD (Langston et al., 1983; Langston and Ballard, 1983). MPTP causes mitochondrial Complex I inhibition which leads to decreased ATP synthesis and formation of ROS (Chiueh et al., 1994). Like PD patients, MPTP users experienced loss of NSDA neurons and axon terminals, and progressive loss of motor function over time (Vingerhoets et al., 1994).

A more direct link between PD and mitochondrial impairment came from description of Complex I deficiency in post-mortem substantia nigra of PD patients (Schapira et al., 1989). Since this discovery, several reports have demonstrated Complex I deficiency in substantia nigra, platelets and skeletal muscles of PD patients (Bindoff et al., 1989; Krige et al., 1992; Mann et al., 1994). Overall, the severity of Complex I deficits have been reported to be about 35% in PD patients when compared to a control population. However, within PD patients there seems to be a heterogeneous population, with some patients showing severe Complex I deficiency and others having normal Complex I activity (Schapira, 2008). From this data, one can hypothesize that Complex I deficits in PD patients may lower the threshold of mitochondria or ROS-mediated apoptosis.

Some genetic cases of PD confirm the involvement of mitochondria and ROS in PD. PTEN induced kinase 1 (PINK1) and oncogene DJ1 (DJ1) are genes associated with familial PD and their products are directly linked to mitochondrial function (Beal, 2005).

PINK1 is a mitochondrial kinase which is present in 5-10% of Lewy bodies for familial and sporadic PD patients (Gandhi et al., 2006). The L166B DJ1 mutation is associated with increased localization of DJ1 to the mitochondrial membrane (Bonifati et al., 2003a), suggesting mitochondrial dysfunction may be involved in familial forms of PD.

With vast evidence for the involvement of mitochondrial dysfunction in PD, its role in the pathogenesis of the disease still remains largely controversial (Coppede et al., 2006). It is unclear, for example, whether mitochondrial deficits are the cause or a downstream effect of the disease.

Protein Degradation

The ubiquitin proteasome system (UPS) is the major intracellular protein degradation system (Hershko 1998). As demonstrated in **Figure 1-4**, in the UPS proteins destined for degradation are covalently tagged with ubiquitin, a 76 amino acid residue protein, through a process that requires the sequential actions of ubiquitin activating (E1), conjugating (E2) and ligating (E3) enzymes (Hershko et al., 1983). Usually, the ubiquitylation process is repeated many times to allow the formation of a polyubiquitin chain on the substrate which is then targeted for degradation by the 26S proteasome. The 26S proteasome is a large protease complex composed of a barrel-shaped 20S proteolytic core and two 19S regulatory caps, one on each side of the barrel's openings. Individual ubiquitin monomers are regenerated in the process by the actions of de-ubiquitylating enzymes. It is noteworthy that a large number of cellular proteins (>1000), comprising various E1s, E2s, E3s and other related members,

are involved in the UPS (Hicke et al., 2005) and therefore the dysfunction of this system could lead to major cellular consequences.

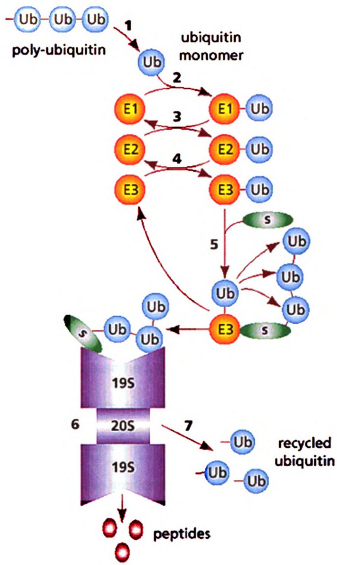

Figure 1-4. The Ubiquitin Proteasome System (UPS). Depiction of the UPS, demonstrating ubiquitin release from pro-ubiquitin (Step 1) followed by ubiquitin conjugation to the substrate by adenylation of ubiquitin by ubiquitin-activating enzyme E1 (Step 2), transfer of activated-ubiquitin to the cysteine of a specific E2 ubiquitin-conjugating enzyme (Step 3), transfer of activated ubiquitin from E2 to a substrate-specific E3 ubiquitin-ligase (Step 4) and formation of a substrate-E3 complex and biosynthesis of the polyubiquitin chain (Step 5). The substrate protein is recognized by the 19S regulatory particle in an ATP-dependent step (Step 6) and must be unfolded and deubiquitinated before it can enter the interior of the 20S particle to come in contact with the proteolytic active sites (Step 7). The passage of the unfolded substrate into the core is called translocation and results in degraded proteins (MacDonald, 1999).

Several discoveries point to UPS dysfunction in PD. There is decreased activity of the 20S proteasome in SNpc of PD patients (McNaught and Jenner, 2001; McNaught et al., 2003) and proteasome activators are suppressed in the PD SNpc (McNaught and Olanow, 2003). Other factors such as increased levels of proteins with oxidative damage, increased protein aggregation and formation of Lewy bodies also implicate the UPS in PD. It is noteworthy to mention that one of the major components of sporadic PD Lewy bodies is aggregated α-synuclein (Spillantini et al., 1997). Duplication, triplications or mutations in the gene for α-synuclein that cause increased expression of WT α-synuclein lead to familial PD (Chartier-Harlin et al., 2004). This suggests that too much of this protein can cause neurotoxicity, potentially by aggregating and blocking proteasome function. This idea is consistent with other neurodegenerative disorders such as Huntington's disease, where aggregating proteins are associated with neurotoxicity.

Other genetic cases have implicated UPS dysfunction in the etiology of PD. The first gene demonstrated to cause autosomal recessive PD, parkin, is an E3 ligase (Kitada et al., 1998). Interestingly, disease causing mutations of parkin were found to compromise its normal role as an E3 enzyme (Sriram et al., 2005). PD patients with mutations in parkin show accumulation of insoluble Pael receptors, a substrate for parkin possibly implicating the UPS pathway (Yamamoto et al., 2005). The discovery of a missense mutation in UCH-L1, a de-ubiquitylating enzyme, in a pair of German siblings with inherited PD (Leroy et al., 1998) also lends support to the role of UPS in PD pathogenesis. The mutated version of UCH-L1 markedly reduces ubiquitin hydrolase

activity *in vitro* (Gong and Leznik, 2007). This evidence, however, remains controversial since UCH-L1 mutations have only been seen in one pair of siblings and the possibility remains that other genes or environmental factors were responsible for PD in these individuals.

As is the case with the mitochondrial pathway, the involvement of the UPS in the pathogenesis of PD should be interpreted with caution. Many cellular processes can lead to proteasome dysfunction and, in turn, proteasome dysfunction can cause impairment of other cellular processes that are implicated in PD pathogenesis. For example, proteasome inhibitors can cause mitochondrial damage (Sullivan et al., 2004) and, vice versa, mitochondrial Complex I inhibitors can decrease proteasome activity (Hoglinger et al., 2003a). The interconnectivity of these pathways makes it difficult to assess the exact role of UPS in PD pathogenesis and discern whether proteasome dysfunction is a result or an active contributor to the disease.

Abnormal DA Metabolism

A major question that has been posed is why there seems to be selective vulnerability of NSDA neurons in PD. Although several brain regions are affected in PD, as demonstrated by presence of pathological abnormalities such as Lewy bodies, the DA neurons of SNpc and noradrenergic neurons of locus ceruelleus exhibit the most extensive cell loss. One element common to these severely affected neuronal populations is that they produce catecholamines. It is therefore not surprising that metabolism of catecholamines, particularly DA, which is also synthesized in

noradrenergic neurons, has been proposed to play a role in the neuronal loss in the PD brain.

It is crucial for DA neurons to closely regulate synthesis, storage, release and reuptake of DA because certain metabolites of DA can be highly toxic to neurons (Graham, 1978; Graham et al., 1978; LaVoie and Hastings, 1999b, 1999a). The enzymatic and non-enzymatic metabolism of DA is depicted in **Figure 1-5**. DA oxidation by MAO results in the formation of dihydroxyphenylacetaldehyde (DOPAL) which is highly toxic (Burke et al., 2003; Legros et al., 2004; Ebadi et al., 2005). Under normal conditions, AD can efficiently and quickly convert DOPAL to DOPAC, a less toxic species that diffuses out of axon terminals. Accumulation of DOPAL in nerve terminals by inhibition of AD can exacerbate neurotoxicity caused by Complex I inhibition (Lamensdorf et al., 2000). The further enzymatic conversion of DOPAL to DOPAC can also damage the cells by producing ROS.

Cytoplasmic DA can also auto-oxidize non-enzymatically to produce a highly reactive DA-quinone molecule, superoxide (O_2^-) and H_2O_2 radicals **(Figure 1-5)**. The DA-quinone molecules bind to cysteine residues causing covalent protein modification, conformational changes and loss of function of intracellular proteins (LaVoie and Hastings, 1999b). Neurons are primarily protected from ROS-induced oxidative damage by glutathione (Cooper and Kristal, 1997), which donates an electron to free radicals (O_2-, OH-, OONO- and H_2O_2) and reduces them to less toxic molecules. If there is an increase in ROS formation or decrease in antioxidant proteins, the cell can undergo oxidative damage. The added stress from abnormal DA metabolism,

combined with other abnormalities such as mitochondrial or proteasomal dysfunction may make catecholamine neurons susceptible to cell death.

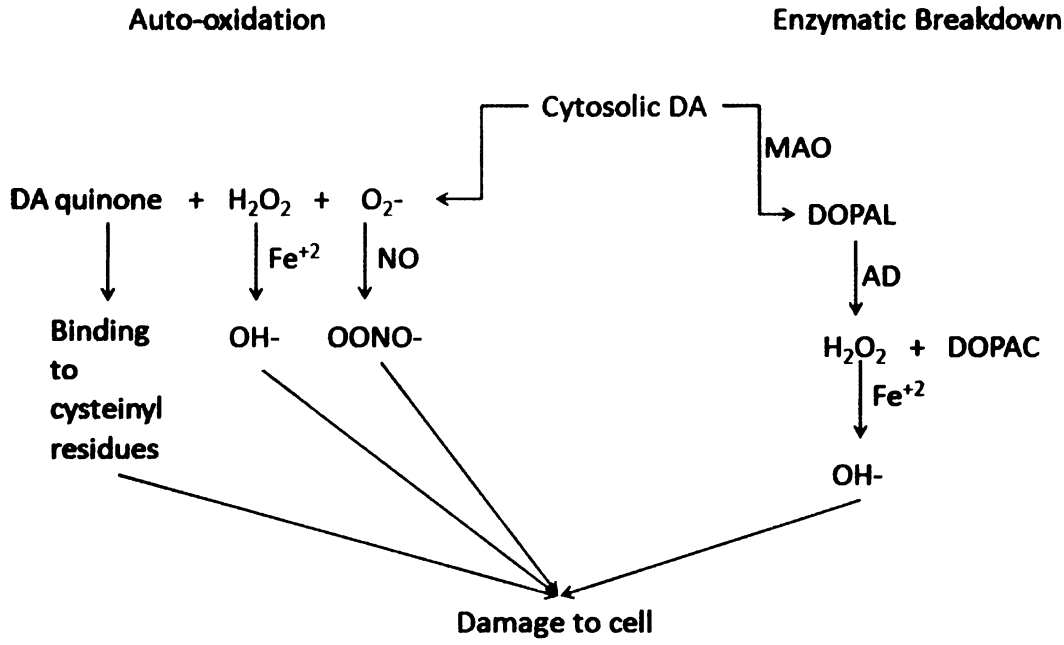

Figure 1-5. DA non-enzymatic (left) and enzymatic (right) metabolic pathways. The enzymatic metabolism of DA results in the formation of DOPAC and a hydrogen peroxide (H_2O_2) molecule which can react with iron to form hydroxyl radical (OH^-) through the Fenton reaction (Dringen et al., 2000). Non-enzymatic DA auto-oxidation results in the formation of DA-quinone molecules as well as H_2O_2 and superoxide (O_2^-). H_2O_2 can produce OH^- while O_2^- can react with nitric oxide (NO) to form peroxynitrite ($OONO^-$).

Genetic cases of PD are consistent with the hypothesis that abnormal metabolism of DA may be involved. For example, α-synuclein and parkin are proposed to be directly involved in regulation of DA metabolism and transmission ((Jiang et al., 2004a; Jiang et al., 2006)), and mutations in the genes for these proteins may cause an imbalance in this tightly regulated system. Furthermore, mitochondrial impairment can affect DA metabolism and therefore the genes involved in mitochondrial function may disrupt normal DA homeostasis and cause further toxicity to the cells.

Overall, much evidence suggests that damage from abnormal metabolism of DA may contribute to the selective loss of NSDA neurons in PD. On the other hand, if DA were the main culprit for extensive cell loss in PD, all DA containing neurons in the brain should be affected to a similar extent. However, as evidence presented in the next section will demonstrate, this is clearly not the case.

F. Differential susceptibility of DA neurons in PD

There are several groups of DA neurons in the brain, located throughout the hypothalamus and midbrain (**Figure 1-6**). While NSDA neurons undergo the most extensive lesion in PD, other DA neurons in the brain are not affected to the same extent (Ahlskog, 2005). NSDA neurons undergo more extensive degeneration compared to the adjacent MLDA neurons in PD. Based on post-mortem analyses of patients with PD, approximately 80-90% of melanin-pigmented neurons are lost in the SNpc compared to 30-40% in the ventral tegmental area (VTA) (German et al., 1989; Fearnley and Lees, 1991) while melanin-pigmented TIDA neurons do not degenerate in

PD (Braak and Braak, 2000). This differential susceptibility is inconsistent with the hypothesis that abnormal DA metabolism underlies the extensive demise of NSDA neurons. Understanding the differences between these distinct neuronal populations and the mechanisms by which they respond to cellular stresses or metabolize cytosolic DA may shed light on protective or deleterious properties that cause the differential susceptibility of these neurons in PD.

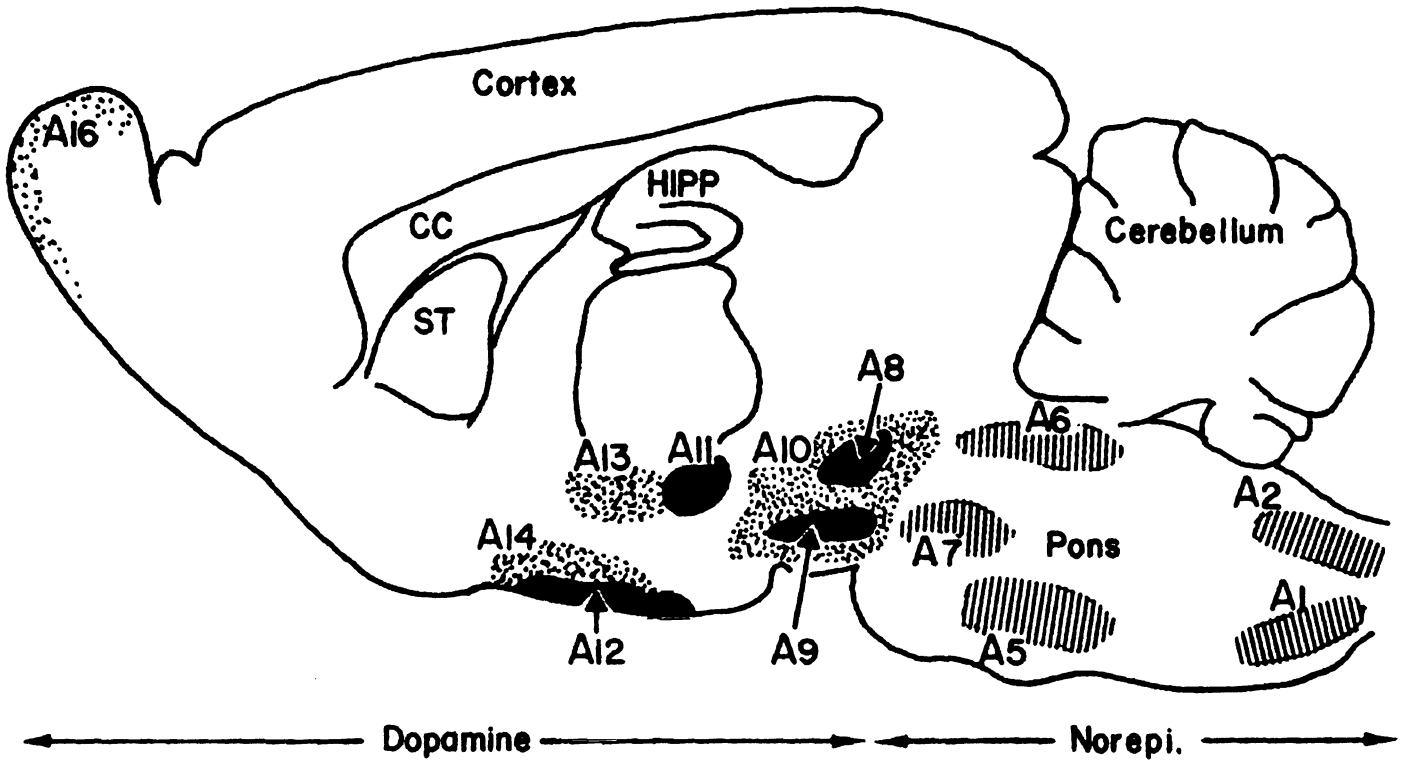

Figure 1-6. Distribution of dopamine and norepinephrine neuronal populations in a sagittal view of the rat brain. A1-A7 are norepinehrine neurons, A8-A16 are dopaminergic neurons. CC = corpus collosum; HIPP = hippocampus; ST = striatum; Norepi = norepinephrine (Dahlstrom and Fuxe 1964; Moore et al. 1987).

MLDA neurons

MLDA neurons are located in the VTA and send axons through the medial forebrain bundle that terminate in the nucleus accumbens (NA) and frontal cortex (Dahlström and Fuxe, 1964; Ungerstedt, 1971c, Cooper et al., 2003). MLDA neurons are involved in the control of motivation, emotions and reward and other higher cognitive functions. These neurons have been extensively studied in regards to addiction and reward-based behaviors (Di chiara et al., 2002) as well as schizophrenia and other affective disorders.

MLDA neurons are very similar to NSDA neurons in that they have long projecting axons and form classic synapses with target medium spiny neurons of NA or pyramidal cells of the frontal cortex. MLDA neurons utilize the same enzymatic machinery to synthesize, package, and release DA (**Figure 1-1**). Furthermore, these neurons use the high affinity DAT for reuptake of DA and utilize DA autoreceptors to regulate their activity.

Some differences between MLDA and NSDA neurons have been noted and may help explain the differential susceptibility of these neuronal populations in PD. One major difference is that the majority of MLDA neurons express the calcium chelator calbindin, whereas only 30% of NSDA neurons express this protein (Lavoie and Parent, 1991; Parent and Lavoie, 1993; Haber et al., 1995). Neurons that express calbindin, both in SNpc and VTA are less susceptible in PD and animal models of PD (Yamada et al., 1990; Lavoie and Parent, 1991), however a direct cause and effect relationship has not been established between calbindin and cell survival. Furthermore, if indeed

protective, the mechanisms underlying the protective properties of calbindin have yet to be elucidated.

MLDA neurons also have lower levels of DAT and D2 receptor mRNA when compared to NSDA neurons (Hurd et al., 1994; Haber et al., 1995). On the other hand, MLDA neurons have a higher turnover rate of DA than NSDA neurons as measured by the ratio of DA metabolites to DA (Behrouz et al., 2007), suggesting DA breakdown may be more efficient in these neurons. The resistance of MLDA neurons is unlikely to be due to lower toxin entry via DAT since these neurons also display resistance to lipophillic toxins that freely enter the cells (Betarbet et al., 2000; Behrouz et al., 2007). On the other hand, the differences in the way these neurons handle DA synthesis, uptake and metabolism may contribute to their partial resistance in PD models and PD and require further examination.

TIDA neurons

TIDA cell bodies are located in the ARC of the hypothalamus and their axons project to ME, where they release DA into the hypophyseal portal blood. DA released into the portal circulation is transported to the anterior pituitary where it tonically inhibits prolactin secretion by activating D2 receptors on pituitary lactotrophs. A portion of the TH positive neurons in the ventrolateral ARC lack L-aromatic amino acid decarboxylase and are not capable of synthesizing DA (Meister et al., 1988). The exact function of these "DOPAergic" neurons is not known and the remainder of this dissertation will focus on the dorsomedial region of ARC, which projects to ME and releases DA.

TIDA neurons possess and utilize the same enzymatic machinery as NSDA and MLDA neurons in order to produce DA from dietary tyrosine (**Figure 1-1**). These neurons also use the highly efficient VMAT-2 to package DA inside of synaptic vesicles so that it may be exocytosed upon propagation of an action potential. Cytosolic DA that is not packaged is rapidly metabolized by MAO and AD to DOPAC in a similar fashion to NSDA and MLDA neurons.

There are two major differences between hypothalamic TIDA neurons and mesotelencephalic NSDA and MLDA neurons. Since TIDA neurons do not form classic synapses with their targets (**Figure 1-7**), they lack the high affinity DAT but instead utilize a low affinity reuptake system (Demarest and Moore, 1979a; Annunziato et al., 1980). Second, TIDA neurons have much lower expression levels of D2 autoreceptors

(Lookingland and Moore, 1984; Gunnet et al., 1987; Weiner et al., 1991) and therefore lack D2 mediated feedback inhibition.

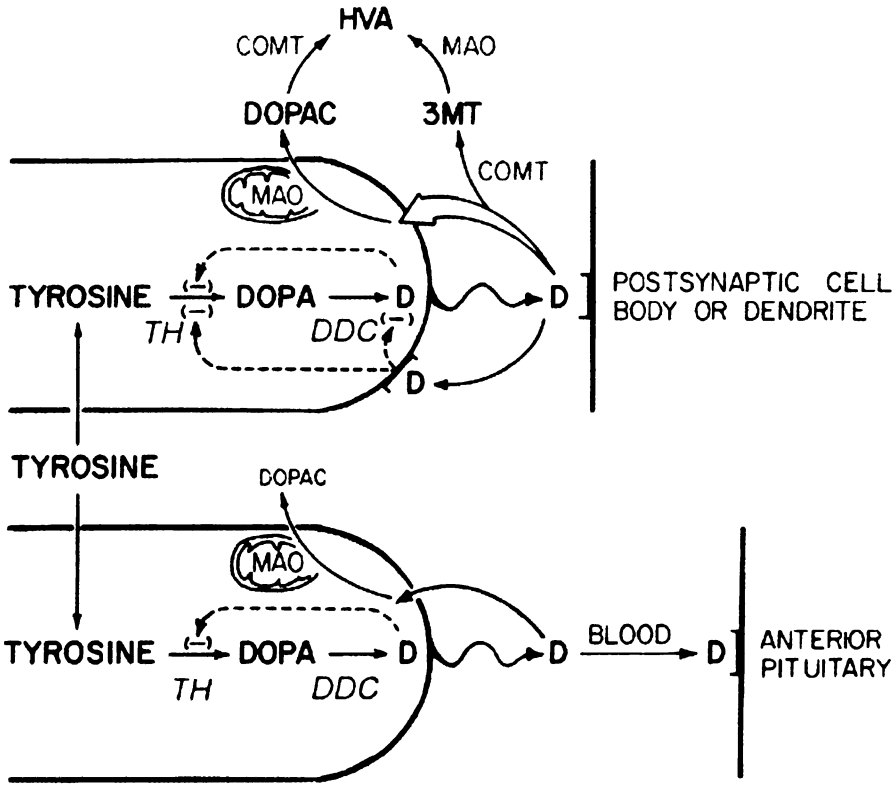

Figure 1-7. Differences in the DA transmission, uptake and feedback inhibition in NSDA or MLDA neurons (top) and TIDA neurons (bottom). NSDA and MLDA neurons (top) which form classical synapses with post-synaptic targets, have high affinity dopamine transporter for reuptake of DA, and utilize D2 receptor mediated feedback inhibition. TIDA neurons (bottom) release DA into the hypophyseal portal blood, utilize a low affinity high volume transporter for uptake of DA, and lack D2 receptor feedback inhibition Figure from Lookingland and Moore (2005).

Due to similarities between TIDA, NSDA and MLDA neurons, it would be plausible to hypothesize that disruptions due to abnormal DA function would affect the TIDA system in PD. However, unlike other central DA neurons there is no loss of TIDA neurons in the post-mortem PD brain (Langston and Forno, 1978; Braak and Braak, 2000) and the mechanisms underlying this selective resistance to neurodegeneration are not known. As such, characterization of the properties of TIDA neurons compared to other DA neurons that degenerate in PD may elucidate mechanisms that impart protection.

The major function of TIDA neurons is to inhibit the release of prolactin from the anterior pituitary. Disrupting TIDA DA synthesis and release, preventing DA access to pituitary lactotrophs, or blocking pituitary D2 receptors, all increase prolactin secretion. TIDA neurons, in turn, are activated by prolactin (Hokfelt and Fuxe, 1972; Lookingland et al., 1987a; Arbogast and Voogt, 1997; Lerant and Freeman, 1998). This serves as a long loop feedback system where prolactin can suppress its own secretion by increasing the activity of TIDA neurons. TIDA neuronal activation by prolactin has two components, a rapid (less than 4 h) activation of TH that does not require protein synthesis and may be associated with the catylitic properties of the enzyme (Pasqualini et al., 1994; Lookingland and Moore, 2005), and a delayed (12-16 h) stimulation of TH which requires ongoing protein synthesis (Arbogast and Voogt, 1991; Lookingland and Moore, 2005).

Several studies have used circulating prolactin concentration as an indirect index of TIDA neuronal integrity since loss of TIDA neuronal function stimulates

prolactin secretion. A majority of studies indicate that basal levels of prolactin are not altered in PD patients, suggesting that TIDA neuronal function is preserved (Lawton and MacDermot, 1980; Agnoli et al., 1981; Eisler et al., 1981; Thorner and Login, 1981; Vogel and Ketsche, 1986; Kirkpatrick and Tamminga, 1988).

G. Animal models of PD

Many animal models of PD have been developed to date and yet no single model, either based on neurotoxins, genetic mutations or a combination of the two, recreates all the key features of disease. Each model has its advantages and disadvantages in regards to studying different aspects of this complicated neurodegenerative disorder. Some of the most commonly used models are discussed here.

Neurotoxin-based Models

Several neurotoxins have been used to model PD, based on the ability of these compounds to induce degeneration of NSDA neurons. The most common toxin models employ MPTP, 6-hydroxydopamine (6-OHDA), rotenone or paraquat. MPTP and rotenone inhibit mitochondrial Complex I and all four toxins cause the formation of ROS. MPTP is the only toxin linked with a human form of parkinsonism, is the most widely studied and will be therefore be most extensively discussed here.

MPTP

MPTP is a lipophillic compound and upon systemic administration penetrates the blood brain barrier and enters the brain. Once inside the brain, the majority of MPTP is taken up by glial cells due to the high number of these cells compared with neurons (Markey et al, 1984). Inside glial cells, MPTP is converted by MAO to 1-methyl, 4-phenyl, 2,3, dihydropyrinium (MPDP) and oxidized to its active and toxic metabolite 1-methyl-4-phenylpyridinium (MPP+). As depicted in **Figure 1-8**, at modest doses MPP+ causes toxicity to DA neurons by gaining access to the cell via DAT and depleting ATP stores via binding to mitochondrial Complex I as well as producing ROS (Chan et al., 1991; Zang and Misra, 1993). MPP+ can also serve as a substrate for MAO inside these DA neurons and result in inhibition of the enzymatic conversion of DA into DOPAC (Takamidoh et al., 1987). In addition, MPP+ can be taken up into vesicles by VMAT-2, thereby displacing vesicular DA into the cytoplasm (Reinhard et al., 1987; Liu et al., 1992).

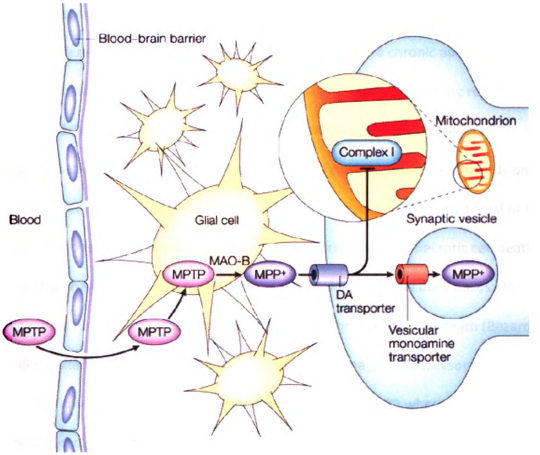

Figure 1-8. Diagram describing distribution, bioactivation and site of action of MPTP. 1-Methyl, 4-phenyl, 1,2,3,6-tetrahydropyridine (MPTP), a lipophillic molecule rapidly crosses the blood brain barrier and is metabolized, primarily by glial cells, to its toxic and active metabolite MPP+. 1-methyl-4-phenylpyridinium (MPP+) can then enter dopaminergic neurons through the dopamine (DA) transporter. Once inside the cell, MPP+ can inhibit Complex I of the mitochondrial electron transport chain, disabling ATP production and causing the formation of reactive oxygen species. MPP+ can also be sequestered inside of synaptic vesicles, thereby displacing DA into the cytoplasm. Figure from Villa and Przedborski (2003).

Acute, sub-chronic and chronic MPTP administration regimens have been used to model different stages of PD, ranging from a single dose to chronic administration via osmotic minipumps over an extended period of time. All these dosing regimens cause loss of DA from the axon terminal region of NSDA neurons followed by retrograde cell death. The extent and mechanism of cell loss, however, depends on the dosing regimen. Paradigms using high daily doses (e.g. acute model with a total of 80 mg/kg MPTP over 4 injections in one day) cause severe, rapid and necrotic cell death. On the other hand, regimens employing repeated exposure to low daily doses (25 mg/kg per day or less) cause less rapid and primarily non-necrotic cell death (Bezard et al., 1997; Tatton and Kish, 1997; Petroske et al., 2001; Smeyne and Jackson-Lewis, 2005). The lower repeated dosing regimen better resembles PD where progressive non-necrotic cell death occurs (Mochizuki et al., 1996; Anglade et al., 1997). Chronic or sub-chronic treatment with MPTP also produces motor dysfunction, and in some cases of prolonged treatment, Lewy body-like inclusions (Petroske et al., 2001). Decreased UPS function has also been reported with MPTP treatment (Fornai et al., 2005), further implicating the mitochondrial and UPS pathways in the etiology of PD.

While NSDA neurons are severely damaged, TIDA neurons are resistant to modest acute doses of MPTP or MPP+ when administered either systemically or centrally (Melamed et al., 1985; Sundstrom et al., 1987; Willis and Donnan, 1987; Mogi et al., 1988). The complete resistance of TIDA neurons to MPTP toxicity is postulated to be due exclusively to extrinsic factors. It is generally believed that decreased MPP+ uptake into these neurons due to lower expression of DAT may underlie the resistance

of TIDA neurons. Others have suggested that differential distribution, reduced bio-activation by astrocytes, or sequestration of MPP+ into vesicles may be responsible for the resistance of TIDA neurons (Hirsch, 1992; Hirsch et al., 1997; Uhl, 1998).

Although the MPTP mouse model mimics several aspects of PD, other aspects of the disease are not replicated in this model. These characteristics include the lack of progressive neurodegeneration after termination of MPTP administration and the lack of Lewy body formation in most regiment dosages of MPTP. Interestingly, people who injected themselves with MPTP have progressive NSDA loss of function (Vingerhoets et al., 1994) suggesting the lack of progressiveness of this model may be due to species differences. The absence of progressive degeneration remains a concern in most other toxin models as well. With its high level of specificity to DA neurons, ease of use, and reproducibility from rodents to primates, MPTP remains the most widely used toxin model of PD.

Rotenone

Rotenone, commonly used as an insecticide and fish poison, can bind to and inhibit the activity of Complex I of the electron transport chain. Rotenone's lipophillic property allows it to easily penetrate the blood-brain barrier and enter all cells in the brain, where it accumulates in mitochondria and binds to nicotinamide adenine dinucleotide (NADH)-ubiquinone reductase (Complex I) and inhibits the transfer of electrons, decreases ATP and increases ROS production from mitochondria (Betarbet et al., 2002).

Chronic treatment of rats with rotenone causes relatively selective loss of NSDA neurons and formation of Lewy body-like inclusions (Betarbet et al., 2000; Thiffault et al., 2000). A loss of UPS function has also been reported in rotenone treated rats, connecting the mitochondrial and UPS pathways in this model of PD. These pathological changes are accompanied by motor dysfunction such as abnormal animal posture and decreased spontaneous movement (Betarbet et al., 2000; Thiffault et al., 2000).

Differential susceptibility amongst DA neuronal populations has also been demonstrated in the chronic rotenone model, with NSDA neurons as the most susceptible, MLDA neurons less susceptible, and no loss of TIDA neurons or axon terminals (Betarbet et al., 2000; Behrouz et al., 2007).

These features make rotenone an attractive model; however several major limitations have hindered the widespread use of this toxin for the study of PD. Although this model has been reproduced by several groups (Betarbet et al., 2000; Behrouz et al., 2007), the NSDA lesions have been consistently reported to be present in only 50% of the animals that received rotenone, the severity of the NSDA lesion was highly variable, and there was non-selective degeneration in other neuronal types not usually affected in PD (Hoglinger et al., 2003b). In addition, the use of rotenone *in vivo* is technically challenging requiring survival surgery and implantation of an osmotic minipump, and while this model has been characterized in rats, there have been no successful reports of its use in mice.

6-OHDA

6-OHDA was used to model PD 40 years ago and was the first neurotoxin to produce selective degeneration of NSDA neurons (Ungerstedt, 1968). 6-OHDA is a hydroxylated analogue of DA (Blum et al., 2001) and selectively damages DA neurons after its entry into cells via DAT and norepinephrine transporter. Once inside the cell, 6-OHDA can accumulate in the cytosol and damage the cell by formation of quinone molecules and ROS (Przedborski and Ischiropoulos, 2005). 6-OHDA can also inhibit mitochondrial Complex I (Betarbet et al., 2002; Schober, 2004). However, it is unclear whether Complex I inhibition is due to a direct binding of 6-OHDA to the enzyme, or indirect effect of ROS damage to mitochondria.

Intracranial 6-OHDA injection produces a selective, potent, rapid and reproducible degeneration of NSDA neurons (Jeon et al., 1995). One advantage of using 6-OHDA is that it can be unilaterally injected in order to kill NSDA neurons on only one side of the brain, allowing the contralateral side of the same brain to be used as a control, as well as creating an asymmetric turning behavior to the contralateral side in response to DA agonist administration that correspond to the extent of the lesion (Ungerstedt, 1968). As such, quantification of the circling provides an *in vivo* index of the NSDA lesion severity.

Disadvantages of this model include the lack of specificity for dopaminergic neurons and the rapid necrotic cell death, which does not mimic the slow, progressive, apoptocic degeneration observed in PD (Luthman et al., 1989; Jeon et al., 1995).

Furthermore, due to its inability to cross the blood brain barrier, 6-OHDA must be stereotaxically injected into the SNpc, medial forebrain bundle or ST to damage NSDA neurons.

Paraquat

The herbicide paraquat has also been used to model PD. Paraquat is structurally similar to MPP+ and enters DA neurons via DAT (Shimizu et al., 2001; Shimizu et al., 2003). Once inside the cell, paraquat can cause ROS formation and damage cells. Systemic paraquat administration leads to the destruction of NSDA neurons (Manning-Bog et al., 2002; McCormack et al., 2005). This loss of neurons is reported to be accompanied by the formation of Lewy body-like inclusions. This model, however, has not been well characterized and it is unclear whether the selectivity, time course and mechanism of cell death mirror that of PD (Thiruchelvam et al., 2000).

Genetic and gene transfer models

In addition to the toxin based models, several genetic models have been developed with null mutations (knock outs; KO), one extra copy of the gene, or point mutations of the genes implicated in PD pathogenesis. These models have provided information about the function of these genes as well as how these functions may relate to PD. Furthermore, combination of genetic and toxin models can mimic gene/environment integrations in PD. Gene transfer models have also been used to

knock down (KD), over express, or express WT or mutated versions of genes in adult animals, which have proven useful in bypassing developmental genetic compensation that occur in KO models (Periquet et al., 2005). These genetic models and their implications in elucidating the etiology of PD are discussed below.

α-Synuclein

α-Synuclein is primarily found in neural tissue and is named for its cellular localization in the pre-synaptic axon terminal regions as well as in nuclei. Several point mutations (A53T, A30P, E46K) as well as duplication and triplication of the gene result in autosomal dominant PD (Polymeropoulos et al., 1997; Kruger et al., 1998; Zarranz et al., 2004). While the functions of α-synuclein are not well understood, it's involvement in several pathways including chaperone function, synaptic plasticity (Abeliovich et al., 2000; Murphy et al., 2000; Cabin et al., 2002), and regulation of reserve vs. readily releasable pool of vesicles (George et al., 1995) have been demonstrated. α-Synuclein is normally unfolded, but under certain conditions such as during oxidative damage it can produce protofibrills and aggregates and is found as a major component of Lewy bodies (Spillantini et al., 1997; Lee and Trojanowski, 2006). Animals with varying expression levels of α-synuclein have been created and have aided in our understanding of the functions of this protein and how it may relate to sporadic PD.

α-Synuclein KO or KD

Several lines of α-synuclein KO mice have been generated that are viable and show little phenotypic abnormalities. While one line of α-synuclein KO mice has a small decrease in ST DA levels and attenuated amphetamine-induced locomotor response (Abeliovich et al., 2000), others have no disruption in locomotor activity following amphetamine and normal ST DA levels (Specht and Schoepfer, 2001; Cabin et al., 2002; Schluter et al., 2003). A small upregulation of β-synuclein was observed in the ST in some but not all KO mice, suggesting possible genetic compensation (Schluter et al., 2003).

α-Synuclein KO mice are resistant to NSDA cell death after either acute or chronic exposure to MPTP (Dauer et al., 2002; Drolet et al., 2004b). The axon terminal regions of NSDA neurons are also partially resistant to MPTP treatment compared to WT littermates (Drolet et al., 2004b). These findings are consistent with the hypothesis that higher levels of α-synuclein are associated with increased risk of PD. While gene transfer approaches have been developed to silence the expression of α-synuclein, this has not been combined with other methods in order to determine if transient knock down of the gene can be protective against various toxins or in PD.

Overexpression of WT or Mutant α-Synuclein

Several α-synuclein transgenic mice have been also described to date, most utilizing a cDNA construct with a heterologous promoter. Overexpression of WT gene recapitulates some features of PD including translocation of α-synuclein into the cell

body from its normal axonal and pre-synaptic location (Kahle et al., 2000; Masliah et al., 2001; Matsuoka et al., 2001; Rockenstein et al., 2002), accumulation of fibrillar accumulation of α-synuclein (Kahle et al., 2000; van der Putten et al., 2000; Masliah et al., 2001), reduced dopaminergic nerve terminal density in the ST and some motor abnormalities (Masliah et al., 2000; van der Putten et al., 2000; Masliah et al., 2001; Fleming et al., 2004). However, loss of NSDA neurons does not occur in α-synuclein overexpressing mice (Matsuoka et al., 2001), making this model less than ideal for studying the etiology of PD.

Mice expressing the human A30P mutant α-synuclein, where an alanine is replaced with a proline, also display mislocation of α-synuclein to the cell body (Kahle et al., 2000; Matsuoka et al., 2001; Lee et al., 2002a; Gomez-Isla et al., 2003) and with the exception of one model, do not display fibrillar inclusions (Kahle et al., 2000). These mice have also been shown to have altered short-term hippocampal synaptic plasticity (Steidl et al., 2003), increased gliosis, and motor dysfunction (Gomez-Isla et al., 2003). However, none of these transgenic lines display NSDA neuron loss, even in aged animals.

Mice expressing the human A53T α-synuclein mutation, where an alanine is replaced with a threonine, seem to be the most affected (Kahle et al., 2000; Matsuoka et al., 2001; Lee et al., 2002b; Gomez-Isla et al., 2003). The A53T transgenics show the abnormal translocation of α-synuclein to the cell bodies (van der Putten et al., 2000; Giasson et al., 2002; Lee et al., 2002b; Gispert et al., 2003) and show drastic and progressive motor abnormalities (van der Putten et al., 2000; Giasson et al., 2002; Lee

et al., 2002b). These mice also have accumulation of non-fibrillar and fibrillar α-synuclein and ubiquitin (van der Putten et al., 2000; Giasson et al., 2002; Lee et al., 2002b). Other deficits observed in these mice include mitochondrial DNA damage including reduced Complex IV activity (Martin et al., 2006). As with other α-synuclein transgenics, even high expression of A53T α-synuclein does not induce NSDA cell death.

Interestingly, mice that express both A53T and A30P mutations do not show exacerbated pathological or motor phenotypes in comparison to the single mutant models described above (Richfield et al., 2002). Transgenic mice expressing the A53T or A30P mutation are more sensitive to lower doses of MPTP (Nieto et al., 2006; Yu et al., 2008). Moreover, treatment with the pesticides paraquat and maneb increases inclusion formation in A53T transgenics (Norris et al., 2007) and worsens behavioral defects without causing cumulative NSDA cell loss (Fernagut et al., 2007). These data suggest increased levels of mutated α-synuclein may render these neurons more susceptible to toxicity. However, both the WT and A53T transgenic mice are resistant to paraquat toxicity (Manning-Bog et al., 2003).

Viral gene delivery in adult animals has provided models that include NSDA neuronal cell loss. Adeno- or lenti-viral delivery of human WT and mutant (A30P or A53T) α-synuclein to the SNpc of rats and primates leads to DA neurons loss as well as neuritic pathology and α-synuclein inclusions (Kirik et al., 2002; Klein et al., 2002; Lo Bianco et al., 2002; Kirik et al., 2003; Lauwers et al., 2003; Yamada et al., 2004). Two rat models also demonstrated drug-induced rotational behavior (Kirik et al., 2002; Lauwers et al., 2003). WT and A53T α-Synuclein delivery into the striatum and the

amygdala of mice using a lentivirus causes changes similar to those seen after nigral delivery, suggesting that the Lewy-like pathology and neurodegeneration are not restricted to DA cells (Lauwers et al., 2003). The fact that this degeneration is not specific to neurons that degenerate in PD suggests the expression levels of α-synuclein may be too high to be physiologically relevant.

LRRK2

Over 20 LRRK2 mutations have been identified, and these are the most common known cause for familial PD (Farrer, 2007) and are clinically indistinguishable from sporadic PD. LRRK2 encodes for a large protein of 2052 amino acids with several functional domains including a kinase, GTPase, WD40, and leucine rich repeat domains. These various domains suggest that the protein has many functions, which include kinase and GTPase activity as well as vesicular trafficking and membrane recycling (Biskup et al., 2007). It is, however, unclear how the normal function of the protein would relate to PD, as the mutations may cause gain of function rather than a disruption in the normal role of the protein.

While LRRK2 KO and transgenic mice have been recently generated, there has only been one report of a transgenic mouse line that has been published in peer-reviewed journals (Melrose et al., 2007). The non-peer reviewed data presented at professional meetings suggests that mice overexpressing WT do not have nigral abnormalities or phenotype. There have been no reports of toxin treatment of LRRK2 transgenic or KO mice.

Parkin

Mutations in parkin are currently recognized as one of the most common causes of early onset Parkinsonism. Parkin aids in the UPS by acting as an E3 ubiquitin ligase. Recent data, however has demonstrated that parkin also has the ability to alter the function of proteins via mono-ubiquination. The ability of parkin to assemble both K48- and K63-linked chains under different conditions is apparently governed by members of the E2s it recruits (Lim et al., 2005).

Parkin KO

Several spontaneous and targeted parkin KO mice have been described (Goldberg et al., 2003; Lorenzetti et al., 2004; Perez et al., 2005). Homozygous 'quaking mice' with spontaneous deletion of parkin and parkin co-regulated gene (PACRG) show locomotor abnormalities, although these motor abnormalities have been attributed to the neighboring locus (Lockhart et al., 2004; Lorenzetti et al., 2004). Interestingly, targeted KO mice deficient in parkin have normal DA neuron numbers and lack major phenotypic or pathological abnormalities. Subtle abnormalities include increased levels of extracellular DA, reduced synaptic excitability in ST (Goldberg et al., 2003) and changes in energy metabolism, synaptic function and protein handling (Periquet et al., 2005) have been observed. Parkin KO mice are not more sensitive to treatment with 6-OHDA, methamphetamine (Perez et al., 2005), or MPTP (Thomas et al., 2007b).

Overexpression of Parkin

Adenoviral delivery of parkin cDNA ameliorates α-synuclein-induced DA neuron loss and consequent motor dysfunction (Yamada et al., 2005). Furthermore, viral delivery of parkin or DJ1 protected against MPTP-induced NSDA cell death (Paterna et al., 2007).

Pink1

Mutations in pink1 cause autosomal recessive PD with a similar phenotype as parkin mutants including early onset and prolonged disease duration. The serine/threonine kinase domain and a mitochondrial localization signal in the pink1 protein make it relatively clear that it is a mitochondrial associated kinase (Cookson et al., 2007).

Pink1 KO mice have impaired mitochondrial respiration in the ST (Gautier et al., 2008), abnormal DA release and synaptic plasticity in ST (Kitada et al., 2007) but no loss of DA neurons or axon terminals. Furthermore, silencing pink1 by conditional RNA interference does not produce DA neuronal loss in mice (Zhou et al., 2007).

Pink1 silencing by RNA interference in SNpc of mice increased neuronal toxicity induced by MPP+ (Haque et al., 2008), suggesting a combination of genetic and environmental factors may contribute to NSDA cell death. Furthermore, WT Pink1, but not the G309D mutant which is linked to familial PD or a kinase-dead mutant, protect neurons against MPTP (Haque et al., 2008), suggesting mutated pink1 loses its protective properties.

DJ1

PD patients with mutations in the DJ-1 gene are phenotypically similar to those with parkin or pink1 mutations, with generally early onset (30-50 yrs) and long disease duration. The normal function of the gene is unknown, but is thought to play a role in maintaining cell survival after exposure to oxidative stress (Bonifati et al., 2003b). DJ1 has been shown to bind to RNA targets (e.g. mitochondrial genes, genes involved in glutathione metabolism and members of the PTEN/PI3K cascade) under normal, but not oxidative stress conditions (van der Brug et al., 2008).

DJ-1 KO mice have been generated and have age-dependent and task-dependent motor deficits. While these behavioral deficits are accompanied by changes in ST DA reuptake rates and elevated DA content, no loss of DA neurons was observed (Chen et al., 2005). DJ-1 KO mice treated with MPTP showed increased DA neuron loss and striatal terminal density compared to WT littermates (Kim et al., 2005). This increased sensitivity is mitigated by adenoviral delivery of DJ-1. Interestingly, WT mice also receiving DJ-1 vector were resistant to MPTP damage.

Overall, genetic models of PD have not been successful at reproducing the NSDA cell loss observed in PD, even with high expression levels of mutated forms of dominant or complete KO of recessive genes. This lack of cell loss may be due to differential aging processes between mice and humans (i.e. an aged mouse may not necessarily represent an old person). Another pitfall may be that these transgenic mice, which are kept in very controlled laboratory environments, are not exposed to

environmental toxins and stressors. Indeed, the few models that have combined genetic and toxin models have been most successful at reproducing most of the pathology seen in PD.

G. Dissertation Objective

The experiments described herein utilize neurochemical, histological, biochemical and molecular biology techniques to test the specific hypotheses listed under the following specific aims with the central overarching hypothesis that discovering factors that protect resistant neurons will lead to development of therapeutic approaches to halt or slow the progressive loss of NSDA neurons in PD.

1. Does the differential susceptibility among NSDA, MLDA and TIDA neurons exist in the chronic MPTP mouse model? **Hypothesis:** NSDA neurons are most susceptible, MLDA neurons are partially susceptible and TIDA neurons are unaffected by chronic treatment with MPTP.
2. Do NSDA, MLDA and TIDA neurons all initially respond to MPTP treatment with loss of DA and the resistant neurons recover? If so, is this recovery dependent on protein synthesis? **Hypothesis:** All DA neuronal populations lose DA in response to a single injection of MPTP, but TIDA neurons depend on synthesis of new proteins that allow them to recover.
3. Are the genomic responses of NSDA and TIDA neurons different when exposed to MPTP? **Hypothesis:** Several genes possibly coding for neuroprotective

proteins are upregulated in TIDA neurons but not NSDA neurons following treatment with MPTP.

Is increased expression of parkin responsible for recovery of TIDA neurons from MPTP-induced DA loss? **Hypothesis:** Parkin is at least partially responsible for allowing TIDA neurons to recover from MPTP-induced DA loss.

Chapter 2. Materials and Methods

A. Animals

All experiments were conducted in male C57Bl/6J mice purchased from Jackson Laboratories (Bar Harbor, MA) unless otherwise indicated. Animals were housed two to four per cage, maintained in a light-controlled (12 h light/dark cycle) and temperature-controlled (22 ± 1°C) room, and provided with food and tap water *ad libitum*. The Michigan State University Institutional Animal Care & Use Committee approved all experiments using live animals (AUF #s 08/08-123-00 and 01/08-004-00.)

Generation of Parkin Knock-Out Mice

Heterozygous parkin knock-out (KO) mice were obtained in breeding pairs from Jackson Laboratories and were bred to yield homozygous parkin KOs, heterozygotes (HT), and homozygous wild type (WT) mice (F1). Heterozygous mice were crossed and the offspring of this cross (F2) and further heterozygous (F2 x F2 and F3 x F3) crosses were performed to expand and maintain the colony for the experiments described herein. Parkin KO and WT littermates were used for experiments after the F6 generation. The viability, fertility and basic biochemical features of these mice have been previously described (Goldberg et al., 2003).

Genotyping

Genotypes for parkin KO mice, HT and WT littermates were confirmed by polymerase chain reaction (PCR) analysis of genomic DNA. Mouse tail snips were dissolved in 600 µl of nuclei lysis buffer with proteinase K (25 mM EDTA, 50 mM NaCl, 0.8 mg/ml proteinase K) at 55°C for 4 h. RNA contamination was removed by

incubation with RNase (0.05 mg/ml) for 30 min. The protein was precipitated with 200µl of protein precipitation solution (4.2 M NaCl, 0.63 M KCL, 10 mM Tris base, pH 8.0) and the mixture was incubated on ice for 5 min, and centrifuged (15,000 x g 10 min) to pellet the protein. The supernatant containing the DNA was placed into a fresh microcentrifuge tube containing 600 µl isopropanol at room temperature. The solution was gently mixed by inversion until white strands of DNA precipitate were visualized. The DNA strands were pelleted by centrifugation at 15,000 x g for 1 min. The supernatant was removed, and the DNA-containing pellet was washed twice with 70% ethanol and resuspended in 100 µl of DNA rehydration solution (10 mM tris-HCL, 1 mM EDTA, pH 7.4).

DNA concentration and purity in each sample was determined by measuring the absorbance using a Nanodrop ND-1000 spectrophotometer (Nanodrop, Wilmington, DE). The concentration of each sample was adjusted to 50 ng/µl with DNA rehydration solution. For the PCR reaction, 5 µl of the DNA sample was added to 20 µl of PCR reaction solution (1 mM PCR buffer, 200 mM dNTP, 2 mM MgCl, 0.18 pm/µl oligo primers, 0.4 u/µl taq polymerase; Invitrogen Carlsbad, CA), mixed and placed into the PCR machine. PCR run parameters were 94°C for 5 min, 30 cycles of 94°C, 65°C, 72°C of 1 min each, followed by 72°C for 5 min. The PCR primers used were CCTACACAGAACTGTGACCTGG, GCAGAATTACAGCAGTTACCTGG, and ATGTTGCCGTCCTCCTTGAAGTCG and have been previously described (Goldberg et al., 2003). Subsequent gel electrophoresis (75 mV, 1 h) on a 1.0% agarose gel was used to separate amplified DNA (10 µl) from each sample. As depicted in **Figure 2-1**, animal

genotype was confirmed for all animals through visualization of the amplified DNA using a UV transilluminator (UVC co., San Gabriel, CA). Only homozygous parkin KO mice or homozygous WT mice were used in the described experiments.

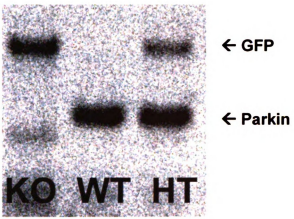

Figure 2-1. Genotyping of wild-type (WT), homozygous parkin knock-out (KO), heterozygous (HT) mice. Ethidium bromide stained 1% agarose gel following electrophoresis of PCR amplification products the Parkin gene and the green fluorescent protein (GFP) construct.

B. Drugs

All drugs were purchased from Sigma-Aldrich (St. Louis, MO). Doses were calculated from the free base of the respective drug. 1-methyl, 4-phenyl, 1,2,3,6-tetrahydropyridine (MPTP), GBR-12909 (GBR), and cycloheximide were dissolved in 0.9% sterile saline. Dipropylsulfamoyl-benzoic acid (probenecid) was dissolved in 0.1 N NaOH and the pH was adjusted to 7.4 using hydrochloric acid (HCL).

Chronic MPTP

Male 8–12 week old mice received injections of either vehicle (10 ml/kg; s.c.) or MPTP (20 mg/kg; s.c.) every 3.5 days, for a total of 10 injections over 5 weeks. Probenecid (250 mg/kg; i.p.) was administered 1 h before each MPTP injection to increase the plasma and central nervous system half-life of MPTP and MPP^+, respectively (Petroske et al., 2001). Probenecid alone does not have an effect on NSDA neurons (Lau et al., 1990). All experiments using MPTP were performed using previously published safety guidelines (Przedborski et al., 2001). Animals treated with MPTP were kept in a separate room and conditions (e.g. light/dark cycle, temperature, etc) were monitored and were similar between the rooms. Experiments were terminated 3 weeks after the last MPTP injection.

Single Injection MPTP

Male 8-12 week old mice received a single injection of either vehicle (10 ml/kg; s.c.) or MPTP (20 mg/kg; s.c.). For the time course study, the experiment was terminated 4, 8, 16 or 32 h after the MPTP injection. Saline treated animals were killed 8 h after injection and were used as zero time controls.

Cycloheximide

Male 8-12 week old mice were treated with 4 injections of vehicle (10 ml/kg; i.p.) or the protein synthesis inhibitor cycloheximide (120 mg/kg; i.p.) every 2 h, with the first cycloheximide injection 15 min prior to a single injection of MPTP.

GBR-12909

Male 8-12 week old mice were treated with an injection of either vehicle (10 ml/kg; i.p.) or the DAT blocker GBR (10 mg/kg; i.p.) 30 min prior to a single injection of MPTP. The experiment was terminated 4 h after MPTP treatment.

Lentiviral shRNA Against Mouse Parkin

Transduction-ready lentiviral particles expressing 1 of 3 parkin shRNA sequences under the control of a U6 promoter were purchased (10^6 TU/ml; Sigma) and were stereotaxically injected bilaterally into the ARC. A non-target shRNA sequence was used as control. Animals were treated with a single injection of MPTP 3-5 weeks after injection with the lentivirus and killed 16 h later. **Table 2-1** lists the shRNA sequences for parkin and non-target shRNA.

Lentiviral Particles	Catalog #	Sequence
Park2 shRNA	TRCN0000041143	CCGGCGTTTCATTATCTGCAACTTTCTCGA GAAAGTTGCAGATAATGAAACGTTTTTG
Park2 shRNA	TRCN0000041145	CCGGCGGAGGATGTATGCACATGAACTC GAGTTCATGTGCATACATCCTCCGTTTTTG
Park2 shRNA	TRCN0000041147	CCGGGACCTGGAACAACAGAGTATTCTC GAGAATACTCTGTTGTTCCAGGTCTTTTTG
Non-target shRNA	SHC002	CCGGCAACAAGATGAAGAGCACCAACTC GAGTTGGTGCTCTTCATCTTGTTGTTTTT

Table 2-1. Sequence and catalog information for parkin and non-target shRNA lentiviral particles purchased from Sigma. 500 nl of each virus containing parkin shRNA was bilaterally injected into the ARC of mice in order to knock down expression of parkin. Non-target shRNA lentivirus was bilaterally injected into ARC of mice that were used as controls.

C. Tissue Preparation

At the appropriate time following drug administration, mice were killed by decapitation and their brains were rapidly removed from the skull and placed on a glass dissecting stage over ice. Under a dissecting microscope, ME was collected. For the chronic MPTP experiments, the brain was bisected along the mid-sagittal axis and half of the brain was drop-fixed for immunohistochemical analysis, while the other half was frozen rapidly on dry ice for neurochemical and Western blot analyses.

In all other experiments, the whole brain was quickly frozen on dry ice after the dissection of ME. Consecutive coronal sections (500 μm) were prepared from the frozen brains using a cryostat set at -10 °C (CTD-Model Harris, International Equipment Co., Needham, MA). Sections were collected through the rostro-caudal extent of the brain beginning approximately 2.5 mM anterior to Bregma (Paxinos and Watson 1986), thaw-mounted onto glass slides, and immediately refrozen. The regions of interest were dissected using a modification of the method described by Palkovits (Palkovits, 1973, 1978). **Figures 2-2** and **2-3** demonstrate the location where tissue samples were obtained. Using a dissecting microscope, bilateral tissue punches from NA and ST were removed using 22- and 18-gauge round punch tools, respectively (**Figure 2-2**). One punch from ARC was obtained using an 18-gauge oval punch tool, and bilateral tissue punches from VTA and SNpc were collected using 18-guage round and oval punch tools, respectively (**Figure 2-3**). These tissue samples were used for neurochemical, Western blotting or RNA analysis and were processed according to the appropriate protocols described below.

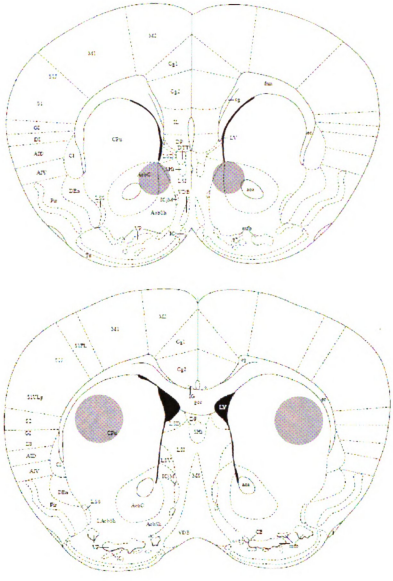

Figure 2-2. Diagrams of coronal brain sections illustrating the location of micropunches used to dissect NA and ST. The brown circles indicate the location of the Palkovits micropunch. NA was dissected (top) from a 500 µM section 1.42 mm rostral to Bregma and ST was microdissected (bottom) from a 500 µM section 0.98 mm rostral to Bregma (Paxinos and Watson, 1986).

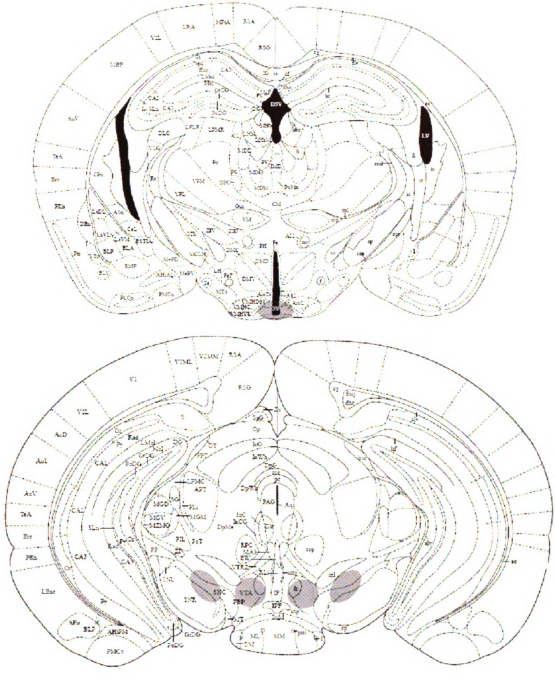

Figure 2-3. Diagrams of coronal brain sections illustrating the sections used to dissect ARC (top), VTA and SNPC (bottom). The brown circles indicate the location of the Palkovits micropunch. ARC was dissected (top) from a 500 µM section 1.94 mm caudal to Bregma and SNpc and VTA were microdissected (bottom) from a 500 µM section 3.08 mm caudal to Bregma (Paxinos and Watson, 1986).

D. Neurochemical Analyses

Microdissected brain regions were placed into cold tissue buffer (0.1M phosphate-citrate buffer pH 2.5) for neurochemical analyses and stored frozen at -20 C. On the day of assay, samples were thawed and sonicated with 3 one second bursts (Heat Systems Ultrasonics, Plainview NY). Protein was pelleted by centrifugation at 16,000 x g (Beckman Coulter Microfuge, Palo Alto, CA) for 1 min. The supernatant containing the neurochemicals of interest was removed using a 100 µl Hamilton syringe, placed into a fresh tube, and used for high pressure liquid chromatography with electrochemical detection (HPLC-EC) analysis.

The pellet from the initial centrifugation containing the protein was resuspended and dissolved in 100 µl of 1 N sodium hydroxide (NaOH) by sonication. The Lowry method was used to determine protein concentrations of the tissue pellets (Lowry et al., 1951). Protein samples were transferred from the microcentrifuge tube to 12 x 75 glass culture tubes. Standard solutions with 6.25, 12.5, 25 or 50 µg of bovine serum albumin (BSA; Sigma) were dissolved in 100 µl of 1 N NaOH and transferred to individual 12 x 75 culture tubes. To each tube, 1.0 ml of Reagent A (0.2 M sodium carbonate, 40 mM cupric sulfate, 70 mM sodium potassium tartrate) was added and mixed by vortexing. The mixture was incubated at room temperature for 10 min, after which 100 µl of Reagent B (Folin reagent diluted 1:2 with dH_2O) was added to the culture tubes. The mixture was vortexed and incubated at room temperature for 30 min. Protein concentrations were quantified by comparing the absorbance of each

sample, read at 700 nm on a Gilford spectrophotometer (Gilford Instruments, Oberlin, OH), to the absorbance of the known protein standards assayed concurrently.

The content of the neurochemicals norepinephrine (NE), DA, DOPAC, HVA, 5-HT, and 5-HIAA were determined with HPLC-EC using a Waters 515 HPLC pump (Waters Corporation, Milford, MA) with a flow rate of 1.0 ml/min and an ESA Coulochem 5100A electrochemical detector with an oxidation potential of +0.4V. Neurochemical standards containing 1.0 ng of the desired neurochemicals and experimental samples were injected onto a C18 reverse phase analytical column (Bioanalytical Systems, West Lafayette, IN). The HPLC-EC mobile phase (0.5M sodium phosphate, 0.03M citrate, 0.1 mM EDTA, sodium octylsulfate, 15-20% methanol, pH 2.5) was adjusted by altering the concentrations of sodium octylsulfate and methanol to optimize neurotransmitter peak resolution.

Neurotransmitter content was quantified by comparing the peak heights of each sample to the peak heights of standards. To correct for differences in sample size the neurotransmitter content was normalized to the amount of protein in each sample and expressed as a concentration in ng/mg protein.

E. Western Blot Analyses

Protein Extraction

Microdissected brain samples were placed into cold homogenization buffer (320 mM sucrose, 5.0 mM HEPES, with Complete Mini Protease Inhibitor Cocktail Tablets, Roche Diagnostics, Mannheim, Germany, pH 7.4), homogenized by sonication

and centrifuged (1000 x g 10 min). The supernatants containing total cytoplasmic protein were removed and placed into fresh microcentrifuge tubes. The samples were assayed for protein content using the bicinchoninic acid protein method (BCA, Sigma). Ten µl of loading buffer (250 mM Tris base, pH 6.8, 20% glycerol, 5% SDS, 0.01% bromophenol blue) was added to the appropriate amount of sample and the mixture was vortexed, boiled at 95°C for 10 min to denature the proteins, and cooled to 4°C.

Electrophoresis/Transfer Conditions

Two 15% polyacrylamide gels (Bio-Rad, Hercules, CA, USA) were placed in the inner chamber of a mini-protean-3 electrophoresis cell (BioRad). The inner chamber was filled with Laemli running buffer (25 mM Tris base, 192 mM glycine, 0.1% SDS) and samples were loaded onto the gel. The volume was adjusted to load 20 µg of protein for each sample. A protein ladder of known molecular weights was also loaded onto each gel. Proteins were separated by applying a 100 mV current for approximately 1 h. Proteins were transferred to 0.45 µm nitrocellulose membranes (Fisher Scientific, Pittsburgh, PA, USA) by electrophoresis at 30 mV for 12 h.

Protein Detection and Quantification

Nitrocellulose membranes containing the proteins of interest were washed in 25 mM Tris buffered saline (TBS; 4 x 5 min), incubated in blocking buffer (Li Cor, Inc., Lincoln, NE, USA) for 1 h and reacted with primary antibody in blocking buffer overnight at 4 C. The source, dilution, and name of the company supplying each primary antibody used in the experiments are listed in **Table 2-2**.

Antibody	Dilution	Source	Company
TH	1:2000	Rabbit	Chemicon,
Parkin	1:1000	Rabbit	Cell Signaling
βIII tubulin	1:5000	Mouse	Chemicon
GAPDH	1:10000	Mouse	Chemicon

Table 2-2. Description of primary antibodies used in the experiments in this dissertation. Antibody characterization is based on the standard dilution used for Western blotting, animal used to generate the antibody (Source) and the company the antibody was purchased from (Company). TH= tyrosine hydroxylase, GAPDH = glyceraldehyde 3-phosphate dehydrogenase.

Nitrocellulose membranes were washed with TBS (3 x 5 min) and incubated with the appropriate IRDye 800-conjugated goat anti-rabbit (Rockland, Gilbertsville, PA, USA) or Alexa Fluor 680-labeled goat anti-mouse (Molecular Probes, Eugene, OR, USA) secondary antibodies (1:15,000 dilution in blocking buffer) for 1 h at room temperature. Membranes were washed in TBS (4 x 5 min) and bound antibodies were visualized with the Odyssey infrared imager (Li-Cor Biosciences, Lincoln NE). The density of each band was quantified by measuring the infrared absorbance using the Odyssey infrared imager and Odyssey software (version 3.0, Li-Cor Biosciences).

Relative density was obtained by normalizing the band density of the protein of interest to that of the control protein used to account for variations in loading of samples onto the gel. GAPDH was used as the control protein and its detection and visualization was linear. **Figure 2-4** demonstrates that expression levels of GAPDH are similar amongst the compared regions (ARC and SNpc) and do not change with treatment (Control and MPTP-treated). Each nitrocellulose membrane contained representative samples from all experimental conditions.

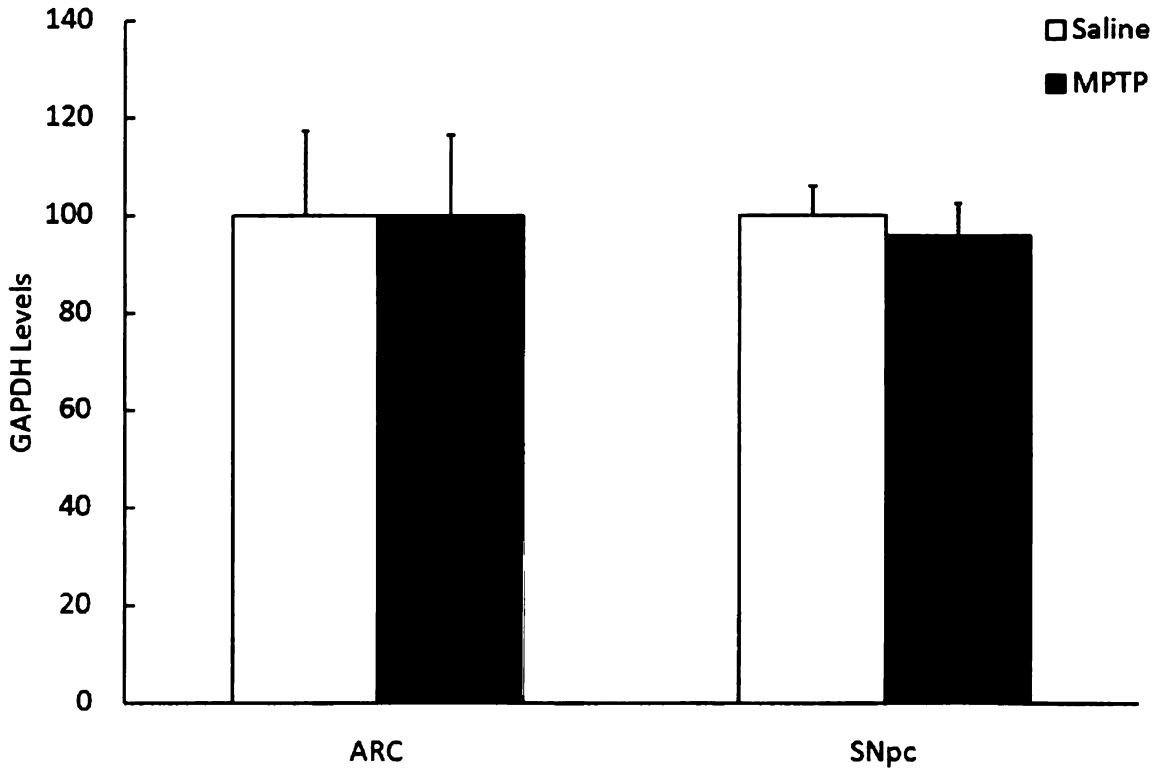

Figure 2-4: GAPDH levels in ARC and SNpc of control and MPTP treated mice. Mice were treated with a single injection of MPTP (20 mg/kg; s.c.) or saline (10 ml/kg; s.c.) and killed 8 h later. ARC and SNpc were microdissected and expression of GAPDH protein was determined using Western blot analysis.

F. Immunohistochemistry

Immunohistochemical staining was performed to visualize and count the number of TH immunoreactive cells in ARC, SNpc and VTA. Following removal from the skull, brains were dissected along the mid-sagittal axis and drop-fixed in 4% paraformaldehyde for 7 days and cryoprotected in 20% sucrose. Coronal sections (60 µm) through the hypothalamus and midbrain (beginning at Bregma –2.5 through –3.7mm; Franklin and Paxinos, 1996) were prepared with a -19°C cryostat using Multiblock™ processing (Neuroscience Associates, Knoxville, TN). Immunohistochemistry was performed on free floating sections using a primary rabbit anti-TH antibody (Chemicon, Temecula, CA), followed by a biotin-conjugated, goat anti-rabbit secondary antibody (Jackson Immunoresearch, West Grove, PA). Bound peroxidase was visualized with 0.05% 3-3'-diaminobenzidine tetrahydrochloride with 0.01% hydrogen peroxide using an ABC Elite kit (Vector Laboratories, Burlingame, VT). Alternate sections were stained with Nissl to determine if decreases in TH-immunoreactive (IR) cell counts corresponded with loss of neurons.

G. Unbiased Stereological cell counting

Using the StereoInvestigator software (version 4.03, MicroBrightfield, Inc. 2000), sections were viewed on the screen at low magnification (4X), ARC, SNpc and VTA were delineated from the rostral through the caudal extent of each nuclei. The first plane was a randomly chosen section within 180 µm of the most rostral plane of

the ARC, SNpc or VTA as determined by a mouse atlas (Franklin and Paxinos, 1996). The delineated sections were evenly spaced apart (240 μm).

TH-IR and Nissl stained neurons were counted using the Optical Fractionator method, an unbiased stereological technique that employs a systematic, random strategy in which cells in a defined region are sampled. This method results in a quantifiable estimate of the total population of cells within a given region (West et al., 1991; Schmitz, 1997; Schmitz and Hof, 2000, 2005). The 3-dimentional probe used to sample the entire ARC, SNpc or VTA yields counts that are independent of cell shape and size or conformational changes in the tissue. A counting frame (60x60μm) was utilized and a fraction of the delineated cells were sampled. Cell counts were made through 78% (14 μm) of the total depth of the tissue (18 μm) allowing for a 2 μm guard zone at the top and bottom of each section. TH-IR and Nissl stained cells were identified with a consistent distribution over the depth of the counting frame, thus confirming sufficient reagent penetration throughout the thickness of the tissue slice.

TH-IR or Nissl counts were performed using a 60X objective and cells were counted only if the top of the nucleus came into focus within the virtual counting frame and within the delineated region of interest. Neurons were counted only if they showed TH-IR or Nissl staining within the cell body. For Nissl stained sections, cells that were larger in size (>15 μm in diameter) and had a defined nucleus were counted as neurons. The smaller cells (<15 μm in diameter) that were amorphous in shape and did not have a well-defined nucleus were considered glia and were not counted. For estimates of number of neurons per half brain, the section periodicity was 4 as every

fourth section was selected for analysis (West et al., 1991, Schmitz, 1997). The coefficient of error for each estimate was calculated and was less than 0.1 (Gundersen, m=1) (Gundersen and Jensen, 1987).

H. Rapid Immunofluorescent staining

A rapid staining technique was used to visualize TH-IR neurons so that they could be selectively dissected by laser capture microscopy for RNA analysis. Coronal 10 μm frozen sections through the midbrain and hypothalamus were obtained in a cryostat set at -10°C, mounted on slides and kept frozen on dry ice. Sections were rapidly fixed in ice-cold 70% acetone for 1 min and rinsed with PBS with 0.1% Triton X-100 (PBS-Tx). Sections were incubated for 2 min in mouse anti-TH antibody (1:40; Zymed, CA. Cat # 32-2100) containing 400 U/ml of RNasin RNase inhibitor (Promega, WI. Cat # N2115), rinsed twice with TBS-Tx and incubated for 2 min in Alexa Fluor 488 goat anti mouse secondary antibody (invitrogen, CA. Cat # A-11001). Slides were rinsed in PBS, dipped in cresyl violet for Nissl stain, and dehydrated in a 70%, 95% and 100% ethanol gradient followed by xylene. Sections were dried in a fume hood and laser capture microscopy (LCM) was performed within 2 h after staining. **Figure 2-5** demonstrates the time course of RNA integrity using this rapid staining technique. This time course demonstrates that leaving section in staining solution for 10 min yields optimal staining without compromising RNA quality.

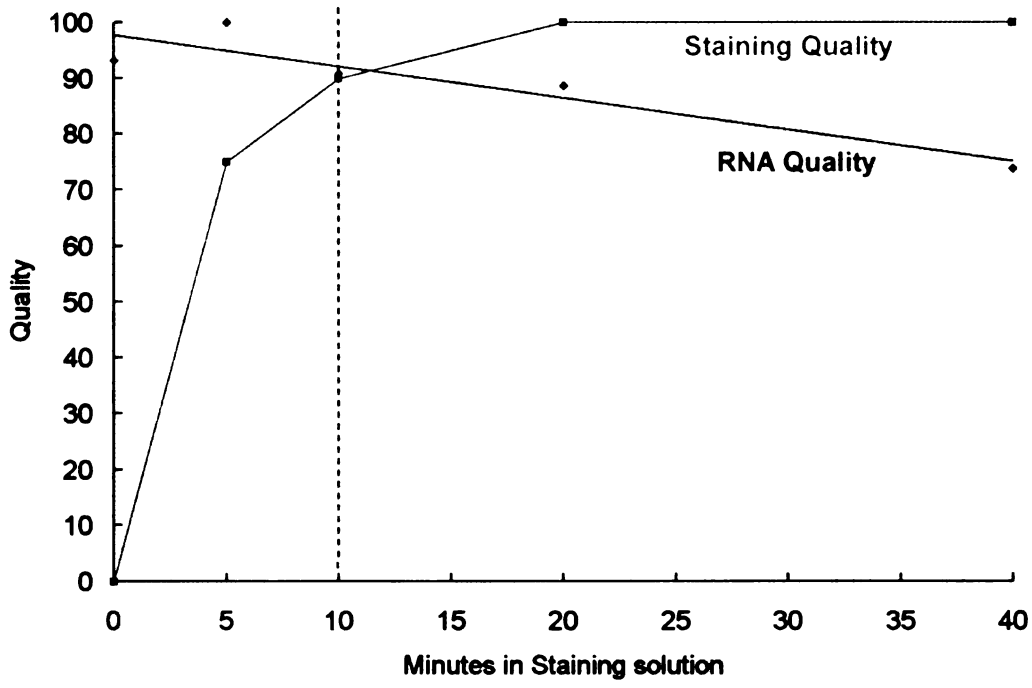

Figure 2-5: Time course of RNA degradation during rapid immunofluorescent staining for TH. Coronal 10 µm frozen sections through the midbrain and hypothalamus were rapidly fixed in ice-cold 70% acetone for 1 min and rinsed with PBS with 0.1% Triton X-100 (PBS-Tx). Sections were incubated in primary and secondary antibodies for a total of 5, 10, 20 or 40 min. The sections were viewed under a microscope to determine staining quality. RNA was extracted from these sections and its quality was determined using a picochip (BioAnalyzer, AGILENT Technologies).

I. Laser Capture Microscopy (LCM)

In LCM, a near-infrared power laser microbeam melts a thermoplastic ethyl vinyl acetate membrane which overlays the tissue of interest. The melted membrane sticks to the selected cells, which can be lifted and secured in a microfuge tube containing the RNA extraction solution. The surrounding tissue remains unchanged. This technique, coupled with rapid immunofluorescent TH staining allows for dissection of DA neurons without major contamination from other neuronal types and glia.

LCM was performed using a PixCell II Laser Microdissection System (Arcturus Engineering Incorporated; Mountain View, California, USA). The following parameters were used for dissection of TH-immunoflurescent cells: spot size = 7 μm; power = 45–85 mW; and duration = 750–1100 μs (Greene et al., 2005). After rapid staining, slides containing the sections were cleaned using a prep strip and placed onto the microscope. Capsure HS caps (Arcturus) were loaded onto the LCM and after focusing on the appropriate sections an HS cap was positioned on top of the tissue so that the cells of interest were in the center of the cap. TH-positive cells were collected from specific brain regions as depicted in **Figure 2-6**. The same HS cap was used to collect 300-500 cells from each brain region per animal. The cap was placed into the alignment tray and 10 μl of extraction buffer was placed into the fill port of the ExtractSure™. The tube was placed into the port, covered with a heating block (preheated to 42 C) and incubated for 30 min at 42 C to extract the cells. The cells were collected at the bottom of the tube by centrifugation for 2 min at 800 x g and were stored frozen at -80 C until RNA extraction.

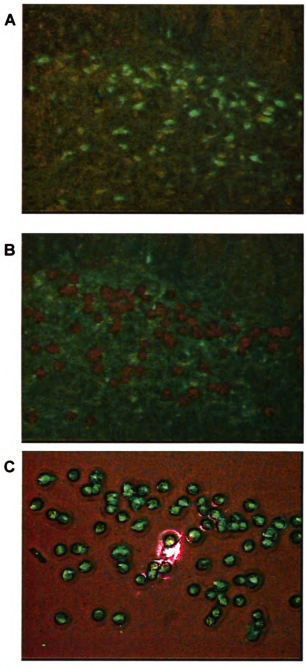

Figure 2-6: Laser capture of tyrosine hydroxylase-immunoreactive (TH-IR) cells of SNpc. A. TH-IR cells before capture, B. section after cells were captured, C. Cap with captured cells.

J. RNA isolation from LCM samples

Total RNA was extracted using the Extractsure adapter and PicoPure Isolation Kit (Arcturus) with DNase digestion (Qiagen RNase-free DNase Set). RNA purification columns were incubated with 250 µl of preconditioning buffer for 5 min at room temperature. The cell extract was mixed with an equal volume (50 µl) of 70% ethanol and loaded onto the purification column. The mixture was centrifuged at 100 x g for 2 min to facilitate nucleic acid binding to the column, followed by centrifugation at 16,000 x g for 30 sec to remove flowthrough. The column containing the nucleic acids was washed using Wash Buffer 1. DNase mix solution (5 µl DNase and 35 µl DNase buffer) was added to the column and incubated at room temperature for 15 min to remove column bound DNA. After DNase treatment, the column was washed with Wash Buffers 1 and 2 and transferred to a new 1.5 ml tube. The column was incubated at room temperature with 12 µl of Elution Buffer and the eluted RNA was collected at the bottom of the tube by centrifuging at 1000 x g for 1 min.

RNA quality was determined for representative samples from each group using a Bioanalyzer Picochip (Agilent Technologies, Santa Clara, CA). The Bioanalyzer uses a microfluidics-based platform to analyze RNA. The individual samples were examined, a pseudo gel image is created and bands were sized and quantified. Total extracted RNA was stored frozen at -80 C.

K. RNA Amplification

Total RNA was amplified for each sample using the MessageAmp II aRNA Amplification Kit (Ambion, Austin, TX). First strand cDNA was synthesized using an oligo-dT primer containing the T7 promoter. E-coli DNA polymerase and RNase H were employed to simultaneously degrade the RNA and synthesize second strand cDNA. cDNA was purified to remove RNA, primers, enzymes and salts. *In vitro* transcription was performed to create multiple copies of aRNA. aRNA was purified to remove unincorporated nucleotides, salts, enzymes and inorganic phosphate. A second round of synthesis was performed as described above.

For the *in vitro* transcription step, biotin labeled UTP (provided with the kit) was used to synthesize biotin labeled aRNA. The samples yielded approximately 400 ng of aRNA after the first round of amplification and approximately 100 μg of aRNA after the second round of amplification. RNA quality was assessed by absorbance readings on a Nanodrop (Thermo Scientific, Wilmington, DE) and RNA was determined to be of good purity (260:280 ratio of around 2.0-2.2). RNA integrity was also determined by running the samples on an agrose gel as well as on a Bioanalyzer picochip. A smear of aRNA bands that extended from 200 – 1000 bases was observed. The RNA was centered on 600 bases, which is consistent with other published records of aRNA after 2 rounds of amplifications (Van Gelder et al., 1990).

L. Microarray Hybridization and Initial Analysis

In order to determine the differences in mRNA levels in ARC and SNpc of control and MPTP treated animals, amplified RNA from each sample was hybridized to an Affymetrix Mouse Genome 430 2.0 Array (Affymetrix, Santa Clara, CA). Microarray and preliminary analyses were performed by the Michigan State University genomics facility according to the methods specified by Affymetrix. Hybridization solution contained 0.05 μg/μl fragmented cRNA, 50pM control oligonucleotide B2, eukaryotic hybridization controls (bioB, bioC, bioD, 1,5, 5; 25 pM, respectively; Affymetrix, Santa Clara, CA), 0.1 mg/ml of herring sperm DNA, 0.5 mg/ml acetylated bovine serum albumin (BSA; Sigma, St. Louis, MO) in hybridization buffer (100 mM MES, 1M NaCl, 20 mM EDTA, 0.01% Tween20). Before being applied to the microarray the hybridization solution was heated to 95 C, cooled to 45 C, and clarified by centrifugation. Hybridization was carried out at 45°C in a hybridization oven for 16 h.

Subsequent washing and staining of the arrays was performed using the GeneChip fluidics station protocol EukGE-WS2. The GeneChip probe arrays were washed 10X at 25°C with Non Stringent Wash Buffer (0.9 M NaCl, 0.06 M NaH_2PO_4, 6 mM EDTA, 0.01% Tween20). The second wash consisted of 4 cycles of 15 mixes per cycle with Stringent Wash Buffer (100 mM MES; 2-N-Morpholinoethanesulfonic acid, Sigma, St. Louis, MO), 0.1 M NaCl, 0.01% Tween-20) at 50 C. The arrays were stained for 10 min in streptavidin-phycoerythrin (SAPE) solution (10 μg/ml SAPE; Molecular Probes, Eugene, OR), 2 μg/μl acetylated BSA (Sigma, St.Lous, MO) in 100 mM MES; 1M NaCl, 0.05% Tween20 at 25 C. The post stain wash consisted of 10 cycles at 25 C in the

fluidics station using the non-stringent solution. The probe arrays were treated for 10 min in antibody solution (2 µg/µl acetylated BSA, 0.1 µg/µl normal goat IgG; Sigma), 3 µg/ml goat-anti-streptavidin, biotinylated antibody (Vector Laboratories, Burlingame, CA); in 100 mM MES; 1M NaCl, 0.05% Tween20) at 25 C. The final wash consisted of 15 cycles of 4 mixes per cycle at 30°C in fluidics station using the non-stringent solution. Following washing and staining, probe arrays were scanned twice at 3 µm resolution using the GeneChip System confocal scanner (Hewlett-Packard, Santa Clara, CA). Visualization of all arrays is included in **Figures 2-7** and **2-8**. Data analysis was performed using Microarray Suite Version 5.0 software and Data Mining Tool Version 2.0 software (Affymetrix).

The Affymetrix arrays also contain probes to control for RNA degradation. These probes target different parts of mRNA from 3' to 5' ends. RNA degradation usually occurs starting from the 3' or 5' ends so RNA degradation can be visualized if probes that target the ends of mRNA bind fewer signals than the probes that target the center of the mRNA. **Figure 2-9** demonstrates that there was equal hybridization to different parts of the probes, indicating good quality RNA with little to no degradation.

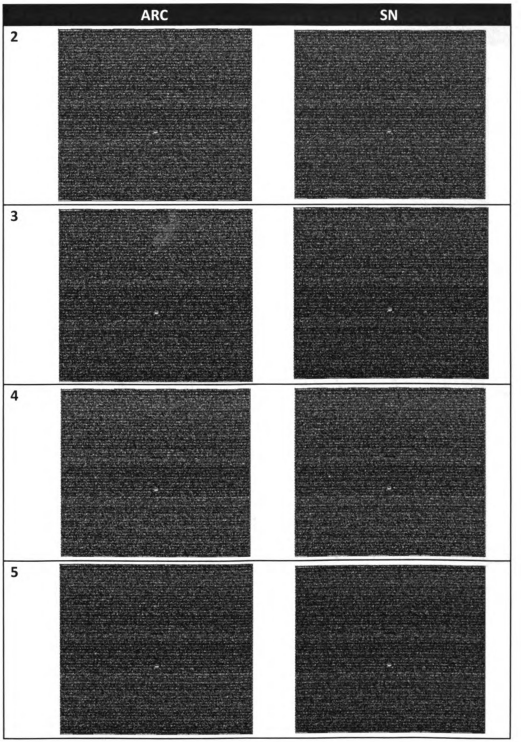

Figure 2-7: Visualization of individual arrays hybridized with amplified mRNA from ARC and SNpc of control animals. All arrays are visualized in order to rule out any artifacts. These pictures show an apparently random ditribution of biotin labled probes. The black bar and white block at the center of each array also demonsrtate proper hybridization.

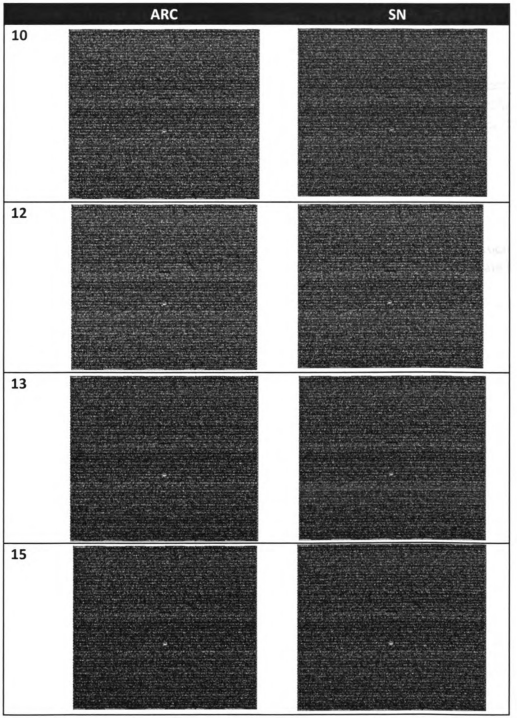

Figure 2-8: Visualization of individual arrays hybridized with amplified mRNA from ARC and SNpc of MPTP treated animals. All arrays are visualized in order to rule out any artifacts. These pictures show an apparently random ditribution of biotin labled probes. The black bar and white block at the center of each array also demonsrtate proper hybridization.

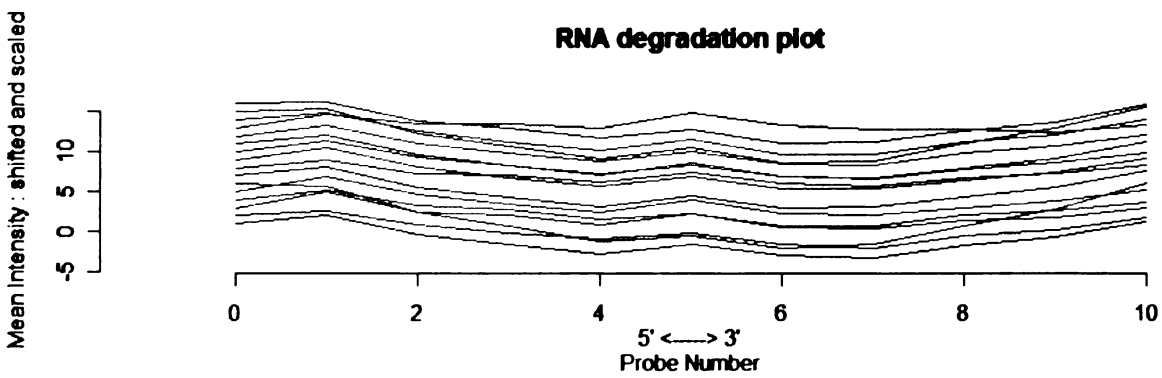

Figure 2-9: Assessment of RNA quality in individual arrays. Each line represents expression of genes hybridized to the 3' through 5' ends of RNA from each array. Flat lines demonstrate lack of RNA degradation in the samples.

M. Microarray Data Analysis and Statistics

Normalization, Background Correction and Data Summarization

Normalization, background correction and data summarization were performed in collaboration with Dr. Marianne Huebner at Michigan State University. GeneChip Robust Multi-array Analysis (GCRMA) was used for normalization of the gene expression data to correct for background noise. Starting with the probe-level data from a set of Gene Chips, the perfect-match (PM) values were background-corrected, normalized and summarized resulting in a set of expression measures.

Background correction is arguably the most crucial step for probe level processing. The non-linear background correction used in GCRMA is done in a per-chip basis. The GCRMA function summarizes probe intensities, adjusts for optical effect and non-specific binding, background-corrects, and generates an expression set all in one step. With GCRMA, the base types (A,T,G or C) at each position (1-25) along the probe determine the affinity of each probe. The parameters of the position specific base contributions to the probe affinity are estimated in an NSB experiment in which only NSB but no gene-specific binding is expected.

Normalization is necessary so that multiple chips can be compared to each other during analysis. The GCRMA normalization procedure is aimed at making the distributions identical across arrays and is quantile, which results in very sharp normalizations. All the arrays are used and no chip is discarded on the basis of extreme value considerations. Once the probe-level values were background-corrected and normalized, they were summarized into expression measures so that the result is a

single expression measure per probe-set, per chip. **Figure 2-10** depicts mean expression levels for each array before and after normalization using GCRMA.

The summarization used is motivated by the assumption that observed log-transformed PM values follow a linear additive model containing a probe affinity effect, a gene specific effect (expression level) and an error term. For GCRMA, the probe affinity effects are assumed to sum to zero, and the gene effect (expression level) is estimated using median polishing. Median polishing is a robust model fitting technique, which protects against outlier probes

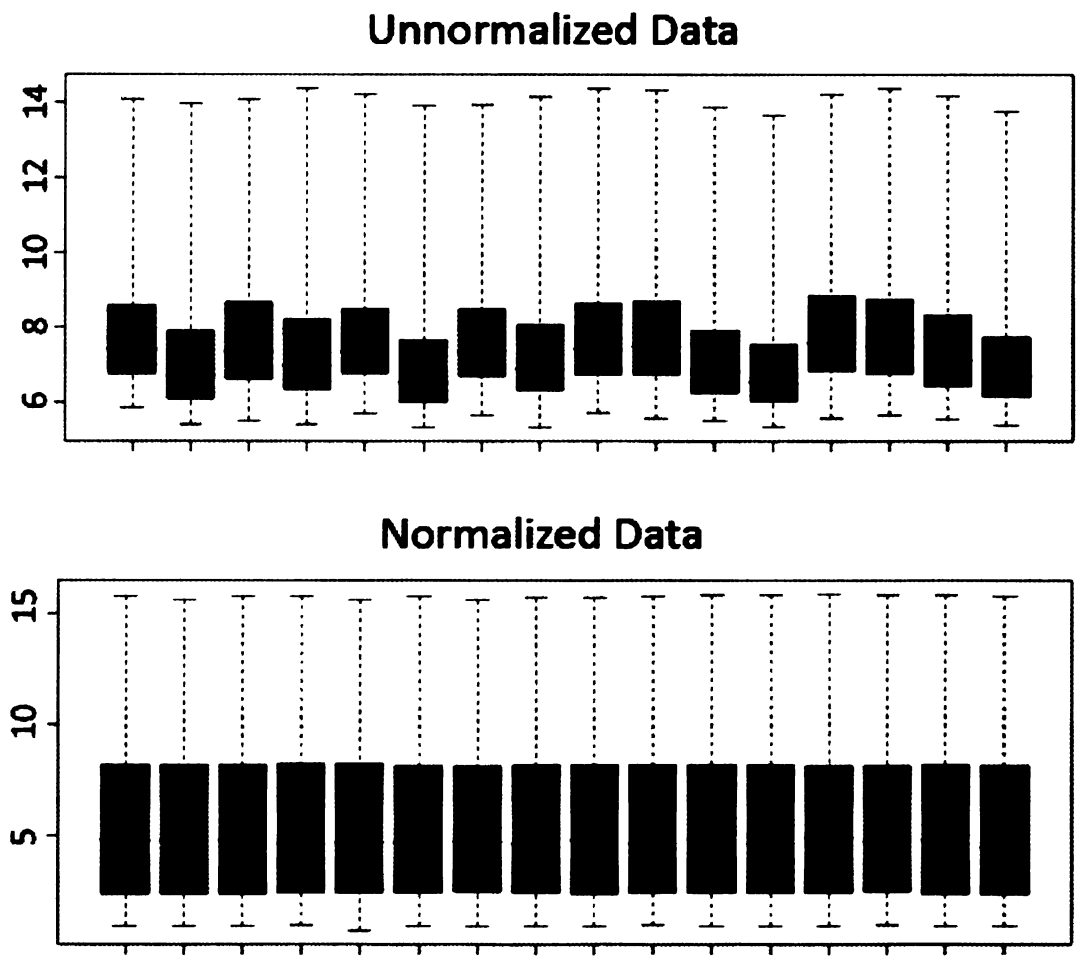

Figure 2-10: Mean expression levels (Y-axis) of all genes in each array (X-axis) before (top) and after (bottom) normalization with GCRMA. The GCRMA method is used to ensure all arrays have similar distribution.

The Use of Updated Annotation Files

Most of the commonly used Affymetrix platforms were designed before the respective genomes were fully sequenced. Therefore, these platforms have many probes that were designed after consensus sequences of clusters of Expressed Sequence Tags were established. In the original Affymetrix definitions many probe sets often map to the same gene (i.e. target different transcript isoforms) and some integrative microarray studies use *ad hoc* heuristics such as the average or maximum to integrate these values into a single expression estimate. To solve these problems, updated probe set definitions have been generated by re-annotating the existing probes on Affymetrix platforms to better reflect the transcript information and gene annotations currently available (Wang et al., 2002; Dai et al., 2005). These pioneering studies have shown that updated probe set definitions will affect approximately 20–30% of all probe sets, thus affecting a large portion of the gene estimates. As a consequence, the genes identified as differentially expressed using the original and updated probe set definition only show 50% overlap (Dai et al., 2005). Updated probe set definitions that map probes to transcript annotations, such as ensEMBL transcripts, Refseq and Entrez GeneID are now available (http://brainarray.mbni.med.umich.edu/Brainarray/default.asp) and were integrated into bioconductor packages such as GCRMA. Updated probe annotations have also been shown to improve the cross-platform reproducibility of microarray experiments (Wang et al., 2002; Dai et al., 2005).

Statistical Analyses

To identify differentially expressed genes a linear model was fit for all genes based on a experimental design comparing two brain regions and two treatments. These estimators exhibit robust behavior even for a small number of arrays and allow for incomplete data arising from spot filtering or spot quality weights. For each gene a moderated t-statistic is calculated using posterior standard deviations to extract those with maximally differential expression (Smyth 2004). This analysis was carried out using the R software (v.2.6.1, http://cran.r-project.org/) and the linear model package Limma available in the R Bioconductor software suite (http://www.bioconductor.org).

P-values were adjusted for multiple testing following Storey's approach of controlling the false discovery rate (FDR). FDR of a set of predictions is the expected percent of false predictions in the set of predictions (Benjamini and Hochberg 1995, Storey 2002).

Cluster Analysis

After obtaining model-based expression values, high-level hierarchical clustering analysis was performed (Eisen et al. 1998) in dCHIP (Li and Wong 2001) to identify groups of genes with similar expression patterns. The clustering algorithm of genes was as follows: the distance between two genes is defined as 1 - r where r is the Pearson correlation coefficient between the standardized expression values of the two genes across the samples used. Two genes with the closest distance are first merged into a super-gene and connected by branches with length representing their distance, and are excluded for subsequent merging events. The expression value of the newly

formed super-gene is the average of standardized expression values of the two genes (centroid-linkage) across samples. The next pair of genes (super-genes) with the smallest distance is chosen to merge and the process is repeated n – 1 times to merge all the n genes. These standardization and clustering methods follow previously documented methods (Eisen et al., 1998; Golub et al., 1999). Centroid linkage can produce branch inversion when the distance between two clusters is smaller than the height of either cluster, dChip truncates the distance to be the larger of the two heights, which prevents the branch inversion in visualization, but the further distance computation is still based on the averaged profile. **Figure 2-11** depicts an example of hierarchial clustering performed in dChip.

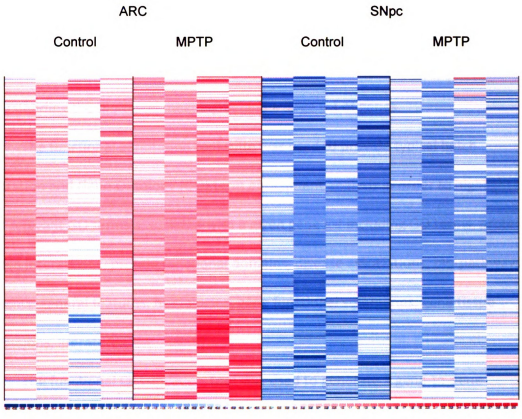

Figure 2-11. Cluster analysis of genes significantly higher in ARC than SNpc after treatment with a single injection of MPTP. Male mice (n=8/group) were treated with a single injection of MPTP (20 mg/kg; s.c.) or saline (10 ml/kg; s.c.) and killed 8 h later. Amplified mRNA from 300-500 laser-captured TH immunofluorescent cells from ARC and SN of each animal were hybridized to an Affymetrix mouse 430 2.0 chip. Data was normalized and cluster analysis was performed to find genes with similar expression patterns. Each row represents a gene and each column represents a treatment group. Genes close to each other have high similarity in their standardized expression values across the 4 treatment groups. On the bottom of the clustering picture is the color scale: the red color represents expression level higher than mean of a gene across all samples, the white color represents mean expression, and the blue color represents expression lower than the mean. Since the expression level for each gene is standardized to have mean 0 and standard deviation 1, the standardized expression values most likely fall within the range of -3 to 3. dChip uses pure white to represent 0, pure red to represent 3 or higher, and pure blue to represent –3 or lower (Golub et al., 1999).

Pathway Analysis with DAVID

The Database for Annotation, Visualization and Integrated Discovery (DAVID) provides a comprehensive set of functional annotation and classification tools for understanding the biological meaning behind a large list of genes.

The functional annotation tool suite was used to provide typical batch annotation and Gene Ontology (GO) term enrichment analysis in order to highlight the most relevant GO terms associated with a given gene list including GO terms, protein-protein interactions, protein functional domains, disease associations, bio-pathways, sequence general features, homologies, gene functional summaries, gene tissue expressions, literatures, etc.

The functional Classification Tool was used to generate a gene-to-gene similarity matrix based upon shared functional annotation using over 75,000 terms from 14 functional annotation sources. The clustering algorithms classified highly functionally related genes into groups, which provided a rapid means to organize large lists of genes to help unravel the biological content determined by the microarray.

Analysis of Candidate KEGG Pathways

KEGG (Kyoto Encyclopedia of Genes and Genomes) PATHWAY™ is a collection of manually drawn pathway maps representing current knowledge of molecular interaction and reaction networks. Candidate KEGG pathways relating to PD were determined and a list of all genes involved in each pathway was generated. These genes were located in our microarray database in order to determine general changes in candidate pathways.

N. RNA isolation from microdissected tissue punches

Total RNA from microdissected tissue was extracted using the MELT total nucleic acid isolation with DNase digestion (Ambion, Austin, TX). Tissue was digested with 100 ul of MELT digestion mastermix (4 µl of MELT cocktail and 96 µl of MELT buffer) and vigorous vortexing for 10 min. The lysate was centrifuged at 10,000 x g for 3 min and transferred to a 96 well plate containing 210 µl of binding bead master mix (10 µl binding beads, 100 µl binding solution and 100 µl of 80% ethanol). The mixture was incubated at room temperature for 2 min, which allowed the RNA to bind to the magnetic binding beads. The beads containing the RNA were magnetically captured during a 3 min incubation and the supernatant was discarded. The beads were washed with 300 µl of Wash Solutions 1 and 2 and were air dried for 5 min at room temperature. DNA contamination was removed from the beads by incubation with 100 µl of TURBO DNase digestion master mix (2 µl TURBO DNase 2U/µl and 98 µl of DNase buffer) for 10 min at room temperature with gentle agitation. The beads were captured again using the magnetic stand and washed twice with 300 µl of Wash Solution 2. The beads containing the RNA were air dried for 5 min and RNA was eluted by incubation in 20 µl of elution buffer. The beads were captured using the magnetic stand and the purified RNA was collected and placed into a fresh elution tube. RNA concentration was determined using a Nanodrop and quality was assessed using a picochip (BioAnalyzer, AGILENT Technologies).

O. Reverse transcription

RNA was incubated with oligo(dT) primers and dNTP mix at 65 C for 5 min to promote primer annealing. The mixture was incubated with 0.1M DTT, a reverse transcriptase (Superscript II, Invitrogen) and RNase inhibitor (RNaseIn, Ambion) at 42 C for 1 h to allow for reverse transcription. The mixture was heated to 70 C for 15 min in order to destroy the reverse transcriptase. And resulting cDNA was stored in -80 C until use with real time PCR.

P. Real Time Quantitative PCR

Primers were identified using Primer3 and synthesized by the macromolecular and structural facility (Michigan State University, East Lansing, MI) and are listed in **Table 2-3**. All primer sets were tested to ensure a single product as assessed by 2% agarose gel electrophoresis and melt-curve analysis. GAPDH was used as the reference gene and **Figure 2-12** demonstrates that GAPDH mRNA levels were similar across regions (ARC and SNpc) and did not change with treatment (Control vs. MPTP). No template reactions were used as negative controls.

Total RNA was reverse transcribed as described above and used as template in a 10 µl PCR reaction with 400 nM primers, and SYBR Green PCR Master Mix (Applied Biosystems). Forty cycles of PCR were performed and samples from 8 mice were run in triplicate. Threshold cycle (C_t) were determined and compared to C_t for the reference genes.

Gene Name	Forward Primer	Reverse Primer
GAPDH	AACTTTGGCATTGTGGAAGG	ACACATTGGGGGTAGGAACA
Parkin	TTCTGACACCAGCATCTTGC	CTT TCCTCCGTGGTCTCTG
UCH-L1	CCCTTGGTTTGCAGCTTTAG	ACACACAGGAGGGAAAGTGC
Pink1	GAGGGCGTGCACCATCTG	AGGATGTTGTCGGACTTGAGA TC
SNCA	AGGCAGCTGGAAAGACAAAA	CAGCTCCCTCCACTGTCTTC
LRRK2	GATGTCAGTACGCCCCTGAT	CTGCCAGCGCTATGATGTTA
DJ-1	GCTTCCAAAAGAGCTCTGGTCA	GCTCTAGTCTTTGAGAACAAGC

Table 2-3. Forward and reverse primers used for real time PCR analysis. All primers were identified using the Primer3 software and used for real time PCR amplification.

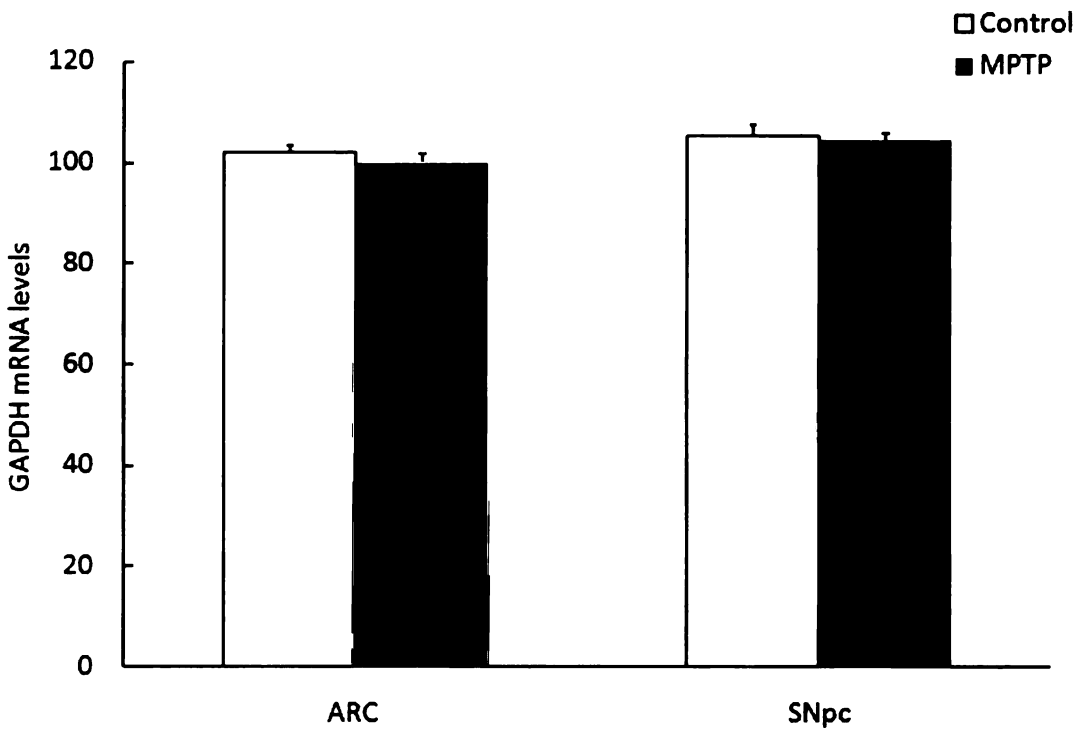

Figure 2-12. GAPDH mRNA levels in ARC and SNpc of control and MPTP-treated mice. Mice were treated with a single injection of MPTP (20 mg/kg; s.c.) or saline (10 ml/kg; s.c.) and killed by decapitation 8 h later. ARC and SNpc were microdissected and expression of GAPDH mRNA was determined using real time PCR.

Fold change between regions was determined using the $\Delta\Delta C_t$ method, which compares the C_t values of the samples of interest with a control or calibrator such as a non-treated sample or RNA from normal tissue. The C_t values of both the calibrator and the samples of interest are normalized to an appropriate endogenous housekeeping gene. The $\Delta\Delta C_t$ method is also known as comparative C_t method where $\Delta\Delta C_t = \Delta C_{t,sample} - \Delta C_{t,reference}$. Here, $\Delta C_{t,sample}$ is the C_t value for any sample normalized to the endogenous housekeeping gene and $\Delta C_{t,reference}$ is the C_t value for the calibrator also normalized to the endogenous housekeeping gene. For the $\Delta\Delta C_t$ calculation to be valid the amplification efficiencies of the target and the endogenous reference must be approximately equal. PCR efficiencies of all primer sets were therefore tested to ensure similarity to the GAPDH primer (85–100%). This was established by determining how ΔC_t varies with template dilution. If the plot of cDNA dilution versus delta C_t is close to zero, it implies that the efficiencies of the target and housekeeping genes are very similar. Significant differences between SNPC and ARC were determined using a one-way ANOVA with one correlated measure ($p \leq 0.05$).

Q. Stereotaxic Lentiviral Injections

Mice were injected bilaterally into the ARC with 500 nl of lentiviral particles expressing a Parkin or non-target shRNA. Stereological injections (David Kopf Instruments, Tujunga, CA) were performed under ketamine : xylazine anesthesia (330 mg/kg : 20 mg/kg ; s.c.). A Hamilton Syringe (Hamilton, Reno, NV) with a 30 gauge blunt-tip needle was used to inject 500 nl of viral particles into the left and right ARC. Each mouse received bilateral injections of lentiviral vectors at a 10 degree angle in the following coordinates from Bregma: rostro-caudal -1.85, latero-medial 1.25 and -1.25, and dorso-ventral -5.8 from the skull surface. The virus was injected over a period of 5 min at a rate of approximately 100nl/min, and the needle was left in place for an additional 10 min. **Figure 2-13** depicts the location of the bilateral stereotaxic injections. **Figure 2-14** shows ARC injected with a lentivitus encoding for Green Fluorescent Protein demonstrating successful transfection of ARC neurons with the lentivirus. **Figure 2-15** demonstrates a lack of microglial activation and inflammatory response with IBA1 staining. Activated microglia become round and detract processes when they become activated under inflammatory conditions. This is not the case in lentivirus treated animals as microglia retain their normal inactive morphology.

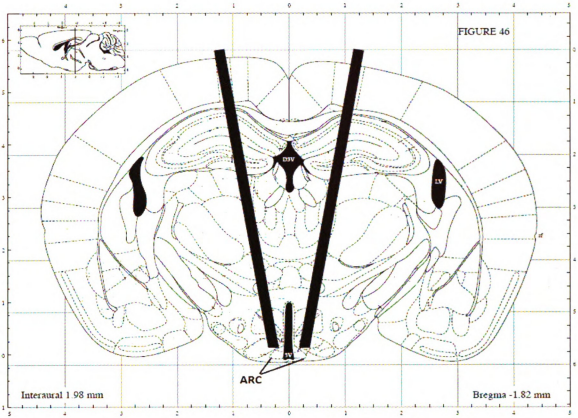

Figure 2-13. Bilateral stereotaxic injection of lentiviral vectors into ARC of control and MPTP-treated mice. Animals received bilateral stereotaxic injections of Parkin shRNA or non-target shRNA lentivirus into the ARC. Three to five weeks later, animals were injected with either MPTP (20 mg/kg; s.c.) or saline (10 ml/kg; s.c.) and killed by decapitation 16 h later. Concentrations of parkin mRNA were determined in ARC of all animals.

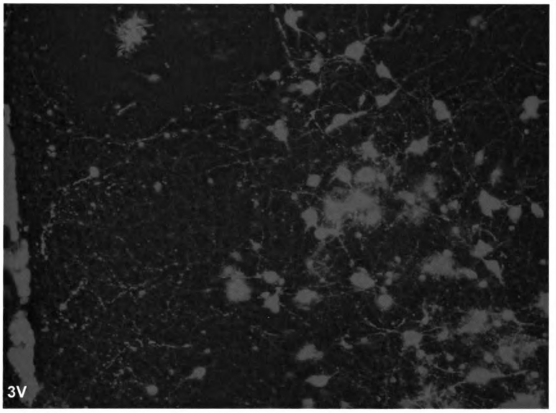

Figure 2-14. Stereotaxic injection of lentiviral vector encoding for green fluorescent protein (GFP) into ARC of mice. Animals received stereotaxic injections of GFP lentivirus into the ARC. Three weeks later, animals were killed and brains were viewed under the microscope for presence of GFP protein.

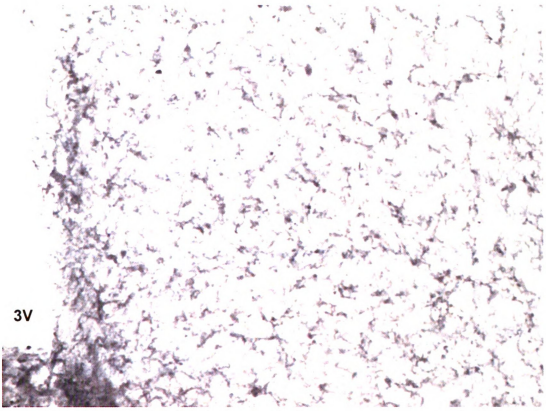

Figure 2-15. IBA1 staining for brain sections from mice that received stereotaxic injection of lentiviral vector encoding for green fluorescent protein into ARC. 3V = third ventricle.

P. Statistical Analysis

Power analyses were conducted to determine optimal sample size required for each experiment. One-way analysis of variance (ANOVA) tests were used to detect statistical significance between two or more groups on a single independent variable. Two-way ANOVA's were used to detect statistical significance between two or more groups when there were two independent variables in the study. Repeated measures ANOVA was used when comparing brain regions within the same animal. A p value of less than or equal to 0.05 was considered statistically significant. If the ANOVA revealed an interaction of statistical significance Tukey's test was used for multiple comparisons among groups.

Chapter 3: Characterization of Differential Susceptibility of TIDA, NSDA and MLDA Neurons in the Chronic MPTP Mouse Model

A. Introduction:

It has been hypothesized that abnormal DA metabolism underlies the selective degeneration of NSDA neurons in PD (Lotharius and O'Malley, 2000; Lotharius and Brundin, 2002; Vergo et al., 2007). However, it is unclear why all DA neuronal populations are not affected to the same extent in PD; with TIDA neurons remaining fully intact while NSDA neurons are severely damaged and MLDA neurons less severely affected (Braak et al., 1996; Braak and Braak, 2000; Braak et al., 2006a; Braak et al., 2006b). In order to study this differential susceptibility, an animal model for PD that mimics this differential susceptibility needs to be established. The ideal model should recapitulate the severe retrograde NSDA neuronal loss, less severe retrograde damage to MLDA neurons and complete preservation of TIDA neurons.

The MPTP mouse model has been commonly used to study PD and its strengths over other toxin-based models have been highlighted in Chapter 1 (Introduction, Section F. Animal Models of PD). Chronic treatment with the toxin mimics the long duration of retrograde degenerative insult to NSDA neurons observed in PD (Petroske et al., 2001; Drolet et al., 2004b). The differential susceptibility of DA neuronal populations, particularly of TIDA neurons, has not been well characterized in the chronic MPTP mouse model. If differential susceptibility exists amongst these DA neuronal populations in response to MPTP administration, then this model can be

utilized to discern the intrinsic properties of these neuronal populations and identify protective and/or deleterious factors that underlie their responsiveness to neurotoxin insult.

B. Hypothesis

This experiment tests the hypothesis that TIDA, NSDA and MLDA neurons are differentially susceptible in the chronic MPTP mouse model, with TIDA neurons being fully spared while NSDA neurons are severely damaged and MLDA neurons are moderately affected.

C. Experimental Design

The chronic MPTP mouse model consisted of injections of MPTP (20 mg/kg; s.c.) or saline (10 ml/kg; s.c.) every 3.5 days for 5 consecutive weeks for a total of 10 injections (**Figure 3-1**). All animals also received probenecid (250 mg/kg; i.p.) with each MPTP/saline injection. Probenecid prevents the transport of organic acids across epithelial membranes and therefore blocks the clearance of MPP+ from the brain (Petroske et al., 2001). Animals were decapitated 3 weeks after the last MPTP injection and the brains were quickly removed. Following the dissection of ME from the ventral surface of the brain, the brain was bisected along the mid-sagittal axis. One half of the brain was frozen for neurochemical analysis and the other half was drop-fixed in 4% paraformaldehyde for immunohistochemical analysis. The details of animal use, drug administration, tissue preparation, neurochemical and immunohistochemical analyses were described previously in Chapter 2 (Methods, Sections. A-F).

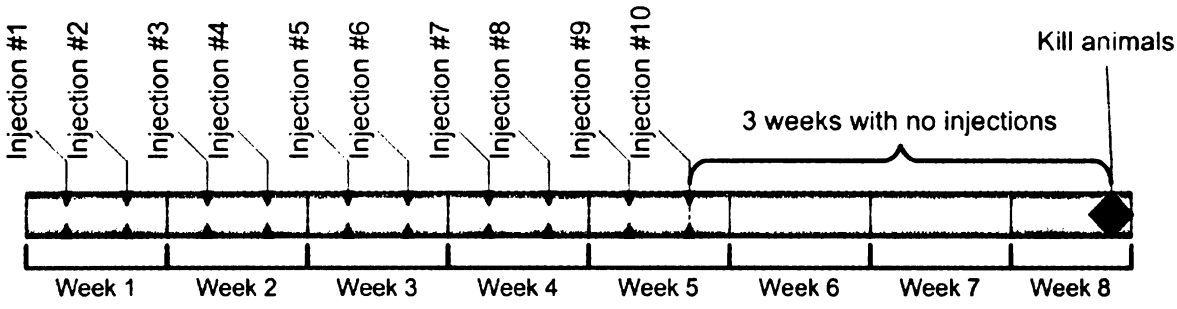

Figure 3-1. Time course of chronic MPTP administration. Male C57bl mice (n=8/group) were injected with either MPTP (20 mg/kg; s.c.) or saline (10 ml/kg; s.c.) every 3.5 days for 5 consecutive weeks. Animals also received probenecid (250 mg/kg; i.p.) with each MPTP or saline injection. Mice were killed by decapitation 3 weeks after the last MPTP or saline injection.

The primary endpoints used to determine axon terminal loss were DA concentrations in ME, ST and NA; the axon terminal regions of TIDA, NSDA and MLDA neurons, respectively. DA concentrations in these regions primarily reflect vesicular, rather than cytoplasmic or extracellular DA (Carlsson, 1975b; Carboni et al., 1992; Di Chiara et al., 1996), as DA not sequestered inside vesicles is rapidly metabolized. DA concentrations reflect the ability of neurons to synthesize, and store neurotransmitter in their axon terminals. Because axon terminals have had 3 weeks to recover from MPTP, DA concentrations in this model reflect the relative density of the remaining functional axon terminals. The concentrations of DA after chronic MPTP are consistent with other indices of axon terminal integrity such as TH and VMAT-2 levels (Wilson et al., 1996; Kilbourn et al., 2000; Reveron et al., 2002). Cytosolic DA is converted in the presynaptic terminals to DOPAC and therefore the concentrations of DOPAC and ratio of DOPAC to DA are commonly used to estimate the activity of central DA neurons (Westerink and Spaan, 1982; Lookingland et al., 1987b; DeMaria et al., 1999).

The endpoint used to determine DA cell body loss was unbiased stereological cell counts of TH positive neurons in the ARC, SNpc and VTA; the cell body regions of TIDA, NSDA and MLDA neurons, respectively. In order to confirm that lower TH positive cell counts were due to loss of neurons rather than down regulation of TH, stereological cell counts were also performed on alternating Nissl stained cells in ARC, SNpc and VTA. For Nissl stained sections, morphological criteria were used to differentiate between neurons and glia. These morphological criteria are described in detail in Chapter 2 (Methods, Section G. Unbiased Stereological Cell Counting).

In order to demonstrate that the dose of MPTP used in these experiments did not damage non-DA neuronal populations, concentrations of NE, as well as 5-HT and its metabolite 5-hydroxyindoleacetic acid (5-HIAA) were determined.

Endpoint	Method	Measure of	Indicates
DA	HPLC-EC	Vesicular DA	DA axon terminal density
DOPAC	HPLC-EC	DA metabolite	DA metabolism
DOPAC/DA	HPLC-EC	Relative amount of DA metabolized to that stored in axon terminals	DA neuron activity
NE	HPLC-EC	Vesicular NE	NE axon terminal density
5-HT	HPLC-EC	Vesicular 5-HT	5-HT axon terminal density
5-HIAA	HPLC-EC	5-HT metabolite	5-HT metabolism
TH cell counts	Stereology	Cells expressing TH	DA cell number
Nissl cell counts	Stereology	All cells	Total neuron number

Table 3-1. The experimental endpoints used for indices of neuronal function in the chronic MPTP mouse model. DA = dopamine, DOPAC = 3,4-dihydroxyphenylacetic acid, NE = norepinephrine, 5-HT = serotonin, 5-HIAA = 5-hydroxyindoleacetic acid, TH = tyrosine hydroxylase and HPLC-EC = high performance liquid chromatography coupled with electrochemical detection.

D. Results

Following chronic treatment with MPTP the concentrations of DA were measured in ME, ST and NA. MPTP did not alter DA concentrations in ME while inducing significant DA loss (~70%) in ST. MLDA neurons were less severely, but significantly, affected with only ~45% DA loss in NA (**Figure 3-2**). Similarly, following treatment with MPTP, DOPAC concentrations remained unchanged in ME, but decreased significantly in ST, and NA (**Figure 3-3**). The ratio of DOPAC/DA was determined and was unchanged in ME, but significantly increased in ST (**Figure 3-4**). There was no change in DOPAC/DA ratio in NA following MPTP administration, suggesting either that these neurons do not have D2 receptor mediated compensatory activation or that insufficient amounts of MLDA axon terminals have been lost following this dose of MPTP to produce compensatory activation unlesioned MLDA neurons.

Following chronic treatment with MPTP, concentrations of NE (**Table 3-2**), as well as 5-HT and its metabolite 5-HIAA (**Table 3-3**) were determined in ME, ST and NA. Concentrations of NE, 5-HT and 5-HIAA were unchanged in all regions examined, demonstrating that MPTP is specific to DA neuronal populations.

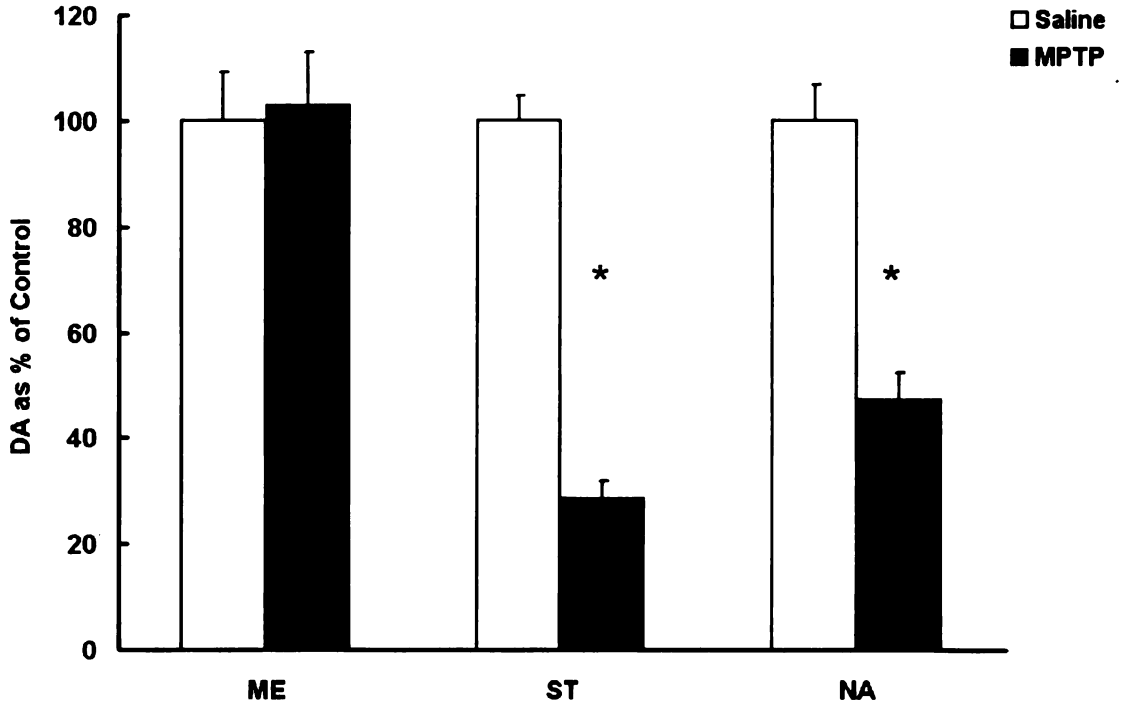

Figure 3-2. The effects of chronic MPTP administration on DA levels in median eminence (ME), striatum (ST) and nucleus accumbens (NA). Male mice (n=8/group) were treated with either MPTP (20mg/kg; s.c.) or saline (10 ml/kg; s.c.) every 3.5 days for 5 consecutive weeks. All animals received an injection of probenecid (250 mg/kg; i.p.) with each MPTP or saline injection. DA levels are presented as % of saline treated. Actual DA concentrations (ng/mg protein) are as follows in saline treated mice: ME: 147±13.5, ST: 140±6.5 and NA: 43±2.9 , and MPTP treated mice: ME: 151±15, ST: 40±5 and NA: 20.4±2.2. Columns represent means of groups and vertical bars represent +1.0 standard error of the mean. (*) indicates values for MPTP treated mice that were significantly different ($p < 0.05$) from saline treated controls.

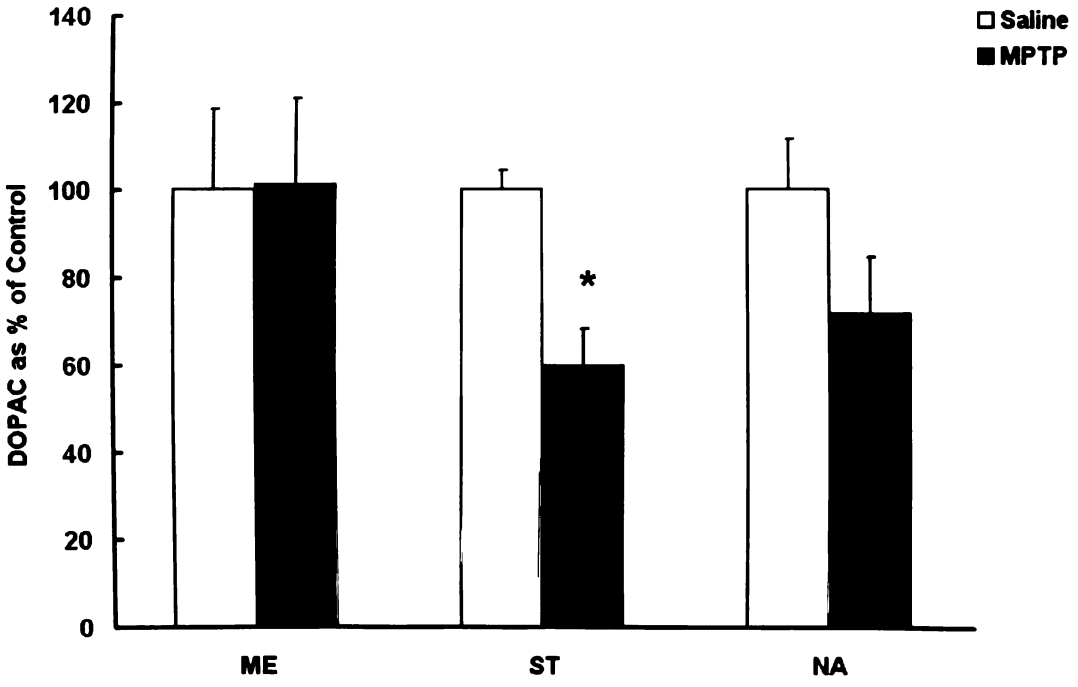

Figure 3-3. The effects of chronic MPTP administration on DOPAC levels in median eminence (ME), striatum (ST) and nucleus accumbens (NA). Male mice (n=8/group) were treated with either MPTP (20mg/kg; s.c.) or saline (10 ml/kg; s.c.) every 3.5 days for 5 consecutive weeks. All animals received an injection of probenecid (250 mg/kg; i.p.) with each MPTP or saline injection. DOPAC levels are presented as % of saline treated. Actual DOPAC concentrations (ng/mg protein) are as follows in saline treated mice: ME: 3.6±0.7, ST: 11.0±0.5 and NA: 7.2±0.8, and MPTP treated mice: ME: 3.6±0.7, ST: 6.6±0.9, and NA: 5.1±0.9. Columns represent means of groups and vertical bars represent +1.0 standard error of the mean. (*) indicates values in MPTP treated mice that were significantly different ($p < 0.05$) from saline treated controls.

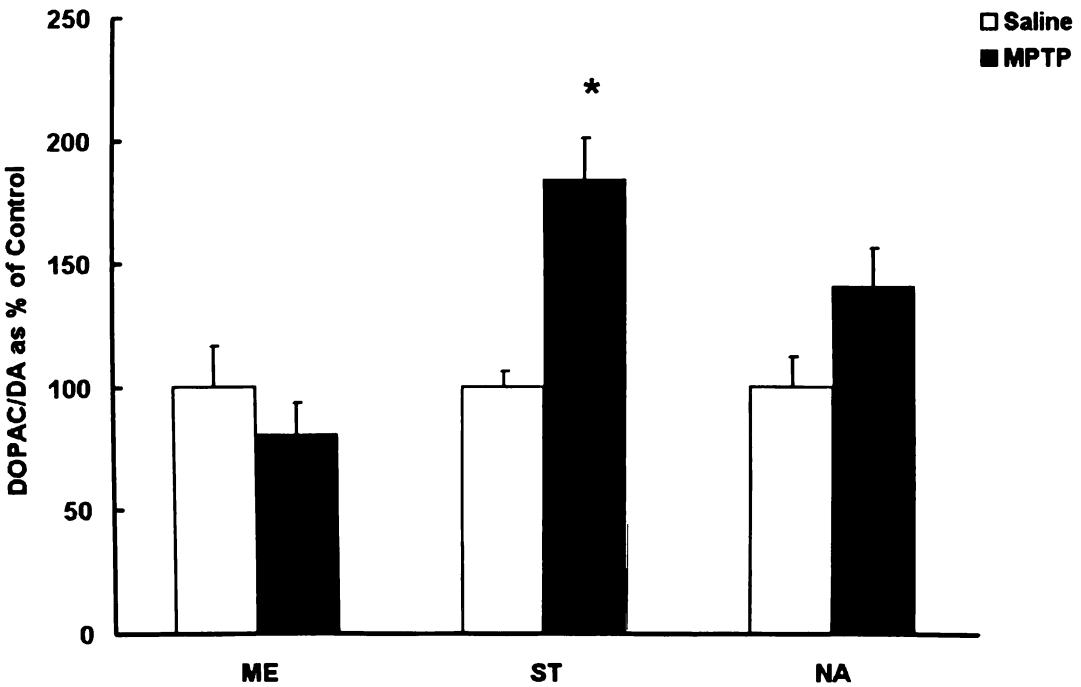

Figure 3-4. The effects of chronic MPTP administration on the ratio of DOPAC/DA in median eminence (ME), striatum (ST) and nucleus accumbens (NA). Male mice (n=8/group) were treated with either MPTP (20mg/kg; s.c.) or saline (10 ml/kg; s.c.) every 3.5 days for 5 consecutive weeks. All animals received an injection of probenecid (250 mg/kg; i.p.) with each MPTP or saline injection. Ratios are presented as % of saline treated controls. Actual DOPAC/DA ratios are as follows in saline treated mice: ME: 0.03±0.01, ST: 0.06±0.01 and NA: 0.14±0.01, and MPTP treated mice: ME:0.02±0.01, ST: 0.11±0.01, and NA: 0.19±0.02. Columns represent means of groups and vertical bars represent +1.0 standard error of the mean. (*) indicates values for MPTP treated mice that were significantly different ($p < 0.05$) from saline treated controls.

Concentrations of NE (ng/mg protein)			
	ME	ST	NA
Control	17.9 ± 1.6	ND	3.0 ± 0.5
MPTP	18.5 ± 4.2	ND	3.9 ± 0.3

Table 3-2. Norepinephrine (NE) concentrations in median eminence (ME), striatum (ST) and nucleus accumbens (NA) of control and MPTP treated mice. Male mice (n=8/group) were treated with either MPTP (20mg/kg; s.c.) or saline (10 ml/kg; s.c.) every 3.5 days for 5 consecutive weeks. All animals received an injection of probenecid (250 mg/kg; i.p.) with each MPTP or saline injection. ND = Not Detectable.

A. Concentrations of 5-HT (ng/mg protein)			
	ME	**ST**	**NA**
Control	8.5 ± 1.2	7.5 ± 1.3	13.2 ± 1.5
MPTP	8.0 ± 1.4	7.4 ± 0.6	15.2 ± 2.7

B. Concentrations of 5-HIAA (ng/mg protein)			
	ME	**ST**	**NA**
Control	16.2 ± 1.3	7.0 ± 2.1	3.4 ± 0.5
MPTP	13.4 ± 4.1	7.5 ± 1.1	4.1 ± 0.6

Table 3-3. Serotonin (5-HT; A) and 5-hydroxyindoleacetic acid (5-HIAA; B) concentrations in median eminence (ME), striatum (ST) and nucleus accumbens (NA) of control and MPTP treated mice. Male mice (n=8/group) were treated with either MPTP (20mg/kg; s.c.) or saline (10 ml/kg; s.c.) every 3.5 days for 5 consecutive weeks. All animals received an injection of probenecid (250 mg/kg; i.p.) with each MPTP or saline injection.

Paraformaldehyde fixed brains were sectioned at 60 μM and every third section was dual-stained for TH (**Figure 3-5**) and Nissl. Unbiased stereological cell counts were performed on TH immunoreactive cells in ARC, SNpc and VTA, the cell body regions of TIDA, NSDA and MLDA neurons, respectively. MPTP administration failed to induce loss of TH cells in ARC or VTA, while treatment with this neurotoxin caused a significant decrease in TH immunoreactive neurons in SNpc (**Figure 3-6**). Alternate sections were stained for Nissl and the number of neurons were counted to determine if lower TH immunoreactive cell counts in SNPC were due to cell loss rather than down regulation of TH. There was a similar ~30% loss of Nissl stained neurons in SNPC following treatment with MPTP (**Figure 3-7**) .

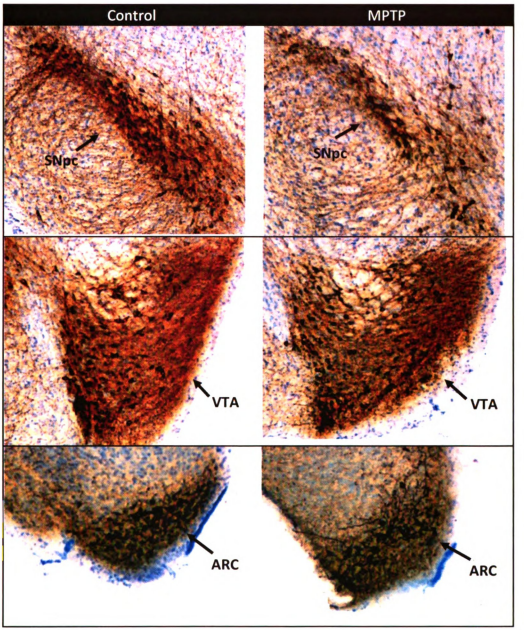

Figure 3-5. Tyrosine hydroxylase immunoreactive (TH-IR) cells in the substantia nigra pars compacta (SNpc), ventral tegmental area (VTA) and arcuate nucleus (ARC) of control and MPTP treated mice. Male mice (n=8/group) were treated with either MPTP (20mg/kg; s.c.) or saline (10 ml/kg; s.c.) every 3.5 days for 5 consecutive weeks. All animals received an injection of probenecid (250 mg/kg; i.p.) with each MPTP or saline injection. Half brains were drop-fixed in paraformaldehyde, 60 μM sections were collected and dual-stained for TH and Nissl. Arrows indicate localization of brown stained TH immunoreactive cells and their processes within each brain region.

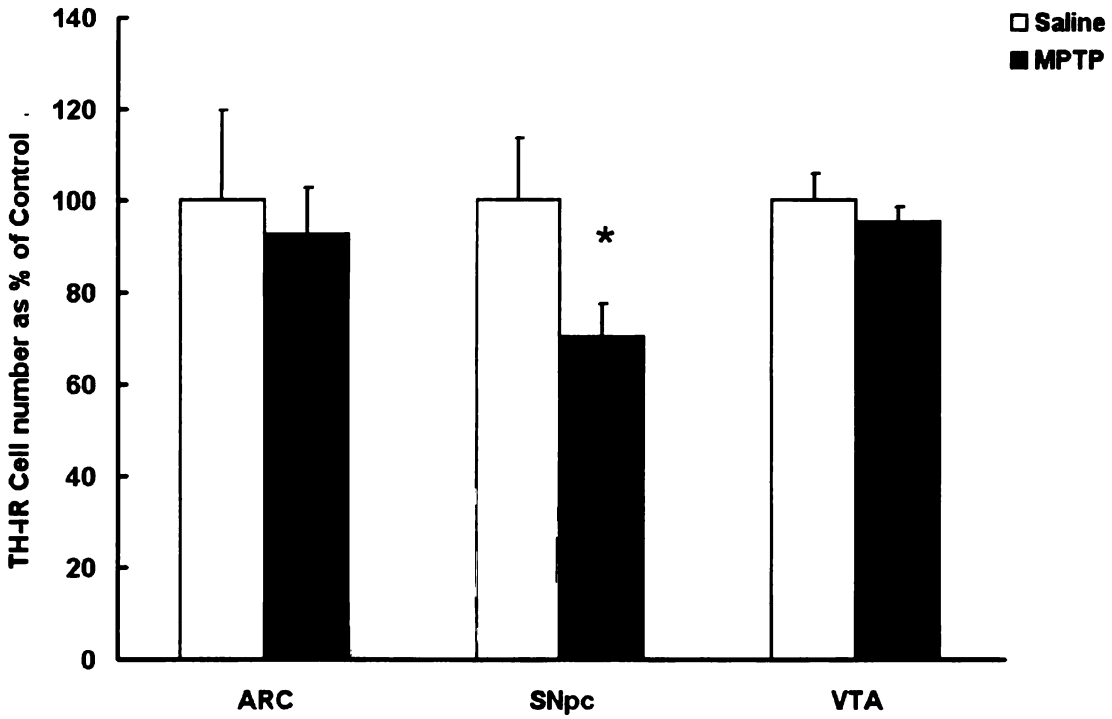

Figure 3-6. The effects of chronic MPTP administration on tyrosine hydroxylase immunoreactive (TH-IR) cell numbers in the arcuate nucleus (ARC), substantia nigra pars compacta (SNpc) and ventral tegmental area (VTA). Male mice (n=8/group) were treated with either MPTP (20mg/kg; s.c.) or saline (10 ml/kg; s.c.) every 3.5 days for 5 consecutive weeks. All animals received an injection of probenecid (250 mg/kg; i.p.) with each MPTP or saline injection. Half brains were drop-fixed in paraformaldehyde, 60 µM sections were collected and dual-stained for TH and Nissl. Numbers of TH-immunoreactive cells are presented as % of saline treated controls. Actual unilateral TH-immunoreactive cell numbers are as follows in saline treated mice: ARC: 1205±237, SNpc: 2687±365 and VTA: 2251±130, and MPTP treated mice: ARC:1117±121, SNpc: 1892±195 and VTA: 2146±76. Columns represent means of groups and vertical bars represent +1.0 Standard error of the mean. (*) indicates values for MPTP treated mice that were significantly different ($p < 0.05$) from saline treated controls.

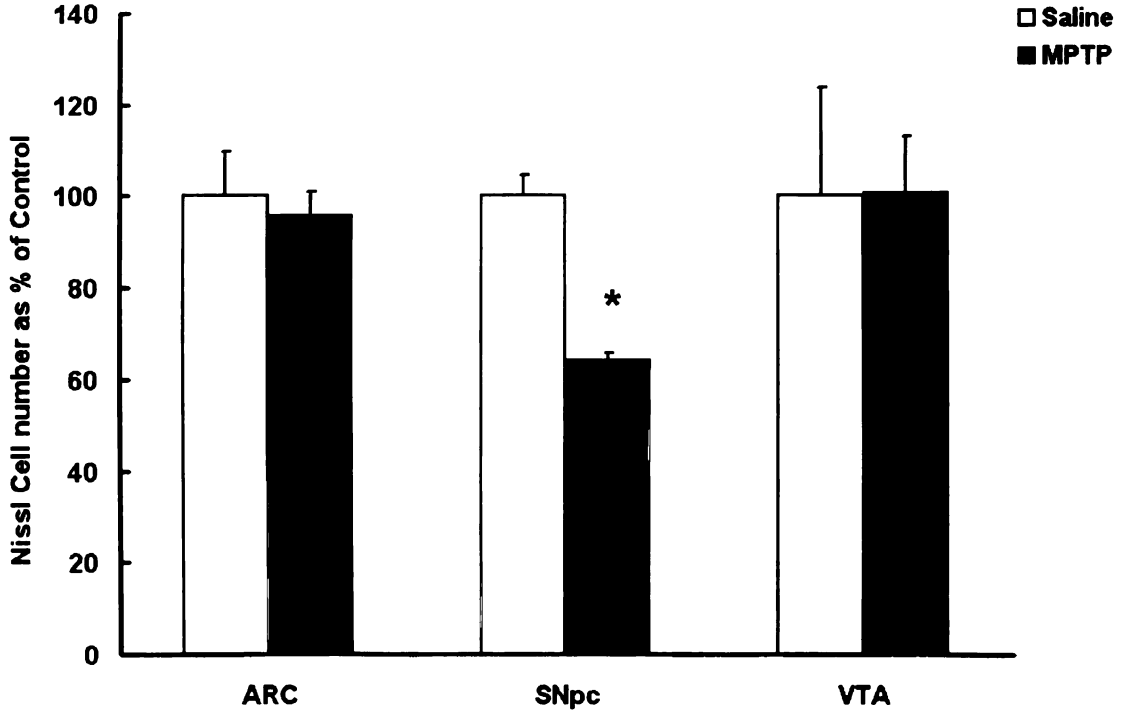

Figure 3-7. The effects of chronic MPTP administration on Nissl positive cell numbers in the arcuate nucleus (ARC), substantia nigra pars compacta (SNpc) and ventral tegmental area (VTA). Male mice (n=8/group) were treated with either MPTP (20mg/kg; s.c.) or saline (10 ml/kg; s.c.) every 3.5 days for 5 consecutive weeks. All animals received an injection of probenecid (250 mg/kg; i.p.) with each MPTP or saline injection. Half brains were drop-fixed in paraformaldehyde, 60 micron sections were collected and stained for Nissl. Neurons were counted using unbiased stereological methods and are presented as % of saline treated controls. Actual unilateral cell numbers are as follows in saline treated mice: ARC: 9410±907, SNpc: 4918±228 and VTA: 3826±907, and MPTP treated mice: ARC: 9016±470, SNpc:3151±84 and VTA: 3855±470. Columns represent means of groups and vertical bars represent +1.0 Standard error of the mean. (*) indicates values for MPTP treated mice that were significantly different ($p < 0.05$) from saline treated controls.

E. Discussion:

These experiments demonstrate that chronic MPTP treatment can successfully model the differential loss of DA neuronal populations observed in PD. Specifically, TIDA neurons are completely spared in the chronic MPTP mouse model of PD, while NSDA neurons are markedly depleted, and MLDA neurons are less severely damaged. These results show that the MPTP mouse model recapitulates the pattern of differential susceptibility seen in PD. This makes the MPTP mouse model an attractive model study mechanisms that contribute to susceptibility in DA neurons.

In accordance with previous reports (Petroske et al., 2001; Drolet et al., 2006), chronic systemic MPTP treatment leads to loss of DA and DOPAC concentrations in ST. This long-term loss of neurotransmitter levels has been consistently mirrored by loss of DA neuron-specific proteins such as TH, DAT and VMAT-2 (Wilson et al., 1996; Kilbourn et al., 2000; Reveron et al., 2002; Drolet et al., 2004b, 2006) and can be reliably used to represent loss of NSDA axon terminal density and integrity. The activation of the remaining axon terminals, as demonstrated by the increased DOPAC/DA ratio, suggests the remaining axon terminals compensate for the severe DA loss. This loss of NSDA axon terminal density and compensatory activation of remaining neurons is also present in the brains of PD patients (Ribeiro et al., 2002; Sossi et al., 2002).

Consistent with previous studies employing the chronic mouse model (Petroske et al., 2001; Drolet et al., 2004a), the loss of axon terminals (~70%) is accompanied by significant, but less severe (~30%) loss of TH immunoreactive cell bodies in SNpc after treatment with MPTP. This loss of TH positive neurons was mirrored by loss of Nissl

stained cell bodies, demonstrating that lower cell counts were due to loss of entire cell bodies, and not transient down-regulation of TH, as previously reported in some MPTP mouse models (Kuhn et al., 2003). The more severe loss of axon terminals after MPTP is supportive of other reports that chronic treatment with the toxin causes retrograde damage to NSDA neurons, affecting the axon terminals before killing the cell bodies (Petroske et al., 2001; Drolet et al., 2006). This retrograde pattern of toxicity of NSDA neurons is also present in the brains of PD patients with 70–80% loss of ST nerve terminals and 50–60% loss of SNpc neurons when clinical symptoms appear (Bernheimer et al., 1973; Agid, 1991).

Unlike NSDA neurons, TIDA axon terminals have unchanged DA and DOPAC levels after chronic treatment with MPTP. This novel finding suggests that TIDA neurons are completely resistant to chronic MPTP treatment with full preservation of axon terminal density and integrity. Stereological cell counts also demonstrate that the cell bodies of these neurons also remain fully intact, which suggests that TIDA neurons remain completely spared. This differential susceptibility between TIDA and NSDA neurons mimicks PD, where no lesion of TIDA neurons, as measured indirectly using circulating prolactin levels or directly using post-mortem cell counts, is accompanied by severe damage to NSDA neurons (Agnoli et al., 1981; Eisler et al., 1981; Matzuk and Saper, 1985; Laihinen and Rinne, 1986; Franceschi et al., 1988).

DA and DOPAC levels in the NA also decrease after treatment with chronic, systemic MPTP, demonstrating that there is some damage to the axon terminals of these neurons. However, the degree of terminal loss in NA (~50%) is less than that

observed for NSDA terminals (~70%). Furthermore, MPTP treatment does not cause loss of MLDA cell bodies demonstrating that these neurons are less susceptible to treatment with MPTP than NSDA neurons. The ratio of DOPAC/DA is not significantly increased in NA following treatment, suggesting that the degree of axon terminal loss may not be sufficient to cause a compensatory increase in activity. These findings reveal that MLDA neurons are relatively resistant to the neurotoxic effects of Complex I inhibition when compared with NSDA neurons, but these neurons are not completely spared. This partial susceptibility following neurotoxic exposure may be due to the presence of a heterogeneous population of cells in the VTA; some that display resistance and some that are vulnerable to neurotoxic insult.

In high doses, MPP+ has an affinity for the norepinephrine (NE) and serotonin (5-HT) transporters and can cause nonselective toxicity to these neuronal populations. Furthermore, lipophillic MPTP may be bioactivated in NE or 5-HT neurons via MAO in sufficient amounts to damage these neuronal types. The cell bodies and some terminal regions of these DA pathways are innervated by NE and 5-HT neurons, originating from the locus coeruleus and raphe nuclei, respectively (Alex and Pehek, 2007). Thus, NE or 5-HT can regulate the function of DA neurons via their actions on DA cell bodies or terminals and complicate findings due to the direct action of MPTP on DA neurons. It is therefore important to determine the effect of MPTP on NE and 5-HT neurons in order to separate direct and indirect effects of MPTP on DA neuronal populations.

While this model has been previously described (Petroske et al., 2001; Drolet et al., 2004b), it has not been determined whether the dose of MPTP is low enough to be

specific only to DA neurons. The experiments in this chapter demonstrate that following treatment with chronic MPTP, concentrations of NE, as well as 5-HT and its metabolite 5-HIAA remain unchanged in all measured regions. This suggests that the MPTP treatment regimen employed in this study does not have any deleterious effects on NE or 5-HT neuronal populations. Accordingly, any toxic effects may be attributed to direct effect of the MPP+ on the DA neurons.

A number of hypotheses have been proposed to explain the preferential susceptibility of NSDA neurons to neurotoxic insult (Hirsch, 1992; Hirsch et al., 1997). These hypotheses include variations in pharmacokinetic factors such as toxin distribution and bio-activation of MPTP to MPP^+ by astrocytes. Others have postulated that differential entry of MPP^+ into the cell via DAT may play a role in the differential susceptibility of these neurons. Finally, differences in cell body size, length of projecting axons and density of innervation of these axons have been proposed to play a role in the differential demise of these neuronal populations.

Several studies have demonstrated that MPTP is readily distributed and converted to MPP^+ in SNpc, VTA and hypothalamus, suggesting that differences in toxin distribution or bio-activation is not a likely explanation for differential sensitivity (Del Zompo et al., 1993; Hung et al., 1995; Speciale et al., 1998). Moreover, exposure to MPP^+ markedly increases apoptosis in TH-IR midbrain primary cultures, but not TH-IR mediobasal primary cultures (Behrouz et al., 2007). Since these cells were exposed to the same concentration of the active toxin for the same amount of time, the

differential sensitivity of NSDA and TIDA neurons cannot be due to bioactivation, distribution or clearance of the toxin.

Differential uptake of MPP^+ via DA transporter (DAT) and intracellular compartmentalization into vesicles via VMAT-2 have also been proposed to explain differential susceptibility to neurotoxins (Uhl, 1998). Variations in transporter expression, however, do not address the selective NSDA neuronal toxicity following exposure to rotenone (Behrouz et al., 2007). Rotenone is a lipophillic molecule that, unlike MPP^+, does not require DAT to enter neurons and is not compartmentalized into vesicles (Le et al., 1999; Betarbet et al., 2000; Masliah et al., 2000; Bywood and Johnson, 2003). Rotenone diffuses into all cells and chronic, systemic rotenone administration decreases Complex I activity uniformly throughout the entire brain (Greenamyre et al., 2001). Differential susceptibility amongst TIDA, NSDA and MLDA neurons can be seen following chronic systemic rotenone treatment (Betarbet et al., 2000; Behrouz et al., 2007), demonstrating this differential susceptibly is not dependent on entry of the toxin into the cells. These *in vivo* results are complemented by data from primary culture studies that demonstrate differential susceptibility of DA neuronal populations to rotenone (Behrouz et al., 2007).

Differences in cell body size, length of projecting axons and density of innervation of these axons have also been proposed as explanations for differential toxicity (Braak and Braak, 2000). The somata of TIDA neurons have a similar diameter and contain the same organelles as those seen in the midbrain cell groups (Van den Pol et al., 1984). NSDA and MLDA neurons have long projecting axons while TIDA neurons

have short axons that terminate locally within the MBH (Björklund A, 1984). The short axons of TIDA neurons are unlikely to be a key resistance phenotype since MLDA neurons, which do have long projecting axons, also show some resistance to these toxins. Density of innervation is also unlikely to explain the differential sensitivity of discrete DA neuronal systems since the resistant TIDA and highly affected NSDA neurons have virtually identical innervation densities to their target neurons and the mildly affected MLDA neurons have a lower density of innervation, as demonstrated by DA concentrations in regions containing axon terminals. Taken together, the present findings suggest that inherent properties of DA neurons related to cell body size, axonal length, and density of innervation of target cells are unlikely explanations for the differential sensitivity of these neurons to neurotoxins.

Differences in intrinsic response of TIDA, NSDA and MLDA neurons, such as expression of protective or deleterious genes may be responsible for the differential susceptibility of these neuronal populations to MPTP. The MPTP mouse model can therefore be used to examine the differential responses of these neuronal populations and analyze intrinsic properties that may infer susceptibility or protection.

Chapter 4: Characterization of the Immediate Neurochemical Responses of TIDA, NSDA and MLDA Neurons to a Single Injection of MPTP

A. Introduction

Chronic systemic treatment with MPTP causes a similar pattern of DA neuron damage observed in symptomatic PD patients. In this model, TIDA neurons remain unaffected with intact cell bodies, while NSDA neurons are extensively and retrogradely lesioned and MLDA neurons are moderately affected. This differential susceptibility of DA neuronal populations is likely dependent upon their intrinsic properties.

The long term response of these neuronal populations after chronic MPTP is an excellent model for studying advanced PD when cell death has already occurred. On the other hand, examination of responses to the first injection of MPTP should mimic early PD, when the most susceptible neurons undergo degeneration. This will allow for assessment of the intrinsic properties of the most susceptible midbrain neurons as they undergo degeneration as compared with resistant TIDA neurons.

The immediate response of NSDA neurons to MPTP has been well characterized. By 1.5 h after a single systemic injection of MPTP, DA is displaced from synaptic vesicles and lost from the axon terminals. Retrograde neurodegeneration proceeds such that by 24 h after treatment with MPTP DA levels in ST remain low, and by 72 h cell bodies in the SNpc express markers of apoptosis (Pileblad et al., 1984; Perry et al., 1985; Pileblad et al., 1985). TIDA neurons are intact and function normally after

chronic treatment with MPTP, but it is possible that these neurons respond to MPTP in a fashion similar to NSDA neurons and later recover. If this is the case, their properties during the period of recovery (when they may express protective factors) can be examined. Determination of the time course of events immediately after MPTP treatment can also address the possibility that MPP+ may not enter these neurons due to lower DAT expression (Demarest and Moore, 1979a). If TIDA neurons respond to treatment with MPTP in a similar fashion to NSDA neurons, it is possible that MPP+ enters these neurons via a DAT-independent mechanism. The results from chronic MPTP experiments described in the Chapter 3 demonstrated that MLDA neurons are partially resistant to the toxic effects of MPTP when compared with NSDA neurons. It would therefore be insightful to learn about the response of this neuronal population as well.

It has been proposed that NSDA neurons produce deleterious proteins in response to toxin exposure that cause their demise (Kuhn et al., 2003). Alternatively, it is possible that TIDA or MLDA neurons may respond to toxin treatment by production of protective proteins. Determining whether the differential susceptibility of NSDA, MLDA and TIDA neurons to toxins is due to mechanisms already in place under normal conditions or through inducible response mechanisms to toxin treatment would allow for identification of intrinsic mechanisms that could determine neuronal fate.

The objectives of the experiments described in this chapter are to examine and compare the short-term neurochemical responses of TIDA, NSDA and MLDA neurons to MPTP administration and determine whether these responses are DAT dependent.

Experiments also determine whether the neurochemical responses of these DA neuronal populations are dependent on synthesis of proteins in response to MPTP treatment.

B. Hypothesis

The experiments in this chapter test the general hypothesis that TIDA and MLDA neurons initiate intrinsic protective mechanisms in response to MPTP.

C. Experimental Design

Time Course of Responses of TIDA, NSDA and MLDA Neurons to a Single Injection of MPTP

A single injection of MPTP (20 mg/kg; s.c.) or saline (10 ml/kg; s.c.) was administered **(Figure 4-1)** and animals were killed by decapitation either 4, 8, 16 or 32 h later. Saline treated animals were killed 8 h after saline injection and were used as zero time controls. Immediately after decapitation brains were removed, ME was dissected from the ventral surface of the brain, and the brain was frozen on dry ice for neurochemical analyses. The details of methods for animal use, drug administration, tissue preparation, and neurochemical analyses are described in Chapter 2 (Methods, Sections. A-D).

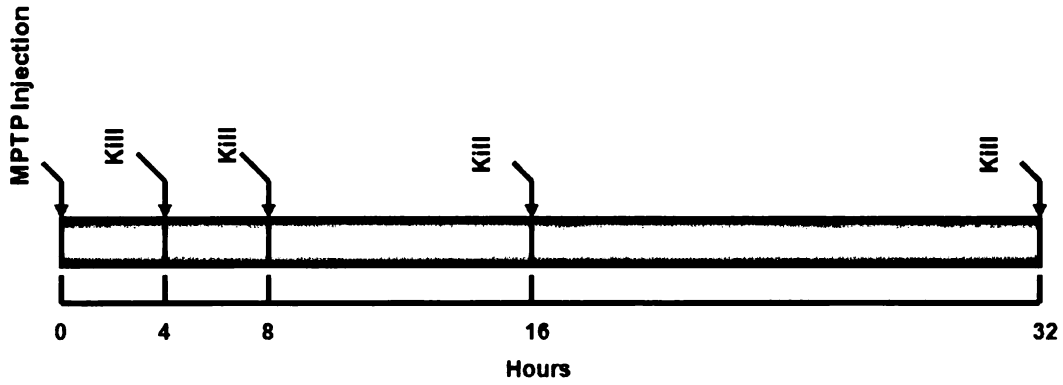

Figure 4-1. Paradigm for the single injection MPTP time course experiment. Male C57bl mice (n=8/group) were injected with MPTP (20 mg/kg; s.c.) and killed by decapitation either 4, 8, 16 or 32 h later. Saline (10 ml/kg; s.c.) treated animals were killed 8 h post-injection and were used as zero time controls.

The primary endpoints **(Table 4-1)** used to determine vesicular DA loss from axon terminal regions were DA concentrations in ME, ST and NA; the axon terminal regions of TIDA, NSDA and MLDA neurons, respectively. Under basal conditions, DA concentrations in these regions primarily reflect vesicular DA (Carlsson, 1975a; Carboni et al., 1992; Di Chiara et al., 1996). Since MPP+ converted from MPTP causes displacement of DA out of vesicles and axon terminals (Chiueh et al., 1994), DA concentrations following a single injection of MPTP reflects a combination of vesicular, cytoplasmic and extracellular DA (see Chapter 1; Introduction, Section E). Accordingly, decreased concentrations of DA shortly after treatment with MPTP should be interpreted as loss of DA stores rather than loss of axon terminal integrity. Only after MPP+ has cleared from the brain and neurons recover in the absence of MPTP (by 32 h post-injection) can the loss of DA be attributed to the loss of axon terminal integrity. Moreover, since MPTP and MPP+ bind to and inhibit the activity of MAO in DA neurons (Takamidoh et al., 1987), changes in DOPAC and DOPAC/DA should not be interpreted solely as DA neuronal activity, but may be contributed partially to MAO inhibition.

In order to demonstrate that the dosage used in these experiments does not directly affect non-DA neuronal populations, concentrations of NE, as well as 5-HT and its metabolite 5-HIAA were measured. If these neurons are directly affected by MPP+, there should be a decrease in neurotransmitter levels. Other changes in NE or 5-HT/5-HIAA levels may be attributed to the response of these neurons to the DA neuronal populations.

Endpoint	Method	Measure of	Indicates
DA	HPLC-EC	Vesicular, cytoplasmic or extracellular DA	DA neuron function
DOPAC	HPLC-EC	DA metabolite	DA metabolism, MAO activity
NE	HPLC-EC	Vesicular NE	NE axon terminal density
5-HT	HPLC-EC	Vesicular 5-HT	5-HT axon terminal density
5-HIAA	HPLC-EC	5-HT metabolite	5-HT metabolism

Table 4-1. The experimental endpoints used for neuronal function following treatment with a single injection of MPTP. DA = dopamine, DOPAC = 3,4-dihydroxyphenylacetic acid, NE = norepinephrine, 5-HT = serotonin, 5-HIAA = 5-hydroxyindoleacetic acid, TH = tyrosine hydroxylase and HPLC-EC = high performance liquid chromatography coupled with electrochemical detection.

Effects of Blockade of DAT on the response of TIDA, NSDA and MLDA Neurons to a Single Injection of MPTP

This experiment tests the hypothesis that the mode of MPP+ entry into TIDA neurons, unlike NSDA and MLDA neurons, is DAT-independent. Mice were pretreated with DAT inhibitor GBR-12909 (GBR, 10 mg/kg; i.p.) or saline (10 ml/kg; i.p.) 30 min prior to a single injection of MPTP (20 mg/kg; s.c.) or saline (10 ml/kg; s.c.). All animals were killed by decapitation 4 h after MPTP administration **(Figure 4-2)** and the brains were quickly removed. Immediately after decapitation, ME was dissected from the ventral surface of the brain, and the brain was frozen on dry ice for neurochemical analyses. The details of methods for animals, drug administration, tissue preparation, and neurochemical analyses are described in Chapter 2 (Methods, Sections. A-D). The primary endpoints (**Table 4-1**) used in this experiment are similar to the previous experiment.

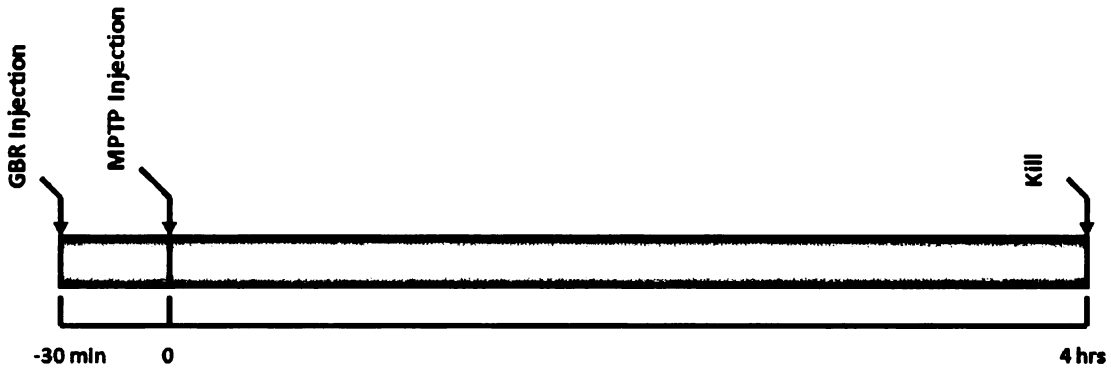

Figure 4-2. Experimental paradigm for the combination of GBR pretreatment with a single injection MPTP. Male C57bl mice (n=8/group) were pretreated with GBR-12909 (GBR; 10 mg/kg; i.p.) or saline (10 ml/kg; i.p.) 30 min prior to a single injection of MPTP (20 mg/kg; s.c.) or saline (10 ml/kg; s.c.). All animals were killed by decapitation 4 h after MPTP.

Effects of Protein Synthesis Inhibition on the Responses of TIDA, NSDA and MLDA Neurons to a Single Injection of MPTP

This experiment tests the hypothesis that the recovery from MPTP-induced DA loss in TIDA neurons is dependent on *de novo* synthesis of proteins. Mice were treated with 4 or 2 injections of cycloheximide (120 mg/kg; i.p.) or saline (10 ml/kg; i.p.) every 2 h, with the first cycloheximide injection 15 min prior to a single injection of MPTP (20 mg/kg; s.c.) or saline (10 ml/kg; s.c.). This dose of cycloheximide has been shown to block protein synthesis in the brain for at least 2 h (Squire and Barondes, 1973; Squire et al., 1973; Squire and Barondes, 1976). Animals receiving 4 cycloheximide injections were decapitated 14 h after MPTP and animals that received 2 cycloheximide injections were decapitated 7 h post MPTP (**Figure 3-4**). Immediately after decapitation, ME was dissected from the ventral surface of the brain, and the brain was frozen on dry ice for neurochemical analysis. The details of methods for animals, drug administration, tissue preparation, and neurochemical analyses are described in Chapter 2 (Methods, Sections. A-D). The primary endpoints (**Table 4-1**) used in this experiment are similar to the previous experiment.

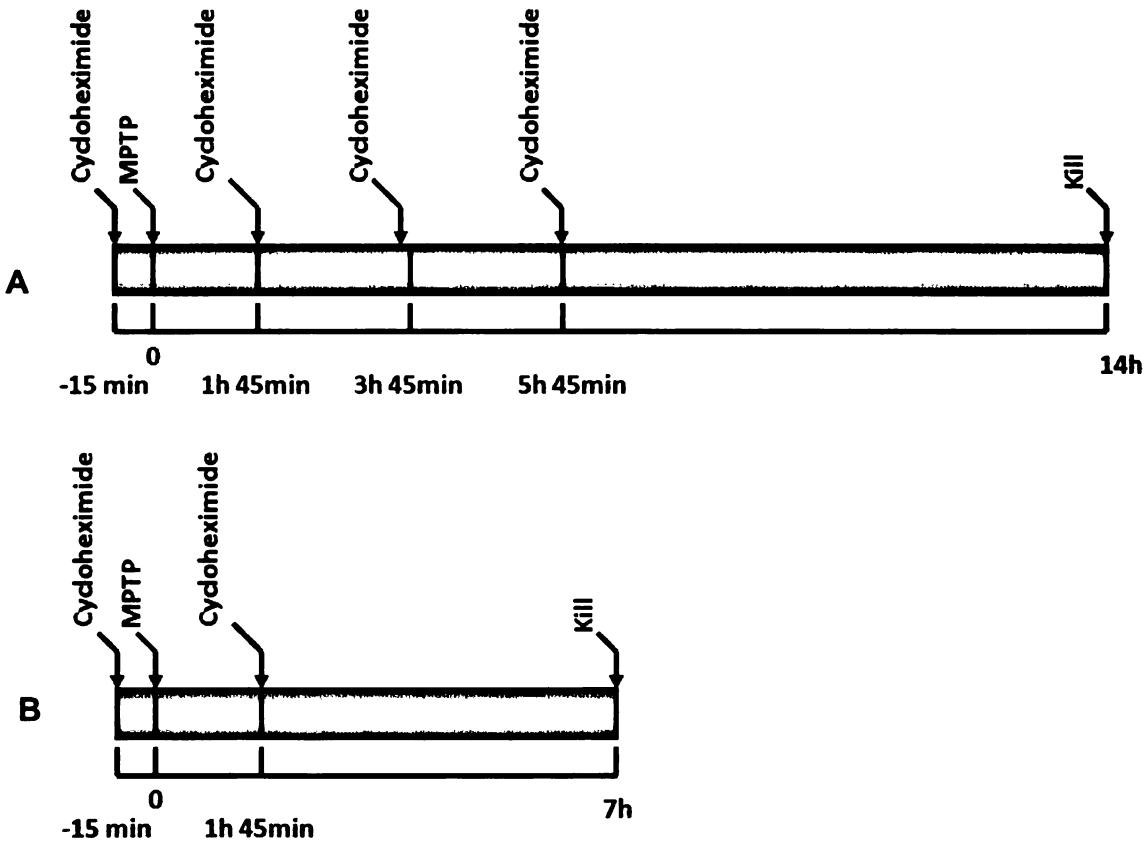

Figure 4-3. Experimental paradigm for the combination of cycloheximide pretreatment with a single injection of MPTP. Male C57bl mice (n=8/group) were treated with 4 (A) or 2 (B) injections of cycloheximide (120 mg/kg; i.p.) or saline (10 ml/kg; i.p.) every 2 h, with the first cycloheximide injection 15 min prior to a single injection of MPTP (20 mg/kg; s.c.) or saline (10 ml/kg; s.c.). Animals receiving 4 cycloheximide (A) injections were killed 14 h after MPTP and animals receiving 2 cycloheximide injections (B) were killed 7 h post MPTP.

Effects of Immediate vs. Delayed Protein Synthesis Inhibition on the Responses of TIDA, NSDA and MLDA Neurons to a Single Injection of MPTP

This experiment tests the hypothesis that *de novo* protein synthesis at different times prevents recovery of TIDA neurons from MPP+ induced DA loss. Mice were treated with 2 injections of cycloheximide (120 mg/kg; i.p.) or saline (10 ml/kg; i.p.) 2 h apart starting either 15 min prior to or 3 h 45 min after a single injection of MPTP (20 mg/kg; s.c.) or saline (10 ml/kg; s.c.). All animals were killed by decapitation 16 h after MPTP (**Figure 3-5**) and the brains were quickly removed. Immediately after decapitation, ME was dissected from the ventral surface of the brain, and the brain was frozen on dry ice for neurochemical analysis. The details of methods for animals, drug administration, tissue preparation, and neurochemical analyses are described in Chapter 2 (Methods, Sections. A-D). The primary endpoints (**Table 4-1**) used in this experiment are similar to the previous experiment.

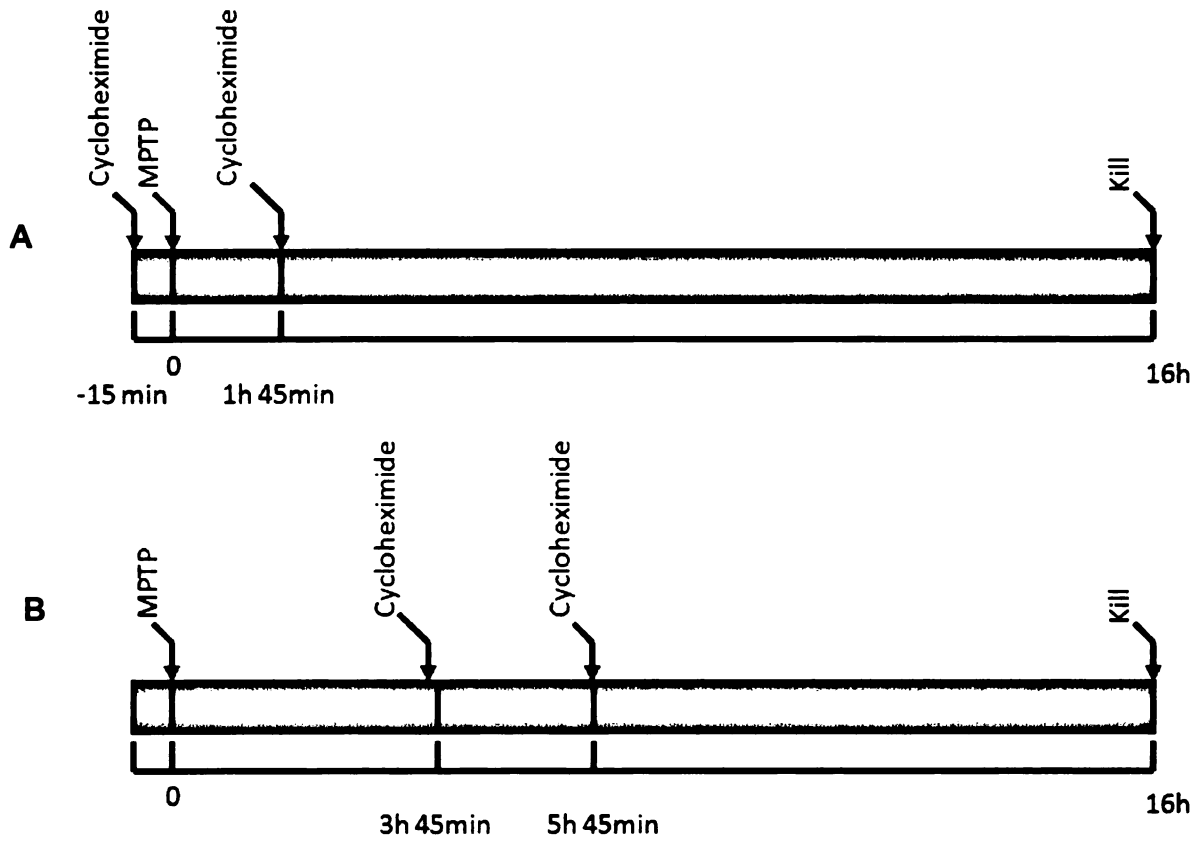

Figure 4-4. Experimental paradigm for the combination of cycloheximide treatment with a single injection MPTP Male C57bl mice (n=8/group) were treated with 2 injections of cycloheximide (120 mg/kg; i.p.) or saline (10 ml/kg; i.p.), 2 h apart, starting either 15 min prior to (A) or 3 h 45 min after (B) a single injection of MPTP (20 mg/kg; s.c.) or saline (10 ml/kg; s.c.). All animals were killed by decapitation 16 h after MPTP.

D. Results

Time Course of Responses of TIDA, NSDA and MLDA Neurons to a Single Injection of MPTP:

Figure 4-5 demonstrates the time-course of the responses of TIDA, NSDA and MLDA neurons to a single systemic injection of MPTP. ME, ST and NA DA levels were significantly decreased by 4 h after MPTP treatment. ME DA levels increased at 8 h, and were similar to controls at 16 and 32 h post-injection. In contrast, DA levels in ST decreased further at 8 h post-MPTP and remained low (~25% of controls) for the remainder of the time. Decreased levels of DA (~70% of control) were maintained in the NA at 8 and 16 h post-MPTP injection, but returned to control levels by 32 h.

As demonstrated in **Figure 4-6**, DOPAC levels mirrored DA levels after treatment with a single injection of MPTP. DOPAC levels in ME, ST and NA decreased significantly by 4 h after MPTP treatment. DOPAC levels returned to control levels in ME by 16 h after treatment, but remained low in ST and NA.

No changes in NE concentrations were observed in NA or ME at any time after treatment with MPTP. Concentrations in ST were not detectable even in zero time controls **(Table 4-2)**. 5-HT levels increased in ST 4 h after MPTP treatment **(Figure 4-7)**, but returned to normal by 8 h post-MPTP and did not change at 16 or 32 h post-treatment. 5-HT levels in ME or NA remained unchanged following MPTP treatment. 5-HIAA levels increased in ST by 4 and 8 h after MPTP, but returned to normal at 16 and 32 h after treatment **(Figure 4-8)**.

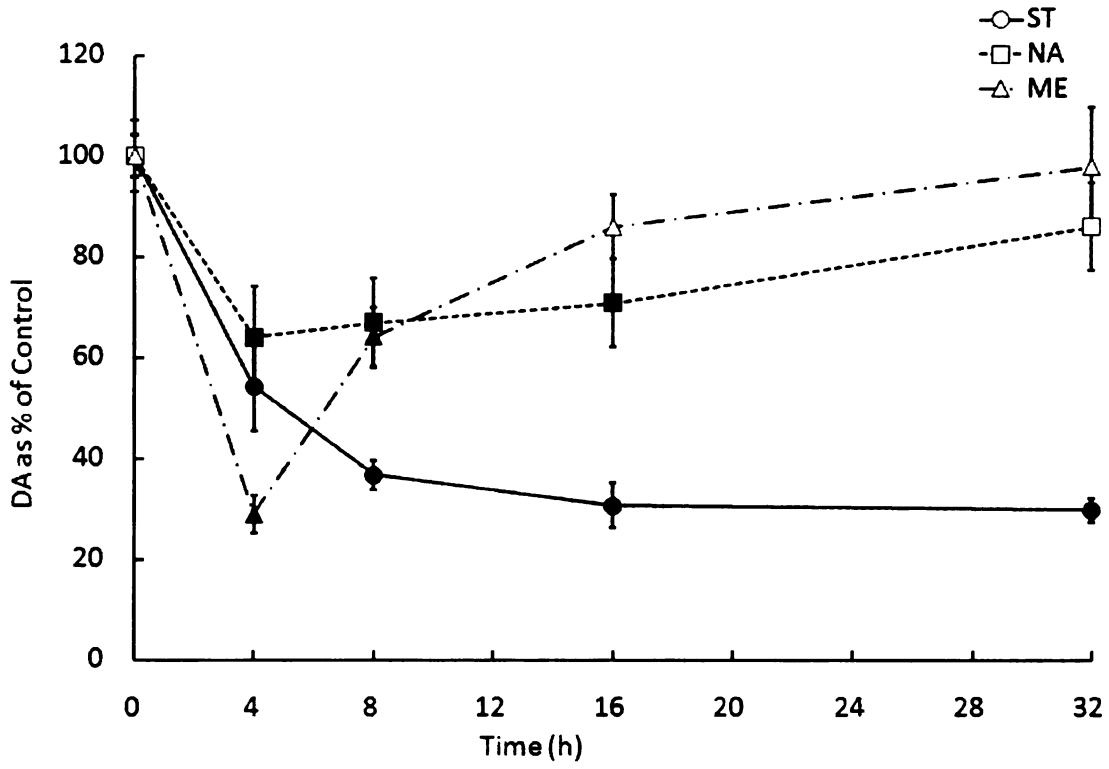

Figure 4-5: The time course of effects of a single injection of MPTP on DA levels in median eminence (ME), striatum (ST) and nucleus accumbens (NA). Male mice (n=8/group) were treated with MPTP (20mg/kg; s.c.) and killed by decapitation either 4,8,16 or 32 h later. Saline (10 ml/kg; s.c.) treated animals were killed 8 h post-injection and were used as zero time controls. DA levels are presented as % of these saline treated controls. Actual DA concentrations (ng/mg protein) are as follows in ME: zero h control : 176±12, MPTP 4 h:51±7, MPTP 8 h: 112±10, MPTP 16 h: 153±11, MPTP 32 h: 172±20; NA: zero h control: 71±3 , MPTP 4 h: 45±7, MPTP 8 h: 48±6, MPTP 16 h: 51±6, MPTP 32 h: 62±6 ; and in ST: zero h control: 172±7 , MPTP 4 h: 94±15, MPTP 8 h: 63±5, MPTP 16 h: 53±8 and MPTP 32 h: 51±4 . Geometric symbols represent means of groups and vertical bars represent ± 1 standard error of the mean. Filled in symbols represent MPTP treated mice that were significantly different ($p < 0.05$) from saline treated controls.

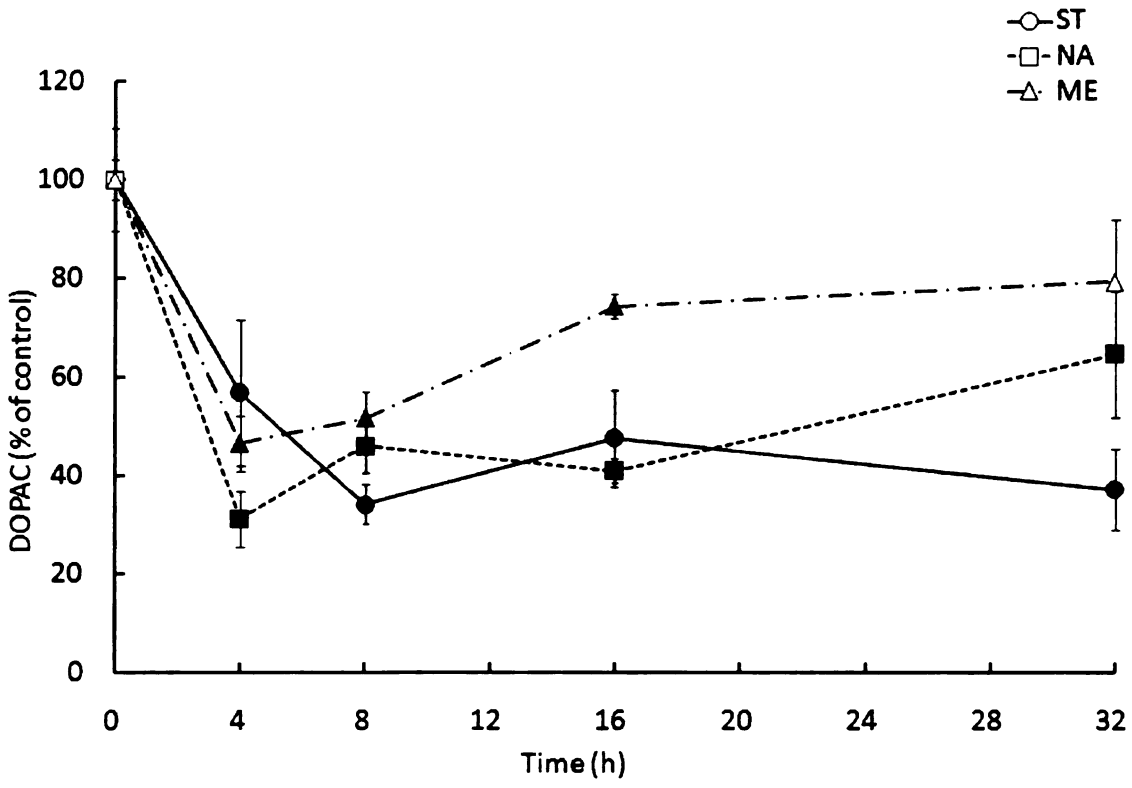

Figure 4-6: The time course of effects of a single injection of MPTP on DOPAC levels in median eminence (ME), striatum (ST) and nucleus accumbens (NA). Male mice (n=8/group) were treated with MPTP (20mg/kg; s.c.) and killed by decapitation either 4, 8, 16 or 32 h later. Saline (10 ml/kg; s.c.) treated animals were killed 8 h post-injection and were used as zero time controls. DOPAC levels are presented as % of saline treated. Actual DOPAC concentrations (ng/mg protein) are as follows in ME: zero h control: 12±1, MPTP 4 h: 6±2, MPTP 8 hr: 6±2, MPTP 16 hr: 9±1, MPTP 32 hr: 10±2, in NA: zero h control: 16±1 , MPTP 4 h: 5±1, MPTP 8 h: 7±1, MPTP 16 h: 6±0, MPTP: 10±2 and in ST: zero h control: 24.2±2 , MPTP 4 h:14±3, MPTP 8 h: 8±1, MPTP 16 h: 12±2, and MPTP 32 h: 9±2 . Geometric symbols represent means of groups and vertical bars represent ± 1 standard error of the mean. Filled in symbols represent MPTP treated mice that were significantly different ($p < 0.05$) from saline treated controls.

Concentrations of NE (ng/mg protein)			
Time (h) after MPTP	**ST**	**NA**	**ME**
0	ND	7.3 ± 1.4	21.8 ± 4.5
4	ND	9.9 ± 1.3	26.3 ± 3.6
8	ND	7.8 ± 1.9	20.9 ± 1.8
16	ND	9.4 ± 1.1	21.8 ± 2.3
32	ND	8.3 ± 1.2	27.2 ± 5.1

Table 4-2. Norepinephrine (NE) concentrations in median eminence (ME), striatum (ST) and nucleus accumbens (NA) of saline control and MPTP treated mice. Male mice (n=8/group) were treated with MPTP (20mg/kg; s.c.) and killed by decapitation either 4, 8, 16 or 32 h later. Saline (10 ml/kg; s.c.) treated animals were killed 8 h post-injection and were used as zero time controls. ND = Not Detectable.

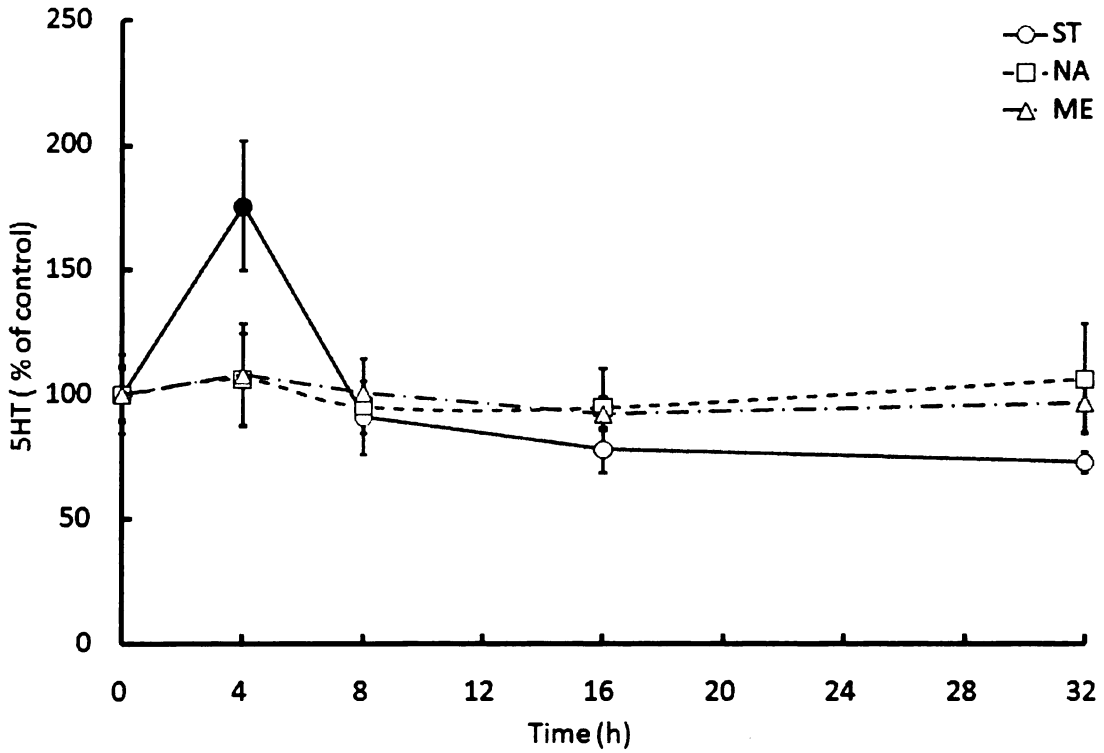

Figure 4-7: The time course of effects of a single injection of MPTP on 5-HT levels in median eminence (ME), striatum (ST) and nucleus accumbens (NA). Male mice (n=8/group) were treated with MPTP (20mg/kg; s.c.) and killed 4,8,16 or 32h later. Saline (10 ml/kg; s.c.) treated animals were killed 8h post-injection and are considered 0 time controls. 5-HT levels are presented as % of saline treated. Actual 5-HT concentrations (ng/mg protein) are as follows in ME: zero h control: 14±2, MPTP 4 h:16±3, MPTP 8 hr:17±2, 16 hr:13±1, MPTP 32 hr: 14±2,in NA: zero h control: 13±2 , MPTP 4 h: 13±2, MPTP 8 h: 12±2, MPTP 16 h: 12±2, MPTP 32 hr:13±3 and in ST: zero h control: 12±1 , MPTP 4 h: 20±3, MPTP 8 h: 10±1, MPTP 16 h: 9±1, MPTP 32 hr: 8±1. Geometric symbols represent means of groups and vertical bars represent ±1.0 standard error of the mean. Filled in symbols represent MPTP treated mice that were significantly different ($p < 0.05$) from saline treated controls.

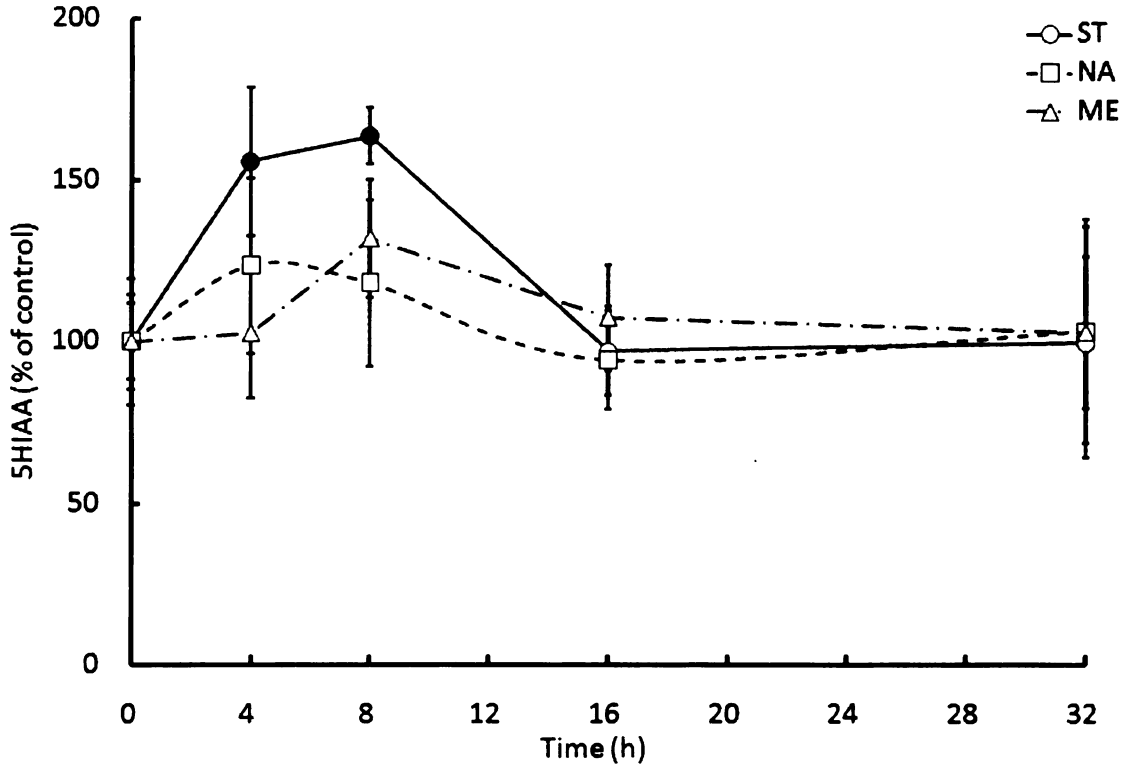

Figure 4-8: The time course of effects of a single injection of MPTP on 5HIAA levels in median eminence (ME), striatum (ST) and nucleus accumbens (NA). Male mice (n=8/group) were treated with MPTP (20mg/kg; s.c.) and killed 4,8,16 or 32h later. Saline (10 ml/kg; s.c.) treated animals were killed 8h post-injection and are considered 0 time controls. 5HIAA levels are presented as % of saline treated. Actual 5HIAA concentrations (ng/mg protein) are as follows in ME: zero h control: 6±1, MPTP 4 h: 9±1, MPTP 8 h: 9±1, MPTP 16 h: 5±1, MPTP 32h: 6±2, in NA: zero h control: 6±1 , MPTP 4 h: 7±1, MPTP 8 h: 7±1, MPTP 16 h: 5±1, MPTP 32 h: 6±2 and in ST: zero h control: 6±1 , MPTP 4 h: 9±1, MPTP 8 h: 9±1, MPTP 16 h: 5±1, MPTP 32 h: 6±1. Geometric symbols represent means of groups and vertical bars represent ±1.0 standard error of the mean. Filled in symbols represent MPTP treated mice that were significantly different ($p < 0.05$) from saline treated controls.

Effects of Blockade of DAT on the Responses of TIDA, NSDA and MLDA Neurons to a Single Injection of MPTP:

As demonstrated in **Figure 4-9**, DA concentrations decreased in ME 4 h following MPTP administration in both control and GBR-treated mice. In ST, a significant loss of DA was observed 4 h after MPTP-treatment, and this DA loss was blocked by GBR-pretreatment **(Figure 4-10)**. **Figure 4-11** demonstrates that there was a loss of DA in NA 4 h after treatment with MPTP, but GBR pre-treatment blocked MPTP induced DA loss in NA. In all three regions, GBR treatment alone did not alter DA levels.

Figure 4-12 demonstrates that DOPAC levels decreased in ME 4 h after MPTP in both control and GBR-treated mice. Moreover, DOPAC levels remained unchanged in ME after GBR treatment alone. MPTP treatment also caused a loss of DOPAC in ST of control and GBR-treated mice **(Figure 4-13)**. ST had decreased levels of DOPAC following GBR treatment alone. DOPAC levels also decreased in NA following MPTP treatment in both control and GBR-treated mice (**Figure 4-14**) and GBR treatment alone did not alter DOPAC concentrations in this region.

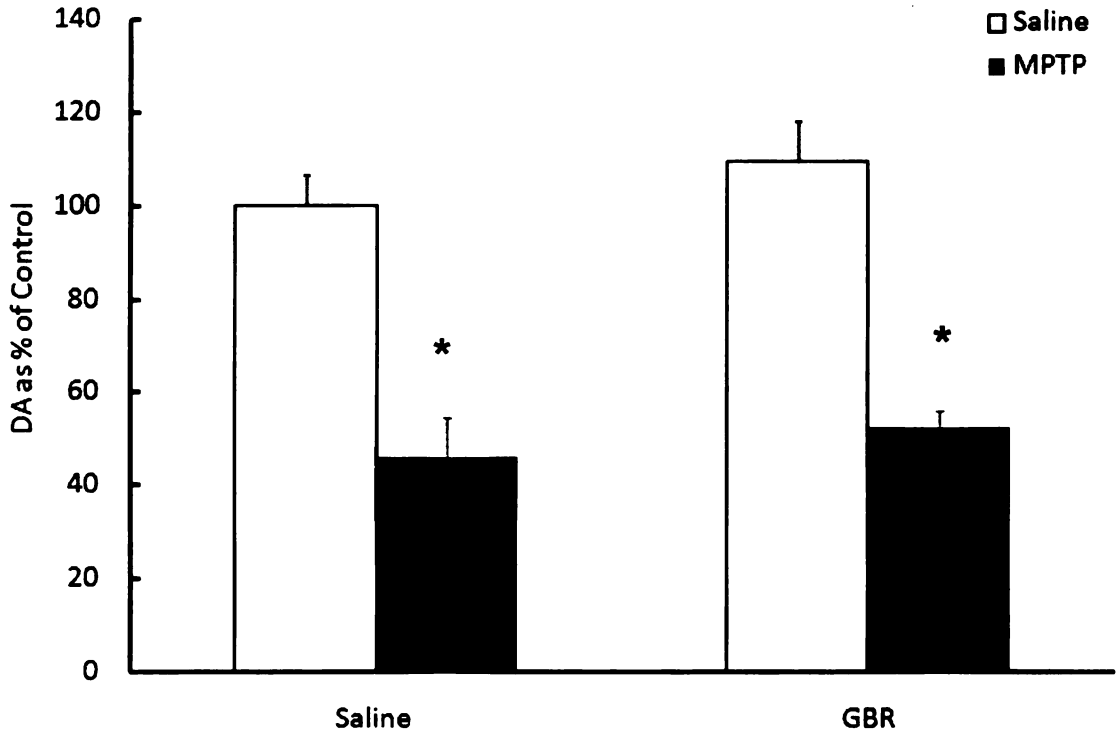

Figure 4-9. The effects of GBR pre-treatment and single injection MPTP administration on DA levels in median eminence (ME). Male mice (n=8/group) were treated with the DAT inhibitor GBR (10 mg/kg; i.p.) or saline (10 ml/kg; i.p.). Thirty min after GBR administration, mice received a single injection of MPTP (20mg/kg; s.c.) or saline (10 ml/kg; s.c.). All animals were decapitated 4 h after MPTP or saline treatment. DA levels are presented as % of saline treated. Actual DA concentrations (ng/mg protein) are as follows: Saline/saline: 131±8, Saline/MPTP: 60±11, GBR/saline: 144±13, and GBR/MPTP: 69±5. Columns represent means of groups and vertical bars represent +1.0 standard error of the mean. (*) indicates values for MPTP treated mice that were significantly different ($p < 0.05$) from saline treated controls.

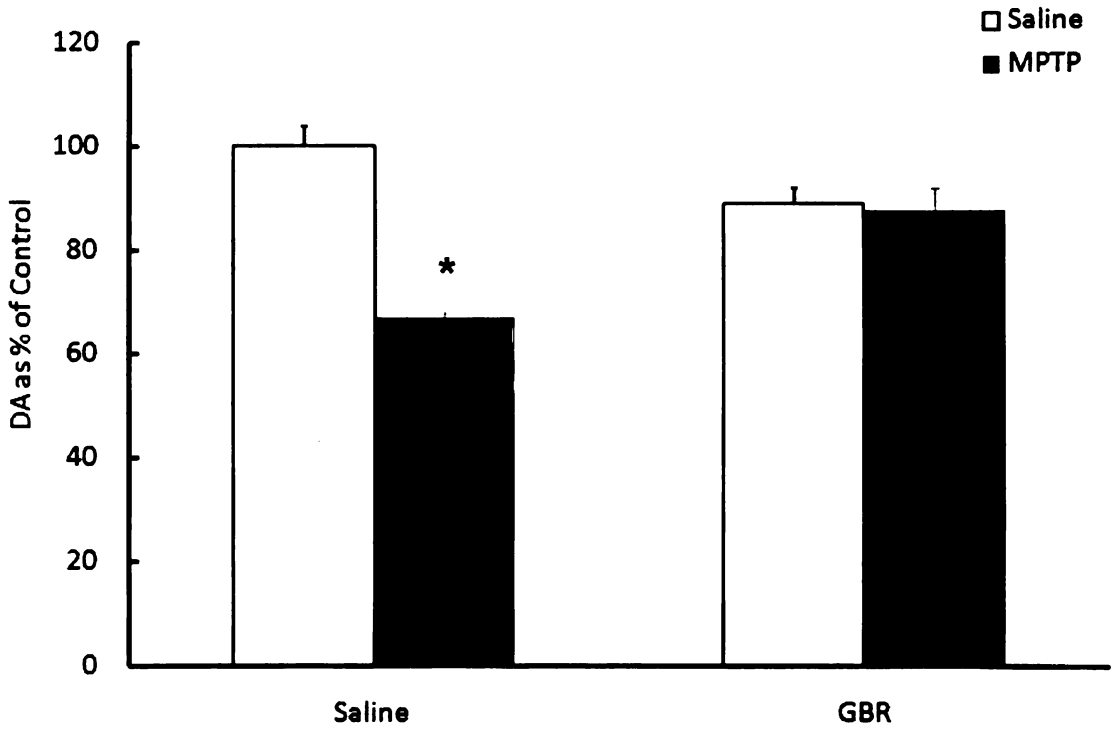

Figure 4-10. The effects of GBR pre-treatment and single injection MPTP administration on DA levels in striatum (ST). Male mice (n=8/group) were treated with the DAT inhibitor GBR (10 mg/kg; i.p.) or saline (10 ml/kg; i.p.). Thirty min after GBR administration, mice received a single injection of MPTP (20 mg/kg; s.c.) or saline (10 ml/kg; s.c.). All animals were decapitated 4 h after MPTP or saline treatment. DA levels are presented as % of saline treated. Actual DA concentrations (ng/mg protein) are as follows: Saline/saline: 182±7, Saline/MPTP: 122±12, GBR/saline: 162±6, and GBR/MPTP: 160±8. Columns represent means of groups and vertical bars represent +1.0 standard error of the mean. (*) indicates values for MPTP treated mice that were significantly different ($p < 0.05$) from saline treated controls.

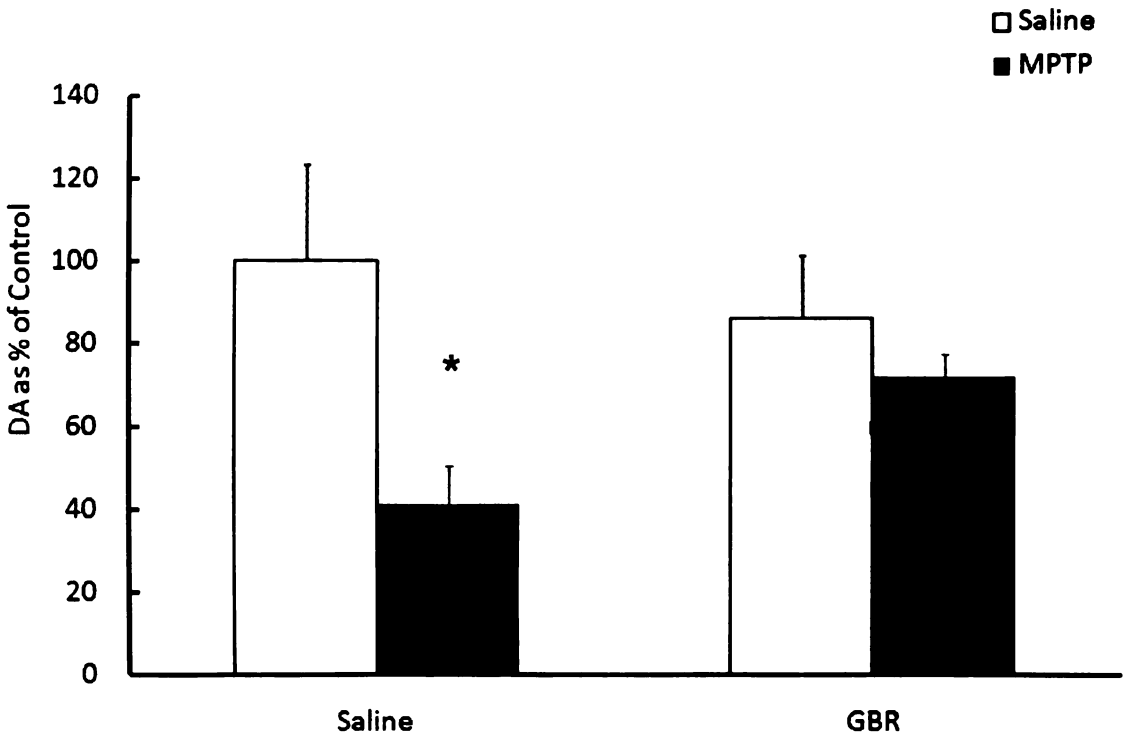

Figure 4-11. The effects of GBR pre-treatment and single injection MPTP administration on DA levels in nucleus accumbens (NA). Male mice (n=8/group) were treated with the DAT inhibitor GBR (10 mg/kg; i.p.) or saline (10 ml/kg; i.p.). Thirty min after GBR administration, mice received a single injection of MPTP (20 mg/kg; s.c.) or saline (10 ml/kg; s.c.). All animals were decapitated 4h after MPTP or saline treatment. DA levels are presented as % of saline treated. Actual DA concentrations (ng/mg protein) are as follows: Saline/saline: 80±19, Saline/MPTP: 33±7, GBR/saline: 69±12, and GBR/MPTP: 57±4. Columns represent means of groups and vertical bars represent +1.0 standard error of the mean. (*) indicates values for MPTP treated mice that were significantly different ($p < 0.05$) from saline treated controls.

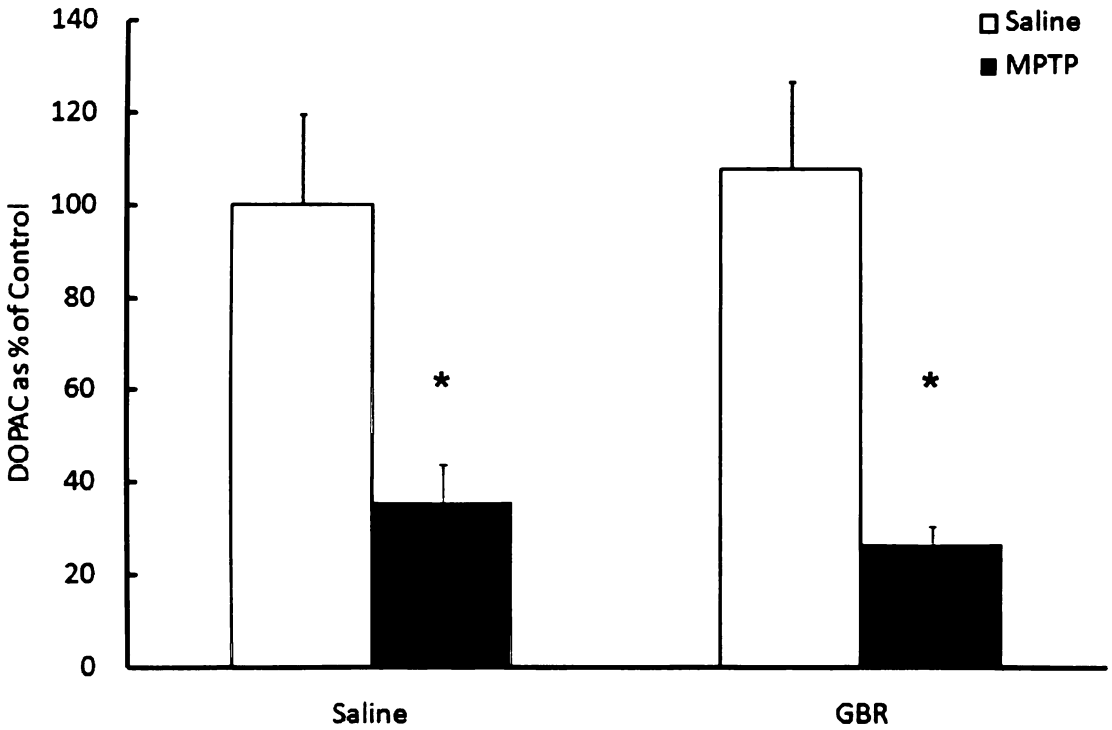

Figure 4-12. The effects of GBR pre-treatment and single injection MPTP administration on DOPAC levels in median eminence (ME). Male mice (n=8/group) were treated with the DAT inhibitor GBR (10 mg/kg; i.p.) or saline (10 ml/kg; i.p.). Thirty min after GBR administration, mice received a single injection of MPTP (20 mg/kg; s.c.) or saline (10 ml/kg; s.c.). All animals were decapitated 4 h after MPTP or saline treatment. DA levels are presented as % of saline treated. Actual DOPAC concentrations (ng/mg protein) are as follows: Saline/saline: 4±1, Saline/MPTP: 2±1, GBR/saline: 4±1, and GBR/MPTP: 1±0. Columns represent means of groups and vertical bars represent +1.0 standard error of the mean. (*) indicates values for MPTP treated mice that were significantly different ($p < 0.05$) from saline treated controls.

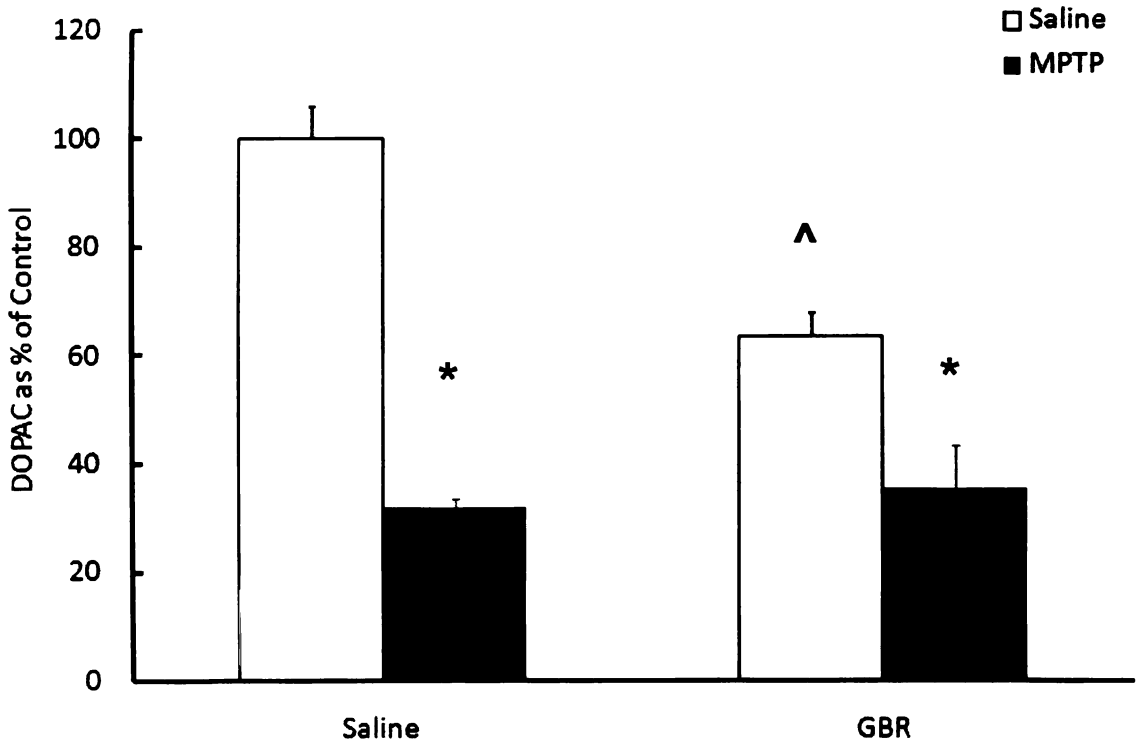

Figure 4-13. The effects of GBR pre-treatment and single injection MPTP administration on DOPAC levels in striatum (ST). Male mice (n=8/group) were treated with the DAT inhibitor GBR (10 mg/kg; i.p.) or saline (10 ml/kg; i.p.). Thirty min after GBR administration, mice received a single injection of MPTP (20 mg/kg; s.c.) or saline (10 ml/kg; s.c.). All animals were decapitated 4 h after MPTP or saline treatment. DA levels are presented as % of saline treated. Actual DOPAC concentrations (ng/mg protein) are as follows: Saline/saline: 17±1, Saline/MPTP: 6±0, GBR/saline: 11±1, and GBR/MPTP: 6±1. Columns represent means of groups and vertical bars represent +1.0 standard error of the mean. (*) indicates values for MPTP treated mice that were significantly different ($p < 0.05$) from saline treated controls.

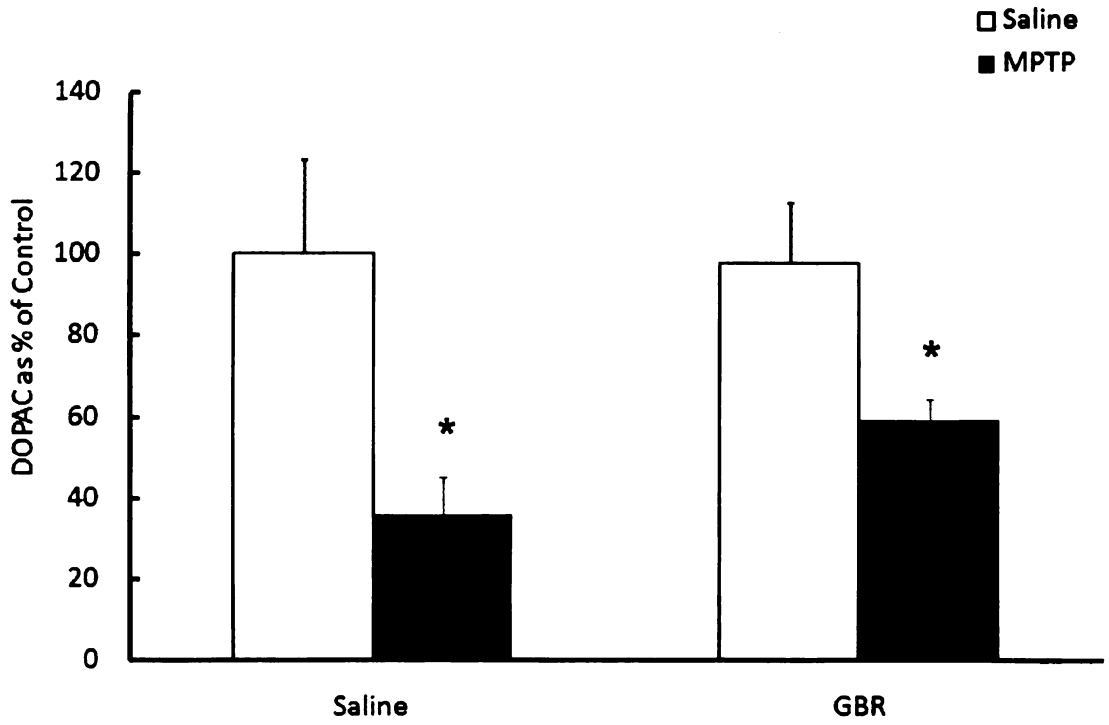

Figure 4-14. The effects of GBR pre-treatment and single injection MPTP administration on DOPAC levels in nucleus accumbens (NA). Male mice (n=8/group) were treated with the DAT inhibitor GBR (10 mg/kg; i.p.) or saline (10 ml/kg; i.p.). Thirty min after GBR administration, mice received a single injection of MPTP (20 mg/kg; s.c.) or saline (10 ml/kg; s.c.). All animals were decapitated 4 h after MPTP or saline treatment. DA levels are presented as % of saline treated. Actual DOPAC concentrations (ng/mg protein) are as follows: Saline/saline: 8±1, Saline/MPTP: 3±1, GBR/saline: 8±2, and GBR/MPTP: 5±1. Columns represent means of groups and vertical bars represent +1.0 standard error of the mean. (*) indicates values for MPTP treated mice that were significantly different ($p < 0.05$) from saline treated controls.

The Impact of Protein Synthesis Inhibition on the Neurochemical Responses of NSDA, MLDA and TIDA Neurons to a Single Injection of MPTP:

Figure 4-15 demonstrates the effects of cycloheximide treatment on DA concentrations in the ME in MPTP treated mice. Treatment with MPTP alone decreased DA levels in ME by 7 h but there was complete recovery of DA to control levels by 14 h post-MPTP. Treatment with cycloheximide prevented MPTP induced loss of ME DA concentrations at 14 h, but not 7 h. In contrast, DA concentrations in ST were significantly decreased 7 and 14 h after treatment with MPTP in both control and cycloheximide treated mice **(Figure 4-16)**. Similarly, DA levels in NA decreased 7 and 14 h following MPTP treatment in both control and cycloheximide treated mice (**Figure 4-17**). Cycloheximide treatment alone did not alter DA levels in ME, ST or NA.

DOPAC levels mirrored DA levels following treatment with cycloheximide and MPTP (**Table 4-3).** DOPAC levels decreased in ME by 7 h after MPTP treatment alone and returned to control levels by 14 h post-MPTP, whereas DOPAC levels did not change in the ME of mice treated with cycloheximide and MPTP. ST and NA DOPAC concentrations decreased with MPTP treatment in control and cycloheximide treated mice. Cycloheximide alone did not alter DOPAC levels in ME, NA, or ST.

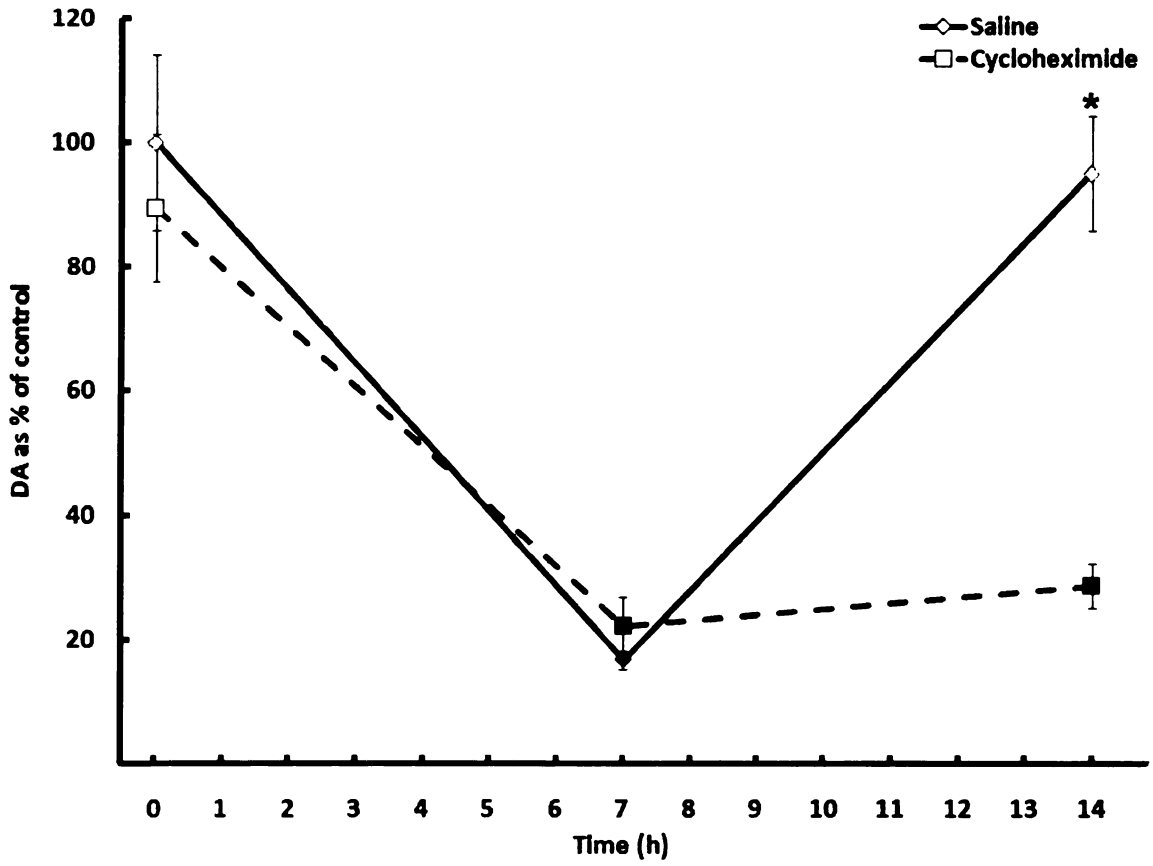

Figure 4-15. The effects of cycloheximide and MPTP administration on DA levels in median eminence (ME). Male C57bl mice (n=8/group) were treated with 2 or 4 injections of cycloheximide (120 mg/kg; i.p.) or saline (10 ml/kg; i.p.) every 2 h, with the first cycloheximide injection 15 min prior to a single injection of MPTP (20 mg/kg; s.c.) or saline (10 ml/kg; s.c.). Animals receiving 2 cycloheximide injections were decapitated 7 h after MPTP and animals receiving 4 cycloheximide injections were decapitated 14 h post MPTP. DA levels are presented as % of saline treated. Actual DA concentrations (ng/mg protein) in ME are as follows in saline treated mice: zero h control: 132±18, MPTP 7 h: 22±2 and MPTP 14 h: 124±14, and Cycloheximide treated mice: zero h control: 118±18, MPTP 7 h: 29±6 and MPTP 14 h: 38±6. Geometric shapes represent means of groups and vertical bars represent +1.0 standard error of the mean. Filled in symbols indicate values for MPTP treated mice that were significantly different ($p < 0.05$) from saline treated controls. (*) indicates values for cycloheximide treated mice that were significantly different ($p < 0.05$) from saline treated controls.

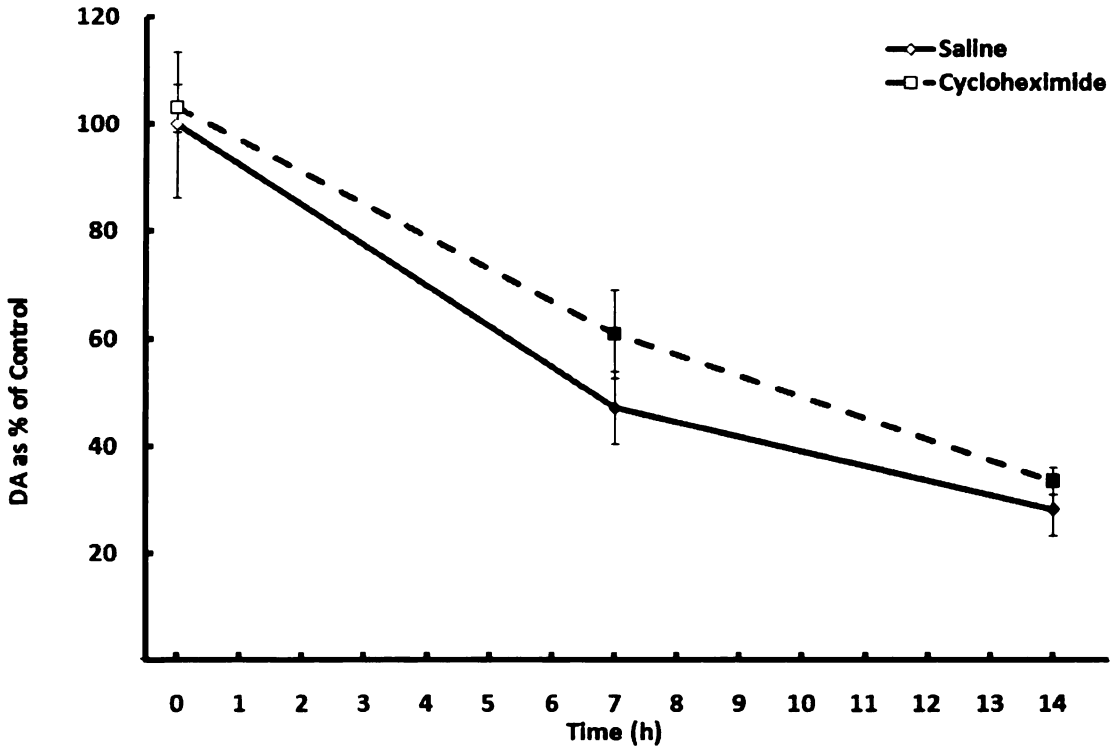

Figure 4-16. The effects of cycloheximide and MPTP administration on DA levels in striatum (ST). Male C57bl mice (n=8/group) were treated with 2 or 4 injections of cycloheximide (120 mg/kg; i.p.) or saline (10 ml/kg; i.p.) every 2 h, with the first cycloheximide injection 15min prior to a single injection of MPTP (20 mg/kg; s.c.) or saline (10 ml/kg; s.c.). Animals receiving 2 cycloheximide injections were decapitated 7 h after MPTP and animals receiving 4 cycloheximide injections were decapitated 14 h post MPTP. DA levels are presented as % of saline treated. Actual DA concentrations (ng/mg protein) in ST are as follows in saline treated mice: zero h control: 187±8, MPTP 7 h: 88±15 and MPTP 14 h: 52±5, and Cycloheximide treated mice: zero h control: 203±23, MPTP 7 h: 114±13 and MPTP 14 h: 63 ± 9. Geometric shapes represent means of groups and vertical bars represent +1.0 standard error of the mean. Filled in symbols indicate values for MPTP treated mice that were significantly different ($p < 0.05$) from saline treated controls. (*) indicates values for cycloheximide treated mice that were significantly different ($p < 0.05$) from saline treated controls.

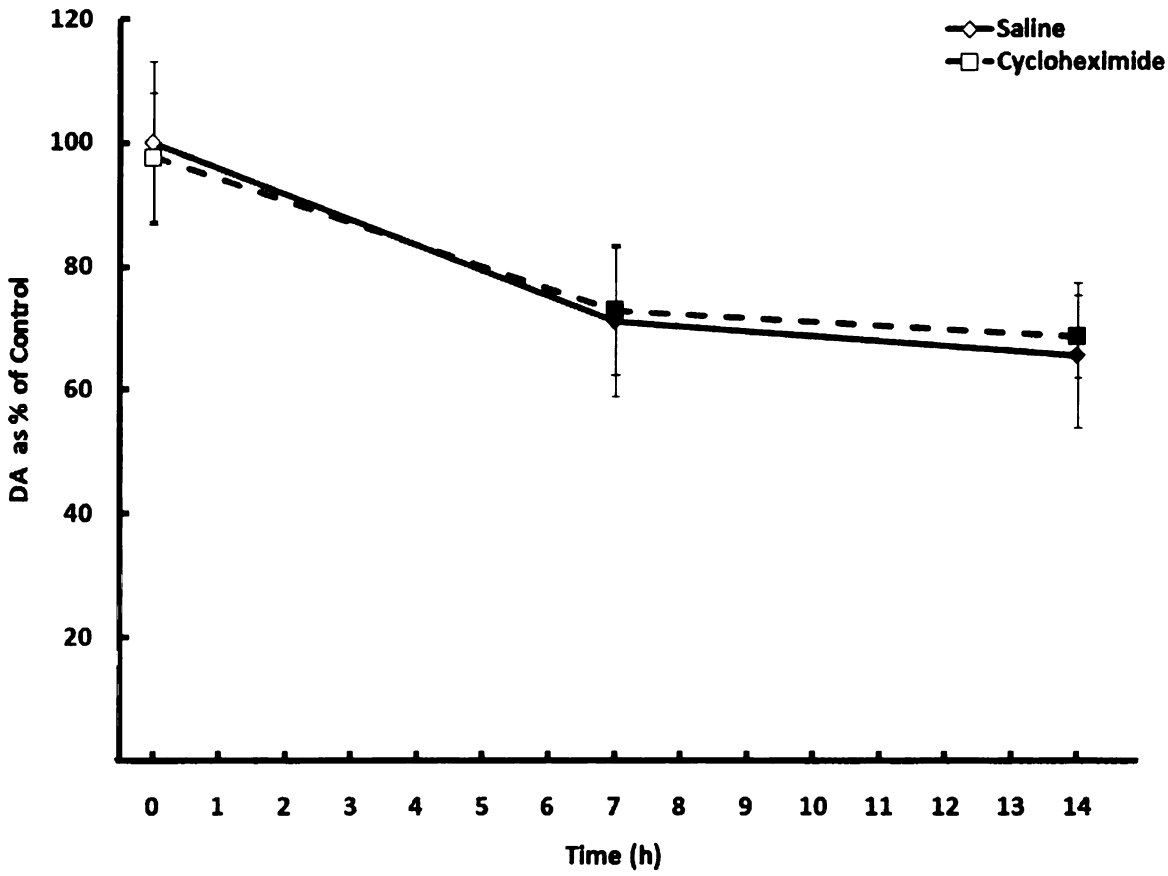

Figure 4-17. The effects of cycloheximide and MPTP administration on DA levels in nucleus accumbens (NA). Male C57bl mice (n=8/group) were treated with 2 or 4 injections of cycloheximide (120 mg/kg; i.p.) or saline (10 ml/kg; i.p.) every 2 h, with the first cycloheximide injection 15 min prior to a single injection of MPTP (20 mg/kg; s.c.) or saline (10 ml/kg; s.c.). Animals receiving 2 cycloheximide injections were decapitated 7 h after MPTP and animals receiving 4 cycloheximide injections were decapitated 14 h post MPTP. DA levels are presented as % of saline treated. Actual DA concentrations (ng/mg protein) in NA are as follows in saline treated mice: zero h control: 94±11, MPTP 7 h: 64±8 and MPTP 14 h: 58±9, and Cycloheximide treated mice: zero h control: 92±10, MPTP 7 h: 69±10 and MPTP 14 h: 65±7. Geometric shapes represent means of groups and vertical bars represent +1.0 standard error of the mean. Filled in symbols indicate values for MPTP treated mice that were significantly different ($p < 0.05$) from saline treated controls. (*) indicates values for cycloheximide treated mice that were significantly different ($p < 0.05$) from saline treated controls.

ME	0 h	7 h	14 h
Saline	6.7 ± 1.7	4.5 ± 0.9	6.0 ± 1.7
Cycloheximide	6.0 ± 1.1	7.1 ± 2.0	5.9 ± 2.0

ST	0 h	7 h	14 h
Saline	17.2 ± 1.9	3.9 ± 1.1*	7.0 ± 1.1*
Cycloheximide	20.5 ± 1.7	5.3 ± 2.0*	6.4 ± 2.0*

NA	0 h	7 h	14 h
Saline	21.7 ± 1.5	7.1 ± 0.7*	9.5 ± 1.1*
Cycloheximide	27.2 ± 2.3	8.0 ± 2.0*	11.5 ± 2.0*

Table 4-3. DOPAC concentrations (ng/mg protein) in ME, ST and NA after a single injection MPTP with protein synthesis inhibition using cycloheximide. Male C57bl mice (n=8/group) were treated with 4 or 2 injections of cycloheximide (120 mg/kg; i.p.) or saline (10 ml/kg; i.p.) every 2 h, with the first cycloheximide injection 15 min prior to a single injection of MPTP (20 mg/kg; s.c.) or saline (10 ml/kg; s.c.). Animals receiving 4 cycloheximide injections were decapitated 14 h after MPTP and animals receiving 2 cycloheximide injections were decapitated 7 h post MPTP.

The Impact of Immediate vs. Delayed Protein Synthesis Inhibition on the Neurochemical Responses of NSDA, MLDA and TIDA Neurons to a Single Injection of MPTP:

Figure 4-18 demonstrates the effects of immediate and delayed cycloheximide treatment on DA concentrations in the ME in MPTP treated mice. DA levels in ME were similar to controls 16 h after treatment with MPTP. Cycloheximide alone had no affect on DA levels, but immediate and delayed cycloheximide treatment significantly decreased DA levels in ME in MPTP treated mice. As depicted in **Figure 4-19**, ST DA levels decreased 16 h after treatment with MPTP. Immediate or delayed treatment with cycloheximide along with MPTP also caused significant loss of DA; however, the magnitude of DA loss was significantly less in early cycloheximide + MPTP treatment than with MPTP alone. DA levels in NA decreased after treatment with MPTP in the control and immediate or delayed cycloheximide treated animals (**Figure 4-20**).

DOPAC levels mirrored DA levels following treatment with cycloheximide and MPTP (**Table 4-4**). DOPAC levels decreased in ST and NA after treatment with MPTP in control and immediate or delayed cycloheximide treated mice. Cycloheximide treatment alone did not alter DOPAC levels in NA, or ST. DOPAC levels were not determined due to experimental error.

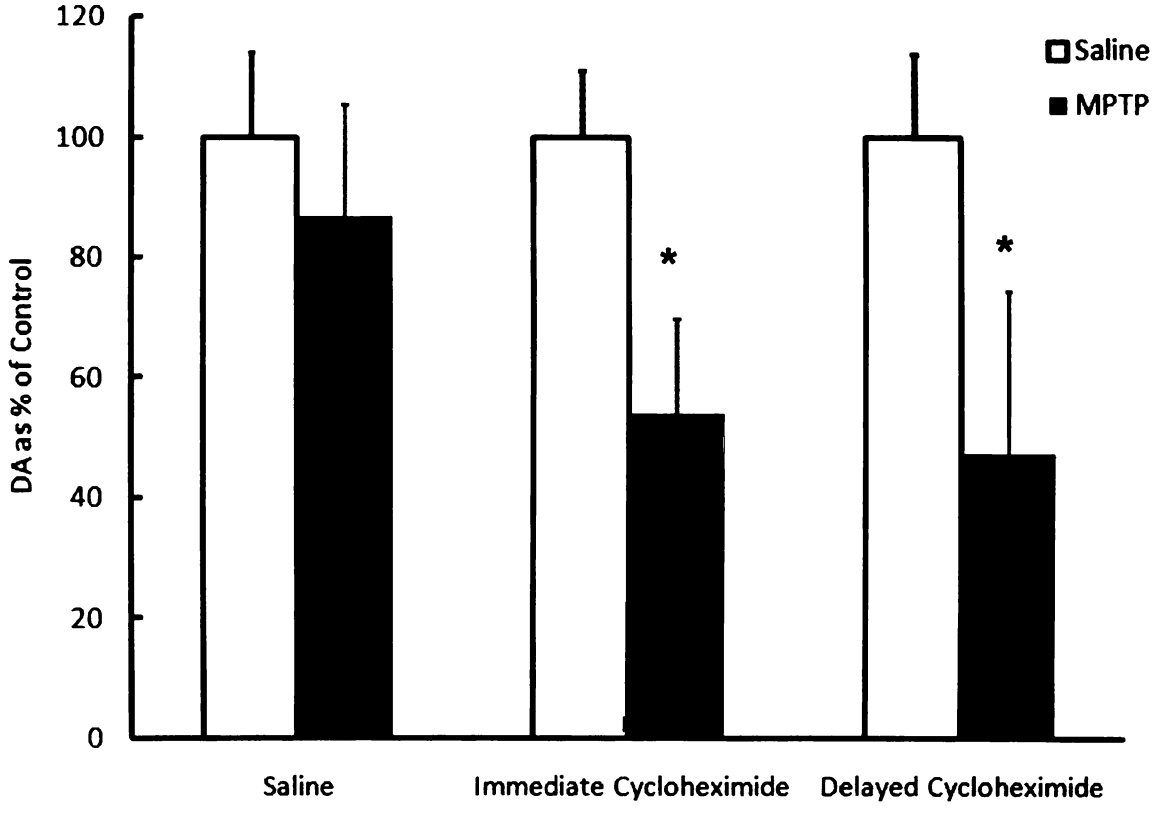

Figure 4-18. The effects of immediate and delayed cycloheximide and single injection MPTP on DA levels in ME. Male C57bl mice (n=8/group) were treated with 2 injections of cycloheximide (120 mg/kg) or saline (10 ml/kg; s.c.), 2h apart, starting either 15 min prior (A) to or 3 h 45 min after (B) a single injection of MPTP (20 mg/kg; s.c.) or saline (10 ml/kg; s.c.). All animals were decapitated 16 h after MPTP. DA levels are presented as % of saline/saline treated. Actual DA concentrations (ng/mg protein) in NA are as follows: saline/saline: 204±38, saline/early cycloheximide: 161±16, saline/late cycloheximide: 187±33, MPTP/saline: 152±22, MPTP/early cycloheximide: 114±15 and MPTP/late cycloheximide: 126± 53. Columns represent means of groups and vertical bars represent +1.0 standard error of the mean. (*) indicates values for MPTP treated mice that were significantly different ($p < 0.05$) from saline treated controls.

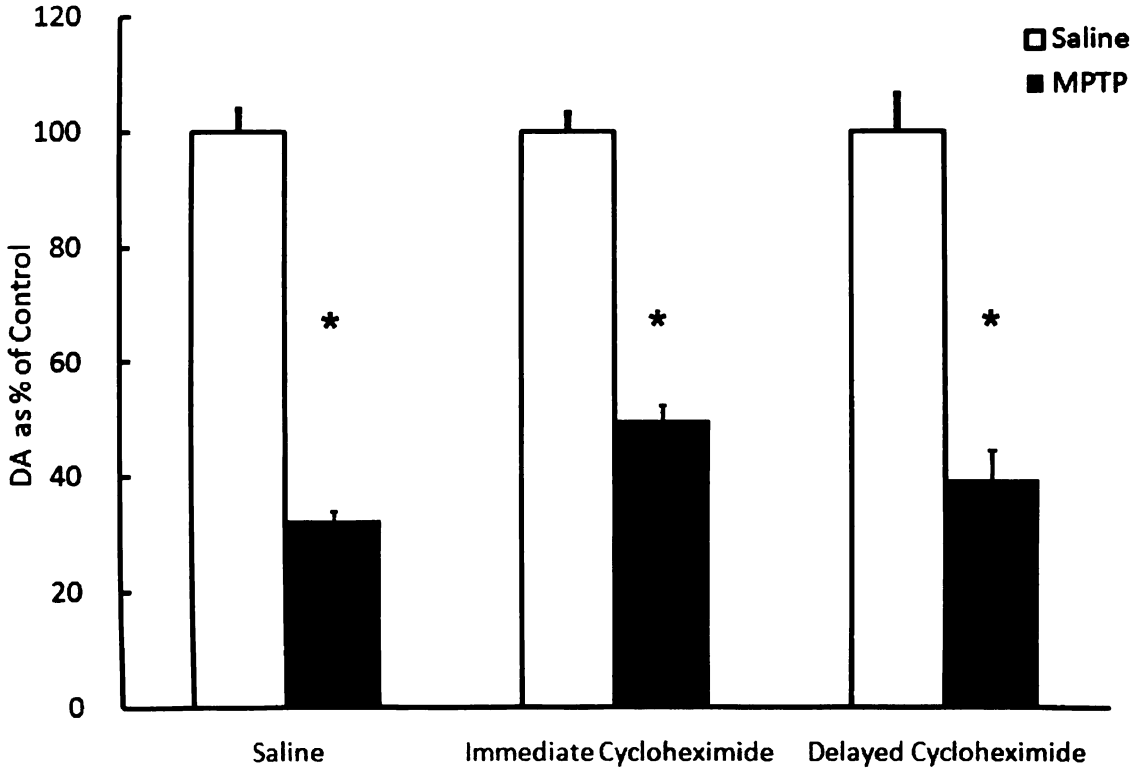

Figure 4-19. The effects of immediate and delayed cycloheximide and single injection MPTP on DA levels in ST. Male C57bl mice (n=8/group) were treated with 2 injections of cycloheximide (120 mg/kg) or saline (10 ml/kg; s.c.), 2 h apart, starting either 15 min prior (A) to or 3 h 45 min after (B) a single injection of MPTP (20 mg/kg; s.c.) or saline (10 ml/kg; s.c.). All animals were decapitated 16 h after MPTP. DA levels are presented as % of saline/saline treated. Actual DA concentrations (ng/mg protein) in ST are as follows in saline treated mice: saline/saline 155± 6, saline/early Cycloheximide: 150±9 and saline/late cycloheximide: 147±4, MPTP/saline: 50±5, MPTP/early cycloheximide: 73±7 and saline/late cycloheximide: 59±2. Columns represent means of groups and vertical bars represent +1.0 standard error of the mean. (*) indicates values for MPTP treated mice that were significantly different ($p < 0.05$) from saline treated controls.

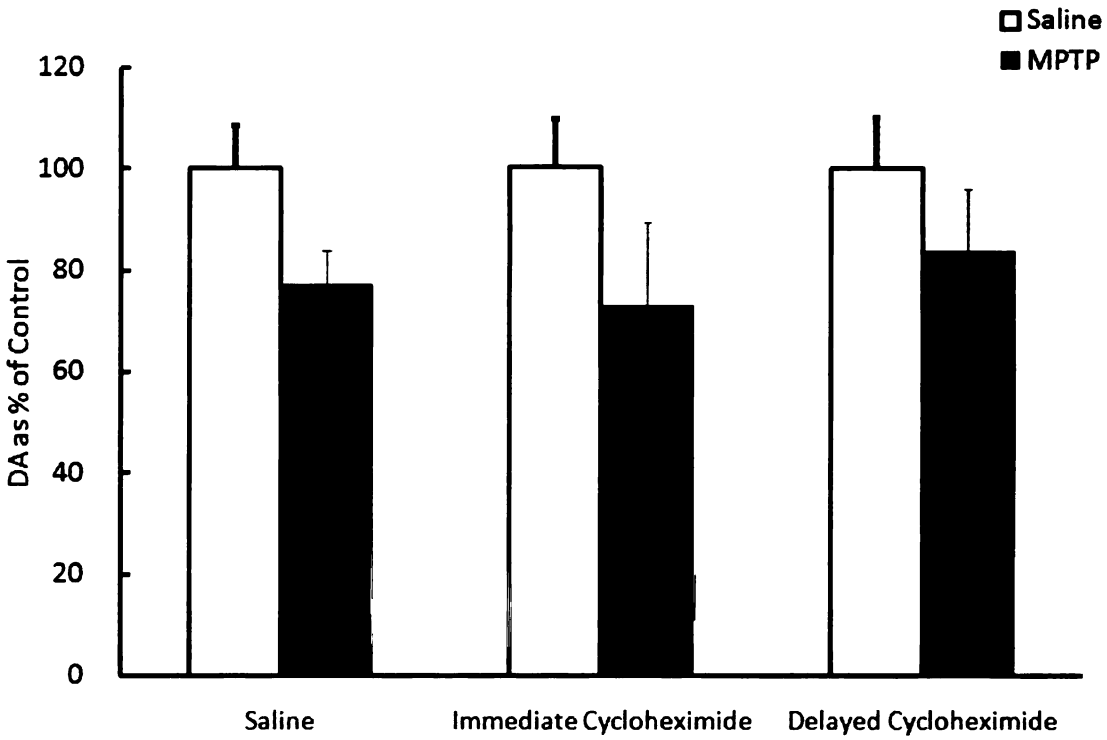

Figure 4-20. The effects of immediate and delayed cycloheximide and single Injection MPTP on DA levels in NA. Male C57bl mice (n=8/group) were treated with 2 injections of cycloheximide (120 mg/kg) or saline (10 ml/kg; s.c.), 2 h apart, starting either 15 min prior (A) to or 3 h 45 min after (B) a single injection of MPTP (20 mg/kg; s.c.) or saline (10 ml/kg; s.c.). All animals were decapitated 16 h after MPTP. DA levels are presented as % of saline/saline treated. Actual DA concentrations (ng/mg protein) in NA are as follows in saline/saline: 67±6, saline/early cycloheximide: 67±7, saline/late cycloheximide: 67±11, MPTP/saline: 53±7, MPTP/early cycloheximide: 56±4 and MPTP/late cycloheximide: 49±8. Columns represent means of groups and vertical bars represent +1.0 standard error of the mean. (*) indicates values for MPTP treated mice that were significantly different ($p < 0.05$) from saline treated controls.

DOPAC Concentrations in ME			
		Cycloheximide	
	Saline	Immediate	Delayed
Saline	ND	ND	ND
MPTP	ND	ND	ND

DOPAC Concentrations in ST			
		Cycloheximide	
	Saline	Immediate	Delayed
Saline	21.3 ± 3.4	24.2 ± 2.0	25.6 ± 2.0
MPTP	13.8 ± 0.8*	13.0 ± 0.2*	16.7 ± 2.0*

DOPAC Concentrations in NA			
		Cycloheximide	
	Saline	Immediate	Delayed
Saline	9.3 ± 1.5	12.2 ± 1.2	11.7 ± 2.0
MPTP	6.5 ± 0.8*	7.5 ± 1.0*	5.4 ± 2.0*

Table 4-4. DOPAC concentrations (ng/mg protein) in ST, NA and ME after a single injection MPTP with protein synthesis inhibition using cycloheximide. Male C57bl mice (n=8/group) were treated with 2 injections of cycloheximide (120 mg/kg) or saline (10 ml/kg; s.c.), 2 h apart, starting either 15 min prior (Immediate) to or 3h 45min after (Delayed) a single injection of MPTP (20 mg/kg; s.c.) or saline (10 ml/kg; s.c.). All animals were decapitated 16h after MPTP.

Discussion:

The experiments in this chapter characterize the time course of neurochemical events following toxin entry into TIDA, NSDA and MLDA neuronal populations. These experiments also address the differential mode of toxin entry into the DA neuronal populations as well as the dependency of their MPTP-induced response on synthesis of new proteins. These results are discussed in detail below.

Differential Response of TIDA, NSDA and MLDA Neurons After a Single Injection of MPTP

A novel temporal profile of neurotoxin-induced neurochemical changes is observed in TIDA, NSDA, and MLDA neurons after treatment with a single injection of MPTP. TIDA, NSDA and MLDA neurons respond in a similar fashion 4 h after treatment with MPTP exhibiting DA loss from their axon terminals. These responses, however, vary greatly after this time point and these differential responses may determine their fate.

TIDA neurons respond to MPTP exposure with a substantial DA loss from axon terminals 4 h after a single injection. This rapid loss of DA likely represents MPP^+-induced displacement of vesicular DA from the axon terminals rather than a reduction in density and integrity of terminals as observed in the chronic model. In agreement, the initial loss of DA in TIDA neurons is followed by a rapid recovery by 8 h that continues to up to 16 h after MPTP treatment. DOPAC levels mirror DA levels in this model and this loss of DOPAC is likely due to a combination of displacement of DA from vesicles and diffusion out of axon terminals, loss of ATP due to Complex I inhibition, as

well as inhibition of MAO by MPP+ (Takamidoh et al., 1987). The transient DA and DOPAC loss from this region correlates with the short half life of MPP+ in the brain (Langston and Irwin, 1986; Irwin et al., 1989; Cosi and Marien, 1999; Saporito et al., 2000). The rapid recovery of TIDA neurons from MPTP-induced DA loss provides a temporal window that may be examined to determine underlying mechanisms that allow for this recovery.

Consistent with previous reports (Pileblad et al., 1984; Pileblad et al., 1985), NSDA axon terminals also lose DA 4 h after MPTP treatment, but unlike TIDA neurons, they do not recover from MPTP toxicity for up to 32 h after toxin exposure. In fact, NSDA neurons have ongoing DA loss between 4 and 8 h post MPTP-injection, during which time TIDA neurons are rapidly recovering. DOPAC levels also mirror DA levels in ST and this loss of DOPAC, at least for up to 8 h after treatment, while MPP+ is present, is likely due to both loss of DA that can be converted to DOPAC and inhibition of MAO by MPTP/MPP+.

These experiments also confirm that MLDA neurons are partially resistant to the toxic effects of MPTP. The initial response of MLDA neurons after 4 h is very similar to that of NSDA neurons, but NSDA terminals continue to lose DA between 4 and 8 h, whereas MLDA terminals maintain moderate DA levels. MLDA neurons, however, do not show the rapid recovery that TIDA neurons experience at 8 and 16 h after MPTP injection. Similar to that observed in TIDA and NSDA neurons, DOPAC levels mirror DA levels in the NA demonstrating lower metabolism of DA due to loss of DA as well as inhibition of MAO by MPTP/MPP+. These results support the hypothesis that MLDA

neurons may be composed of a heterogeneous group of neurons; some that display resistance and some that are vulnerable to neurotoxic insult and do not recover, whereas TIDA neurons are homogeneously resistant. There is some evidence for this hypothesis, as a group of MLDA neurons that express the protein calbindin are protected from MPTP-induced toxicity (Lavoie and Parent, 1991; Lavoie et al., 1991; Parent and Lavoie, 1993).

NE levels remain unchanged in the ME and NA suggesting that MPP+ does not enter noradrenergic neurons via the NE transporter in sufficient quantities to disrupt neurotransmitter stores. This explains why noradrenergic neurons are not lesioned after chronic treatment with MPTP in experiments described in Chapter 3. 5-HT concentrations, on the other hand, increase by 4 h after treatment with MPTP, but only in ST. It is unlikely that this change in 5-HT concentrations is due to a direct effect of MPP+ on these neurons. If MPP+ entered these neurons in sufficient amounts to cause damage, the neurotransmitter levels would have decreased so it is likely that the increase in 5-HT levels is actually due to indirect effects of DA systems on the serotoninergic neurons. It is known that 5-HT release both in SNpc and in ST act on 5-HT 2B/C receptors on NSDA cell bodies and axon terminals to inhibit DA release (De Deurwaerdere et al., 1996; De Deurwaerdere and Spampinato, 1999). It is therefore not surprising that large displacement of DA from NSDA axon terminals would cause activation of this "brake" system.

Mechanism of MPP+ uptake is different in TIDA neurons vs. NSDA and MLDA neurons:

The time-course of toxin-induced neurochemical changes in TIDA neurons suggests that, even though DAT expression is low in TIDA terminals (Demarest and Moore, 1979a, 1979b), MPP+ entry into these cells is sufficient to disrupt neurotransmitter storage. Treatment with the DAT blocker GBR has no affect in MPTP-induced DA loss in TIDA axon terminals, revealing that MPP+ enters these cells via DAT-independent mechanisms. Furthermore, blocking DAT does not change DOPAC concentrations in the ME, consistent with the conclusion that TIDA neurons do not utilize DAT for uptake of extracellular DA under basal conditions (Demarest and Moore, 1979b, 1979a).

One way that MPP+ could gain access inside TIDA neurons is through direct conversion of MPTP to MPP+ by MAO located inside these cells. However, this remains an unlikely explanation because NSDA and MLDA neurons also express MAO but do not show this DAT-independent response to MPTP. Furthermore, since TIDA neurons have a lower DOPAC/DA ratio than NSDA or MLDA neurons, it is unlikely that MAO is more active or has higher expression in these neurons. It is also unlikely that MPP+ is entering these neurons via non-specific transporters, since other neuronal populations, including 5-HT or NE neuronal types, do not show neurotransmitter loss in response to MPTP treatment. It is possible that MPP+ enters TIDA neurons via a specific transporter that is unique to these neurons. Although not well characterized, a unique high volume, low affinity transporter has been described in TIDA neurons (Annunziato et al., 1980), supporting the hypothesis that a unique mode of MPP+ entry may exist in

these neurons. Lack of specific antibodies, agonists or antagonists to characterize this transporter makes it difficult to test this hypothesis. It is possible that the fate of molecules taken up via this unique transporter is different from those taken up by DAT. For example, molecules taken up via this transporter may be more or less likely to be packaged inside vesicles or metabolized. It is, however, unlikely that MPP+ sequestration into vesicles plays a role in the differential susceptibility of these neurons since a similar pattern of susceptibility can be observed with toxins such as rotenone that are not transported into synaptic vesicles (Betarbet et al., 2000; Behrouz et al., 2007).

In accordance with previous reports (Pileblad and Carlsson, 1985), NSDA and MLDA neurons showed complete protection against MPTP-induced DA loss, suggesting that entry via DAT is the only way sufficient amounts of MPP+ can enter these neurons. This difference in response between TIDA neurons and NSDA or MLDA neurons suggests that MPP+ enters TIDA neurons via different mechanisms. Moreover, DOPAC levels in ST were significantly decreased after GBR alone, supporting previous data that demonstrates NSDA neurons normally utilize DAT to uptake extracellular DA (Bannon, 2005). On the other hand, DOPAC levels in NA do not decrease after GBR treatment alone, suggesting that either less DA is taken up through DAT in these neurons or that DA normally taken up through DAT in MLDA neurons may be more efficiently packaged. Previous reports that demonstrate lower levels of DAT expression in MLDA neurons than NSDA neurons support the former of the two possibilities (Freed et al., 1995; Haber et al., 1995).

Recovery of TIDA Neurons is Dependent on Synthesis of New Proteins after MPTP Treatment:

Since the axon terminals of TIDA neurons are outside the blood brain barrier, they are likely exposed to toxic chemicals and oxidative stress to a greater extent than NSDA or MLDA neurons. It is evolutionarily sensible that these neurons have a mechanism in place that protects them from extracellular stresses and allows recovery from neurotoxin-induced toxicity. The experiments in this chapter demonstrate that inhibition of protein synthesis blocks the ability of TIDA neurons to recover by 16 h post-treatment. This suggests that TIDA neurons may constitutively synthesize or upregulate expression of protective proteins in response to MPTP exposure. These experiments also demonstrate that blocking protein synthesis either immediately or 4 h after treatment with MPTP blocks the ability of TIDA neurons to recovery from MPTP-induced DA loss. Since low levels of DA in TIDA terminals at 4 h are likely to lead to increased prolactin secretion from the anterior pituitary, which in turn feed back to increase the activity of TIDA neurons, it would be plausible to hypothesize that prolactin may be responsible for the recovery of these neurons. It has been previous demonstrated, however, that the immediate prolactin control over TIDA neuron activity is not dependent on protein synthesis. Only after 16 h following prolactin changes this control become dependent on synthesis of new proteins. Since the recovery of these neurons is dependent on synthesis of new proteins, prolactin control is unlikely to be responsible for this recovery.

On the other hand, blocking protein synthesis in NSDA neurons does not alter their neurochemical profile 7 or 14 h after treatment with MPTP. This suggests that synthesis of new proteins following treatment with MPTP does not play a role in causing the deleterious effects observed at this time point. This is perhaps not surprising, since the immediate response of all neurons is to maintain homeostasis and perform their function. Instead, it is likely that NSDA neurons lack the neuroprotective mechanisms that are in place in TIDA neurons.

General Conclusions

The experiments in this chapter reveal that TIDA neurons have protein synthesis dependent protective mechanisms that are activated in response to treatment with MPTP. The timeline of this recovery has been established. Studying these neurons 8 h after treatment with MPTP should prove useful in identifying proteins that infer protection to these neurons. Indeed, 8 h after MPTP the susceptible NSDA neurons are disrupted but are still viable. This makes the sampling of neurons 8 h after MPTP treatment a very attractive model for further comparison of the properties of NSDA and TIDA neurons.

MLDA neurons lie somewhere between the fully resistant TIDA and susceptible NSDA neurons. Based on the neurochemical profile of these neurons after treatment with a single injection of MPTP (or chronic repeated exposure as shown in Chapter 3) it is likely that there is a heterogeneous population of these neurons, one that is susceptible to neurotoxic insult (like NSDA neurons) and another that is resistant (like

TIDA neurons). Without knowing the phenotype that makes some of these neurons resistant and some susceptible, it would be difficult to assess their protective properties especially if these populations are heterogeneously distributed within the VTA rather than clustered into discrete groups.

Gene expression differences in key cellular pathways may account for the differential susceptibility of TIDA and NSDA neurons to cell death. A recent study providing an initial analysis of gene expression profile comparisons of NSDA and MLDA neurons suggested several molecular pathways that may be involved in neuroprotection (Greene et al., 2005). These pathways include energy metabolism, neuropeptide neurotransmission, and aberrant kinase or phosphatase signaling pathways. Studying gene expression profiles of TIDA neurons would undoubtedly identify novel neuroprotective properties that are distinct from those observed in NSDA neurons. Identification of protective and deleterious properties in DA neuronal populations with divergent responses to neurotoxins can provide a method to discover targets that can subsequently be translated into neuroprotective treatments for patients with PD.

Chapter 5: Characterization of the Genomic Responses of TIDA and NSDA Neurons to a Single Injection of MPTP

F. Introduction

The previous chapter demonstrated that treatment with a single systemic injection of MPTP causes loss of DA from axon terminals of TIDA and NSDA neurons, but that only TIDA neurons are able to recover from this DA loss. Moreover, the recovery of TIDA neurons was demonstrated to be dependent on synthesis of new proteins. It's unclear what proteins are responsible for the recovery of TIDA neurons. Identification of genes with increased expression following MPTP in TIDA neurons will allow for functional studies aimed at determining which proteins protect TIDA neurons from MPTP toxicity. The results from these studies may be exploited in the development of strategies to protect NSDA neurons from toxicity.

The objective of the experiments outlined in this chapter is to determine the genomic profile of TIDA and NSDA neurons under normal basal conditions and 8 h after treatment with MPTP when NSDA neurons continue to lose axon terminal DA while TIDA neurons are rapidly recovering from DA loss.

G. Hypothesis:

The experiments in this chapter test the hypothesis that several genes are upregulated in the resistant TIDA neurons, but not susceptible NSDA neurons, in response to treatment with systemic MPTP.

H. Experimental Procedures

Mice were treated with a single injection of MPTP (20 mg/kg; s.c.) or saline (10 ml/kg; s.c.) and killed by decapitation 8 h later. Immediately after decapitation brains were removed in RNase free conditions and frozen on dry ice. Sections (10 μm) through the hypothalamus and midbrain were obtained and rapidly stained for TH, and 300-500 TH-immunofluorescent cells were microdissected from ARC and SNpc of each animal using LCM. RNA was isolated for each region and amplified linearly. Amplified RNA for each sample was biotin labeled and hybridized to an Affymetrix Mouse 430 2.0 genechip. Data was analyzed using the software R. The details of methods for animal use, drug administration, tissue preparation, rapid immunofluorescent staining, LCM, RNA isolation and amplification, microarray hybridization and analysis, reverse transcription and quantitative real time PCR are described in Chapter 2 (Methods, Sections. A-D; H-M).

For real time PCR experiments, mice were treated with a single systemic injection of MPTP (20 mg/kg; s.c.) or saline (10 ml/kg; s.c.) and killed by decapitation 8 h later. Immediately after decapitation brains were removed in RNase free conditions and frozen on dry ice. Sections (500 μm) were obtained and the ARC and SNpc were microdissected and RNA was collected from each sample. mRNA was reverse transcribed and real time PCR was performed to assess expression levels of each gene. The details of methods for animal use, drug administration, tissue preparation, reverse

transcription and quantitative real time PCR are described in Chapter 2 (Methods, Sections. A-D; N-Q).

I. Results

Genes with Differential Expression in ARC and SNpc in Control and MPTP Treated Mice

The number of genes with an adjusted p-value of 0.05 or less that were differentially expressed between ARC and SNpc by at least 2 fold (log_2 1 fold) were determined (**Figure 5-1**). The details of these genes are available in the Appendix. **Figure 5-2** demonstrates the number of genes significantly higher in ARC or SNpc under control conditions and 8 h after treatment with a single injection of MPTP. Overall, 348 genes had higher expression in ARC than SNpc in control animals, 254 of which also had higher expression in ARC 8 h after treatment with MPTP. There were 156 genes with higher expression in ARC when compared to SNpc after treatment with MPTP but not in saline treated controls. Under control conditions, 309 genes were expressed in higher levels in SNpc, and 253 of these genes had higher expression in SNpc even after treatment with MPTP. There were 153 genes with higher expression in SNpc when compared to ARC of MPTP treated but not saline treated controls.

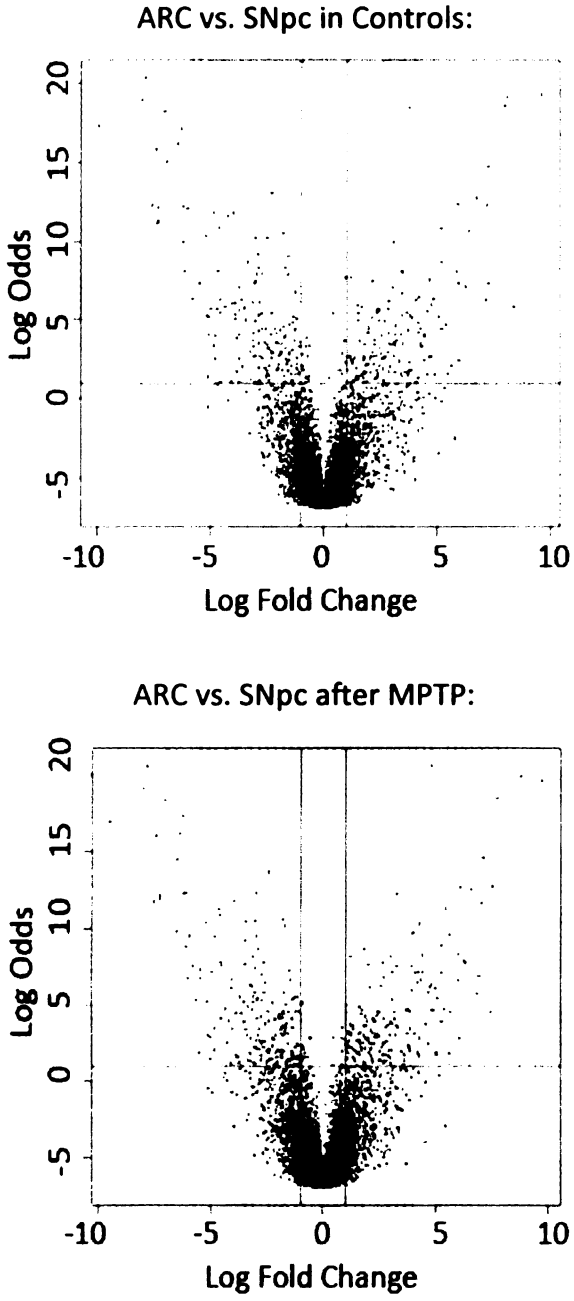

Figure 5-1: The pattern of expression of genes differentially expressed among regions in the control (top) and MPTP treated (bottom) animals. Male mice (n=8/group) were treated with a single injection of MPTP (20 mg/kg; s.c.) or saline (10 ml/kg; s.c.). All animals were killed 8 h after MPTP or saline treatment. Amplified mRNA from 300-500 laser-captured TH immunofluorescent cells from ARC and SNpc of each mouse were hybridized to an Affymetrix mouse 430 2.0 chip. Data was normalized and genes that were significantly different between the two regions by at least 2 fold were identified.

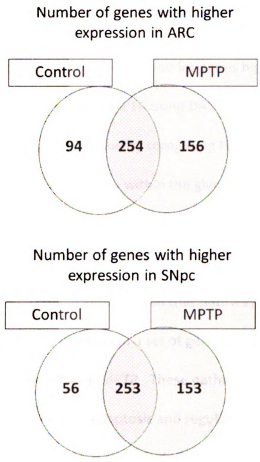

Figure 5-2: The number of genes with statistically higher expression in ARC (top) and SNpc (bottom) under control and MPTP treated conditions. Male mice (n=8/group) were treated with a single injection of MPTP (20 mg/kg; s.c.) or saline (10 ml/kg; s.c.). All animals were killed 8 h after MPTP or saline treatment. Amplified mRNA from 300-500 laser-captured TH immunofluorescent cells from ARC and SN of each mouse were hybridized to an Affymetrix mouse 430 2.0 chip. Data was normalized and genes that were significantly different between the two regions by at least 2 fold were identified.

Unbiased Pathway Analysis of Microarray Data with DAVID:

Unbiased pathway analysis was performed for genes higher in ARC when compared to SNpc after treatment with MPTP using DAVID annotation tools. DAVID uses a modification of Fisher Exact P-value by comparing the ratio of the occurrence rate of each Gene Ontology (GO) pathway within the given gene list to the ratio of occurrence of the pathway within the entire genome by chance alone. The GO pathways that had significantly higher occurrence than would be expected by chance alone were identified ($P \leq 0.05$) and genes within that pathway were further analyzed. **Table 5-1** depicts biological GO pathways in a set of genes that were significantly higher in ARC than SNpc after treatment with MPTP. These pathways include general cellular processes, RNA metabolic processes, apoptosis and regulators of gene expression. The number of genes that overlap within each biological pathway are indicated in **Table 5-1**. **Figure 5-3** demonstrates the relative expression levels of genes that overlap with the apoptosis pathway and have higher expression in ARC following treatment with MPTP. The genes apolipoprotein E, HSPA1A, Kainate 2 glutamate receptor, BCL-2 associated anthanogene 3, FC receptor, CD1D1 antigen, angiopietin-like 4, SIR2 α, mitogen activated protein kinase 7, and TAIL1 are all proteins that regulate apoptosis and had higher expression in ARC when compared with SNpc after treatment with MPTP but not in saline treated controls.

DAVID annotation tools were also utilized to examine differences between SNpc and ARC levels in saline treated controls. Several general and specific pathways were

implicated and are listed in **Table 5-2**. These pathways include general synaptic transmission as well as neurotransmitter metabolism and secretion amongst others. The genes listed on this table that were specific to DA metabolism, transport and secretion are depicted in **Figure 5-4**. These results confirm previous findings that D2 receptors and DAT have higher expression in NSDA neurons when compared to TIDA neurons. Other DA related genes that had higher expression in SNpc when compared to ARC were synphilin, TH, nuclear receptor 4A2, synaptic vesicle glycoprotein 2C, complexin 1, VMAT-2, islet cell autoantigen 1 and nicotinic cholinergic receptors α4 and α6.

Gene Ontology Pathway	# of genes in pathway	P-value
GO:0065007~biological regulation	46	7.25E-05
GO:0050789~regulation of biological process	43	9.33E-05
GO:0050794~regulation of cellular process	39	2.87E-04
GO:0010467~gene expression	31	0.005062
GO:0016070~RNA metabolic process	26	0.011584
GO:0009987~cellular process	83	0.015522
GO:0048518~positive regulation of biological process	13	0.017751
GO:0006915~apoptosis	10	0.020681
GO:0012501~programmed cell death	10	0.022838
GO:0008380~RNA splicing	5	0.025273
GO:0008219~cell death	10	0.028062
GO:0009605~response to external stimulus	8	0.028087
GO:0016265~death	10	0.028496
GO:0042108~positive regulation of cytokine biosynthetic process	3	0.029302
GO:0006139~nucleobase, nucleoside, nucleotide and nucleic acid metabolic process	30	0.029917
GO:0010468~regulation of gene expression	23	0.030603
GO:0019222~regulation of metabolic process	24	0.036963
GO:0007268~synaptic transmission	5	0.036987
GO:0048522~positive regulation of cellular process	11	0.03955
GO:0045727~positive regulation of translation	3	0.039564
GO:0006350~transcription	22	0.039712
GO:0045059~positive thymic T cell selection	2	0.040871
GO:0043368~positive T cell selection	2	0.040871
GO:0031323~regulation of cellular metabolic process	23	0.044313
GO:0031328~positive regulation of cellular biosynthetic process	3	0.045134

Table 5-1: DAVID Pathway analysis of genes expressed higher in ARC than SNpc after treatment with MPTP. Male mice (n=8/group) were treated with a single injection of MPTP (20 mg/kg; s.c.) or saline (10 ml/kg; s.c.) and killed 8 h later. Amplified mRNA from 300-500 laser-captured TH immunofluorescent cells from ARC and SNpc of each animal were hybridized to an Affymetrix mouse 430 2.0 chip. Data was normalized and pathway analysis was performed for genes that were significantly higher in ARC than SNpc after MPTP treatment. The biological Gene Ontology (GO) pathways that had the most genes of interest were determined and are listed above.

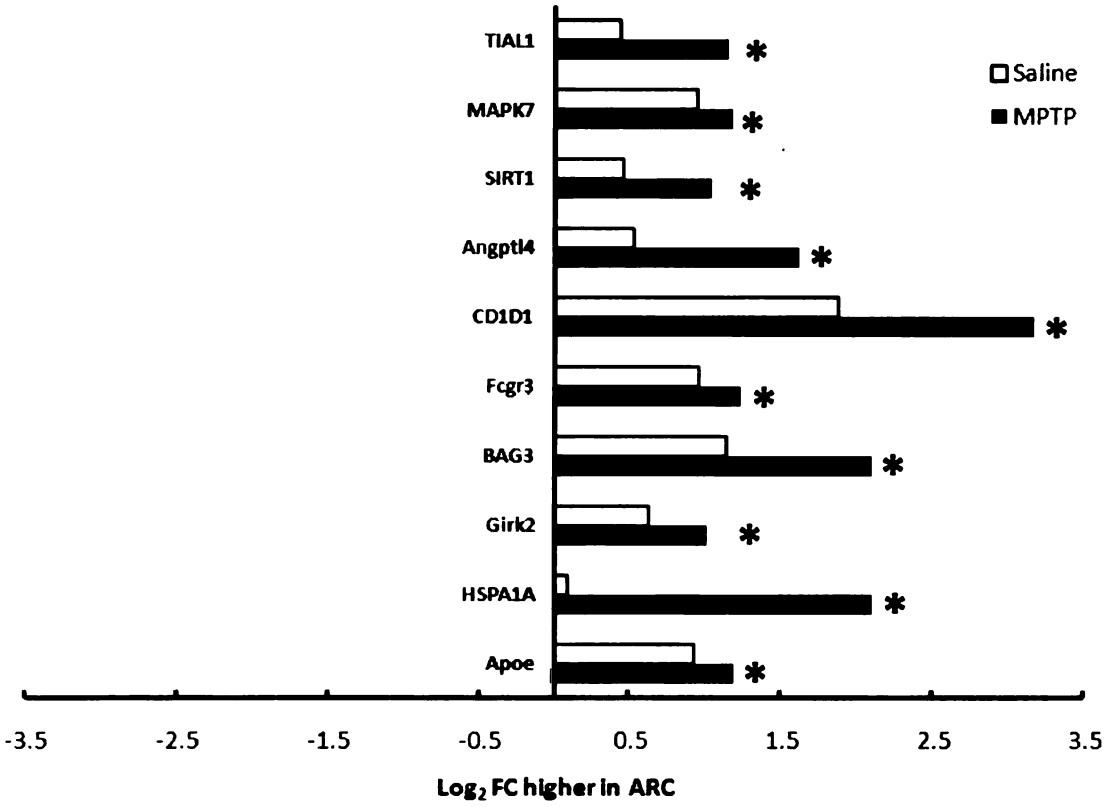

Figure 5-3. Relative expression levels of genes that regulate apoptosis in ARC vs. SNpc of saline and MPTP treated mice. Male mice (n=8/group) were treated with a single injection of MPTP (20 mg/kg; s.c.) or saline (10 ml/kg; s.c.) and killed 8 h later. Amplified mRNA from 300-500 laser-captured TH immunofluorescent cells from ARC and SNpc of each animal were hybridized to an Affymetrix mouse 430 2.0 chip. Data was normalized and DAVID annotation tools were utilized to determine important biological pathways. Genes involved in regulation of apoptosis are depicted here. Horizontal bars represent means of groups and (*) indicates values of expression levels in ARC that were significantly ($p \leq 0.05$) higher than SNpc of the same animals.

Table 5-2: DAVID Pathway analysis of genes higher in SNpc than ARC only after treatment with MPTP. Male mice (n=8/group) were treated with a single injection of MPTP (20 mg/kg; s.c.) or saline (10 ml/kg; s.c.) and killed 8 h later. Amplified mRNA from 300-500 laser-captured TH immunofluorescent cells from ARC and SNpc of each animal were hybridized to an Affymetrix mouse 430 2.0 chip. Data was normalized and pathway analysis was performed for genes that were significantly higher in SNpc than ARC in saline treated controls. The biological Gene Ontology (GO) pathways that had the most genes of interest were determined and are listed above.

Gene Ontology Pathway	# of genes in pathway	P-value
GO:0019226~transmission of nerve impulse	17	0.00
GO:0007268~synaptic transmission	15	0.00
GO:0001505~regulation of neurotransmitter levels	11	0.00
GO:0046928~regulation of neurotransmitter secretion	6	0.00
GO:0007267~cell-cell signaling	17	0.00
GO:0007271~synaptic transmission, cholinergic	5	0.00
GO:0007269~neurotransmitter secretion	7	0.00
GO:0042417~dopamine metabolic process	5	0.00
GO:0045055~regulated secretory pathway	7	0.00
GO:0044255~cellular lipid metabolic process	18	0.00
GO:0006584~catecholamine metabolic process	5	0.00
GO:0018958~phenol metabolic process	5	0.00
GO:0014070~response to organic cyclic substance	4	0.00
GO:0042133~neurotransmitter metabolic process	5	0.00
GO:0030534~adult behavior	6	0.00
GO:0051046~regulation of secretion	6	0.00
GO:0043279~response to alkaloid	4	0.00
GO:0003001~generation of a signal involved in cell-cell signaling	7	0.00
GO:0006629~lipid metabolic process	18	0.00
GO:0006776~vitamin A metabolic process	4	0.00
GO:0006066~alcohol metabolic process	11	0.00
GO:0007399~nervous system development	18	0.00
GO:0014059~regulation of dopamine secretion	3	0.00
GO:0014046~dopamine secretion	3	0.00
GO:0045045~secretory pathway	10	0.00
GO:0050433~regulation of catecholamine secretion	3	0.00
GO:0035094~response to nicotine	3	0.00
GO:0006775~fat-soluble vitamin metabolic process	4	0.00
GO:0006836~neurotransmitter transport	5	0.00
GO:0042391~regulation of membrane potential	5	0.00
GO:0022008~neurogenesis	12	0.00
GO:0007628~adult walking behavior	4	0.00
GO:0007626~locomotory behavior	9	0.00
GO:0050432~catecholamine secretion	3	0.00
GO:0035264~multicellular organism growth	5	0.00
GO:0032940~secretion by cell	10	0.00
GO:0048699~generation of neurons	11	0.00

Table 5-2 continued Gene Ontology Pathway	# of genes in pathway	P-value
GO:0048699~generation of neurons	11	0.00
GO:0048666~neuron development	9	0.00
GO:0048878~chemical homeostasis	9	0.01
GO:0051179~localization	48	0.01
GO:0030182~neuron differentiation	10	0.01
GO:0050801~ion homeostasis	8	0.01
GO:0008202~steroid metabolic process	7	0.01
GO:0008610~lipid biosynthetic process	9	0.01
GO:0007417~central nervous system development	9	0.01
GO:0010033~response to organic substance	4	0.01
GO:0006694~steroid biosynthetic process	5	0.01
GO:0051234~establishment of localization	43	0.01
GO:0006576~biogenic amine metabolic process	5	0.01
GO:0006810~transport	42	0.01
GO:0048732~gland development	5	0.01
GO:0030902~hindbrain development	4	0.01
GO:0001964~startle response	3	0.01
GO:0006725~aromatic compound metabolic process	6	0.01
GO:0007610~behavior	10	0.01
GO:0055082~cellular chemical homeostasis	7	0.01
GO:0006873~cellular ion homeostasis	7	0.01
GO:0046903~secretion	10	0.01
GO:0008344~adult locomotory behavior	4	0.01
GO:0048856~anatomical structure development	34	0.01
GO:0046879~hormone secretion	4	0.02
GO:0021983~pituitary gland development	3	0.02
GO:0050793~regulation of developmental process	9	0.02
GO:0006575~amino acid derivative metabolic process	5	0.02
GO:0051899~membrane depolarization	3	0.02
GO:0035270~endocrine system development	4	0.02
GO:0042445~hormone metabolic process	5	0.02
GO:0021536~diencephalon development	3	0.02
GO:0009653~anatomical structure morphogenesis	22	0.02
GO:0040014~regulation of multicellular organism growth	4	0.02
GO:0022604~regulation of cell morphogenesis	4	0.02
GO:0022603~regulation of anatomical structure morphogenesis	4	0.02

Table 5-2 continued Gene Ontology Pathway	# of genes in pathway	P-value
GO:0008360~regulation of cell shape	4	0.02
GO:0042592~homeostatic process	10	0.02
GO:0007420~brain development	7	0.02
GO:0019725~cellular homeostasis	8	0.02
GO:0065008~regulation of biological quality	15	0.03
GO:0040018~positive regulation of multicellular organism growth	3	0.03
GO:0009058~biosynthetic process	23	0.03
GO:0000902~cell morphogenesis	12	0.03
GO:0032989~cellular structure morphogenesis	12	0.03
GO:0007270~nerve-nerve synaptic transmission	3	0.03
GO:0006766~vitamin metabolic process	4	0.04
GO:0042416~dopamine biosynthetic process	2	0.04

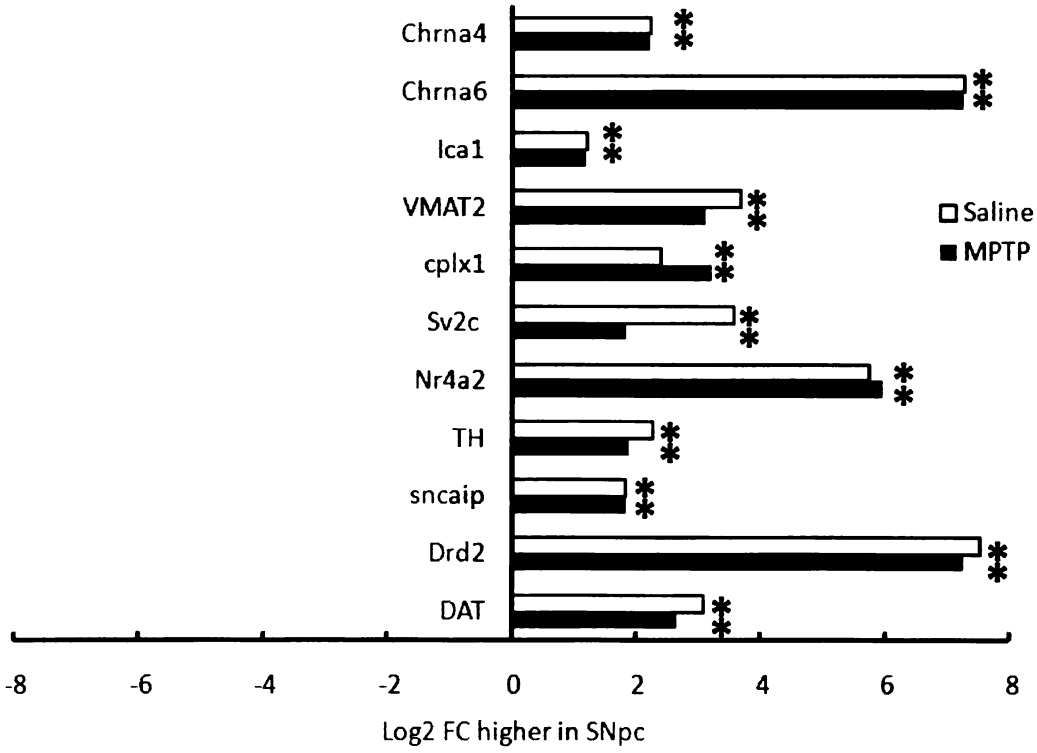

Figure 5-4: Expression levels of genes related to DA metabolism, transport and secretion in ARC vs. SNpc of Saline and MPTP treated Mice. Male mice (n=8/group) were treated with a single injection of MPTP (20 mg/kg; s.c.) or saline (10 ml/kg; s.c.) and killed 8 h later. Amplified mRNA from 300-500 laser-captured TH immunofluorescent cells from ARC and SNpc of each animal were hybridized to an Affymetrix mouse 430 2.0 chip. Data was normalized and DAVID annotation tools were utilized to determine important biological pathways. Genes involved in DA metabolism, transport and secretion are depicted here. Horizontal bars represent means of groups and (*) indicates values of expression levels in SNpc that were significantly higher ($p \leq 0.05$) than ARC of the same animals.

Cluster Analysis of Genes Significantly Higher in ARC than SNpc in MPTP-Treated Mice

Hierarchial cluster analysis was performed for genes with higher expression in ARC than SNpc after treatment with MPTP. **Figure 5-5** depicts the pattern of expression of a small cluster of genes that increase expression in ARC but not SNpc after treatment with MPTP. Further analysis of this small cluster using DAVID demonstrated that at least 2 of these 15 genes, HSP1A and HSP 8, are chaperones that respond to cellular stress and are involved in pathways such as responding to protein stimulus or unfolded (or misfolded) proteins (**Table 5-3**).

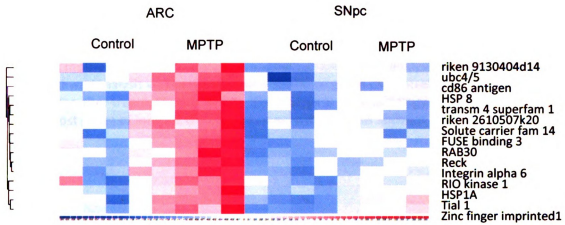

Figure 5-5: Cluster Analysis of genes up-regulated in ARC but not SNpc after treatment with MPTP. Male mice (n=8/group) were treated with a single injection of MPTP (20 mg/kg; s.c.) or saline (10 ml/kg; s.c.) and killed 8 h later. Amplified mRNA from 300-500 laser-captured TH immunofluorescent cells from ARC and SNpc of each animal were hybridized to an Affymetrix mouse 430 2.0 chip. Data was normalized and cluster analysis was performed to identify genes with similar expression patterns. A cluster was identified with genes that have higher expression in ARC after MPTP than in Controls. Blue = low expression, white = moderate expression, and red = high expression.

GO pathway	Genes implicated	P-value
GO:0051789~response to protein stimulus	HSP1A, HSP8	0.04
GO:0006986~response to unfolded protein	HSP1A, HSP8	0.04

Table 5-3: DAVID Pathway analysis of genes higher in SNpc than ARC only after treatment with MPTP. Male mice (n=8/group) were treated with a single injection of MPTP (20 mg/kg; s.c.) or saline (10 ml/kg; s.c.) and killed 8 h later. Amplified mRNA from 300-500 laser-captured TH immunofluorescent cells from ARC and SNpc of each animal were hybridized to an Affymetrix mouse 430 2.0 chip. Data was normalized and cluster analysis was performed using dCHIP. Pathway analysis was performed for a cluster of genes that increased expression in ARC but not SNpc after treatment with MPTP. The biological Gene Ontology (GO) pathways that had the most genes of interest were determined and are listed above.

Analysis of Candidate Genes

There have been several genes linked to PD. The relative expression levels of these candidate genes were determined in SNpc and ARC of control and MPTP treated animals and are depicted in **Figure 5-6**. Synphilin had higher expression in SNpc under both saline and MPTP treatment and α-synuclein had higher expression in SNpc only after treatment with MPTP. None of the genes analyzed were significantly higher in ARC when compared to SNpc of control or MPTP-treated animals.

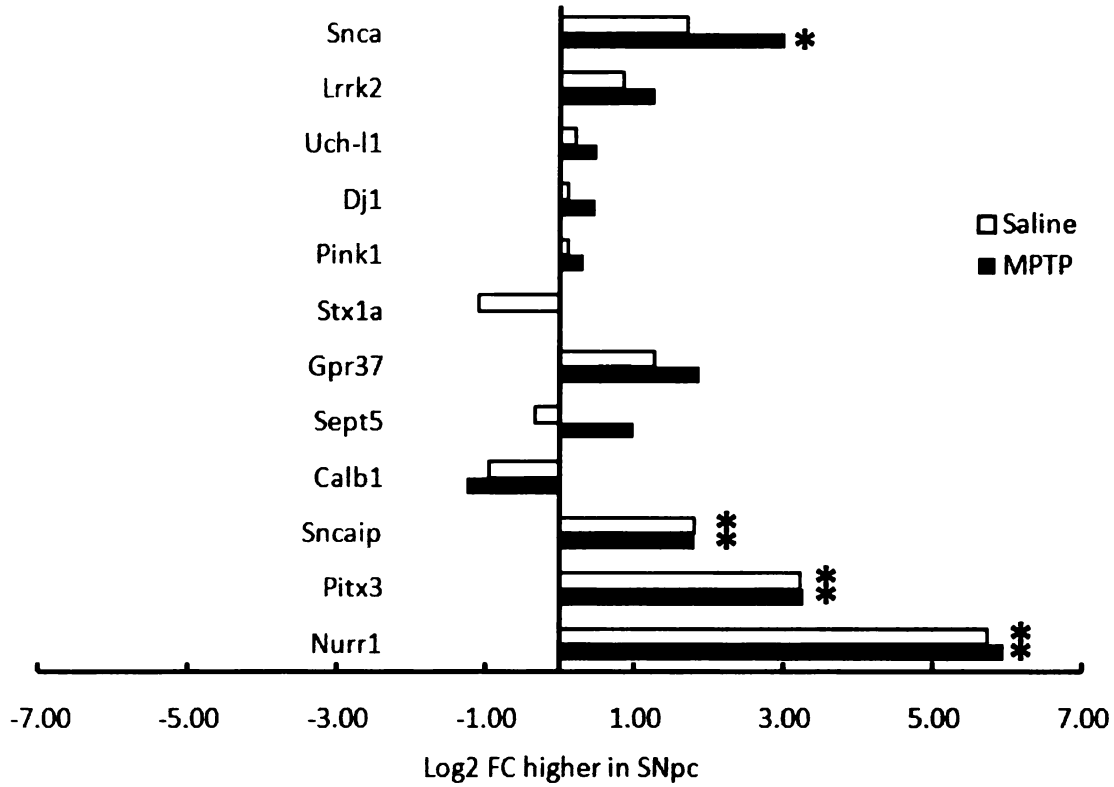

Figure 5-6: Expression levels of Parkinson's disease related genes in ARC vs. SNpc of Saline and MPTP treated Mice. Male mice (n=8/group) were treated with a single injection of MPTP (20 mg/kg; s.c.) or saline (10 ml/kg; s.c.) and killed 8 h later. Amplified mRNA from 300-500 laser-captured TH immunofluorescent cells from ARC and SNpc of each animal were hybridized to an Affymetrix mouse 430 2.0 chip. Data was normalized and genes that have been implicated in Parkinson's disease were identified. Horizontal bars represent means of groups and (*) indicates values of expression levels in SNpc that were significantly different ($p < 0.05$) from ARC of the same animals. SNCA = α-synuclein, LRRK2 = Leucine rich repeat kinase, UCH-L1 = Ubiquitin carboxyl-terminal esterase L1, DJ1 = oncogene DJ1, Pink1 = PTEN induced putative kinase 1, pitx3 = Paired-like homeodomain transcription factor 3, and Nurr1 = Nuclear receptor subfamily 4, group A, member 2.

Real Time PCR Analysis of Candidate Genes

The mRNA expression levels of candidate genes were analyzed in tissue punches containing ARC and SNpc of control and MPTP-treated mice using real time PCR. **Figure 5-7** demonstrates that parkin mRNA was significantly increased after treatment with MPTP in ARC, but not in SNpc. UCH-L1 levels also increased following treatment with MPTP in ARC, but remain unchanged in SNpc (**Figure 5-8**). Several other genes including LRRK2, synuclein, DJ1 and Pink1 had no change in expression after treatment with MPTP (**Table 5-4**). All of the examined genes had similar expression levels between ARC and SNpc in saline treated controls.

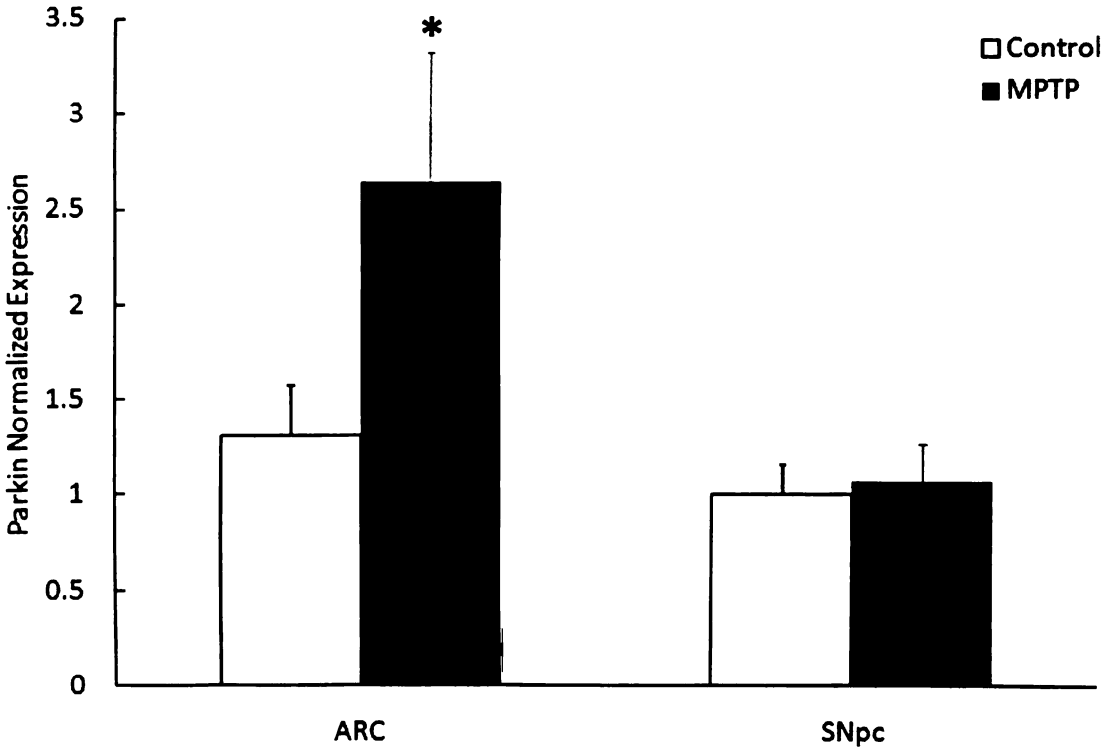

Figure 5-7: RT-PCR analysis of normalized parkin expression levels in ARC and SNpc in controls and MPTP treated mice. Male mice (n=8/group) were treated with a single injection of MPTP (20 mg/kg; s.c.) or saline (10 ml/kg; s.c.) and killed 8 h later. ARC and SNpc were microdissected and mRNA was isolated from each region. Real time PCR analysis was performed and expression levels of parkin were normalized to GAPDH expression levels in each region. Columns represent means of groups and vertical bars represent +1.0 standard error of the mean. (*) indicates values for MPTP treated mice that were significantly different ($p < 0.05$) from saline treated controls.

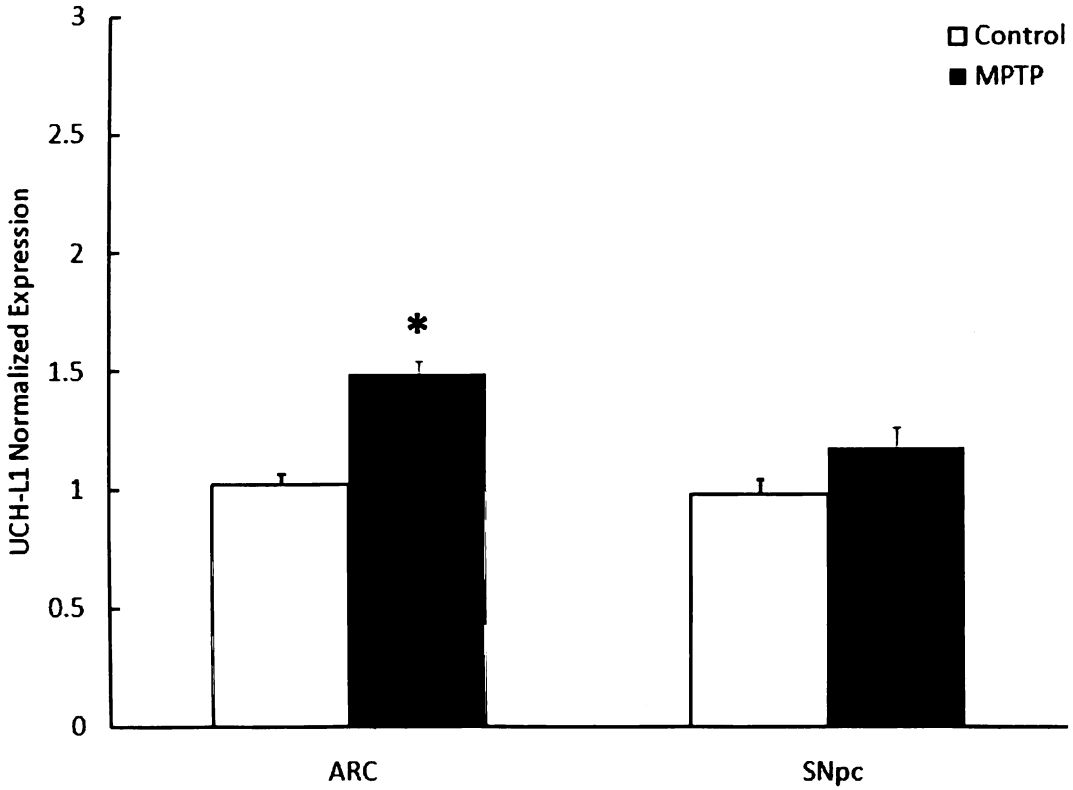

Figure 5-8: RT-PCR analysis of normalized UCH-L1 expression levels in ARC and SNpc in controls and MPTP treated mice. Male mice (n=8/group) were treated with a single injection of MPTP (20 mg/kg; s.c.) or saline (10 ml/kg; s.c.) and killed 8 h later. ARC and SNpc were microdissected and mRNA was isolated from each region. Real time PCR analysis was performed and expression levels of UCH-L1 were normalized to GAPDH expression levels in each region. * indicates significant difference from control. Columns represent means of groups and vertical bars represent +1.0 standard error of the mean. (*) indicates values for MPTP treated mice that were significantly different ($p < 0.05$) from saline treated controls.

A. Normalized LRRK2 Expression		
	ARC	**SNpc**
Saline	1.3 ± 0.1	1.0 ± 0.1
MPTP	1.1 ± 0.1	0.8 ± 0.1

B. Normalized α-synuclein Expression		
	ARC	**SNpc**
Saline	0.7 ± 0.1	1.0 ± 0.2
MPTP	0.7 ± 0.1	1.0 ± 0.2

C. Normalized DJ1 Expression		
	ARC	**SNpc**
Saline	1.3 ± 0.1	1.0 ± 0.1
MPTP	1.4 ± 0.1	1.4 ± 0.1

D. Normalized Pink1 Expression		
	ARC	**SNpc**
Saline	0.8 ± 0.0	1.0 ± 0.0
MPTP	0.8 ± 0.1	1.0 ± 0.1

Table 5-4: Normalized mRNA expression levels of LRRK2, synuclein, DJ1, and Pink1 in ARC and SNpc of mice injected with saline or MPTP. Male mice (n=8/group) were treated with a single injection of MPTP (20 mg/kg; s.c.) or saline (10 ml/kg; s.c.) and killed 8 h later. ARC and SNpc were microdissected and mRNA was isolated from each region. Real time PCR analysis was performed and expression levels of LRRK2, synuclein, DJ1 and Pink1 were normalized to GAPDH expression levels in each region.

Discussion:

The experiments in this chapter demonstrate the genomic response of TIDA and NSDA neurons under normal control conditions and after treatment with MPTP. These genomic responses were analyzed based on two general hypotheses; that TIDA neurons may upregulate expression of protective genes that allow them to recover from neurotoxic insult, and that NSDA neurons may have mechanisms in place under basal conditions that do not allow these neurons to recover from MPTP treatment. Evidence for the first hypothesis is particularly strong as the recovery of TIDA neurons from DA loss is dependent on synthesis of new proteins following MPTP. Several methods, including unbiased pathway analysis, cluster analysis and examination of candidate genes were utilized to identify these potentially protective or deleterious genes.

Analysis of Pathways using DAVID Annotation Tools:

Genes that have higher expression in ARC compared with SNpc after MPTP but not after saline treatment are parts of several general and specific biological pathways. Interestingly, one of the pathways is regulation of apoptosis. Certain genes involved in regulation of apoptosis delay cell death and thereby protect the cells from self-destruction in response to MPTP. Some of these genes have been well studied whereas others are relatively unknown. For example, HSPA1A is a member of the HSP70 family of chaperones and can stabilize existing proteins against aggregation and mediate the folding of newly translated proteins in the cytosol and organelles. The

involvement of HSPA1A in the UPS and its ability to correct misfolded proteins has previously implicated this gene in PD pathogenesis (Bucci et al., 2000; Sittler et al., 2001; Auluck et al., 2002; Neckers, 2002; Shen et al., 2005). The HSP70 family has been shown to be protective in a variety of PD models, including α-synuclein toxicity and MPTP treatment (Auluck et al., 2002; Shen et al., 2005; Nagel et al., 2008). One property shared by the genes in **Figure 5-3** is that they down regulate cell death and their increased expression in ARC following MPTP may be protecting these neurons. In depth functional analysis of these genes, separately and in concert, would be helpful in determining which may act to protect TIDA neurons from toxicity.

Pathway analysis of genes that have higher expression in SNpc than ARC under control conditions may reveal pathways that could hinder the ability of NSDA neurons to recover following MPTP treatment. For example, several genes that regulate DA synthesis, transport and secretion are highly expressed in SNpc compared with the ARC under normal conditions (**Figure 5-4**). Interestingly, genes that are involved in breakdown of cytosolic DA, such as MAO B and mitochondrial AD had similar expression between the two regions. This may indicate that although NSDA neurons have a higher capacity to synthesize, package and secrete more DA, they may not be as efficient in metabolizing cytosolic DA. This may become a problem if large amounts of DA accumulate in the cytosol and is shunted into metabolic pathways that generate ROS or toxic DA adducts. On the other hand, the fact that the recovery of TIDA neurons is dependent on synthesis of new proteins suggests that differences in basal DA metabolism alone cannot underlie the differential susceptibility of NSDA and TIDA

neurons. It is possible that after MPTP treatment, NSDA neurons have both increased oxidative stress due to cytosolic DA, and lack the ability to upregulate anti-apoptotic factors and chaperones that can help alleviate oxidative damage. Further investigation into differences in the regulation of DA synthesis, metabolism and release would be required to examine the importance of these processes in determining the differential susceptibility of NSDA and TIDA neurons to acute MPTP.

Identification of Candidate Clusters:

Cluster analysis of genes with higher expression in ARC than SNpc after MPTP treatment implicates 16 genes with a similar pattern of upregulation following MPTP exclusively in the ARC. Pathway analyses of these genes demonstrate that at least two genes, HSPA1A and HSP 8 are chaperones that respond to stress by properly folding misfolded or damaged proteins. Chaperones are important in situations when oxidative stress can modify proteins and cause them to lose their function or aggregate (Beaucamp et al., 1998; Buzzard et al., 1998; Nagel et al., 2008). As expected, there is much overlap in the genes implicated with cluster analysis with those identified using pathway analysis. Cluster analysis, however, can also serve to implicate genes whose functions are unknown. In this cluster, there are at least 2 genes with unknown function, and it is likely that these genes work in concert with other genes that are also upregulated and may have protective properties. Further functional analysis of the genes in this cluster would be required to determine whether they are protective to

TIDA neurons and if so, whether these protective properties can be utilized to rescue NSDA neurons.

Analysis of Candidate Genes:

There are several genes that have been previously implicated in the pathogenesis of PD. Some of these genes, including Pitx3 and Nurr2, have been reported to have higher expression in the susceptible NSDA neurons versus the resistant TIDA neurons. The results from the microarray analysis confirm previous findings that Pitx3, and Nurr1 have higher expression in SNpc than ARC (Backman et al., 1999; Hwang et al., 2003; van den Munckhof et al., 2003; Chu et al., 2006; Katunar et al., 2008). Surprisingly, microarray analysis did not strongly implicate genes with causative PD mutations. The only gene significantly different amongst the two regions was α-synuclein after treatment with MPTP. While increased expression of α-synuclein has been associated with increased toxicity (Abeliovich et al., 2000; Singleton et al., 2003; Chartier-Harlin et al., 2004; Drolet et al., 2004b), this is unlikely the case in NSDA neurons following MPTP, since blocking protein synthesis does not alter their response to MPTP (**Figure 4-16**).

Furthermore, Affymetrix microarrays provide a 'present' call for genes that can be reliably detected beyond background noise. Due to this, sometimes genes with low signals are not detected. One of the candidate genes, parkin, which has been shown to be protective in several models of PD, did not show as present on the array. Follow up real time PCR analysis of the 6 genes directly involved in familial PD demonstrates that

parkin mRNA levels are similar between the two regions under control conditions but increase significantly only in ARC after treatment with MPTP. The levels of UCH-L1 also increase in ARC after treatment with MPTP, although the magnitude of this change is smaller than that seen with parkin. Interestingly, both parkin and UCH-L1 are components of the ubiquitin proteasome pathway, with parkin acting as an E3 ligase and UCH-L1 as a deubiquinating enzyme. Upregulation of these two genes along with the HSPA1A and HSP 8 chaperones implicate the ubiquitin proteasome pathway as important player in the differential response of NSDA and TIDA neurons to MPTP. Further examination of parkin, UCH-L1 and the chaperones may provide insight about their role in protecting TIDA neurons from toxicity.

Genes and Pathways that Potentially Protect TIDA Neurons from Toxicity.

There are several genomic differences between NSDA and TIDA neurons under basal conditions, as well as in response to MPTP treatment that may explain differential susceptibility to the toxin. Basal DA synthesis and metabolism, upregulation of anti-apoptotic factors, as well as chaperones and proteins involved in protein breakdown may play a role in determining susceptibility. Examination of all of these factors is an extensive process that is beyond the scope of this dissertation. However, one factor that stands out after this genomic analysis of the two regions is parkin. Mutations in parkin cause autosomal recessive PD (Kitada et al., 1998; Sriram et al., 2005), which suggests this protein is essential for the survival of NSDA neurons. Furthermore, increased levels of parkin have been shown to protect against a variety of models

including α-synuclein toxicity (Petrucelli et al., 2002; Yamada et al., 2005), kainate excitotoxicity (Staropoli et al., 2003), and MPTP toxicity (Paterna et al., 2007). This suggests that the increased levels of parkin in response to MPTP may protect TIDA neurons and allow them to recover from MPTP toxicity. If parkin can protect TIDA neurons, either alone or in concert with other proteins, it can be utilized to protect NSDA neurons.

Chapter 6: The Involvement of Parkin in the Recovery of TIDA Neurons from MPTP-Induced DA Loss

A. Introduction:

Parkin is one of several genes upregulated in resistant TIDA neurons but not in susceptible NSDA neurons following treatment with MPTP. Mutations in this gene cause early onset autosomal recessive PD (Kitada et al., 1998) with largely similar pathology to sporadic PD, with the exception that most patients carrying the parkin mutation lack Lewy bodies (Cookson, 2005).

Parkin protein has long been demonstrated to have protective properties in several models of neurodegeneration as well as tumorigenesis (Staropoli, 2008). Two general approaches have been utilized to determine the protective functions of parkin: genetic KO models and transient KD or overexpression. Models utilizing transient expression or KD of parkin have been particularly successful at showing its protective properties. Lentiviral delivery of parkin prevents degeneration of NSDA neurons caused by overexpression of α-synuclein in the rat brain (Petrucelli et al., 2002). Adeno-associated viral delivery of parkin in rat NSDA neurons can also protect these neurons from 6-OHDA toxicity (Vercammen et al., 2006; Manfredsson et al., 2007). Parkin also protects cells *in vitro* from MPP+, hydrogen peroxide, and serum withdrawal (Hyun et al., 2005). Transient knock down of parkin using RNA interference makes neurons more susceptible to kainate excitotoxicity (Staropoli et al.,

2003) suggesting that increase in parkin is protective and decrease in the levels of this protein cause the cells to become more susceptible.

On the other hand, none of the transgenic lines of mice with mutations in parkin show NSDA neuron pathology or hypersensitivity in response to toxin administration (Perez and Palmiter, 2005; Thomas et al., 2007b). This is interesting because the same mutations in humans cause autosomal recessive PD. There is considerable evidence for genetic compensation in parkin KO mice. For example, one would expect that loss of parkin would lead to accumulation of substrates that are normally tagged by this E3 ligase, however this is not the case in parkin KO mice suggesting other members of the UPS may be upregulated to compensate for loss of parkin (Periquet et al., 2005). Indeed upregulation of several members of the UPS, as well as chaperones and other proteins has been reported in these KO mice suggesting data gathered from these KO mice should be interpreted with caution (Goldberg et al., 2003; Perez et al., 2005; Perez and Palmiter, 2005). It should be mentioned that this genetic compensation seems to be limited to mouse models. Drosophila missing the parkin homologue have severe mitochondrial pathology and loss of DA neurons that can be rescued by expression of human parkin (Clark et al., 2006). In the mouse transient manipulation of gene expression has provided a better tool for studying the functions of parkin without confounding genetic compensations.

The 12 exons making up the parkin gene encode a 465 amino acid protein with a pair of Really Interesting New Gene (RING) finger motifs, and in-between RING finger

(IBR) and ubiquitin-like domains (**Figure 6-1**). As with many other proteins with RING domains (Jackson et al., 2000), parkin can act as part of the UPS and tag substrates with poly-ubiquitin chains at their lysine residues. Parkin interacts with E2 conjugating enzymes and its many substrates include (but are not limited to) synphilin-1, o-glycosylated α-synuclein, C-terminus of the HSC70 interacting protein (CHIP), Parkin-associated endothelin receptor (PAELR), Cell division cycle related 1A (cdc-Rel1A), cyclin E, synaptotagmin XI, Septin 5 (sept5) and PARK2 co-regulated (PACRG) (Cookson, 2005). **Figure 6-1** demonstrates how E3 ligase activity of parkin may protect cells against build up of parkin substrates such as o-glycosylated α-synuclein. Of the known parkin substrates, synphilin has higher expression in NSDA neurons when compared with TIDA neurons (**Figure 5-7**) suggesting its accumulation may contribute to toxicity in this subset of neurons.

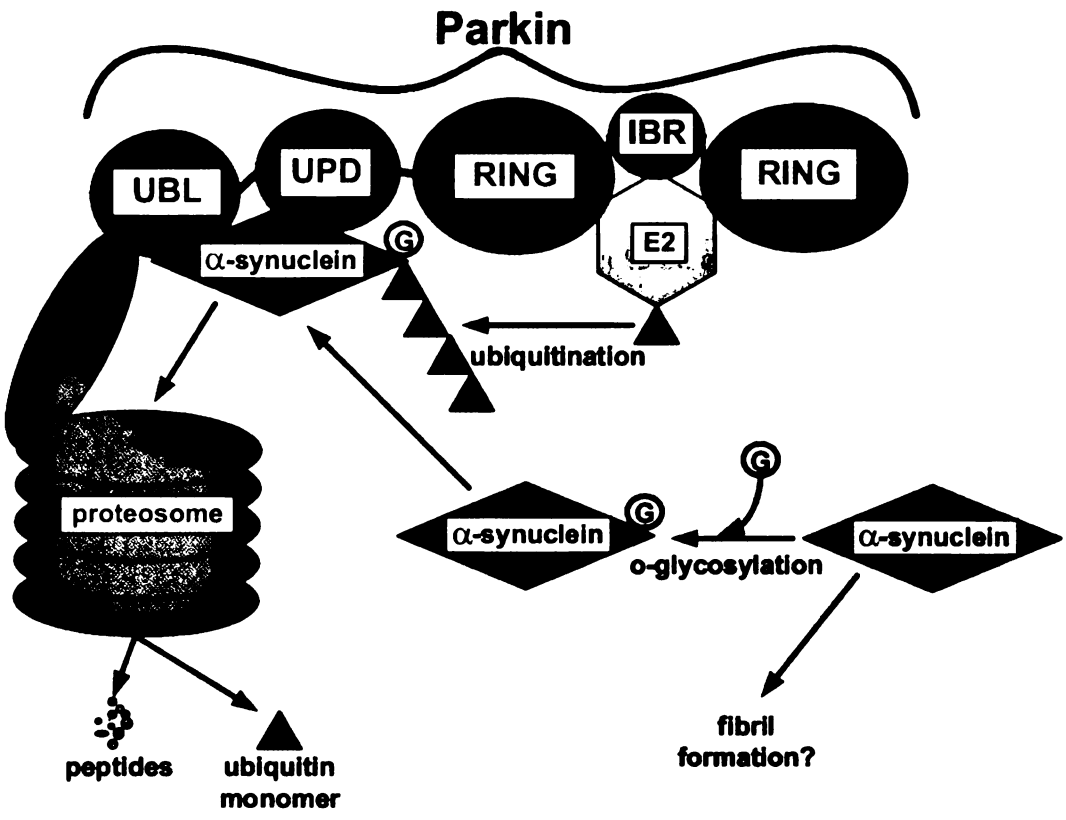

Figure 6-1. Structure and E3 ligase activity of parkin. The parkin protein consists of the Ubiquitin-like Domain (UBL)/Unique Parkin Domain (UPD) region that binds substrates such as glycosylated α-synuclein and two Really Interesting New Gene (RING) finger domains with an In Between Ring domain (IBR) which can recruit specific E2 ubiquitin conjugating enzymes and add ubiquitin monomers to substrates. The UBL domain can also interact with the proteasome, targeting poly-ubiqutin tagged substrates for degradation. Figure from Haywood and Staveley (2004)

Recently, parkin has also been shown to modify proteins via mono-ubiquitylation (Hampe et al., 2006), which modifies the molecular chaperone HSP70 without tagging it for degradation. This mono-ubiquitylated HSP70 is likely to change its function (Moore et al., 2008) in ways that are yet to be elucidated Interestingly, HSP70 mRNA levels increase in TIDA neurons following MPTP treatment, suggesting the mono-ubiquitylating function of parkin may be important in protecting these neurons following MPTP treatment.

Parkin has also been shown to be protective against mitochondrial dysfunction. In PC12 cells, increased expression of parkin delays mitochondrial swelling and cytochrome c release induced by the mitochondrial toxin ceramide (Darios et al., 2003). Furthermore, Drosophila lacking the parkin homologue have mitochondrial dysfunction that can be rescued by replacement with human parkin (Clark et al., 2006). Interestingly, pink1 KO flies have similar mitochondrial pathology as parkin KO flies. The Pink1 gene codes for a mitochondrial kinase and mutations in this gene lead to autosomal recessive PD with similar pathology to patients with parkin mutations. The functions of parkin and Pink1 have been connected because parkin overexpression can rescue the mitochondrial dysfunction and DA loss caused by loss of Pink1. On the other hand, Pink1 overexpression cannot rescue pathology seen in parkin KO flies, suggesting parkin's protective function is downstream of Pink1 (Clark et al., 2006).

The ability of parkin to be protective in so many different pathways implicated in the pathogenesis of PD is dependent on its ability to attach ubiquitin molecules to its

substrates, thereby tagging these proteins for breakdown or altering their function or localization within the cell (Cookson, 2005). As depicted in **Figure 6-2**, it has been proposed that selective vulnerability of DA neurons in PD is due to the attachment of DA adducts to cystenyl residues of parkin, which abolishes its E3 ligase activity (LaVoie et al., 2005). A major criticism of this hypothesis has been that parkin can be damaged by other stressors such as hydrogen peroxide or nitric oxide, and if DA plays a major role in PD pathogenesis, one would expect neurodegeneration of all DA neurons in PD (Cookson, 2005). **Figure 5-7** suggests that parkin mRNA is upregulated in TIDA (but not NSDA) neurons following MPTP treatment. Upregulation of this molecule may be neuroprotective during a time when large amounts of DA are displaced into the cytoplasm, and in combination with MPP+-induced ROS, can damage the cells. This upregulation of parkin, alone or in concert with other protective proteins, may therefore explain the differential susceptibility of these DA neuronal populations to MPTP.

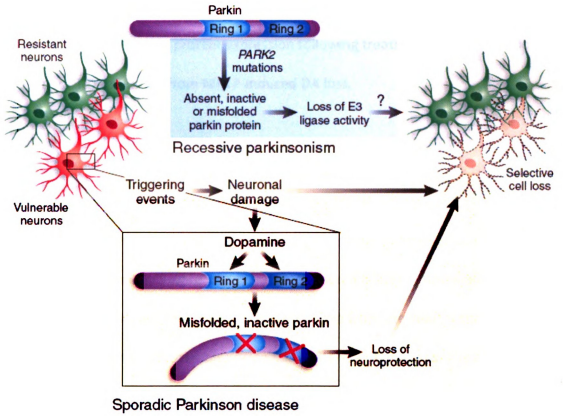

Figure 6-2. The proposed role of parkin in selective degeneration of DA neurons. Parkin may contribute to sporadic PD as well as familial forms caused by mutations in the gene. Auto-oxidized DA in the cytosol can react with parkin RING finger cystenyl residues and thereby inactivate this protective molecule. This loss of parkin function can lead to enhanced cell death in DA neuron populations. This hypothesis does not address differential susceptibility amongst DA neuronal populations in PD, as well as other factors known to inactivate parkin such as hydrogen peroxide and nitric oxide. Figure from Cookson (2005).

B. Hypothesis

Induction of parkin protein expression following treatment with MPTP allows recovery of TIDA neurons from MPTP-induced DA loss.

C. Experimental Design

Parkin Protein Levels Following a Single Injection of MPTP

A single injection of MPTP (20 mg/kg; s.c.) or saline (10 ml/kg; s.c.) was administered and animals were killed by decapitation 8 h later. Immediately after decapitation brains were removed, ME was dissected from the ventral surface of the brain, and the brain was frozen on dry ice for Western blot analyses. The details of methods for animal use, drug administration, tissue preparation, and Western blot analyses are described in Chapter 2 (Methods, Sections. A-F).

Neurochemical Responses of TIDA neurons to MPTP in Parkin KO and WT Mice

Parkin KO mice (F6) and WT littermates were injected with MPTP (20 mg/kg; s.c.) or saline (10 ml/kg; s.c.) and killed by decapitation 16 h later. Immediately after decapitation brains were removed, ME was dissected from the ventral surface of the brain, and the brain was frozen on dry ice for neurochemical analyses. Immediately following decapitation, tail snips were collected and DNA isolated from these samples was used to confirm genotype. The details of methods for animal use, drug administration, tissue preparation, genotyping and neurochemical analyses are described in Chapter 2 (Methods, Sections. A-D).

Neurochemical Responses of TIDA Neurons to MPTP Following Lentiviral Knock Down of Parkin

Lentivirus expressing one of 3 shRNA constructs against parkin or a non-target shRNA under the control of the U6 promoter was bilaterally injected into the ARC of C57bl/6 mice. A non injected control group was also included that did not undergo surgery. Animals were injected with MPTP (20 mg/kg; s.c.) or saline (10 ml/kg; s.c.) 20-28 days following viral injection and animals were killed by decapitation 16 h later. Immediately after decapitation brains were removed, ME was dissected from the ventral surface of the brain, and the brain was frozen on dry ice for neurochemical and Western blot analyses. The details of methods for animal use, drug administration, tissue preparation, and neurochemical and Western blot analyses, as well as details of lentivirus injections are described in Chapter 2 (Methods, Sections. A-E and Q).

D. Results

Parkin Protein Levels Following a Single Injection of MPTP

Figure 6-3 demonstrates that 8 h following treatment with MPTP, there is a significant increase in parkin protein levels in the ME but not in ST of C57bl/6 mice. In saline treated controls, parkin protein levels were similar between ME and ST.

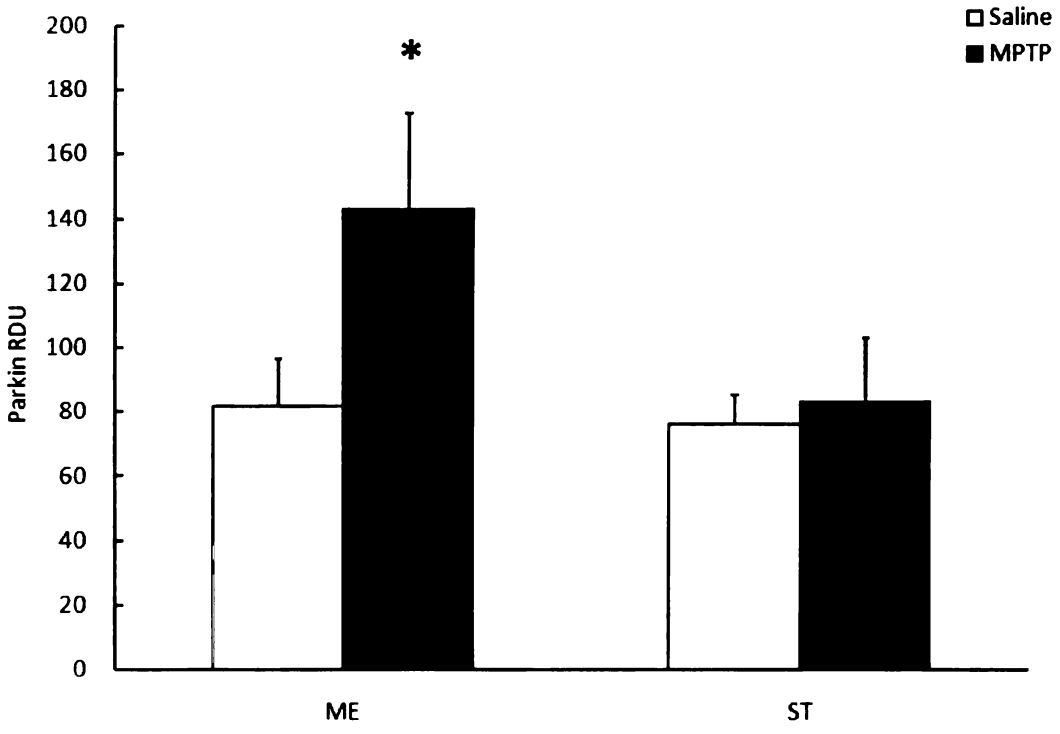

Figure 6-3. The effects of a single injection of MPTP on parkin levels in median eminence (ME) and striatum (ST). Male mice (n=8/group) were treated with either MPTP (20 mg/kg; s.c.) or saline (10 ml/kg; s.c.) and killed 8 h later. Parkin levels were determined by Western blotting and normalized to GAPDH to get relative density units (RDU). Columns represent means of groups and vertical bars represent +1.0 standard error of the mean. (*) indicates values for MPTP treated mice that were significantly different ($p < 0.05$) from saline treated controls.

Neurochemical Responses of TIDA Neurons to MPTP in Parkin KO and WT Mice

Figure 6-4 demonstrates that no significant change can be detected in DA concentrations in ME 16 h following treatment with MPTP in parkin KO or WT littermate mice. ST DA levels were significantly lower 16 h following MPTP treatment in both parkin KO and WT mice (**Figure 6-5**).

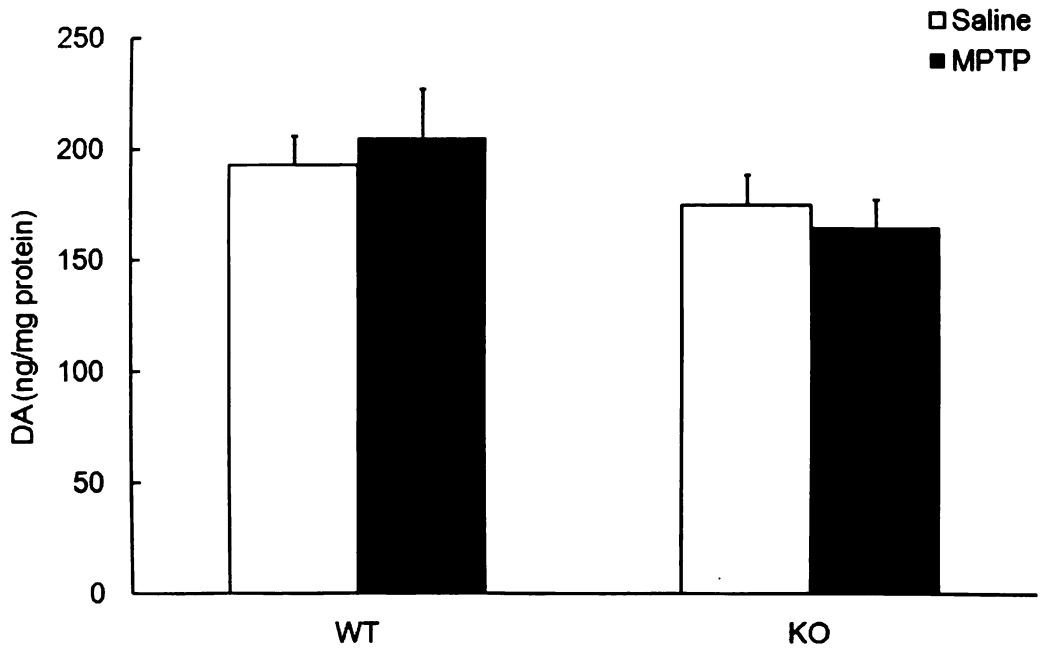

Figure 6-4. The effects of a single injection of MPTP on DA levels in the median eminence (ME) of parkin knock out (KO) and wild type (WT) mice. Male parkin KO and WT littermate (F6) mice (n=8/group) were treated with either MPTP (20 mg/kg; s.c.) or saline (10 ml/kg; s.c.) and killed 16 h later. Columns represent means of groups and vertical bars represent +1.0 standard error of the mean.

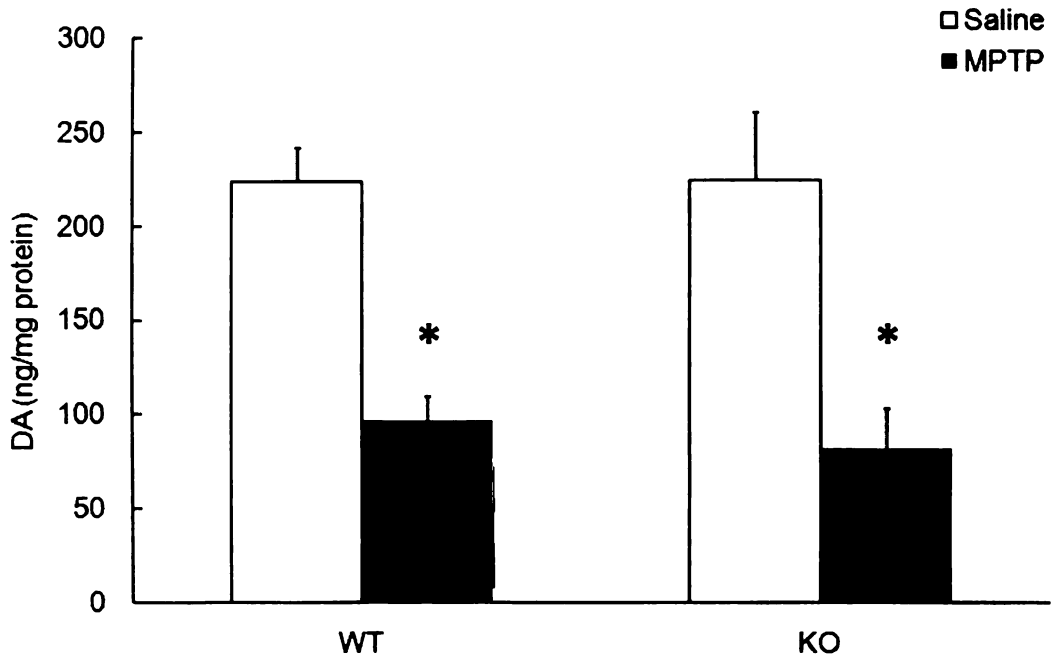

Figure 6-5. The effects of a single injection of MPTP on DA levels in the striatum (ST) of parkin knock out (KO) and wild type (WT) mice. Male parkin KO and WT littermate (F6) mice (n=8/group) were treated with either MPTP (20 mg/kg; s.c.) or saline (10 ml/kg; s.c.) and killed 16 h later. Columns represent means of groups and vertical bars represent +1.0 standard error of the mean. (*) indicates values for MPTP treated mice that were significantly different ($p < 0.05$) from saline treated controls.

Neurochemical Responses of TIDA Neurons to MPTP Following Lentiviral Knock Down of Parkin

Figure 6-6 demonstrates that C57bl/6 mice that received lentiviral particles carrying one of 3 parkin shRNA constructs had significantly lower DA levels in ME 16 h following MPTP treatment. Non-injected control mice that did not undergo surgery and those injected with lentiviral particles carrying a non-target shRNA had unchanged DA levels after injection with MPTP. Stereotaxic injection of lentiviral particles carrying parkin or non-target shRNA alone did not alter DA levels in ME. DA levels in ME of MPTP-treated mice injected with parkin shRNA significantly correlates ($r=0.61$; p-value <0.01) with parkin levels in ARC of the same animals (**Figure 6-7**). There was no correlation between parkin levels and DA concentrations in animals that received parkin shRNA lentivirus ($r= -0.32$, $p= 0.18$), animals that received non-target shRNA and saline ($r= -0.52$, $p= 0.18$) or MPTP ($r= -0.33$, $p= 0.66$) or animals that did not undergo surgery and received saline ($r= -0.04$, $p= 0.93$) or MPTP ($r= 0.17$, $p= 0.78$). No differences in NE, 5HT or 5-HIAA concentrations were detected in ME of mice injected with MPTP, lentivirus or a combination of the two (**Table 6-1**).

ST DA levels decreased following MPTP treatment in all groups, and the magnitude of DA decrease did not differ between animals that received stereotaxic lentiviral injections of scrambled non-target or parkin shRNA and non-injected controls (**Figure 6-8**).

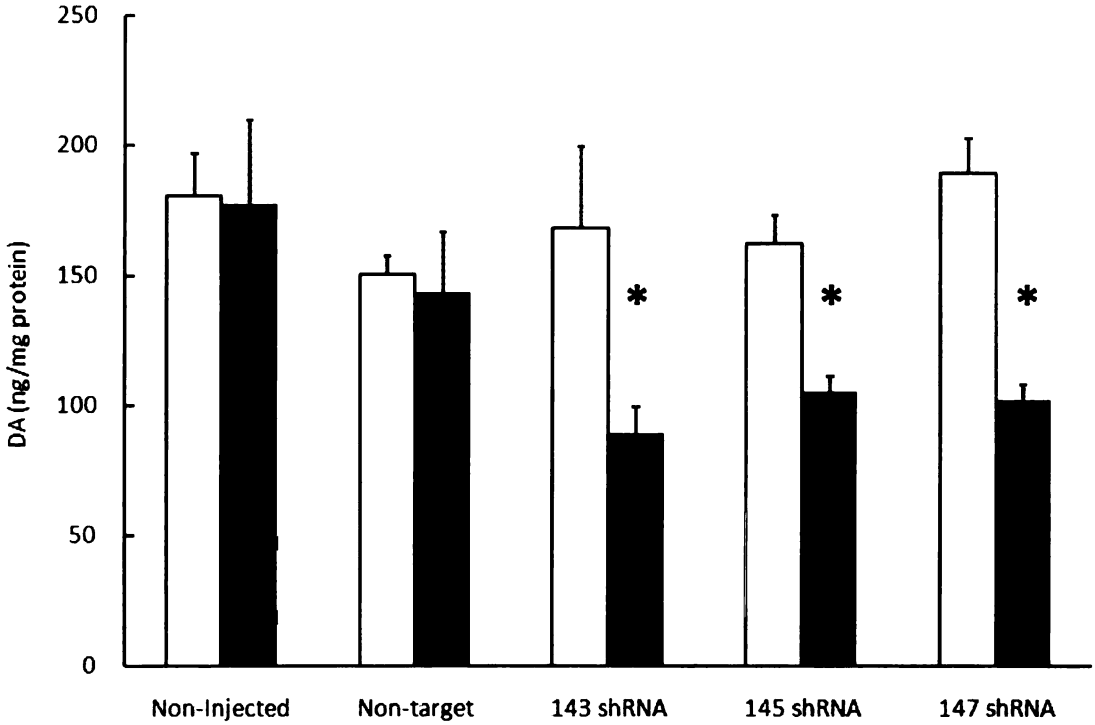

Figure 6-6. The effects of parkin shRNA administration and a single injection of MPTP on DA levels in the median eminence (ME). Male c57bl/6 mice (n=9/group) received bilateral stereotaxic injections of lentivirus (500 nl) containing non-target or one of 3 parkin shRNA sequences (143, 145 or 147). A non-injected group was also included in the study and did not undergo stereotaxic surgery. All mice were treated 20-28 days following surgery with either MPTP (20 mg/kg; s.c.) or saline (10 ml/kg; s.c.) and killed 16 h later. Columns represent means of groups and vertical bars represent +1.0 standard error of the mean. (*) indicates values for MPTP treated mice that were significantly different ($p < 0.05$) from saline treated controls.

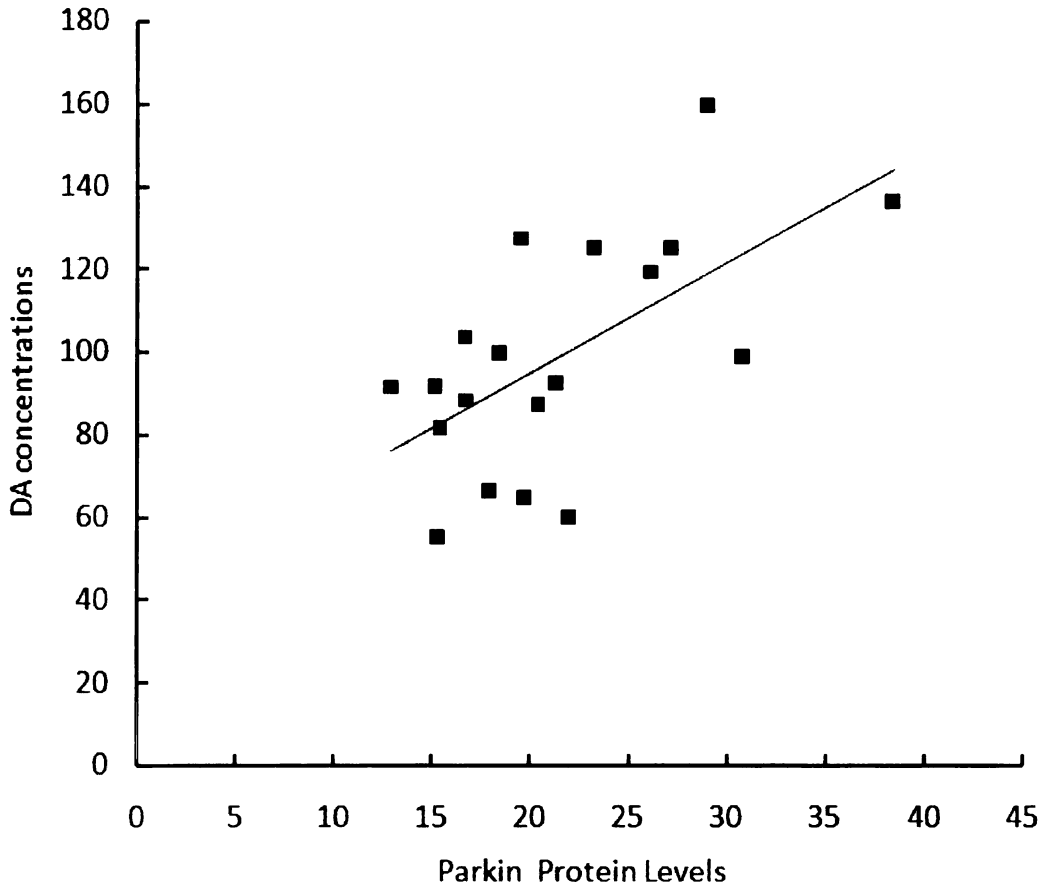

Figure 6-7. The relationship between DA concentrations and parkin levels in ARC of MPTP treated mice injected with parkin shRNA (143, 145, or 147 sequences). Male c57bl/6 mice (n=9/group) received bilateral stereotaxic injections of lentivirus (500 nl) containing non-target or one of 3 parkin shRNA sequences (143, 145, or 147). A non-injected group was also included in the study and did not undergo stereotaxic surgery. All mice were treated 20-28 days following surgery with either MPTP (20 mg/kg; s.c.) or saline (10 ml/kg; s.c.) and killed 16 h later. Pearson's correlation was performed to determine the relationship between DA concentrations and parkin levels in mice receiving parkin shRNA.

NE concentrations (ng/mg protein) in ME					
	Non-Injected	**Non-Target**	**143 shRNA**	**145 shRNA**	**147 shRNA**
Control	48.5 ± 10.8	48.3 ± 4.0	53.9 ± 10.7	53.1 ± 4.2	53.1 ± 4.2
MPTP	57.6 ± 8.8	56.5 ± 6.5	45.6 ± 5.9	45.6 ± 5.9	53.4 ± 3.4

5-HT concentrations (ng/mg protein) in ME					
	Non-Injected	**Non-Target**	**143 shRNA**	**145 shRNA**	**147 shRNA**
Control	13.5 ± 1.7	12.7 ± 1.6	14.4 ± 6.6	13.0 ± 1.2	13.0 ± 3.4
MPTP	17.7 ± 4.4	12.1 ± 2.4	19.1 ± 4.5	12.2 ± 1.5	11.1 ± 1.9

5-HIAA concentrations (ng/mg protein) in ME					
	Non-Injected	**Non-Target**	**143 shRNA**	**145 shRNA**	**147 shRNA**
Control	8.7 ± 0.9	7.3 ± 0.4	8.4 ± 2.9	8.6 ± 0.7	7.7 ± 1.0
MPTP	9.9 ± 1.0	7.8 ± 0.6	7.8 ± 1.3	8.8 ± 1.2	7.4 ± 0.7

Table 6-1. Norepinephrine (NE), serotonin (5-HT) and (5-HIAA) concentrations in the median eminence (ME) following administration of shRNA to control and MPTP-treated mice. Male c57bl/6 mice (n=9/group) received bilateral stereotaxic injections of lentivirus (500 nl) containing non-target or one of 3 parkin shRNA sequences (143, 145 or 147). A non-injected group was also included in the experiment that did not undergo stereotaxic surgery. All mice were treated 20-28 days following surgery with either MPTP (20 mg/kg; s.c.) or saline (10 ml/kg; s.c.) and killed 16 h later.

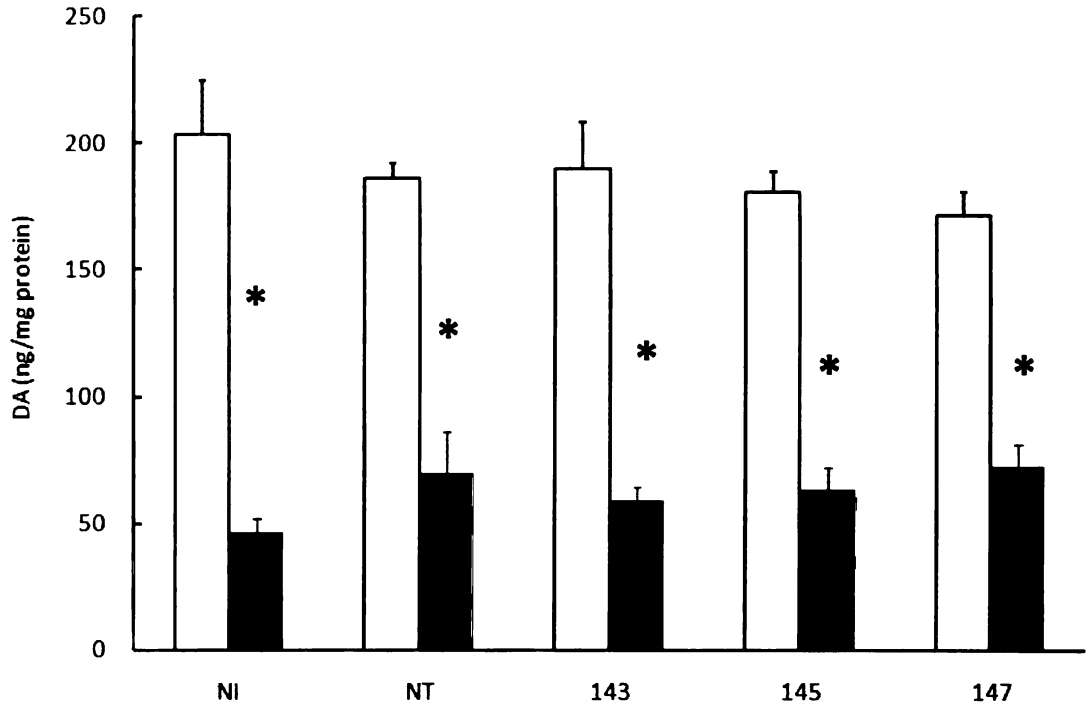

Figure 6-8. The effects of parkin shRNA administration and a single injection of MPTP on DA levels in the striatum (ST). Male c57bl/6 mice (n=9/group) received bilateral stereotaxic injections of lentivirus (500 nl) containing non-target or one of 3 parkin shRNA sequences (143, 145 or 147). A non-injected group was also included in the experiment that did not undergo stereotaxic surgery. All mice were treated 20-28 days following surgery with either MPTP (20 mg/kg; s.c.) or saline (10 ml/kg; s.c.) and killed 16 h later. Columns represent means of groups and vertical bars represent +1.0 standard error of the mean. (*) indicates values for MPTP treated mice that were significantly different ($p < 0.05$) from saline treated controls.

Discussion:

The experiments in this chapter demonstrate that mice that received lentiviral parkin shRNA had stunted recovery of MPTP-induced DA loss in TIDA neurons. These results are consistent with previously described protective properties of parkin (Petrucelli et al., 2002; Darios et al., 2003; Staropoli et al., 2003; Haywood and Staveley, 2004; Jiang et al., 2004b; Cha et al., 2005; Hyun et al., 2005; Yamada et al., 2005; Vercammen et al., 2006; Manfredsson et al., 2007; Poole et al., 2008) and suggest that upregulation of this protein in TIDA neurons following treatment with MPTP. On the other hand, TIDA neurons in parkin KO mice had no deficits in recovery following MPTP treatment, directly contradicting data from the KD study. The lack of difference between KO mice and their WT littermates mirrors other studies showing no difference in susceptibility of other neuronal populations in parkin KO mice (Goldberg et al., 2003; Perez et al., 2005; Perez and Palmiter, 2005; Periquet et al., 2005; Thomas et al., 2007a). This is likely due to genetic compensation in parkin KO mice which makes this an inferior model to study of the functions of this protein (Periquet et al., 2005).

Parkin protein levels are upregulated in the axon terminal regions of TIDA neurons 8 h following MPTP treatment. The upregulation of this protein likely plays a role in the recovery of TIDA neurons from MPTP-induced DA loss. Parkin protein levels are not upregulated in NSDA neurons following MPTP treatment, suggesting this difference may underlie the differential susceptibility of these neuronal populations.

The results of experiments presented in this chapter confirm previous findings that NSDA neurons of parkin KO mice and WT littermates have a similar loss of DA

following treatment with MPTP (Thomas et al., 2007b). Interestingly, TIDA neurons of parkin KO and WT littermates both recover from MPTP-induced DA loss by 16 h post-treatment. This leads to two possible hypotheses; 1) that parkin is not responsible for the DA recovery, or that 2) parkin KO mice have upregulation of other protective genes that compensate for the lack of parkin. Compelling evidence in the literature argues for the latter hypothesis since parkin KO mice are reported to have higher expression levels of chaperones as well as members of the UPS (Periquet et al., 2005). These upregulated proteins likely compensate for lack of parkin and explain why loss of parkin function causes PD in humans but does not cause pathology in aged KO mice or alter the sensitivity to toxins such as MPTP, 6-OHDA, and paraquat (Perez et al., 2005; Perez and Palmiter, 2005; Thomas et al., 2007a). Alternatively, the lack of difference could be due to species differences since several studies have demonstrated that disease causing mutations do not necessarily cause symptoms or altered sensitivity to toxins in mouse models, but do mimic disease pathogenesis in other species such as drosophila (Feany and Bender, 2000; Hashimoto et al., 2003; Clark et al., 2006; Thomas et al., 2007b).

There is a general discrepancy about the protective role of parkin between studies utilizing parkin KO mice and those that transiently KD or overexpress the protein. Since the KD and overexpression strategies utilize various delivery methods of the protein or shRNA, it is unlikely that these techniques are flawed and more likely that parkin KO mice have upregulation of other proteins that compensate for protective roles of parkin. As such, parkin KO mice are not the best model for studying

the protective role of parkin and it would be premature to dismiss the possibility that parkin may be protecting TIDA neurons based on negative results from KO mice.

Viral delivery of 1 of 3 parkin shRNA sequences, but not a non-target shRNA sequence prevents the full recovery of TIDA neurons from MPTP-induced DA loss. This establishes a cause and effect relationship between parkin and DA recovery in TIDA neurons. While ME, a small region of less than 15 μg of total protein, was used to determine neurochemical content and therefore could not be used to confirm parkin KD in this region, parkin protein levels in ARC and DA levels in ME demonstrate a statistically significant relationship in mice treated with any of the parkin shRNA sequences and MPTP. This positive correlation ($r=0.61$, $p\text{-value}<0.01$) demonstrates that mice with lower levels of parkin protein in ARC have lower DA concentrations in ME following MPTP administration. This correlation was absent in mice that received the non-target shRNA virus, or animals that did not undergo surgery but received MPTP. This correlation was also absent in all groups treated with saline, suggesting low parkin levels alone do not cause loss of DA.

The fact that DA concentrations were not lower after MPTP treatment in mice receiving lentiviral delivery of non-target shRNA suggests factors such as stereotaxic surgery, off-target effects of virus or shRNA, inflammatory response due to presence of virus did not contribute to lower DA levels in mice receiving parkin shRNA lentivirus. One pitfall of this experiment was that due to the time required for each stereotaxic surgery, animals had to be injected with virus over a period of 2 weeks, with the non-target shRNA lentivirus animals injected first, followed by 143, 145 and 147 parkin

shRNA constructs. It is unlikely that the short time between surgeries accounts for differences amongst non-target shRNA and parkin shRNA groups since lentiviral delivery provides non-transient expression of the shRNA due to incorporation into the host genome. Furthermore, the fact that parkin protein levels in ARC correlate significantly with DA levels in parkin shRNA treated animals suggests that the decreased DA levels in these animals is dependent on the efficiency of parkin KD.

Other controls such as animals that did not undergo surgery confirm previous findings that TIDA neurons have full recovery from MPTP-induced DA loss by 16 h post injection. Comparison of other groups with non-injected mice also demonstrate that surgery, delivery of a non-target shRNA, or parkin shRNA alone do not alter DA levels in ME. ST DA concentrations demonstrate that similar levels of MPTP successfully penetrated the brain across different groups and that the differences in DA levels in ME are specific to TIDA neurons and not a global non-specific effect. Unchanged NE, 5-HT and 5-HIAA levels in ME also demonstrate that the decrease in DA following MPTP in animals that received parkin shRNA is specific to DA containing neurons.

Overall, the experiments in this chapter demonstrate that parkin plays an important role in the recovery of TIDA neurons from MPTP-induced DA loss. Further characterization of the time course of events following MPTP treatment in mice with low parkin levels will provide a temporal window and future mechanistic studies will determine how parkin exerts its protective effects. Examination of other upregulated factors may also bring into play the mechanisms by which parkin infers protection and whether its protective properties in this region rely on co-expression of other proteins.

Upregulation of parkin levels may be used as an approach to protect the susceptible NSDA neurons in PD models and eventually translated to a protective mechanism for NSDA neurons in PD. Furthermore, the exact mechanism by which parkin promotes the recovery of DA in the axon terminal region of TIDA neurons remains unclear. Parkin interacts with enzymes in the DA metabolism pathway and may affect the recovery of TIDA neurons following MPTP by directly interfering in this pathway. Parkin inhibits the expression of MAO (Jiang et al., 2006) and may therefore prevent DA from being broken down and allow for more packaging of DA, although this is counter-intuitive if cytosolic DA is harmful to cells. Parkin can also increase surface expression of DAT (Jiang et al., 2004a) but it is unclear whether it can do the same for the low affinity high volume DA transporter. If so, more DA may be taken back up and repackaged following MPTP treatment in TIDA neurons accounting for the DA recovery. On the other hand parkin may act indirectly to diffuse oxidative stress thereby allowing the cell to return to a state where it can synthesize and package DA again in a normal fashion resulting in replenishment of DA stores.

Chapter 7. Concluding Remarks

PD is a progressive and devastating disease causing motor abnormalities that disable patients who are forced to give up activities they enjoy, acquire considerable medical costs and have increased mortality (Wermuth et al., 1995; Schenkman et al., 2001; D'Amelio et al., 2006). Based upon 2004 estimates, each year PD costs $34 billion in direct health-related expenses, disability-related costs and lost productivity in the US alone (Whetten-Goldstein et al., 1997; Noyes et al., 2006). Yet symptomatic treatments are only effective for a short time and do nothing to slow the disease process. As the average age of the world's population rises, more people are likely to be affected by diseases such as PD that have increased prevalence in the elderly. A therapeutic approach aiming to decrease or halt the progressive neurodegeneration in NSDA neurons is critical for improving the quality and duration of life for millions affected with PD. Once neuroprotective therapies have been developed, assays can be put into place to detect PD since half of NSDA neurons have already undergone degeneration at initial clinical presentation.

DA Theory for Selective Vulnerability of NSDA Neurons in PD

One property of PD is that while several groups of neurons show pathological abnormalities such as Lewy body formation, only a subset of neurons undergo selective degeneration in PD (Braak and Braak, 2000). This feature of the disease allows for

investigation of properties of the susceptible neurons in comparison with resistant neurons in hopes of discovering neuroprotective agents present only in the resistant neurons. Because the major characteristic of the susceptible neurons is synthesis and transmission of catecholamines such as DA and NE, deleterious properties of these neurotransmitters, particularly DA (which is also the precursor to NE) have been heavily studied and proposed to underlie degeneration. On the other hand, other DA neuronal populations including TIDA neurons do not degenerate in the PD brain.

The major purpose of this dissertation was to examine differences between susceptible and resistant DA neurons in PD, with the overall goal of indentifying factors that could be utilized in development of therapies to protect the susceptible neurons. These studies characterize a toxin model that mimics the long progressive degeneration of NSDA, but not TIDA neurons in PD (Chronic MPTP), as well as examine the response of these neuronal populations that mimics early PD (single injection MPTP), before the most susceptible neurons have been lost.

Basal Differences Between NSDA and TIDA Neuronal Populations

Characterization of basal differences between NSDA and TIDA neurons, a goal of this dissertation, provides new insights about potential factors that may influence susceptibility. Interestingly, while ME is a much smaller region than ST, the concentration of stored DA within these regions is similar, suggesting disruptions in DA stores should affect both groups of neurons. On the other hand, genomic analysis of

these neuronal populations demonstrates that while both groups are DA neurons, the major differences between NSDA and TIDA neurons is in the way they synthesize, store, secrete and uptake DA. Metabolism of DA, however, is similar between these DA neuronal systems. It could therefore be argued that the ability of NSDA neurons to synthesize and store more DA, but not adequately metabolize this DA could contribute to their demise when exposed to neurotoxic insult. Conversely, since the concentration of DA stores is similar between these two groups of neurons, disruptions in DA should make both neuronal populations susceptible. Indeed, these neuronal populations both displace DA following MPTP administration, suggesting both are exposed to high levels of cytosolic DA that can cause damage by formation of DA quinones and ROS. Even more direct evidence against the role of DA as the only culprit comes when TIDA neurons become unable to recover from MPTP damage when protein synthesis is inhibited. This evidence strongly argues that the differential susceptibility of these neuronal populations to toxic stimuli is due to the evoked response of TIDA neurons to MPTP, in the form of synthesis of new proteins. Nevertheless, it is important to keep these basal differences in mind when comparing NSDA and TIDA neurons since a combination of basal differences (that may pre-dispose these neurons) and lack of neuroprotective responses may together underlie susceptibility.

Response of TIDA Neurons to MPTP

The ME is a circumventricular organ, which means it lies in a region that has weakened blood brain barrier. These circumventricular organs serve to monitor the concentrations of toxins in the blood that cannot otherwise cross the blood brain barrier and communicate this to the rest of the brain, which adjusts its responses accordingly. Since these neurons are routinely exposed to stressors that other neuronal populations do not encounter, it is not surprising that they respond to toxic insult with synthesis of protective factors that allow for their recovery. Several genes only have higher expression in these protected TIDA neurons when compared with NSDA neurons following treatment with MPTP, but not under basal conditions. These genes encompassed chaperones, anti-apoptotic factors and components of the UPS. Perhaps not surprisingly, positive regulators of transcription and translation were also upregulated in TIDA neurons following MPTP, suggesting proteomic, as well as genomic increase of protective properties may play a role in the ability of TIDA neurons to recover.

One of the factors identified, parkin, is particularly interesting because not only has it been demonstrated to have protective effects in a wide array of degeneration models, mutations in this gene lead to autosomal recessive early onset PD, directly implicating the function of this gene in NSDA neuronal degeneration. One of the major findings in this dissertation is that parkin is upregulated in protected TIDA neurons following MPTP and transient downregulation of parkin via lentiviral delivery of parkin shRNA causes stunted recovery of the resistant TIDA neurons in response to MPTP.

This clearly demonstrates that presence and upregulation of parkin in TIDA neurons contributes to their recovery from MPTP-induced DA loss. Interestingly, parkin is not upregulated in the susceptible NSDA neurons following MPTP treatment, and this is accompanied by a lack of recovery of NSDA neurons from MPTP-induced DA loss and eventually cell death. It is important to determine if increased expression of parkin can alter the time course of response of NSDA neurons to MPTP. If parkin allows for recovery of TIDA neurons, it is likely that increased expression of parkin in NSDA neurons can also protect these neurons from toxicity.

Hypotheses Regarding the Involvement of Parkin in Recovery of TIDA Neurons

In furthering our knowledge of differential susceptibility of NSDA and TIDA neurons, the results from this dissertation have created additional questions regarding the exact mechanisms by which protective factors such as parkin may be functioning. It will be interesting to determine whether mice with KD of parkin can recover from MPTP-induced DA loss at a later time. A time course of the neurochemical and genomic responses of TIDA neurons following parkin KD would serve to determine whether these neurons can eventually recover. Alternatively, decreased parkin expression may lead to permanent damage including cell death. If TIDA neurons of parkin KD mice fully recover at a later time point it would suggest other factors are also involved in this recovery. Identification of other factors upregulated besides parkin may provide clues as to whether these factors work with or independently of parkin to promote cell survival and will serve to identify which pathways are essential for the

survival of the cell. The upregulation of these other protective factors in parkin KO mice may account for their lack of deficits when compared with WT mice. Other upregulated genes may use the same promoter or transcription factors to increase alongside parkin and may be important. While the parkin promoter has been identified (West et al., 2001), it is unclear whether any of the other genes that were co-upregulated with parkin in TIDA neurons following MPTP use the same promoter region. Overlap amongst genes upregulated alongside parkin and in parkin KO mice may suggest other proteins that work with parkin, perhaps with similar function, to protect the cells. The only gene that upregulates following MPTP microarray analysis from Chapter 5 and the proteomics data from parkin KO mice (Periquet et al., 2005) was HSPA1A, an inducible member of the HSP70 group. While this protein has been shown to be protective in PD models (Bucci et al., 2000; Auluck et al., 2002; Shen et al., 2005), it would be interesting to determine whether this protective chaperone can work in concert with parkin to protect cells from toxicity. On the other hand, if parkin KD alone can cause cell death, it will provide a model in which physiologically important and relevant mechanisms by which parkin provides protection can be determined.

Whether parkin works alone or in concert with other protective factors, the mechanisms by which it exerts protection should be examined. These mechanisms likely include one or all of the pathways highlighted in **Figure 7-1**. Parkin has been shown to protect against proteolytic stress, oxidative damage, and recently some have suggested it may protect cells by mono-ubiquitylation of other proteins (Petrucelli et al., 2002; Darios et al., 2003; Greene et al., 2003; Staropoli et al., 2003; Haywood and

Staveley, 2004; Jiang et al., 2004b; Pesah et al., 2004; Cha et al., 2005; Hyun et al., 2005; Lim et al., 2005; Clark et al., 2006; Hampe et al., 2006; Haywood and Staveley, 2006; Vercammen et al., 2006; Yang et al., 2006; Manfredsson et al., 2007; Paterna et al., 2007; Deng et al., 2008; Moore et al., 2008; Olzmann and Chin, 2008; Poole et al., 2008).

While much attention has been focused its E3 ligase activity due to its importance in protecting against proteolytic stress, it is unlikely to be parkin's only critical function considering that some PD causing parkin mutations do not disturb its E3 ligase activity (Hampe et al., 2006; Matsuda et al., 2006). On the other hand, these mutations may change parkin's tertiary structure and thereby preventing some of its substrates from being tagged. The fact that chaperones and other members of UPS are upregulated in TIDA neurons following MPTP suggests that pathways dealing with protein refolding or breakdown may be equally as important in the recovery of TIDA neurons from MPTP-induced DA loss. It would be interesting to examine if KD of parkin along with expression of E3 inactive parkin can still induce DA recovery in TIDA neurons. If so, it would suggest the E3 ligase activity of parkin is not the protective function.

The ability of parkin to alter the functions of other proteins by lysine-63 linked mono-ubiquitylation may also be important for its neuroprotective effects. While this function of parkin has only been elucidated recently (Lim et al., 2005; Hampe et al., 2006; Moore et al., 2008), one of the few proteins already discovered to be mono-ubiquitylated by parkin, HSP70 is also upregulated in TIDA neurons following MPTP. It

would be interesting to determine if these proteins work in concert to protect TIDA neurons from toxicity. KD of HSP70 alone, parkin alone, or a combination of the two followed by MPTP treatment could determine whether these proteins work together to protect TIDA neurons. It would also be interesting to examine whether other proteins that are upregulated following MPTP are mono-ubiquitylated and if so, how this affects the function of these proteins.

Finally, it would be interesting to determine whether parkin protects these neurons directly against mitochondrial induced oxidative stress via proteasome independent mechanisms. Parkin KO flies have mitochondrial pathology (Clark et al., 2006) and parkin has been proposed to work downstream of another PD related gene, Pink1, to protect against mitochondrial damage. The loss of mitochondrial and tissue integrity in PINK1 and parkin mutant flies is proposed to derive from reduced mitochondrial fission (Deng et al., 2008; Poole et al., 2008) and independent of its proteasome activity. It would be important to determine if transient KD of parkin causes mitochondrial deficits in TIDA and NSDA neurons in a mouse model and determine whether parkin infers protection, partially by preserving mitochondrial function.

Parkin's involvement in a variety of pathways leads to the hypothesis that it protects the cells via several different mechanisms that are likely to occur in parallel all resulting in promotion of cell survival and inhibition of cell death (**Figure 7-1**). NSDA neurons may be particularly susceptible to toxicity because of their inability to upregulate this protein and the damage caused by cytosolic DA. In PD patients carrying

the parkin mutations, one would expect other DA systems to be affected as well, since they lose the ability to upregulate this protective protein. Unfortunately no data has been published about TIDA neurons in these patients so far.

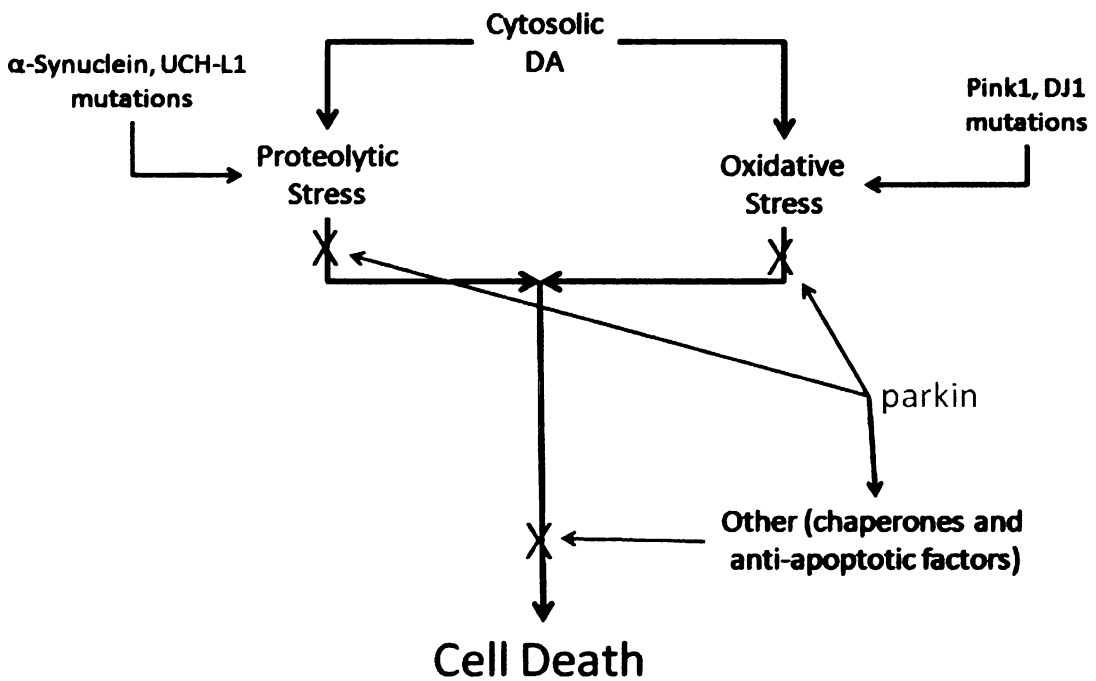

Figure 7-1. The proposed involvement of parkin in pathways that lead to cell death in Parkinson's disease. Oxidative and proteomic stress have long been implicated in pathogenesis of PD and death of NSDA neurons. Cytosolic DA, as well as mutations in various genes can exacerbate the effects of abnormalities in these pathways. Chaperones and anti-apoptotic factors, on the other hand, are known to protect cells from proteolytic or oxidative stress. Here we propose that parkin likely functions by altering all of the above pathways. Parkin's E3 ligase activity can reduce proteolytic stress, it can rescue neurons from oxidative stress by unknown mechanisms and it can modify function of chaperones and anti-apoptotic factors to further protect the cells. The differences in the way parkin expression is regulated in neuronal types can contribute to their differential susceptibility in PD and models of PD.

Protection of NSDA Neurons in PD

The studies in this dissertation shed light on several pathways and intrinsic factors that likely protect TIDA neurons in a toxin-based model of PD. The fact that these molecules are not upregulated in NSDA neurons may render these neurons susceptible. Experiments aimed at increasing the expression of these proteins, both individually and together, will determine whether these factors can protect the susceptible neurons. Further examination of these molecules and pathways should promote development of therapies, such as parkin overexpression in NSDA neurons of PD patients, which may halt or slow the progressive loss of these neurons in PD.

Gene therapy approaches have been brought into light recently in hopes of providing more than just symptomatic treatment for PD patients. Before these models can be routinely employed in PD patients, clinical trials that test the safety and efficacy of gene delivery methods must be established (Lewis and Standaert, 2008). In animal models alone, gene therapy has provided many challenges with both safety and efficacy particularly with viral therapy (Hartman et al., 2008; Sakurai et al., 2008), although delivery of adeno-associated virus has been less problematic in terms of safety (Buch et al., 2008). These issues become even more challenging with clinical trials when the risks of viral therapy and need for sham-surgeries complicate matters greatly. Furthermore, trials of agents that are expected to slow the progression of the disease require longitudinal studies that can take decades. Nonetheless, clinical trials are being conducted with great care and show promise. One study utilizing an adeno-associated viral vector to deliver neurotrophic factors demonstrates some motor

improvements in patients but also that the virus is well tolerated for at least one year following surgery (Marks et al., 2008). Clinical studies utilizing delivery of parkin in PD patients may prove helpful in slowing the degenerative loss of NSDA neurons in the disease.

Appendix:

Figure A-1: Genes with statistically higher expression in ARC than SNpc of saline treated controls. Male mice (n=8/group) were treated with a single injection of MPTP (20 mg/kg; s.c.) or saline (10 ml/kg; s.c.). All animals were killed 8 h after MPTP or saline treatment. Amplified mRNA from 300-500 laser-captured TH immunofluorescent cells from ARC and SNpc of each mouse were hybridized to an Affymetrix mouse 430 2.0 chip. Data was normalized and genes that were significantly higher in ARC than SNpc by at least 2 fold in saline treated controls were identified.

Table A-1. Genes with Higher Expression in ARC than SNpc in Control Mice		
Unigene ID	Description	Log_2 FC
Mm.277996	Pro-opiomelanocortin-alpha	9.62
Mm.154796	Neuropeptide Y	8.42
Mm.140765	Endothelin converting enzyme-like 1	8.15
Mm.57138	Sine oculis-related homeobox 6 homolog (Drosophila)	8.02
Mm.434306	Distal-less homeobox 1	7.28
Mm.75498	CART prepropeptide	7.26
Mm.2453	Somatostatin	7.19
Mm.42242	ISL1 transcription factor, LIM/homeodomain	6.80
Mm.336070	G protein-coupled receptor 101	6.44
Mm.414399	Transcribed locus	6.29
Mm.389327	Growth hormone releasing hormone	6.00
Mm.393566	Estrogen receptor 1 (alpha)	6.00
Mm.34797	Cellular retinoic acid binding protein I	5.95
Mm.4655	Galanin	5.89
Mm.2509	Procollagen, type VI, alpha 1	5.65
Mm.200916	Glutathione peroxidase 3	5.41
Mm.1528	Glypican 4	5.38
Mm.208287	FXYD domain-containing ion transport regulator 6	5.24
Mm.102196	RIKEN cDNA 2900001G08 gene	5.22
Mm.22650	Serine (or cysteine) peptidase inhibitor, clade A, member 3N	5.21
Mm.41638	RIKEN cDNA 6330527O06 gene	5.21
Mm.45054	Guanine deaminase	4.97
Mm.70980	Sortilin-related VPS10 domain containing receptor 3	4.92
Mm.277812	Villin 2	4.85
Mm.150401	Serine/threonine kinase 32A	4.78
Mm.42096	G substrate	4.76
Mm.429391	Transcribed locus	4.71
Mm.20108	Aldehyde oxidase 3	4.70
Mm.283194	Kelch domain containing 8B	4.67
Mm.335953	Diacylglycerol kinase kappa	4.61
Mm.36006	Adenylate kinase 7	4.58
Mm.330975	G protein-coupled receptor 103	4.47
Mm.44305	RIKEN cDNA 1100001E04 gene	4.47
Mm.154093	Procollagen, type XXIII, alpha 1	4.47
Mm.405529	Transcribed locus	4.43
Mm.434981	Transcribed locus	4.41
Mm.1440	Tachykinin 1	4.38
Mm.186404	Coiled-coil domain containing 108	4.37
Mm.434527	Transcribed locus	4.36
Mm.2374	Tachykinin 2	4.34
Mm.332425	Corin	4.30

Table A-1. Continued

Unigene ID	Description	Log_2 FC
Mm.402016	Transcribed locus	4.30
Mm.284102	Expressed sequence AI467606	4.23
Mm.4489	Potassium voltage-gated channel, subfamily H (eag-related), member 1	4.22
Mm.397887	Unc-5 homolog D (C. elegans)	4.21
Mm.246573	RIKEN cDNA 9130014G24 gene	4.20
Mm.296819	RIKEN cDNA 3100002J23 gene	4.19
Mm.41580	RAB3B, member RAS oncogene family	4.18
Mm.383568	Adult male hypothalamus cDNA, RIKEN full-length enriched library, clone:A230069K02 product:hypothetical protein, full insert sequence	4.18
Mm.4672	G protein-coupled receptor 83	4.15
Mm.128861	Protocadherin 20	4.12
Mm.5137	Double C2, beta	4.09
Mm.64201	Neurotensin	4.08
Mm.77895	Chondrolectin	3.92
Mm.290693	G protein-coupled receptor 6	3.90
Mm.396927	Transcribed locus	3.90
Mm.435441	Laminin, beta 3	3.87
Mm.45207	Melanoma antigen, family L, 2	3.85
Mm.34980	Transcribed locus	3.80
Mm.31056	Coiled-coil domain containing 109B	3.79
Mm.126464	Transcribed locus	3.79
Mm.337409	Complement component 1, q subcomponent-like 2	3.79
Mm.6239	Prodynorphin	3.78
Mm.124728	AarF domain containing kinase 4	3.76
Mm.402920	Transcribed locus	3.75
Mm.273114	Gamma-aminobutyric acid (GABA-A) receptor, subunit alpha 5	3.74
Mm.273285	Tescalcin	3.70
Mm.3896	Distal-less homeobox 2	3.69
Mm.392524	G protein-coupled receptor 83	3.62
Mm.416176	Transcribed locus	3.62
Mm.39617	Plexin domain containing 1	3.56
Mm.341593	Transmembrane protein 132E	3.54
Mm.262135	Protein kinase inhibitor beta, cAMP dependent, testis specific	3.53
Mm.329578	Neuropilin (NRP) and tolloid (TLL)-like 1	3.50
Mm.38674	Synaptotagmin-like 4	3.49
Mm.41395	Neuroglobin	3.49
Mm.42202	R-spondin homolog (Xenopus laevis)	3.49
Mm.101811	Dynein, axonemal, heavy chain 1	3.48
Mm.330649	Hypothetical LOC433485	3.46
Mm.285934	Monooxygenase, DBH-like 1	3.46

Table A-1. Continued

Unigene ID	Description	Log_2 FC
Mm.372587	RIKEN cDNA C730029A08 gene	3.43
Mm.395558	Forkhead box O1	3.43
Mm.435516	Synaptic nuclear envelope 1	3.42
Mm.1791	Dual specificity phosphatase 6	3.39
Mm.10299	Procollagen, type V, alpha 2	3.36
Mm.171378	Uncoupling protein 2 (mitochondrial, proton carrier)	3.36
Mm.287867	Neuronal PAS domain protein 4	3.36
Mm.70775	Cerebellin 2 precursor protein	3.31
Mm.266301	Double C2, alpha	3.24
Mm.413640	Transcribed locus	3.24
Mm.32622	G protein-coupled receptor 179	3.23
Mm.4629	Intercellular adhesion molecule 5, telencephalin	3.16
Mm.344095	Scavenger receptor class A, member 3	3.16
Mm.159995	RIKEN cDNA A930021C24 gene	3.16
Mm.188617	ATPase, Ca++ transporting, plasma membrane 4	3.15
Mm.51187	RIKEN cDNA 6030405A18 gene	3.14
Mm.347711	Procollagen, type IV, alpha 4	3.14
Mm.159201	RIKEN cDNA 4932442L08 gene	3.13
Mm.17993	RIKEN cDNA 1700027N10 gene	3.12
Mm.20355	Wingless-related MMTV integration site 4	3.12
Mm.74610	CDNA sequence BC023892	3.11
Mm.28385	Transmembrane protein 176B	3.07
Mm.27086	Reprimo, TP53 dependent G2 arrest mediator candidate	3.04
Mm.78373	Coiled-coil domain containing 19	3.02
Mm.423531	Neuropilin 1	2.99
Mm.23297	Retrotransposon gag domain containing 4	2.98
Mm.266341	Neuropilin 2	2.97
Mm.283777	Prokineticin receptor 2	2.97
Mm.281700	Huntingtin-associated protein 1	2.94
Mm.287187	Sphingomyelin phosphodiesterase, acid-like 3B	2.92
Mm.40173	Potassium voltage-gated channel, subfamily F, member 1	2.92
Mm.19316	GRAM domain containing 1C	2.91
Mm.296806	SEC14-like 3 (S. cerevisiae)	2.91
Mm.119	Nuclear receptor subfamily 4, group A, member 1	2.90
Mm.29891	Forkhead box O1	2.90
Mm.42257	Tektin 1	2.88
Mm.23114	Dynein light chain roadblock-type 2	2.88
Mm.38450	Septin 9	2.87
Mm.16347	Prepronociceptin	2.86
Mm.976	Flavin containing monooxygenase 1	2.86
Mm.238343	Annexin A2	2.86

Table A-1. Continued

Unigene ID	Description	Log_2 FC
Mm.395657	Transcribed locus	2.83
Mm.4965	LIM homeobox protein 1	2.82
Mm.34901	GH regulated TBC protein 1	2.79
Mm.126193	TRAF2 and NCK interacting kinase	2.78
Mm.35708	Leprecan-like 2	2.75
Mm.329622	CDC42 binding protein kinase gamma (DMPK-like)	2.75
Mm.435439	Neuronal guanine nucleotide exchange factor	2.72
Mm.384976	Expressed sequence AW492955	2.71
Mm.20164	Glutathione peroxidase 7	2.68
Mm.401213	Transcribed locus	2.65
Mm.387697	Forkhead-associated (FHA) phosphopeptide binding domain 1	2.65
Mm.364830	Transcription elongation regulator 1-like	2.64
Mm.100144	S100 calcium binding protein A6 (calcyclin)	2.63
Mm.5304	Gamma-aminobutyric acid (GABA-A) receptor, subunit alpha 2	2.62
Mm.4876	Reticulocalbin 1	2.61
Mm.4351	Arginine vasopressin receptor 1A	2.59
Mm.272814	Paraneoplastic antigen MA1	2.59
Mm.96057	RIKEN cDNA A730017D01 gene	2.56
Mm.433973	Protein tyrosine phosphatase, receptor type, K	2.55
Mm.336898	Ngfi-A binding protein 2	2.53
Mm.334207	RIKEN cDNA 4932409I22 gene	2.52
Mm.110505	Immunoglobulin superfamily, member 1	2.48
Mm.275648	PDZ and LIM domain 7	2.48
Mm.130952	Stam binding protein like 1	2.47
Mm.131530	Calcium/calmodulin-dependent protein kinase II alpha	2.47
Mm.39884	Receptor (calcitonin) activity modifying protein 3	2.44
Mm.20916	Wolfram syndrome 1 homolog (human)	2.44
Mm.268378	Calcium channel, voltage-dependent, T type, alpha 1H subunit	2.44
Mm.100167	Phosphodiesterase 8B	2.43
Mm.281298	Growth arrest and DNA-damage-inducible 45 gamma	2.43
Mm.46662	Dapper homolog 1, antagonist of beta-catenin (xenopus)	2.42
Mm.2899	Preproenkephalin 1	2.41
Mm.315382	CDNA sequence BC040758	2.40
Mm.39600	RIKEN cDNA C030019I05 gene	2.38
Mm.3468	Suppressor of cytokine signaling 3	2.37
Mm.433558	Transcribed locus	2.37
Mm.356184	EF hand calcium binding protein 2	2.36
Mm.4352	Procollagen, type XVIII, alpha 1	2.36
Mm.132155	RIKEN cDNA C030009J22 gene	2.35
Mm.39905	Copine V	2.33
Mm.220358	Glucokinase	2.31
Mm.45741	RIKEN cDNA 1110032F04 gene	2.30

Table A-1. Continued

Unigene ID	Description	Log_2 FC
Mm.434783	Transcribed locus	2.29
Mm.208662	CDNA sequence BC029169	2.29
Mm.360398	Transmembrane channel-like gene family 4	2.29
Mm.275409	Transmembrane protein 46	2.27
Mm.400754	Transcribed locus	2.26
Mm.294225	Parathyroid hormone receptor 2	2.25
Mm.330890	Par-3 partitioning defective 3 homolog B (C. elegans)	2.24
Mm.3957	CDNA sequence BC034204	2.24
Mm.1451	Milk fat globule-EGF factor 8 protein	2.22
Mm.186678	CDNA sequence BC022687	2.21
Mm.308296	UDP-N-acetyl-alpha-D-galactosamine:polypeptide N-acetylgalactosaminyltransferase-like 1	2.21
Mm.334569	RIKEN cDNA 4732435N03 gene	2.21
Mm.93193	RIKEN cDNA 4432405B04 gene	2.20
Mm.51340	Ankyrin repeat and SOCS box-containing protein 4	2.20
Mm.23895	Tektin 2	2.19
Mm.32760	RIKEN cDNA 1700009P17 gene	2.15
Mm.398518	Calcium channel, voltage-dependent, gamma subunit 4	2.14
Mm.403263	Transcribed locus	2.13
Mm.332102	Pleckstrin homology domain containing, family G (with RhoGef domain) member 5	2.12
Mm.435564	Ephrin A5	2.12
Mm.87051	Thymocyte selection-associated HMG box gene	2.12
Mm.33304	Potassium channel, subfamily K, member 2	2.11
Mm.40322	Slit homolog 1 (Drosophila)	2.11
Mm.158903	Hepatic leukemia factor	2.10
Mm.142856	LIM homeobox protein 2	2.10
Mm.36446	CDNA sequence BC007180	2.09
Mm.1433	Neuropeptide Y receptor Y2	2.09
Mm.251774	Peroxidasin homolog (Drosophila)	2.09
Mm.25785	LIM domain binding 2	2.07
Mm.3475	Retinoid X receptor gamma	2.06
Mm.28331	Zinc finger, MYND domain containing 10	2.06
Mm.434650	Transcribed locus	2.04
Mm.433168	Transcribed locus	2.01
Mm.283273	Inhibitor of DNA binding 4	2.01
Mm.40038	Apoptosis-inducing factor, mitochondrion-associated 3	2.00
Mm.359762	Peptidylprolyl isomerase (cyclophilin)-like 6	1.99
Mm.222496	Guanine nucleotide binding protein (G protein), gamma 7 subunit	1.99
Mm.80685	Ciliary rootlet coiled-coil, rootletin	1.99
Mm.332684	Kinetochore associated 1	1.96
Mm.390161	Apolipoprotein C-III	1.96

Table A-1. Continued

Unigene ID	Description	Log_2 FC
Mm.284863	BMP and activin membrane-bound inhibitor, homolog (Xenopus laevis)	1.96
Mm.20615	Peroxisomal biogenesis factor 11a	1.95
Mm.290207	E26 avian leukemia oncogene 2, 3' domain	1.92
Mm.261591	Insulin receptor substrate 4	1.91
Mm.22708	Serine (or cysteine) peptidase inhibitor, clade H, member 1	1.91
Mm.156919	Cathepsin Z	1.90
Mm.370334	Ataxin 2 binding protein 1	1.90
Mm.24005	Adhesion molecule with Ig like domain 2	1.89
Mm.27063	Thyroid hormone receptor interactor 6	1.89
Mm.121705	RIKEN cDNA A530088I07 gene	1.88
Mm.135129	ATPase, class V, type 10A	1.88
Mm.44561	RAS protein-specific guanine nucleotide-releasing factor 1	1.87
Mm.403636	Transcribed locus	1.86
Mm.425110	Hypothetical protein LOC620695	1.84
Mm.181021	Procollagen, type IV, alpha 2	1.84
Mm.391678	Odd Oz/ten-m homolog 4 (Drosophila)	1.83
Mm.342160	Carbonic anhydrase 10	1.82
Mm.394928	RIKEN cDNA 9430029N19 gene	1.82
Mm.348844	Transmembrane protein 132D	1.82
Mm.7821	Tumor protein D52-like 1	1.81
Mm.393388	0 day neonate thymus cDNA, RIKEN full-length enriched library, clone:A430010E21 product:unclassifiable, full insert sequence	1.81
Mm.4541	SRY-box containing gene 2	1.81
Mm.264210	Dynein, axonemal, heavy chain 9	1.81
Mm.275845	Synapsin II	1.81
Mm.32582	Early B-cell factor 4	1.81
Mm.392175	CREB regulated transcription coactivator 3	1.80
Mm.89201	Zinc finger protein 179	1.80
Mm.258746	RIKEN cDNA 1190002N15 gene	1.80
Mm.35324	Somatostatin receptor 4	1.80
Mm.31203	Glutathione S-transferase, mu 4	1.79
Mm.327654	LON peptidase N-terminal domain and ring finger 3	1.79
Mm.317947	Nuclear factor I/B	1.78
Mm.158282	RIKEN cDNA 1700029J07 gene	1.78
Mm.402837	Transcribed locus	1.78
Mm.28896	START domain containing 10	1.77
Mm.316890	RIKEN cDNA 5330417C22 gene	1.76
Mm.334108	Dachsous 1 (Drosophila)	1.76
Mm.155887	RIKEN cDNA 1600021P15 gene	1.75
Mm.193272	CDNA sequence BC068157	1.74
Mm.436351	Transcribed locus	1.71

Table A-1. Continued

Unigene ID	Description	Log_2 FC
Mm.295397	DEP domain containing 6	1.71
Mm.337647	Zinc finger, BED domain containing 4	1.71
Mm.357108	Transmembrane protein 178	1.71
Mm.422738	WT1-interacting protein	1.69
Mm.386906	Hypothetical protein C430010C01	1.68
Mm.39691	15 days embryo head cDNA, RIKEN full-length enriched library, clone:D930025C07 product:unclassifiable, full insert sequence	1.63
Mm.295230	Serine protease inhibitor, Kunitz type 2	1.62
Mm.295660	Tetratricopeptide repeat domain 28	1.62
Mm.28534	Leucine rich repeat containing 1	1.62
Mm.132391	6-phosphofructo-2-kinase/fructose-2,6-biphosphatase 4	1.62
Mm.17649	RIKEN cDNA 1700026D08 gene	1.62
Mm.29389	Tensin like C1 domain-containing phosphatase	1.61
Mm.18889	Park2 co-regulated	1.59
Mm.390357	RIKEN cDNA 3010026O09 gene	1.59
Mm.248445	Tripartite motif protein 25	1.59
Mm.248337	Vasorin	1.58
Mm.28244	CDNA sequence BC022623	1.58
Mm.276279	Zinc finger protein 667	1.58
Mm.87448	Fibronectin type 3 and ankyrin repeat domains 1	1.57
Mm.136238	Zinc finger and BTB domain containing 20	1.57
Mm.419530	Transcribed locus	1.56
Mm.33964	RIKEN cDNA 1110004B13 gene	1.55
Mm.379020	Sparc/osteonectin, cwcv and kazal-like domains proteoglycan 1	1.55
Mm.11545	Rhomboid family 1 (Drosophila)	1.54
Mm.435847	Expressed sequence AV025504	1.54
Mm.232525	Anthrax toxin receptor 1	1.54
Mm.328503	Retinoic acid induced 2	1.54
Mm.395887	SET domain containing 6	1.51
Mm.17964	KH domain containing, RNA binding, signal transduction associated 3	1.50
Mm.6442	Polycystic kidney disease 2	1.50
Mm.269088	Acidic (leucine-rich) nuclear phosphoprotein 32 family, member A	1.50
Mm.434173	Transcribed locus	1.50
Mm.213204	Kv channel-interacting protein 2	1.48
Mm.40329	Calcium/calmodulin-dependent protein kinase I gamma	1.46
Mm.292567	Cysteine-rich with EGF-like domains 2	1.46
Mm.41033	Transformation related protein 53 inducible protein 11	1.45
Mm.236928	START domain containing 8	1.45
Mm.275547	Aristaless related homeobox gene (Drosophila)	1.45
Mm.84294	RIKEN cDNA 3110082I17 gene	1.45
Mm.130607	LY6/PLAUR domain containing 6	1.43

Table A-1. Continued

Unigene ID	Description	Log_2 FC
Mm.204834	Solute carrier family 1 (glial high affinity glutamate transporter), member 3	1.43
Mm.1786	Adenine phosphoribosyl transferase	1.41
Mm.1485	Ubiquitin-conjugating enzyme E2E 3, UBC4/5 homolog (yeast)	1.39
Mm.70979	G protein-coupled receptor 176	1.38
Mm.196464	Guanine nucleotide binding protein, alpha inhibiting 2	1.37
Mm.389552	F-box protein 10	1.36
Mm.378951	Kinesin family member C3	1.35
Mm.250731	Microtubule associated serine/threonine kinase 3	1.34
Mm.3390	Myosin IB	1.34
Mm.394224	Androgen receptor	1.34
Mm.28520	Sloan-Kettering viral oncogene homolog	1.34
Mm.81916	Gene model 266, (NCBI)	1.33
Mm.434093	Transcribed locus	1.32
Mm.287163	Btg3 associated nuclear protein	1.31
Mm.331751	Syntaxin binding protein 5 (tomosyn)	1.31
Mm.400752	RIKEN cDNA 2900054C01 gene	1.29
Mm.408473	Transcribed locus	1.29
Mm.416039	Transcribed locus	1.29
Mm.393348	RIKEN cDNA 4930562D19 gene	1.29
Mm.320691	Potassium voltage-gated channel, Shal-related family, member 2	1.29
Mm.128580	DNA methyltransferase (cytosine-5) 1	1.28
Mm.76659	Secretion regulating guanine nucleotide exchange factor	1.28
Mm.193212	Hydroxypyruvate isomerase homolog (E. coli)	1.27
Mm.7852	RIKEN cDNA 2410008K03 gene	1.27
Mm.392845	Androgen receptor	1.27
Mm.424974	MARCKS-like 1	1.27
Mm.170515	Nuclear factor of kappa light chain gene enhancer in B-cells inhibitor, alpha	1.26
Mm.103477	Natriuretic peptide receptor 2	1.25
Mm.25181	Zinc finger, CCHC domain containing 11	1.24
Mm.152121	Recoverin	1.23
Mm.41702	SRY-box containing gene 11	1.23
Mm.87663	Calcium channel, voltage-dependent, gamma subunit 5	1.23
Mm.235590	Leucine rich repeat containing 8 family, member B	1.23
Mm.396682	RIKEN cDNA C030009O12 gene	1.22
Mm.89564	Pregnancy upregulated non-ubiquitously expressed CaM kinase	1.22
Mm.252561	Heparan sulfate 6-O-sulfotransferase 2	1.19
Mm.279872	PRP3 pre-mRNA processing factor 3 homolog (yeast)	1.19
Mm.400798	Transcribed locus	1.19
Mm.46675	Kelch repeat and BTB (POZ) domain containing 11	1.18
Mm.388573	Tubulin tyrosine ligase-like family, member 3	1.18

Table A-1. Continued

Unigene ID	Description	Log_2 FC
Mm.394313	Transcribed locus	1.17
Mm.131572	P21 (CDKN1A)-activated kinase 7	1.17
Mm.41681	Transmembrane protein 119	1.17
Mm.246674	DnaJ (Hsp40) homolog, subfamily C, member 1	1.13
Mm.177761	Chloride channel 2	1.12
Mm.427613	ATP-binding cassette, sub-family G (WHITE), member 1	1.11
Mm.42652	N-acetyltransferase 14	1.10
Mm.291864	Hypothetical LOC629059	1.10
Mm.41642	Regulator of G-protein signaling 4	1.09
Mm.314338	Activin receptor IIA	1.07
Mm.37199	Glutathione S-transferase, mu 1	1.07
Mm.738	Procollagen, type IV, alpha 1	1.07
Mm.330055	Aldehyde dehydrogenase 9, subfamily A1	1.06
Mm.338361	G protein-coupled receptor 75	1.06
Mm.311809	Protein tyrosine phosphatase, receptor type, M	1.06
Mm.23258	RAB, member of RAS oncogene family-like 2A	1.06
Mm.38607	N-acetylglucosamine-1-phosphotransferase, gamma subunit	1.05
Mm.100065	RIKEN cDNA 1300012G16 gene	1.05
Mm.133607	Leucine rich repeat and fibronectin type III domain containing 2	1.04
Mm.223717	MAD homolog 1 (Drosophila)	1.03
Mm.205421	Fibronectin type III domain containing 3a	1.02
Mm.218844	Annexin A9	1.02
Mm.29253	Exosome component 8	1.01
Mm.268369	Leucine rich repeat containing 47	1.01
Mm.317293	Neuronal growth regulator 1	1.00

Figure A-2: Genes with statistically higher expression in SNpc than ARC of saline treated controls. Male mice (n=8/group) were treated with a single injection of MPTP (20 mg/kg; s.c.) or saline (10 ml/kg; s.c.). All animals were killed 8 h after MPTP or saline treatment. Amplified mRNA from 300-500 laser-captured TH immunofluorescent cells from ARC and SNpc of each mouse were hybridized to an Affymetrix mouse 430 2.0 chip. Data was normalized and genes that were significantly higher in SNpc than ARC in saline treated controls by at least 2 fold were identified.

Table A-2. Genes with higher expression in SNpc than ARC in saline treated controls

Unigene ID	Description	Log_2 FC
Mm.14609	Aldehyde dehydrogenase family 1, subfamily A7	9.91
Mm.397323	Expressed sequence AI853839	7.99
Mm.276829	Solute carrier family 39 (zinc transporter), member 4	7.83
Mm.41970	Dopamine receptor 2	7.51
Mm.72070	Riken cDNA C130021I20 gene	7.33
Mm.84118	Predicted gene, EG639426	7.33
Mm.283137	Cholinergic receptor, nicotinic, alpha polypeptide 6	7.28
Mm.427936	Transcribed locus	7.27
Mm.222729	Guanylate cyclase 2c	6.89
Mm.4298	Transcribed locus	6.40
Mm.39825	Transcribed locus	6.25
Mm.57199	Ret proto-oncogene	6.16
Mm.110444	Cholinergic receptor, nicotinic, beta polypeptide 3	6.15
Mm.308735	Kelch-like 1 (Drosophila)	6.09
Mm.103778	Cholinergic receptor, nicotinic, alpha polypeptide 5	5.96
Mm.3507	Nuclear receptor subfamily 4, group A, member 2	5.74
Mm.23782	Glycosyltransferase 25 domain containing 2	5.45
Mm.268521	Insulin-like growth factor 1	5.16
Mm.5076	Tolloid-like	5.10
Mm.288474	Secreted phosphoprotein 1	5.06
Mm.412897	Transcribed locus	5.05
Mm.258708	Early B-cell factor 3	5.01
Mm.52392	RIKEN cDNA A930038C07 gene	5.00
Mm.406232	Transcribed locus	4.93
Mm.358581	Calmegin	4.81
Mm.405570	POU domain, class 3, transcription factor 2	4.79
Mm.239941	Pre B-cell leukemia transcription factor 3	4.77
Mm.71924	Ankyrin repeat domain 38	4.75
Mm.74324	Solute carrier family 35, member D3	4.67
Mm.29221	Transcribed locus	4.66
Mm.295917	Gene model 540, (NCBI)	4.61
Mm.63569	Cholinergic receptor, nicotinic, alpha polypeptide 3	4.58
Mm.282800	Synuclein, gamma	4.55
Mm.393273	Transcribed locus	4.54
Mm.420796	Transcribed locus	4.53
Mm.37882	CDNA sequence BC065085	4.29
Mm.317854	Pregnancy-associated plasma protein A	4.19
Mm.113278	Potassium voltage-gated channel, delayed-rectifier, subfamily S, member 3	4.17
Mm.42190	Unc4.1 homeobox (C. elegans)	4.05

Table A-2. Continued

Unigene ID	Description	Log_2 FC
Mm.408043	Transcribed locus	3.99
Mm.217412	Multiple C2 domains, transmembrane 2	3.94
Mm.39599	GSG1-like	3.87
Mm.275374	Nuclear receptor interacting protein 3	3.86
Mm.292983	Vitrin	3.85
Mm.288805	DEP domain containing 7	3.83
Mm.292100	Fibrinogen-like protein 2	3.81
Mm.361919	Solute carrier family 18 (vesicular monoamine), member 2	3.68
Mm.282751	Anillin, actin binding protein (scraps homolog, Drosophila)	3.67
Mm.154541	RIKEN cDNA 3830431G21 gene	3.67
Mm.129387	POU domain, class 3, transcription factor 2	3.66
Mm.10651	GTP cyclohydrolase 1	3.60
Mm.272976	Synaptic vesicle glycoprotein 2c	3.57
Mm.156558	Synaptotagmin XVII	3.46
Mm.30013	RIKEN cDNA 2010011I20 gene	3.45
Mm.83817	Villin-like	3.41
Mm.425860	Leucine rich repeat containing 3B	3.36
Mm.331690	RIKEN cDNA 5930437A14 gene	3.33
Mm.100125	SH3 domain binding glutamic acid-rich protein like 2	3.20
Mm.141275	RIKEN cDNA E130009J12 gene	3.17
Mm.72799	Transmembrane protease, serine 5 (spinesin)	3.10
Mm.30172	Ras association (RalGDS/AF-6) domain family 6	3.08
Mm.41993	Solute carrier family 6 (neurotransmitter transporter, dopamine), member 3	3.08
Mm.1333	Proprotein convertase subtilisin/kexin type 1	3.08
Mm.39151	Transcribed locus	3.04
Mm.422608	RIKEN cDNA 1190017O12 gene	2.99
Mm.89682	Membrane bound O-acyltransferase domain containing 1	2.97
Mm.115970	A disintegrin-like and metallopetidase (reprolysin type) with thrombospondin type 1 motif, 16	2.96
Mm.415763	Transcribed locus	2.95
Mm.220765	Cadherin 8	2.95
Mm.293363	Spindlin family, member 2	2.94
Mm.4860	Protein tyrosine phosphatase, receptor type, U	2.90
Mm.27789	FERM domain containing 4B	2.90
Mm.246595	Hypocretin (orexin) receptor 1	2.86
Mm.159989	RIKEN cDNA 2810022L02 gene	2.86
Mm.102211	RIKEN cDNA 9330109K16 gene	2.84
Mm.101836	RIKEN cDNA 9630033F20 gene	2.84
Mm.384353	Mab-21-like 1 (C. elegans)	2.82
Mm.391931	Membrane protein, palmitoylated 7 (MAGUK p55 subfamily member 7)	2.82

Table A-2. Continued

Unigene ID	Description	Log_2 FC
Mm.425526	Fibroblast growth factor 20	2.82
Mm.151332	Peroxin 2	2.81
Mm.39723	Kelch domain containing 8A	2.81
Mm.91728	Transcribed locus	2.81
Mm.397113	Transcribed locus	2.79
Mm.379143	Regulator of G-protein signaling 8	2.78
Mm.250866	Aldehyde dehydrogenase family 1, subfamily A1	2.77
Mm.384108	Immunoglobulin superfamily, member 4	2.77
Mm.318710	RIKEN cDNA 3632451O06 gene	2.71
Mm.186779	G protein-coupled receptor 151	2.70
Mm.7995	Fibroblast growth factor 13	2.69
Mm.125650	Apolipoprotein L, 2	2.68
Mm.360649	RIKEN cDNA A830006F12 gene	2.68
Mm.235938	Fragile histidine triad gene	2.67
Mm.102899	Transcribed locus	2.67
Mm.333264	Glutamate receptor interacting protein 2	2.66
Mm.280624	Testis expressed gene 15	2.64
Mm.211850	Arylsulfatase G	2.60
Mm.133293	Membrane protein, palmitoylated 7 (MAGUK p55 subfamily member 7)	2.58
Mm.392745	10 days embryo whole body cDNA, RIKEN full-length enriched library, clone:2610306G12 product:unclassifiable, full insert sequence	2.57
Mm.133615	RIKEN cDNA 2810457I06 gene	2.56
Mm.253736	Palmdelphin	2.55
Mm.209715	Procollagen, type XI, alpha 1	2.52
Mm.39649	RIKEN cDNA B230216G23 gene	2.50
Mm.30767	RIKEN cDNA 1300003B13 gene	2.49
Mm.289643	Cysteine conjugate-beta lyase 2	2.47
Mm.3944	Kallikrein related-peptidase 6	2.46
Mm.130696	RIKEN cDNA 4930589M24 gene	2.45
Mm.434415	Acyl-CoA synthetase long-chain family member 4	2.45
Mm.155708	Ets variant gene 5	2.43
Mm.169261	Von Willebrand factor C and EGF domains	2.43
Mm.5195	Complexin 1	2.40
Mm.211477	Pleckstrin homology-like domain, family B, member 2	2.40
Mm.345834	0 day neonate cerebellum cDNA, RIKEN full-length enriched library, clone:C230096I08 product:hypothetical protein, full insert sequence	2.38
Mm.69013	RIKEN cDNA B430201A12 gene	2.38
Mm.30221	Insulin induced gene 1	2.37
Mm.209232	Contactin associated protein-like 4	2.33
Mm.432481	Forkhead box P2	2.32

Table A-2. Continued

Unigene ID	Description	Log_2 FC
Mm.274308	N-ethylmaleimide sensitive fusion protein attachment protein beta	2.30
Mm.101707	SLIT and NTRK-like family, member 4	2.30
Mm.42012	Laminin, alpha 3	2.29
Mm.1292	Tyrosine hydroxylase	2.26
Mm.23462	Elastin microfibril interfacer 2	2.26
Mm.380993	Phosphatidylinositol-specific phospholipase C, X domain containing 2	2.26
Mm.198414	Serine/threonine kinase 39, STE20/SPS1 homolog (yeast)	2.25
Mm.400451	Musashi homolog 2 (Drosophila)	2.24
Mm.252369	Cholinergic receptor, nicotinic, alpha polypeptide 4	2.24
Mm.407309	Transcribed locus	2.23
Mm.394300	Transcribed locus	2.23
Mm.34235	Williams Beuren syndrome chromosome region 27 (human)	2.23
Mm.253	Regulator of chromosome condensation 2	2.22
Mm.285060	FCH and double SH3 domains 1	2.14
Mm.212855	Myosin regulatory light chain interacting protein	2.12
Mm.78923	Phosphatidylinositol-4-phosphate 5-kinase-like 1	2.11
Mm.268536	Myotubularin related protein 11	2.10
Mm.80318	Transmembrane protein 169	2.09
Mm.337023	Membrane-associated ring finger (C3HC4) 4	2.07
Mm.34175	RIKEN cDNA A530047J11 gene	2.06
Mm.37214	Transferrin	2.06
Mm.316210	FAT tumor suppressor homolog 4 (Drosophila)	2.04
Mm.291799	Retinol dehydrogenase 11	2.03
Mm.87676	Transmembrane protein 16K	2.03
Mm.51259	CDNA sequence BC035537	2.01
Mm.51434	Transcribed locus	1.99
Mm.43358	Pre B-cell leukemia transcription factor 1	1.99
Mm.11869	Expressed sequence AI427122	1.98
Mm.435523	Hypothetical protein LOC574403	1.96
Mm.426628	Expressed sequence C87490	1.96
Mm.428708	Special AT-rich sequence binding protein 1	1.95
Mm.226435	UDP-Gal:betaGlcNAc beta 1,3-galactosyltransferase, polypeptide 1	1.95
Mm.224306	Kelch-like 13 (Drosophila)	1.95
Mm.435789	Transcribed locus	1.94
Mm.268317	Pleckstrin homology domain containing, family H (with MyTH4 domain) member 1	1.92
Mm.255246	Cytochrome P450, family 26, subfamily b, polypeptide 1	1.89
Mm.133193	Keratin 222	1.88
Mm.435077	Transcribed locus	1.88
Mm.306954	Anterior pharynx defective 1a homolog (C. elegans)	1.86
Mm.158289	Myosin, heavy polypeptide 14	1.86

Table A-2. Continued

Unigene ID	Description	Log_2 FC
Mm.56097	RIKEN cDNA D330017J20 gene	1.86
Mm.53865	Ankyrin repeat domain 29	1.85
Mm.4744	Growth differentiation factor 5	1.84
Mm.398133	Transcribed locus	1.83
Mm.292168	Synuclein, alpha interacting protein (synphilin)	1.82
Mm.70371	RIKEN cDNA 2310005E10 gene	1.82
Mm.406348	Transcribed locus	1.82
Mm.41945	Tetratricopeptide repeat domain 22	1.82
Mm.45533	RIKEN cDNA 2310026E23 gene	1.82
Mm.153013	Regulator of G-protein signaling 6	1.81
Mm.335395	RAB6B, member RAS oncogene family	1.81
Mm.435503	AT motif binding factor 1	1.80
Mm.27469	Tetraspanin 2	1.80
Mm.338690	Solute carrier family 35, member F1	1.78
Mm.1892	Corticotropin releasing hormone receptor 1	1.77
Mm.306021	UDP galactosyltransferase 8A	1.76
Mm.32744	Opsin (encephalopsin)	1.75
Mm.240912	Ribulose-5-phosphate-3-epimerase	1.75
Mm.208125	A disintegrin-like and metallopeptidase (reprolysin type) with thrombospondin type 1 motif, 6	1.74
Mm.434125	Transcribed locus	1.74
Mm.282257	Vav 3 oncogene	1.73
Mm.27005	Visinin-like 1	1.71
Mm.28893	RAP1, GTP-GDP dissociation stimulator 1	1.71
Mm.40068	Tubulin, beta 3	1.70
Mm.407234	Transcribed locus	1.69
Mm.213623	RIKEN cDNA 6430502M16 gene	1.69
Mm.426957	Transcribed locus	1.68
Mm.247457	Secernin 3	1.68
Mm.157069	Delta-like 1 homolog (Drosophila)	1.68
Mm.10214	Tuftelin 1	1.67
Mm.30119	Sterol-C4-methyl oxidase-like	1.67
Mm.431124	CDNA, clone:Y2G0147N17, strand:unspecified	1.64
Mm.393375	Transcribed locus	1.63
Mm.316418	Arginine/serine-rich coiled-coil 1	1.62
Mm.393717	Transcribed locus	1.62
Mm.26479	Zinc fingerprotein 618	1.61
Mm.39330	Heat shock protein 4 like	1.60
Mm.87027	Cell cycle exit and neuronal differentiation 1	1.60
Mm.153566	Meteorin, glial cell differentiation regulator-like	1.59
Mm.248096	RUN and SH3 domain containing 2	1.58
Mm.20453	FK506 binding protein 1b	1.56

Table A-2. Continued

Unigene ID	Description	Log_2 FC
Mm.2445	Acyl-Coenzyme A dehydrogenase, long-chain	1.56
Mm.133370	24-dehydrocholesterol reductase	1.55
Mm.275332	Autophagy-related 7 (yeast)	1.54
Mm.432562	Myelin-associated oligodendrocytic basic protein	1.54
Mm.3093	Serine (or cysteine) peptidase inhibitor, clade E, member 2	1.54
Mm.127058	StAR-related lipid transfer (START) domain containing 4	1.54
Mm.32550	DnaJ (Hsp40) homolog, subfamily C, member 12	1.54
Mm.140158	Cytochrome P450, family 51	1.53
Mm.3970	ELAV (embryonic lethal, abnormal vision, Drosophila)-like 4 (Hu antigen D)	1.52
Mm.196701	Protocadherin beta 12	1.52
Mm.31263	RIKEN cDNA B230118H07 gene	1.52
Mm.275387	RIKEN cDNA 1810041L15 gene	1.49
Mm.154303	RIKEN cDNA 4930544G21 gene	1.49
Mm.166647	G protein-coupled receptor 158	1.48
Mm.44721	Leucine-rich repeat LGI family, member 2	1.48
Mm.21995	Fatty acid desaturase domain family, member 6	1.47
Mm.125503	RAN binding protein 6	1.47
Mm.410111	Transcribed locus	1.46
Mm.434311	Cytochrome P450, family 2, subfamily u, polypeptide 1	1.46
Mm.102147	16 days neonate cerebellum cDNA, RIKEN full-length enriched library, clone:9630041I08 product:unclassifiable, full insert sequence	1.44
Mm.289915	Damage specific DNA binding protein 1	1.43
Mm.29098	Galactose mutarotase	1.43
Mm.1517	Synaptobrevin like 1	1.42
Mm.29646	CNDP dipeptidase 2 (metallopeptidase M20 family)	1.42
Mm.377099	Melanoma antigen, family A, 7	1.42
Mm.264036	NAD(P)H dehydrogenase, quinone 2	1.42
Mm.124595	RIKEN cDNA A330008L17 gene	1.41
Mm.41523	RIKEN cDNA 6330416G13 gene	1.41
Mm.380683	HIV-1 Rev binding protein	1.40
Mm.220817	Histidine acid phosphatase domain containing 1	1.40
Mm.432488	Male sterility domain containing 1	1.38
Mm.341423	Dedicator of cytokinesis 4	1.38
Mm.182574	Isochorismatase domain containing 1	1.38
Mm.18962	Catenin (cadherin associated protein), alpha 1	1.37
Mm.151962	Cache domain containing 1	1.37
Mm.26564	Oxysterol binding protein-like 11	1.37
Mm.72979	RIKEN cDNA 6430550H21 gene	1.36
Mm.397953	Transcribed locus	1.36
Mm.46782	La ribonucleoprotein domain family, member 2	1.35

Table A-2. Continued

Unigene ID	Description	Log_2 FC
Mm.386792	Zinc finger protein 364	1.35
Mm.24183	Transgelin 3	1.34
Mm.314113	ELOVL family member 6, elongation of long chain fatty acids (yeast)	1.34
Mm.176695	Tripartite motif-containing 59	1.34
Mm.259191	O-linked N-acetylglucosamine (GlcNAc) transferase (UDP-N-acetylglucosamine:polypeptide-N-acetylglucosaminyl transferase)	1.34
Mm.93796	Mcf.2 transforming sequence	1.34
Mm.271620	Golgi-specific brefeldin A-resistance factor 1	1.34
Mm.192162	Calsyntenin 2	1.32
Mm.119646	Mitogen-activated protein kinase kinase kinase 7 interacting protein 3	1.32
Mm.194	FMS-like tyrosine kinase 3	1.32
Mm.158827	RIKEN cDNA 2410003P15 gene	1.31
Mm.138434	GRAM domain containing 1B	1.31
Mm.40110	G patch domain containing 3	1.30
Mm.196596	RIKEN cDNA 3110002H16 gene	1.30
Mm.193670	Eukaryotic translation initiation factor 5A2	1.29
Mm.54183	Olfactomedin 3	1.28
Mm.302755	Trinucleotide repeat containing 9	1.27
Mm.433866	Transcribed locus	1.26
Mm.291854	Pleckstrin homology domain containing, family G (with RhoGef domain) member 3	1.26
Mm.425171	RIKEN cDNA 6430524H05 gene	1.25
Mm.341004	ATP-binding cassette, sub-family A (ABC1), member 8b	1.25
Mm.284654	WD repeat domain 37	1.25
Mm.371580	Sorbitol dehydrogenase	1.24
Mm.255026	Acyl-CoA synthetase short-chain family member 2	1.24
Mm.219675	G elongation factor, mitochondrial 2	1.22
Mm.425766	Neurexin III	1.22
Mm.41728	Enoyl Coenzyme A hydratase domain containing 1	1.22
Mm.222685	Ceramide kinase	1.22
Mm.298283	Neurofilament, heavy polypeptide	1.21
Mm.275683	Islet cell autoantigen 1	1.21
Mm.130063	RIKEN cDNA 9330182L06 gene	1.20
Mm.258932	RIKEN cDNA 1810012P15 gene	1.20
Mm.425467	Solute carrier organic anion transporter family, member 3a1	1.19
Mm.247143	GDP-mannose 4, 6-dehydratase	1.19
Mm.298251	Leucine-rich repeat LGI family, member 1	1.19
Mm.195932	CDC42 effector protein (Rho GTPase binding) 2	1.19
Mm.170855	RIKEN cDNA B230380D07 gene	1.18
Mm.945	Protein tyrosine phosphatase, receptor type, E	1.17
Mm.389061	PFTAIRE protein kinase 1	1.17

Table A-2. Continued

Unigene ID	Description	Log_2 FC
Mm.302793	Synaptotagmin IX	1.16
Mm.290085	Cereblon	1.16
Mm.3676	Golgi transport 1 homolog B (S. cerevisiae)	1.16
Mm.5163	Ras-like without CAAX 2	1.15
Mm.33120	Histamine N-methyltransferase	1.15
Mm.275639	Glycine receptor, beta subunit	1.15
Mm.86472	RIKEN cDNA 1200014M14 gene	1.15
Mm.146332	Receptor accessory protein 1	1.14
Mm.433835	Transcribed locus	1.13
Mm.57225	Phosphoglucomutase 2-like 1	1.12
Mm.414514	Transcribed locus	1.11
Mm.291826	Adiponectin receptor 2	1.11
Mm.58836	Citrate synthase	1.11
Mm.251228	RNA terminal phosphate cyclase domain 1	1.10
Mm.34326	Zinc finger, DHHC domain containing 2	1.10
Mm.331630	A kinase (PRKA) anchor protein 2	1.10
Mm.38816	WD repeat domain 36	1.09
Mm.312233	TAF4B RNA polymerase II, TATA box binding protein (TBP)-associated factor	1.09
Mm.289441	Claudin 1	1.08
Mm.54201	Hypothetical protein C030014L02	1.08
Mm.33490	GA repeat binding protein, beta 2	1.07
Mm.432944	Chromatin modifying protein 2B	1.07
Mm.397106	Expressed sequence AI848218	1.07
Mm.6306	ATPase, Ca++ transporting, ubiquitous	1.07
Mm.30737	F-box protein 28	1.06
Mm.44068	RIKEN cDNA 3830406C13 gene	1.05
Mm.24431	TAF13 RNA polymerase II, TATA box binding protein (TBP)-associated factor	1.05
Mm.4065	RIKEN cDNA C230093N12 gene	1.04
Mm.219433	Zinc finger, SWIM domain containing 6	1.03
Mm.2942	Asparagine synthetase	1.03
Mm.347625	Phosphatidylinositol glycan anchor biosynthesis, class Z	1.02
Mm.419813	CUB and Sushi multiple domains 1	1.01
Mm.145488	Tyrosyl-tRNA synthetase	1.01
Mm.146984	Proteasome (prosome, macropain) inhibitor subunit 1	1.00

Figure A-3: Genes with statistically higher expression in ARC than SNpc of animals treated with MPTP. Male mice (n=8/group) were treated with a single injection of MPTP (20 mg/kg; s.c.) or saline (10 ml/kg; s.c.). All animals were killed 8 h after MPTP or saline treatment. Amplified mRNA from 300-500 laser-captured TH immunofluorescent cells from ARC and SNpc of each mouse were hybridized to an Affymetrix mouse 430 2.0 chip. Data was normalized and genes that were significantly higher in ARC than SNpc by at least 2 fold in MPTP treated animals were identified.

Table A-3. Genes with higher expression in ARC than SNpc 8h after MPTP treatment		
Unigene ID	Description	Log_2 FC
Mm.277996	Pro-opiomelanocortin-alpha	9.74
Mm.140765	Endothelin converting enzyme-like 1	8.79
Mm.57138	Sine oculis-related homeobox 6 homolog (Drosophila)	7.74
Mm.154796	Neuropeptide Y	7.48
Mm.434306	Distal-less homeobox 1	7.13
Mm.336070	G protein-coupled receptor 101	7.02
Mm.75498	CART prepropeptide	6.94
Mm.2453	Somatostatin	6.86
Mm.42242	ISL1 transcription factor, LIM/homeodomain	6.60
Mm.393566	Estrogen receptor 1 (alpha)	6.29
Mm.34797	Cellular retinoic acid binding protein I	6.11
Mm.2509	Procollagen, type VI, alpha 1	6.09
Mm.414399	Transcribed locus	6.02
Mm.4655	Galanin	6.02
Mm.42096	G substrate	5.69
Mm.429391	Transcribed locus	5.62
Mm.389327	Growth hormone releasing hormone	5.62
Mm.102196	RIKEN cDNA 2900001G08 gene	5.48
Mm.200916	Glutathione peroxidase 3	5.43
Mm.208287	FXYD domain-containing ion transport regulator 6	5.40
Mm.150401	Serine/threonine kinase 32A	5.29
Mm.22650	Serine (or cysteine) peptidase inhibitor, clade A, member 3N	5.28
Mm.283194	Kelch domain containing 8B	5.27
Mm.1528	Glypican 4	5.20
Mm.44305	RIKEN cDNA 1100001E04 gene	5.09
Mm.64201	Neurotensin	5.07
Mm.70980	Sortilin-related VPS10 domain containing receptor 3	5.04
Mm.402016	Transcribed locus	5.00
Mm.2374	Tachykinin 2	4.94
Mm.277812	Villin 2	4.85
Mm.332425	Corin	4.83
Mm.6239	Prodynorphin	4.82
Mm.246573	RIKEN cDNA 9130014G24 gene	4.74
Mm.335953	Diacylglycerol kinase kappa	4.72
Mm.397887	Unc-5 homolog D (C. elegans)	4.71
Mm.1440	Tachykinin 1	4.56
Mm.296806	SEC14-like 3 (S. cerevisiae)	4.46
Mm.5137	Double C2, beta	4.44
Mm.45054	Guanine deaminase	4.40

Table A-3. Continued

Unigene ID	Description	Log_2 FC
Mm.45207	Melanoma antigen, family L, 2	4.35
Mm.290693	G protein-coupled receptor 6	4.31
Mm.262135	Protein kinase inhibitor beta, cAMP dependent, testis specific	4.31
Mm.159201	RIKEN cDNA 4932442L08 gene	4.28
Mm.3896	Distal-less homeobox 2	4.26
Mm.4672	G protein-coupled receptor 83	4.25
Mm.284102	Expressed sequence AI467606	4.23
Mm.154093	Procollagen, type XXIII, alpha 1	4.21
Mm.41395	Neuroglobin	4.12
Mm.34980	Transcribed locus	4.08
Mm.238343	Annexin A2	4.07
Mm.128861	Protocadherin 20	4.04
Mm.38674	Synaptotagmin-like 4	4.02
Mm.287187	Sphingomyelin phosphodiesterase, acid-like 3B	3.98
Mm.36006	Adenylate kinase 7	3.97
Mm.413640	Transcribed locus	3.95
Mm.41580	RAB3B, member RAS oncogene family	3.89
Mm.126464	Transcribed locus	3.88
Mm.20108	Aldehyde oxidase 3	3.86
Mm.124728	AarF domain containing kinase 4	3.85
Mm.330975	G protein-coupled receptor 103	3.85
Mm.392524	G protein-coupled receptor 83	3.84
Mm.77895	Chondrolectin	3.80
Mm.391246	RIKEN cDNA 2610018G03 gene	3.79
Mm.4489	Potassium voltage-gated channel, subfamily H (eag-related), member 1	3.75
Mm.17993	RIKEN cDNA 1700027N10 gene	3.74
Mm.74610	CDNA sequence BC023892	3.72
Mm.273285	Tescalcin	3.71
Mm.35708	Leprecan-like 2	3.64
Mm.402920	Transcribed locus	3.63
Mm.273114	Gamma-aminobutyric acid (GABA-A) receptor, subunit alpha 5	3.58
Mm.396927	Transcribed locus	3.58
Mm.416176	Transcribed locus	3.57
Mm.171378	Uncoupling protein 2 (mitochondrial, proton carrier)	3.54
Mm.23297	Retrotransposon gag domain containing 4	3.50
Mm.405529	Transcribed locus	3.47
Mm.34901	GH regulated TBC protein 1	3.46
Mm.39617	Plexin domain containing 1	3.36
Mm.41854	Raftlin lipid raft linker 1	3.36
Mm.387697	Forkhead-associated (FHA) phosphopeptide binding domain 1	3.36
Mm.435441	Laminin, beta 3	3.34

Table A-3. Continued

Unigene ID	Description	Log_2 FC
Mm.23895	Tektin 2	3.31
Mm.101811	Dynein, axonemal, heavy chain 1	3.31
Mm.31056	Coiled-coil domain containing 109B	3.27
Mm.42257	Tektin 1	3.27
Mm.296819	RIKEN cDNA 3100002J23 gene	3.26
Mm.327654	LON peptidase N-terminal domain and ring finger 3	3.20
Mm.976	Flavin containing monooxygenase 1	3.20
Mm.1894	CD1d1 antigen	3.17
Mm.38450	Septin 9	3.15
Mm.384976	Expressed sequence AW492955	3.14
Mm.372587	RIKEN cDNA C730029A08 gene	3.14
Mm.28385	Transmembrane protein 176B	3.11
Mm.285934	Monooxygenase, DBH-like 1	3.10
Mm.126193	TRAF2 and NCK interacting kinase	3.10
Mm.42202	R-spondin homolog (Xenopus laevis)	3.08
Mm.423621	CD44 antigen	3.06
Mm.329622	CDC42 binding protein kinase gamma (DMPK-like)	3.05
Mm.324305	Gem-interacting protein	3.05
Mm.227117	Solute carrier family 30, member 10	3.05
Mm.39600	RIKEN cDNA C030019I05 gene	3.03
Mm.46662	Dapper homolog 1, antagonist of beta-catenin (xenopus)	3.02
Mm.32622	G protein-coupled receptor 179	3.02
Mm.336244	Nuclear RNA export factor 3	3.02
Mm.398480	RIKEN cDNA 3830409H07 gene	3.00
Mm.347711	Procollagen, type IV, alpha 4	3.00
Mm.78373	Coiled-coil domain containing 19	2.99
Mm.334207	RIKEN cDNA 4932409I22 gene	2.98
Mm.341593	Transmembrane protein 132E	2.96
Mm.281700	Huntingtin-associated protein 1	2.95
Mm.220358	Glucokinase	2.90
Mm.4876	Reticulocalbin 1	2.90
Mm.16347	Prepronociceptin	2.88
Mm.1239	Glial fibrillary acidic protein	2.88
Mm.187372	RIKEN cDNA 4632412N22 gene	2.86
Mm.287421	RIKEN cDNA 1700086L19 gene	2.85
Mm.19316	GRAM domain containing 1C	2.84
Mm.10099	Neuronal pentraxin 2	2.84
Mm.2899	Preproenkephalin 1	2.83
Mm.303386	Laminin, alpha 1	2.82
Mm.4352	Procollagen, type XVIII, alpha 1	2.80
Mm.113877	Glycine receptor, alpha 2 subunit	2.79

Table A-3. Continued

Unigene ID	Description	Log_2 FC
Mm.266301	Double C2, alpha	2.77
Mm.1791	Dual specificity phosphatase 6	2.77
Mm.435516	Synaptic nuclear envelope 1	2.75
Mm.292568	Leucine rich repeat transmembrane neuronal 1	2.75
Mm.12743	Testis specific gene A2	2.75
Mm.20916	Wolfram syndrome 1 homolog (human)	2.73
Mm.329578	Neuropilin (NRP) and tolloid (TLL)-like 1	2.72
Mm.110505	Immunoglobulin superfamily, member 1	2.72
Mm.39884	Receptor (calcitonin) activity modifying protein 3	2.71
Mm.315382	CDNA sequence BC040758	2.70
Mm.1433	Neuropeptide Y receptor Y2	2.70
Mm.360398	Transmembrane channel-like gene family 4	2.70
Mm.284863	BMP and activin membrane-bound inhibitor, homolog (Xenopus laevis)	2.68
Mm.51340	Ankyrin repeat and SOCS box-containing protein 4	2.61
Mm.159995	RIKEN cDNA A930021C24 gene	2.59
Mm.132535	Inositol 1,4,5-trisphosphate 3-kinase B	2.59
Mm.87155	Protein phosphatase, EF hand calcium-binding domain 2	2.58
Mm.356184	EF hand calcium binding protein 2	2.58
Mm.130952	Stam binding protein like 1	2.58
Mm.953	Sphingomyelin phosphodiesterase 2, neutral	2.56
Mm.335337	Similar to Protein C6orf117	2.55
Mm.425110	Hypothetical protein LOC620695	2.51
Mm.10299	Procollagen, type V, alpha 2	2.50
Mm.3475	Retinoid X receptor gamma	2.50
Mm.29891	Forkhead box O1	2.49
Mm.5304	Gamma-aminobutyric acid (GABA-A) receptor, subunit alpha 2	2.48
Mm.275409	Transmembrane protein 46	2.46
Mm.308296	UDP-N-acetyl-alpha-D-galactosamine:polypeptide N-acetylgalactosaminyltransferase-like 1	2.44
Mm.251774	Peroxidasin homolog (Drosophila)	2.43
Mm.256249	Paraneoplastic antigen MA3	2.41
Mm.4965	LIM homeobox protein 1	2.41
Mm.40322	Slit homolog 1 (Drosophila)	2.39
Mm.275751	Coiled-coil domain containing 57	2.39
Mm.272814	Paraneoplastic antigen MA1	2.38
Mm.132391	6-phosphofructo-2-kinase/fructose-2,6-biphosphatase 4	2.38
Mm.434650	Transcribed locus	2.37
Mm.40173	Potassium voltage-gated channel, subfamily F, member 1	2.35
Mm.4351	Arginine vasopressin receptor 1A	2.35
Mm.400754	Transcribed locus	2.35
Mm.275648	PDZ and LIM domain 7	2.34

Table A-3. Continued

Unigene ID	Description	Log_2 FC
Mm.433168	Transcribed locus	2.32
Mm.28244	CDNA sequence BC022623	2.31
Mm.3957	CDNA sequence BC034204	2.30
Mm.261591	Insulin receptor substrate 4	2.29
Mm.150294	Procollagen-proline, 2-oxoglutarate 4-dioxygenase (proline 4-hydroxylase), alpha polypeptide III	2.29
Mm.344095	Scavenger receptor class A, member 3	2.28
Mm.24005	Adhesion molecule with Ig like domain 2	2.26
Mm.93193	RIKEN cDNA 4432405B04 gene	2.26
Mm.268378	Calcium channel, voltage-dependent, T type, alpha 1H subunit	2.25
Mm.398518	Calcium channel, voltage-dependent, gamma subunit 4	2.24
Mm.281298	Growth arrest and DNA-damage-inducible 45 gamma	2.23
Mm.100167	Phosphodiesterase 8B	2.22
Mm.276747	Visual cortex cDNA, RIKEN full-length enriched library, clone:K530032J01 product:unclassifiable, full insert sequence	2.22
Mm.225096	Integrin alpha 6	2.22
Mm.433973	Protein tyrosine phosphatase, receptor type, K	2.20
Mm.20164	Glutathione peroxidase 7	2.18
Mm.41033	Transformation related protein 53 inducible protein 11	2.17
Mm.334569	RIKEN cDNA 4732435N03 gene	2.16
Mm.241063	Expressed sequence AI894139	2.16
Mm.394928	RIKEN cDNA 9430029N19 gene	2.16
Mm.158282	RIKEN cDNA 1700029J07 gene	2.15
Mm.96057	RIKEN cDNA A730017D01 gene	2.15
Mm.435564	Ephrin A5	2.14
Mm.291877	Bromodomain and PHD finger containing, 3	2.14
Mm.71498	Ligand dependent nuclear receptor corepressor-like	2.14
Mm.290207	E26 avian leukemia oncogene 2, 3' domain	2.13
Mm.33304	Potassium channel, subfamily K, member 2	2.11
Mm.33832	Solute carrier family 14 (urea transporter), member 1	2.11
Mm.84073	Bcl2-associated athanogene 3	2.10
Mm.7214	Annexin A3	2.10
Mm.205421	Fibronectin type III domain containing 3a	2.10
Mm.6388	Heat shock protein 1A	2.10
Mm.435439	Neuronal guanine nucleotide exchange factor	2.09
Mm.80685	Ciliary rootlet coiled-coil, rootletin	2.09
Mm.403263	Transcribed locus	2.08
Mm.276279	Zinc finger protein 667	2.06
Mm.275845	Synapsin II	2.04
Mm.44561	RAS protein-specific guanine nucleotide-releasing factor 1	2.02
Mm.436351	Transcribed locus	2.02
Mm.4541	SRY-box containing gene 2	2.01

Table A-3. Continued

Unigene ID	Description	Log_2 FC
Mm.295397	DEP domain containing 6	2.01
Mm.32760	RIKEN cDNA 1700009P17 gene	2.00
Mm.36446	CDNA sequence BC007180	2.00
Mm.132155	RIKEN cDNA C030009J22 gene	1.99
Mm.285	Kinase insert domain protein receptor	1.99
Mm.433558	Transcribed locus	1.98
Mm.283273	Inhibitor of DNA binding 4	1.96
Mm.390712	Potassium channel tetramerisation domain containing 4	1.95
Mm.57175	CD83 antigen	1.95
Mm.121705	RIKEN cDNA A530088I07 gene	1.94
Mm.392156	Transcribed locus, weakly similar to NP_608540.1 [Drosophila melanogaster]	1.93
Mm.279932	RIKEN cDNA B230342M21 gene	1.93
Mm.403692	Transcribed locus	1.92
Mm.18635	Regulator of G-protein signalling 10	1.91
Mm.252561	Heparan sulfate 6-O-sulfotransferase 2	1.91
Mm.403636	Transcribed locus	1.91
Mm.7821	Tumor protein D52-like 1	1.91
Mm.347452	Kinesin family member 17	1.89
Mm.157091	Adenylate cyclase 6	1.89
Mm.24262	Ankyrin repeat domain 54	1.89
Mm.11171	Dorso-medial telencephalon gene 2	1.88
Mm.329991	Scm-like with four mbt domains 2	1.88
Mm.250030	Ribosomal protein L12	1.88
Mm.181021	Procollagen, type IV, alpha 2	1.88
Mm.20355	Wingless-related MMTV integration site 4	1.88
Mm.208662	CDNA sequence BC029169	1.88
Mm.45888	RIKEN cDNA 2210417D09 gene	1.88
Mm.89201	Zinc finger protein 179	1.86
Mm.391678	Odd Oz/ten-m homolog 4 (Drosophila)	1.86
Mm.393388	0 day neonate thymus cDNA, RIKEN full-length enriched library, clone:A430010E21 product:unclassifiable, full insert sequence	1.86
Mm.89976	Zinc finger, imprinted 1	1.85
Mm.183114	Transcribed locus	1.84
Mm.186678	CDNA sequence BC022687	1.83
Mm.316890	RIKEN cDNA 5330417C22 gene	1.83
Mm.139192	Guanine nucleotide binding protein, beta 4	1.83
Mm.379388	RIKEN cDNA A230106D06 gene	1.83
Mm.4940	RIKEN cDNA 1110036O03 gene	1.83
Mm.156919	Cathepsin Z	1.82
Mm.40588	Ring finger protein 182	1.81
Mm.201493	Kruppel-like factor 12	1.79

Table A-3. Continued

Unigene ID	Description	Log_2 FC
Mm.136238	Zinc finger and BTB domain containing 20	1.79
Mm.154284	Solute carrier family 22 (organic cation transporter), member 21	1.78
Mm.326526	Zinc finger protein 516	1.77
Mm.29293	SEC24 related gene family, member D (S. cerevisiae)	1.76
Mm.332684	Kinetochore associated 1	1.75
Mm.262113	RIKEN cDNA 5730593F17 gene	1.75
Mm.38832	Fibronectin type III domain containing 3B	1.74
Mm.394729	RIKEN cDNA 4632427E13 gene	1.74
Mm.186943	Transmembrane protein 131	1.73
Mm.297949	Phytanoyl-CoA dioxygenase domain containing 1	1.73
Mm.10685	Neuropeptide Y receptor Y5	1.73
Mm.252862	D-aspartate oxidase	1.72
Mm.20325	N-acetyl galactosaminidase, alpha	1.71
Mm.25181	Zinc finger, CCHC domain containing 11	1.71
Mm.158143	Nuclear receptor subfamily 2, group F, member 2	1.70
Mm.248337	Vasorin	1.70
Mm.402837	Transcribed locus	1.70
Mm.360537	Predicted gene, EG619719	1.70
Mm.39691	15 days embryo head cDNA, RIKEN full-length enriched library, clone:D930025C07 product:unclassifiable, full insert sequence	1.68
Mm.396273	STIP1 homology and U-Box containing protein 1	1.67
Mm.87051	Thymocyte selection-associated HMG box gene	1.67
Mm.24684	Fos-like antigen 2	1.67
Mm.155887	RIKEN cDNA 1600021P15 gene	1.67
Mm.381165	Polycomb group ring finger 5	1.67
Mm.337647	Zinc finger, BED domain containing 4	1.67
Mm.333327	Histamine receptor H 1	1.66
Mm.434173	Transcribed locus	1.65
Mm.18889	Park2 co-regulated	1.64
Mm.29253	Exosome component 8	1.63
Mm.404309	Transcribed locus	1.63
Mm.320691	Potassium voltage-gated channel, Shal-related family, member 2	1.63
Mm.196189	Angiopoietin-like 4	1.62
Mm.420886	Transcribed locus	1.61
Mm.279872	PRP3 pre-mRNA processing factor 3 homolog (yeast)	1.60
Mm.38548	Regulator of G-protein signaling 9	1.59
Mm.76237	Transcribed locus	1.58
Mm.407113	Transcribed locus	1.58
Mm.331842	Major facilitator superfamily domain containing 2	1.58
Mm.40038	Apoptosis-inducing factor, mitochondrion-associated 3	1.58
Mm.184971	RIKEN cDNA A930009L07 gene	1.57
Mm.292567	Cysteine-rich with EGF-like domains 2	1.57

Table A-3. Continued

Unigene ID	Description	Log_2 FC
Mm.17649	RIKEN cDNA 1700026D08 gene	1.57
Mm.8149	Male germ cell-associated kinase	1.57
Mm.183650	Zinc finger protein 647	1.56
Mm.422738	WT1-interacting protein	1.56
Mm.159842	Calcium channel, voltage-dependent, alpha2/delta subunit 1	1.55
Mm.408606	Transcribed locus	1.55
Mm.89564	Pregnancy upregulated non-ubiquitously expressed CaM kinase	1.53
Mm.738	Procollagen, type IV, alpha 1	1.53
Mm.434093	Transcribed locus	1.53
Mm.248445	Tripartite motif protein 25	1.53
Mm.204834	Solute carrier family 1 (glial high affinity glutamate transporter), member 3	1.52
Mm.397123	RIKEN cDNA 6330404F12 gene	1.51
Mm.24204	Alanine and arginine rich domain containing protein	1.51
Mm.392175	CREB regulated transcription coactivator 3	1.49
Mm.314338	Activin receptor IIA	1.49
Mm.17964	KH domain containing, RNA binding, signal transduction associated 3	1.49
Mm.91794	Transcribed locus	1.48
Mm.33171	Ankyrin repeat and SOCs box-containing protein 5	1.48
Mm.435847	Expressed sequence AV025504	1.46
Mm.87663	Calcium channel, voltage-dependent, gamma subunit 5	1.46
Mm.272517	RWD domain containing 2	1.45
Mm.41364	RIKEN cDNA D330038O06 gene	1.45
Mm.359762	Peptidylprolyl isomerase (cyclophilin)-like 6	1.45
Mm.28534	Leucine rich repeat containing 1	1.45
Mm.275071	Jun oncogene	1.44
Mm.394224	Androgen receptor	1.44
Mm.272120	Glutamic acid decarboxylase 1	1.44
Mm.193212	Hydroxypyruvate isomerase homolog (E. coli)	1.43
Mm.24626	RIKEN cDNA 4921526F01 gene	1.43
Mm.434145	Transcribed locus	1.43
Mm.392845	Androgen receptor	1.42
Mm.331573	Reversion-inducing-cysteine-rich protein with kazal motifs	1.42
Mm.21926	DNA segment, Chr 5, ERATO Doi 40, expressed	1.42
Mm.31203	Glutathione S-transferase, mu 4	1.40
Mm.258746	RIKEN cDNA 1190002N15 gene	1.40
Mm.103477	Natriuretic peptide receptor 2	1.39
Mm.128580	DNA methyltransferase (cytosine-5) 1	1.39
Mm.295686	Zinc finger CCCH type containing 12C	1.39
Mm.32582	Early B-cell factor 4	1.38
Mm.329416	Coiled-coil domain containing 112	1.37

Table A-3. Continued

Unigene ID	Description	Log_2 FC
Mm.287163	Btg3 associated nuclear protein	1.37
Mm.292016	Splicing factor, arginine/serine-rich 7	1.36
Mm.133607	Leucine rich repeat and fibronectin type III domain containing 2	1.36
Mm.223717	MAD homolog 1 (Drosophila)	1.36
Mm.70979	G protein-coupled receptor 176	1.35
Mm.383297	Inositol 1,4,5-trisphosphate 3-kinase B	1.35
Mm.22418	Peroxisome biogenesis factor 5	1.35
Mm.390409	Proline-rich polypeptide 6	1.34
Mm.597	Platelet-activating factor acetylhydrolase, isoform 1b, alpha1 subunit	1.34
Mm.136736	Endothelial differentiation, sphingolipid G-protein-coupled receptor, 3	1.34
Mm.155573	WD repeat domain 31	1.34
Mm.153643	Protocadherin 17	1.33
Mm.393348	RIKEN cDNA 4930562D19 gene	1.32
Mm.395887	SET domain containing 6	1.32
Mm.2930	Peter pan homolog (Drosophila)	1.31
Mm.10812	Phosphodiesterase 9A	1.31
Mm.196464	Guanine nucleotide binding protein, alpha inhibiting 2	1.31
Mm.379020	Sparc/osteonectin, cwcv and kazal-like domains proteoglycan 1	1.31
Mm.240435	Oxysterol binding protein-like 6	1.30
Mm.35324	Somatostatin receptor 4	1.30
Mm.246674	DnaJ (Hsp40) homolog, subfamily C, member 1	1.29
Mm.6988	Aminolevulinate, delta-, dehydratase	1.29
Mm.171304	Integrator complex subunit 2	1.27
Mm.424974	MARCKS-like 1	1.27
Mm.250731	Microtubule associated serine/threonine kinase 3	1.27
Mm.42191	Odd Oz/ten-m homolog 3 (Drosophila)	1.27
Mm.281800	Solute carrier family 35 (UDP-glucuronic acid/UDP-N-acetylgalactosamine dual transporter), member D1	1.26
Mm.247537	Ankyrin repeat domain 39	1.26
Mm.182434	Follistatin-like 1	1.25
Mm.317293	Neuronal growth regulator 1	1.24
Mm.1786	Adenine phosphoribosyl transferase	1.24
Mm.3255	Proprotein convertase subtilisin/kexin type 7	1.24
Mm.400798	Transcribed locus	1.23
Mm.389552	F-box protein 10	1.23
Mm.389966	RAB30, member RAS oncogene family	1.23
Mm.6442	Polycystic kidney disease 2	1.23
Mm.22119	Fc receptor, IgG, low affinity III	1.23
Mm.425327	Glutamate receptor, ionotropic, delta 2	1.22
Mm.226704	Gamma-aminobutyric acid (GABA-A) receptor, subunit beta 1	1.22

Table A-3. Continued

Unigene ID	Description	Log_2 FC
Mm.200203	RUN and TBC1 domain containing 2	1.21
Mm.38607	N-acetylglucosamine-1-phosphotransferase, gamma subunit	1.21
Mm.29678	Polypyrimidine tract binding protein 1	1.21
Mm.41702	SRY-box containing gene 11	1.20
Mm.347	RIKEN cDNA 1810007M14 gene	1.20
Mm.33421	RIKEN cDNA 1110012J17 gene	1.19
Mm.116769	Quiescin Q6-like 1	1.19
Mm.40329	Calcium/calmodulin-dependent protein kinase I gamma	1.19
Mm.305152	Apolipoprotein E	1.19
Mm.209711	RIKEN cDNA A730017C20 gene	1.19
Mm.46675	Kelch repeat and BTB (POZ) domain containing 11	1.18
Mm.38172	Mitogen activated protein kinase 7	1.18
Mm.26237	Cryptochrome 1 (photolyase-like)	1.18
Mm.24028	Rap guanine nucleotide exchange factor (GEF) 3	1.17
Mm.390108	CKLF-like MARVEL transmembrane domain containing 3	1.17
Mm.279427	Zinc finger, CCHC domain containing 8	1.17
Mm.286892	Procollagen, type IV, alpha 5	1.17
Mm.396682	RIKEN cDNA C030009O12 gene	1.16
Mm.3390	Myosin IB	1.15
Mm.242072	Tia1 cytotoxic granule-associated RNA binding protein-like 1	1.15
Mm.19119	LysM, putative peptidoglycan-binding, domain containing 2	1.14
Mm.136586	Spermine oxidase	1.14
Mm.3468	Suppressor of cytokine signaling 3	1.13
Mm.28853	Pituitary tumor-transforming 1 interacting protein	1.13
Mm.378951	Kinesin family member C3	1.12
Mm.363427	HIRA interacting protein 3	1.12
Mm.208955	CDNA sequence BC031353	1.12
Mm.232525	Anthrax toxin receptor 1	1.10
Mm.384704	Transmembrane protein 108	1.09
Mm.234641	RAR-related orphan receptor beta	1.09
Mm.42652	N-acetyltransferase 14	1.09
Mm.102305	Trinucleotide repeat containing 6a	1.08
Mm.249966	V-rel reticuloendotheliosis viral oncogene homolog A (avian)	1.07
Mm.275864	RAB34, member of RAS oncogene family	1.07
Mm.393354	CUG triplet repeat, RNA binding protein 1	1.07
Mm.291831	Glycosylphosphatidylinositol specific phospholipase D1	1.06
Mm.32959	Androgen-induced proliferation inhibitor	1.06
Mm.28765	Translocating chain-associating membrane protein 1	1.04
Mm.351459	Sirtuin 1 ((silent mating type information regulation 2, homolog) 1 (S. cerevisiae)	1.04
Mm.274784	Heterogeneous nuclear ribonucleoprotein H3	1.03
Mm.416039	Transcribed locus	1.03

Table A-3. Continued

Unigene ID	Description	Log_2 FC
Mm.426078	Gene model 967, (NCBI)	1.03
Mm.54460	Vmyotubularin related protein 12	1.03
Mm.391777	Max dimerization protein 4	1.02
Mm.155896	Heterogeneous nuclear ribonucleoprotein A2/B1	1.01
Mm.332838	Glutamate receptor, ionotropic, kainate 2 (beta 2)	1.01
Mm.433262	Transcribed locus	1.01
Mm.275304	RAB22A, member RAS oncogene family	1.00
Mm.31324	Debranching enzyme homolog 1 (S. cerevisiae)	1.00

Figure A-4: Genes with statistically higher expression in SNpc than ARC of animals treated with MPTP. Male mice (n=8/group) were treated with a single injection of MPTP (20 mg/kg; s.c.) or saline (10 ml/kg; s.c.). All animals were killed 8 h after MPTP or saline treatment. Amplified mRNA from 300-500 laser-captured TH immunofluorescent cells from ARC and SN of each mouse were hybridized to an Affymetrix mouse 430 2.0 chip. Data was normalized and genes that were significantly higher in SNpc than ARC by at least 2 fold in MPTP treated animals were identified.

Table A-4. Genes with Higher Expression in SNpc than ARC 8h after MPTP treatment		
Unigene ID	Description	Log_2 FC
Mm.14609	Aldehyde dehydrogenase family 1, subfamily A7	9.49
Mm.397323	Expressed sequence AI853839	7.97
Mm.276829	Solute carrier family 39 (zinc transporter), member 4	7.79
Mm.427936	Transcribed locus	7.51
Mm.72070	Riken cDNA C130021I20 gene	7.40
Mm.283137	Cholinergic receptor, nicotinic, alpha polypeptide 6	7.25
Mm.41970	Dopamine receptor 2	7.24
Mm.84118	Predicted gene, EG639426	6.49
Mm.222729	Guanylate cyclase 2c	6.49
Mm.4298	Transcribed locus	6.35
Mm.39825	Transcribed locus	6.24
Mm.110444	Cholinergic receptor, nicotinic, beta polypeptide 3	6.19
Mm.103778	Cholinergic receptor, nicotinic, alpha polypeptide 5	6.07
Mm.393273	Transcribed locus	6.06
Mm.3507	Nuclear receptor subfamily 4, group A, member 2	5.95
Mm.57199	Ret proto-oncogene	5.90
Mm.308735	Kelch-like 1 (Drosophila)	5.75
Mm.52392	RIKEN cDNA A930038C07 gene	5.60
Mm.414106	Transcribed locus	5.46
Mm.23782	Glycosyltransferase 25 domain containing 2	5.42
Mm.406232	Transcribed locus	5.41
Mm.268521	Insulin-like growth factor 1	5.17
Mm.5076	Tolloid-like	5.10
Mm.9431	Protease, serine, 12 neurotrypsin (motopsin)	5.09
Mm.297371	POU domain, class 3, transcription factor 1	5.09
Mm.239941	Pre B-cell leukemia transcription factor 3	4.97
Mm.74324	Solute carrier family 35, member D3	4.97
Mm.420796	Transcribed locus	4.89
Mm.412897	Transcribed locus	4.88
Mm.405570	POU domain, class 3, transcription factor 2	4.83
Mm.30013	RIKEN cDNA 2010011I20 gene	4.79
Mm.358581	Calmegin	4.58
Mm.63569	Cholinergic receptor, nicotinic, alpha polypeptide 3	4.57
Mm.258708	Early B-cell factor 3	4.52
Mm.295917	Gene model 540, (NCBI)	4.49
Mm.39599	GSG1-like	4.44
Mm.137991	Eph receptor A5	4.38
Mm.29221	Transcribed locus	4.27
Mm.113278	Potassium voltage-gated channel, delayed-rectifier, subfamily S,	4.24

Table A-4. Continued

Unigene ID	Description	Log$_2$ FC
	member 3	
Mm.392745	10 days embryo whole body cDNA, RIKEN full-length enriched library, clone:2610306G12 product:unclassifiable, full insert sequence	4.23
Mm.141275	RIKEN cDNA E130009J12 gene	4.16
Mm.42190	Unc4.1 homeobox (C. elegans)	4.05
Mm.332576	Meningioma 1	4.03
Mm.379143	Regulator of G-protein signaling 8	4.02
Mm.408043	Transcribed locus	4.00
Mm.129387	POU domain, class 3, transcription factor 2	4.00
Mm.384108	Immunoglobulin superfamily, member 4	3.84
Mm.425860	Leucine rich repeat containing 3B	3.83
Mm.388885	POU domain, class 3, transcription factor 1	3.80
Mm.288805	DEP domain containing 7	3.78
Mm.71924	Ankyrin repeat domain 38	3.76
Mm.125650	Apolipoprotein L, 2	3.71
Mm.40875	0 day neonate cerebellum cDNA, RIKEN full-length enriched library, clone:C230022P04 product:unclassifiable, full insert sequence	3.65
Mm.30172	Ras association (RalGDS/AF-6) domain family 6	3.65
Mm.275374	Nuclear receptor interacting protein 3	3.64
Mm.412261	Transcribed locus, strongly similar to XP_001055606.1 similar to Oxysterol-binding protein-related protein 3 (OSBP-related protein 3) (ORP-3) [Rattus norvegicus]	3.57
Mm.154541	RIKEN cDNA 3830431G21 gene	3.51
Mm.100125	SH3 domain binding glutamic acid-rich protein like 2	3.47
Mm.83817	Villin-like	3.47
Mm.39723	Kelch domain containing 8A	3.46
Mm.220765	Cadherin 8	3.43
Mm.193274	R-spondin 2 homolog (Xenopus laevis)	3.42
Mm.101836	RIKEN cDNA 9630033F20 gene	3.41
Mm.37882	CDNA sequence BC065085	3.40
Mm.246595	Hypocretin (orexin) receptor 1	3.39
Mm.333264	Glutamate receptor interacting protein 2	3.32
Mm.102899	Transcribed locus	3.31
Mm.6255	Paired-like homeodomain transcription factor 3	3.27
Mm.102211	RIKEN cDNA 9330109K16 gene	3.25
Mm.115970	A disintegrin-like and metallopetidase (reprolysin type) with thrombospondin type 1 motif, 16	3.21
Mm.334011	Malic enzyme 3, NADP(+)-dependent, mitochondrial	3.20
Mm.5195	Complexin 1	3.20
Mm.394300	Transcribed locus	3.16
Mm.380993	Phosphatidylinositol-specific phospholipase C, X domain containing	3.16

Table A-4. Continued

Unigene ID	Description	Log_2 FC
	2	
Mm.26751	Synaptotagmin-like 2	3.14
Mm.156558	Synaptotagmin XVII	3.13
Mm.317854	Pregnancy-associated plasma protein A	3.11
Mm.361919	Solute carrier family 18 (vesicular monoamine), member 2	3.11
Mm.14099	Zinc finger protein 385	3.11
Mm.293363	Spindlin family, member 2	3.11
Mm.415763	Transcribed locus	3.02
Mm.39090	Glutamate receptor, ionotropic, NMDA2C (epsilon 3)	3.01
Mm.72799	Transmembrane protease, serine 5 (spinesin)	3.01
Mm.141936	Insulin-like growth factor binding protein 2	3.01
Mm.17484	Synuclein, alpha	3.01
Mm.4860	Protein tyrosine phosphatase, receptor type, U	3.00
Mm.331690	RIKEN cDNA 5930437A14 gene	2.99
Mm.276248	Sphingosine-1-phosphate phosphotase 2	2.98
Mm.89682	Membrane bound O-acyltransferase domain containing 1	2.97
Mm.298731	Immunoglobin superfamily, member 21	2.97
Mm.159989	RIKEN cDNA 2810022L02 gene	2.95
Mm.360649	RIKEN cDNA A830006F12 gene	2.92
Mm.345834	0 day neonate cerebellum cDNA, RIKEN full-length enriched library, clone:C230096I08 product:hypothetical protein, full insert sequence	2.90
Mm.82308	Protocadherin beta 3	2.89
Mm.428708	Special AT-rich sequence binding protein 1	2.89
Mm.7995	Fibroblast growth factor 13	2.87
Mm.151332	Peroxin 2	2.85
Mm.292983	Vitrin	2.81
Mm.403758	Transcribed locus	2.81
Mm.384353	Mab-21-like 1 (C. elegans)	2.81
Mm.268536	Myotubularin related protein 11	2.79
Mm.169261	Von Willebrand factor C and EGF domains	2.77
Mm.255246	Cytochrome P450, family 26, subfamily b, polypeptide 1	2.75
Mm.211477	Pleckstrin homology-like domain, family B, member 2	2.75
Mm.425526	Fibroblast growth factor 20	2.74
Mm.292100	Fibrinogen-like protein 2	2.74
Mm.103351	ATP-binding cassette, sub-family A (ABC1), member 7	2.73
Mm.133615	RIKEN cDNA 2810457I06 gene	2.72
Mm.282751	Anillin, actin binding protein (scraps homolog, Drosophila)	2.71
Mm.35141	Mannoside acetylglucosaminyltransferase 5, isoenzyme B	2.69
Mm.27789	FERM domain containing 4B	2.68
Mm.318710	RIKEN cDNA 3632451O06 gene	2.68
Mm.435467	Testis-specific kinase 2	2.68

Table A-4. Continued

Unigene ID	Description	Log_2 FC
Mm.41993	Solute carrier family 6 (neurotransmitter transporter, dopamine), member 3	2.65
Mm.17629	Caspase recruitment domain family, member 10	2.65
Mm.155708	Ets variant gene 5	2.62
Mm.253736	Palmdelphin	2.62
Mm.46782	La ribonucleoprotein domain family, member 2	2.61
Mm.422608	RIKEN cDNA 1190017O12 gene	2.61
Mm.210857	Myelin oligodendrocyte glycoprotein	2.60
Mm.273082	Synaptic vesicle glycoprotein 2 b	2.59
Mm.53865	Ankyrin repeat domain 29	2.58
Mm.235938	Fragile histidine triad gene	2.57
Mm.10651	GTP cyclohydrolase 1	2.56
Mm.46797	Adrenergic receptor, beta 1	2.55
Mm.42012	Laminin, alpha 3	2.55
Mm.376140	Sushi domain containing 5	2.55
Mm.39151	Transcribed locus	2.51
Mm.30221	Insulin induced gene 1	2.50
Mm.240912	Ribulose-5-phosphate-3-epimerase	2.47
Mm.34608	Citrate lyase beta like	2.45
Mm.316210	FAT tumor suppressor homolog 4 (Drosophila)	2.44
Mm.397113	Transcribed locus	2.44
Mm.40915	ST6 (alpha-N-acetyl-neuraminyl-2,3-beta-galactosyl-1,3)-N-acetylgalactosaminide alpha-2,6-sialyltransferase 5	2.43
Mm.236287	RIKEN cDNA 1700019D03 gene	2.42
Mm.426321	LEM domain containing 1	2.42
Mm.40550	Transcribed locus	2.42
Mm.250866	Aldehyde dehydrogenase family 1, subfamily A1	2.41
Mm.78923	Phosphatidylinositol-4-phosphate 5-kinase-like 1	2.39
Mm.34344	Pseudouridylate synthase 7 homolog (S. cerevisiae)-like	2.38
Mm.39649	RIKEN cDNA B230216G23 gene	2.38
Mm.80318	Transmembrane protein 169	2.37
Mm.198414	Serine/threonine kinase 39, STE20/SPS1 homolog (yeast)	2.37
Mm.20453	FK506 binding protein 1b	2.37
Mm.285060	FCH and double SH3 domains 1	2.36
Mm.406348	Transcribed locus	2.35
Mm.192699	Phospholipase C, gamma 2	2.34
Mm.407111	Transcribed locus	2.34
Mm.434385	RIKEN cDNA C330011K17 gene	2.32
Mm.289643	Cysteine conjugate-beta lyase 2	2.31
Mm.209715	Procollagen, type XI, alpha 1	2.31
Mm.34235	Williams Beuren syndrome chromosome region 27 (human)	2.28
Mm.435077	Transcribed locus	2.26

Table A-4. Continued

Unigene ID	Description	Log_2 FC
Mm.212855	Myosin regulatory light chain interacting protein	2.26
Mm.3944	Kallikrein related-peptidase 6	2.25
Mm.28893	RAP1, GTP-GDP dissociation stimulator 1	2.24
Mm.23462	Elastin microfibril interfacer 2	2.23
Mm.252369	Cholinergic receptor, nicotinic, alpha polypeptide 4	2.22
Mm.130696	RIKEN cDNA 4930589M24 gene	2.20
Mm.30767	RIKEN cDNA 1300003B13 gene	2.20
Mm.432481	Forkhead box P2	2.19
Mm.435523	Hypothetical protein LOC574403	2.18
Mm.407309	Transcribed locus	2.17
Mm.11869	Expressed sequence AI427122	2.15
Mm.138434	GRAM domain containing 1B	2.14
Mm.133193	Keratin 222	2.13
Mm.65316	Nitric oxide synthase 1 (neuronal) adaptor protein	2.12
Mm.153013	Regulator of G-protein signaling 6	2.12
Mm.341377	Aryl-hydrocarbon receptor	2.12
Mm.27005	Visinin-like 1	2.10
Mm.125874	Hormonally upregulated Neu-associated kinase	2.10
Mm.432488	Male sterility domain containing 1	2.08
Mm.291824	Transmembrane protein 32	2.08
Mm.426628	Expressed sequence C87490	2.07
Mm.64962	Matrix-remodelling associated 7	2.06
Mm.45533	RIKEN cDNA 2310026E23 gene	2.06
Mm.274308	N-ethylmaleimide sensitive fusion protein attachment protein beta	2.06
Mm.435789	Transcribed locus	2.05
Mm.391931	Membrane protein, palmitoylated 7 (MAGUK p55 subfamily member 7)	2.04
Mm.69013	RIKEN cDNA B430201A12 gene	2.03
Mm.158289	Myosin, heavy polypeptide 14	2.03
Mm.43358	Pre B-cell leukemia transcription factor 1	2.00
Mm.381	Adipose differentiation related protein	2.00
Mm.392499	Transcribed locus	1.99
Mm.395863	Transcribed locus	1.97
Mm.426957	Transcribed locus	1.97
Mm.335395	RAB6B, member RAS oncogene family	1.95
Mm.87676	Transmembrane protein 16K	1.95
Mm.136116	Leucine rich repeat containing 20	1.94
Mm.40068	Tubulin, beta 3	1.94
Mm.5162	Serine dehydratase-like	1.93
Mm.87027	Cell cycle exit and neuronal differentiation 1	1.92
Mm.209232	Contactin associated protein-like 4	1.92
Mm.12239	Geminin	1.91

Table A-4. Continued

Unigene ID	Description	Log_2 FC
Mm.400451	Musashi homolog 2 (Drosophila)	1.91
Mm.46764	CDP-diacylglycerol synthase 1	1.89
Mm.396875	Regulator of G-protein signalling 7 binding protein	1.88
Mm.226435	UDP-Gal:betaGlcNAc beta 1,3-galactosyltransferase, polypeptide 1	1.88
Mm.23639	RIKEN cDNA 6330530A05 gene	1.88
Mm.1292	Tyrosine hydroxylase	1.87
Mm.70371	RIKEN cDNA 2310005E10 gene	1.86
Mm.49665	T-cell lymphoma breakpoint associated target 1	1.86
Mm.86823	NAT9	1.83
Mm.41290	GTPase activating RANGAP domain-like 3	1.82
Mm.292168	Synuclein, alpha interacting protein (synphilin)	1.82
Mm.4744	Growth differentiation factor 5	1.81
Mm.432562	Myelin-associated oligodendrocytic basic protein	1.81
Mm.29646	CNDP dipeptidase 2 (metallopeptidase M20 family)	1.80
Mm.176695	Tripartite motif-containing 59	1.80
Mm.435503	AT motif binding factor 1	1.80
Mm.282257	Vav 3 oncogene	1.79
Mm.100348	Regulator of G-protein signalling 7 binding protein	1.78
Mm.338690	Solute carrier family 35, member F1	1.78
Mm.60061	Regulating synaptic membrane exocytosis 1	1.78
Mm.4654	Protein tyrosine phosphatase, non-receptor type 5	1.78
Mm.51434	Transcribed locus	1.78
Mm.27969	UDP-N-acetylglucosamine pyrophosphorylase 1	1.78
Mm.153566	Meteorin, glial cell differentiation regulator-like	1.78
Mm.247457	Secernin 3	1.78
Mm.433275	Transcribed locus	1.77
Mm.306021	UDP galactosyltransferase 8A	1.77
Mm.27469	Tetraspanin 2	1.76
Mm.41945	Tetratricopeptide repeat domain 22	1.76
Mm.44075	Fibronectin type III domain containing 5	1.76
Mm.390803	Pannexin 2	1.75
Mm.337023	Membrane-associated ring finger (C3HC4) 4	1.75
Mm.412289	Transcribed locus	1.75
Mm.298251	Leucine-rich repeat LGI family, member 1	1.74
Mm.32744	Opsin (encephalopsin)	1.74
Mm.275332	Autophagy-related 7 (yeast)	1.73
Mm.314113	ELOVL family member 6, elongation of long chain fatty acids (yeast)	1.73
Mm.44721	Leucine-rich repeat LGI family, member 2	1.73
Mm.393375	Transcribed locus	1.72
Mm.56946	POU domain, class 3, transcription factor 4	1.72
Mm.124595	RIKEN cDNA A330008L17 gene	1.72

Table A-4. Continued

Unigene ID	Description	Log_2 FC
Mm.57225	Phosphoglucomutase 2-like 1	1.70
Mm.316418	Arginine/serine-rich coiled-coil 1	1.70
Mm.403011	Transcribed locus	1.69
Mm.55143	Dickkopf homolog 3 (Xenopus laevis)	1.69
Mm.224306	Kelch-like 13 (Drosophila)	1.68
Mm.1892	Corticotropin releasing hormone receptor 1	1.68
Mm.3970	ELAV (embryonic lethal, abnormal vision, Drosophila)-like 4 (Hu antigen D)	1.67
Mm.407200	Transcribed locus	1.67
Mm.264036	NAD(P)H dehydrogenase, quinone 2	1.65
Mm.275387	RIKEN cDNA 1810041L15 gene	1.65
Mm.18962	Catenin (cadherin associated protein), alpha 1	1.65
Mm.334029	Predicted gene, EG622320	1.64
Mm.27687	RUN and SH3 domain containing 1	1.63
Mm.41203	Solute carrier family 2 (facilitated glucose transporter), member 6	1.62
Mm.391904	Glutamate receptor, metabotropic 1	1.62
Mm.10214	Tuftelin 1	1.62
Mm.37214	Transferrin	1.61
Mm.29098	Galactose mutarotase	1.61
Mm.139607	CDNA sequence BC003266	1.60
Mm.317049	RIKEN cDNA 5730508B09 gene	1.60
Mm.127058	StAR-related lipid transfer (START) domain containing 4	1.60
Mm.259470	Oxysterol binding protein-like 1A	1.59
Mm.9870	Centromere protein Q	1.59
Mm.205422	Sterile alpha motif domain containing 10	1.57
Mm.34175	RIKEN cDNA A530047J11 gene	1.56
Mm.291799	Retinol dehydrogenase 11	1.56
Mm.229342	Acetyl-Coenzyme A acetyltransferase 2	1.55
Mm.41728	Enoyl Coenzyme A hydratase domain containing 1	1.55
Mm.101707	SLIT and NTRK-like family, member 4	1.54
Mm.146332	Receptor accessory protein 1	1.53
Mm.386754	Leucine-rich repeats and transmembrane domains 1	1.53
Mm.392637	Solute carrier family 36 (proton/amino acid symporter), member 1	1.53
Mm.298283	Neurofilament, heavy polypeptide	1.53
Mm.212927	Transmembrane protein 38a	1.53
Mm.27589	Lactate dehydrogenase D	1.52
Mm.89646	Lactation elevated 1	1.52
Mm.289702	Synaptotagmin I	1.52
Mm.407234	Transcribed locus	1.52
Mm.172720	Leucine rich repeat containing 59	1.50
Mm.19133	Amyloid beta (A4) precursor-like protein 2	1.50
Mm.945	Protein tyrosine phosphatase, receptor type, E	1.50

Table A-4. Continued

Unigene ID	Description	Log_2 FC
Mm.423496	Hypothetical protein LOC636791	1.49
Mm.392829	Hypothetical protein C130006E23	1.49
Mm.398492	Transcribed locus	1.49
Mm.1517	Synaptobrevin like 1	1.48
Mm.389247	Nebulin	1.48
Mm.39330	Heat shock protein 4 like	1.48
Mm.388924	Potassium voltage-gated channel, shaker-related subfamily, beta member 2	1.47
Mm.41523	RIKEN cDNA 6330416G13 gene	1.47
Mm.12057	Hypothetical protein C130086A10	1.46
Mm.3093	Serine (or cysteine) peptidase inhibitor, clade E, member 2	1.46
Mm.268317	Pleckstrin homology domain containing, family H (with MyTH4 domain) member 1	1.45
Mm.289915	Damage specific DNA binding protein 1	1.45
Mm.433866	Transcribed locus	1.45
Mm.194	FMS-like tyrosine kinase 3	1.45
Mm.390807	Protein tyrosine phosphatase 4a3	1.44
Mm.173826	Dymeclin	1.43
Mm.336158	CDNA sequence AK129302	1.43
Mm.40110	G patch domain containing 3	1.43
Mm.434311	Cytochrome P450, family 2, subfamily u, polypeptide 1	1.43
Mm.336329	RALBP1 associated Eps domain containing protein 2	1.42
Mm.140158	Cytochrome P450, family 51	1.42
Mm.158827	RIKEN cDNA 2410003P15 gene	1.42
Mm.5915	DPH5 homolog (S. cerevisiae)	1.41
Mm.103560	Jun dimerization protein 2	1.41
Mm.2942	Asparagine synthetase	1.40
Mm.26479	Zinc fingerprotein 618	1.40
Mm.21108	Monoamine oxidase A	1.40
Mm.109840	Regulator of G-protein signaling 11	1.40
Mm.259191	O-linked N-acetylglucosamine (GlcNAc) transferase (UDP-N-acetylglucosamine:polypeptide-N-acetylglucosaminyl transferase)	1.39
Mm.210447	EH domain binding protein 1-like 1	1.38
Mm.425467	Solute carrier organic anion transporter family, member 3a1	1.38
Mm.132583	Kelch-like 4 (Drosophila)	1.38
Mm.153111	Required for meiotic nuclear division 1 homolog (S. cerevisiae)	1.38
Mm.280254	Abhydrolase domain containing 5	1.37
Mm.133370	24-dehydrocholesterol reductase	1.37
Mm.290802	Guanosine monophosphate reductase	1.37
Mm.193670	Eukaryotic translation initiation factor 5A2	1.36
Mm.157119	Sortilin 1	1.36
Mm.27844	ATP synthase, H+ transporting, mitochondrial F0 complex, subunit s	1.36

Table A-4. Continued

Unigene ID	Description	Log_2 FC
Mm.33490	GA repeat binding protein, beta 2	1.36
Mm.392446	Mus musculus, clone IMAGE:1512359, mRNA	1.36
Mm.302793	Synaptotagmin IX	1.35
Mm.268902	Complexin 2	1.34
Mm.192162	Calsyntenin 2	1.34
Mm.245297	Cytochrome P450, family 4, subfamily v, polypeptide 3	1.34
Mm.386792	Zinc finger protein 364	1.34
Mm.31263	RIKEN cDNA B230118H07 gene	1.33
Mm.18036	E2F transcription factor 1	1.32
Mm.341423	Dedicator of cytokinesis 4	1.32
Mm.38037	MON1 homolog A (yeast)	1.32
Mm.96867	Ring finger protein 141	1.31
Mm.347625	Phosphatidylinositol glycan anchor biosynthesis, class Z	1.31
Mm.3645	Myosin Va	1.31
Mm.125503	RAN binding protein 6	1.31
Mm.377099	Melanoma antigen, family A, 7	1.31
Mm.24641	RIKEN cDNA 2810405J04 gene	1.31
Mm.290534	SH3 binding domain protein 5 like	1.30
Mm.435680	Transcribed locus	1.29
Mm.252316	Glutathione synthetase	1.28
Mm.26134	Protein phosphatase 2 (formerly 2A), regulatory subunit B (PR 52), beta isoform	1.28
Mm.21995	Fatty acid desaturase domain family, member 6	1.27
Mm.247143	GDP-mannose 4, 6-dehydratase	1.27
Mm.209503	Tetratricopeptide repeat domain 27	1.27
Mm.30737	F-box protein 28	1.27
Mm.33120	Histamine N-methyltransferase	1.27
Mm.240434	Apoptosis-inducing factor, mitochondrion-associated 1	1.25
Mm.190774	Basonuclin 2	1.25
Mm.397953	Transcribed locus	1.24
Mm.414514	Transcribed locus	1.24
Mm.121789	POU domain, class 3, transcription factor 3	1.24
Mm.21109	Gelsolin	1.24
Mm.392075	Calumenin	1.24
Mm.257067	Ly6/neurotoxin 1	1.23
Mm.312233	TAF4B RNA polymerase II, TATA box binding protein (TBP)-associated factor	1.23
Mm.219675	G elongation factor, mitochondrial 2	1.23
Mm.170855	RIKEN cDNA B230380D07 gene	1.23
Mm.341747	RIKEN cDNA 6330442E10 gene	1.23
Mm.331630	A kinase (PRKA) anchor protein 2	1.22
Mm.222685	Ceramide kinase	1.22

Table A-4. Continued

Unigene ID	Description	Log_2 FC
Mm.40477	0 day neonate lung cDNA, RIKEN full-length enriched library, clone:E030046E07 product:unclassifiable, full insert sequence	1.22
Mm.29580	Stathmin-like 2	1.21
Mm.2445	Acyl-Coenzyme A dehydrogenase, long-chain	1.21
Mm.38433	Tryptophanyl-tRNA synthetase	1.21
Mm.258932	RIKEN cDNA 1810012P15 gene	1.20
Mm.157069	Delta-like 1 homolog (Drosophila)	1.19
Mm.275683	Islet cell autoantigen 1	1.19
Mm.141054	RIKEN cDNA 1110011C06 gene	1.17
Mm.389061	PFTAIRE protein kinase 1	1.17
Mm.41022	RNA binding motif protein 19	1.15
Mm.425766	Neurexin III	1.15
Mm.406721	Transcribed locus	1.14
Mm.54183	Olfactomedin 3	1.14
Mm.6306	ATPase, Ca++ transporting, ubiquitous	1.13
Mm.38816	WD repeat domain 36	1.12
Mm.3676	Golgi transport 1 homolog B (S. cerevisiae)	1.12
Mm.386776	Estrogen related receptor, alpha	1.11
Mm.255026	Acyl-CoA synthetase short-chain family member 2	1.11
Mm.219433	Zinc finger, SWIM domain containing 6	1.10
Mm.419813	CUB and Sushi multiple domains 1	1.10
Mm.397106	Expressed sequence AI848218	1.09
Mm.433835	Transcribed locus	1.09
Mm.389855	RIKEN cDNA C230052I12 gene	1.08
Mm.434709	Transcribed locus	1.08
Mm.26564	Oxysterol binding protein-like 11	1.08
Mm.29150	Dynein light chain Tctex-type 3	1.08
Mm.27925	Dysbindin (dystrobrevin binding protein 1) domain containing 1	1.07
Mm.24431	TAF13 RNA polymerase II, TATA box binding protein (TBP)-associated factor	1.07
Mm.409762	Transcribed locus	1.06
Mm.432777	Transcribed locus, strongly similar to XP_225688.3 similar to zinc finger protein [Rattus norvegicus]	1.05
Mm.380683	HIV-1 Rev binding protein	1.05
Mm.74208	Periphilin 1	1.05
Mm.197441	Protocadherin beta 16	1.05
Mm.277242	RIKEN cDNA A530089I17 gene	1.05
Mm.46722	PDZ domain containing 1	1.04
Mm.211429	Ectonucleotide pyrophosphatase/phosphodiesterase 6	1.04
Mm.58836	Citrate synthase	1.04
Mm.251228	RNA terminal phosphate cyclase domain 1	1.04
Mm.182912	Growth hormone inducible transmembrane protein	1.04

Table A-4. Continued

Unigene ID	Description	Log_2 FC
Mm.340211	COX10 homolog, cytochrome c oxidase assembly protein, heme A: farnesyltransferase (yeast)	1.03
Mm.289441	Claudin 1	1.03
Mm.216217	RIKEN cDNA 2900011O08 gene	1.03
Mm.405108	Transcribed locus	1.03
Mm.28309	RIKEN cDNA 0610033I05 gene	1.03
Mm.36507	Nudix (nucleoside diphosphate linked moiety X)-type motif 12	1.02
Mm.210095	ATPase, Ca++ transporting, plasma membrane 3	1.02
Mm.432944	Chromatin modifying protein 2B	1.02
Mm.290085	Cereblon	1.02
Mm.290704	RIKEN cDNA C330007P06 gene	1.02
Mm.160172	Kv channel interacting protein 4	1.00
Mm.41761	5',3'-nucleotidase, mitochondrial	1.00

Abeliovich A, Schmitz Y, Farinas I, Choi-Lundberg D, Ho WH, Castillo PE, Shinsky N, Verdugo JM, Armanini M, Ryan A, Hynes M, Phillips H, Sulzer D, Rosenthal A (2000) Mice lacking alpha-synuclein display functional deficits in the nigrostriatal dopamine system. Neuron 25:239-252.

Agid Y (1991) Parkinson's disease: pathophysiology. Lancet 337:1321-1324.

Agnoli A, Baldassarre M, Ruggieri S, Falaschi P, Urso RD, Rocco A (1981) Prolactin response as an index of dopaminergic receptor function in Parkinson's disease. Correlation with clinical findings and therapeutic response. J Neural Transm 51:123-134.

Ahlskog JE (2005) Challenging conventional wisdom: the etiologic role of dopamine oxidative stress in Parkinson's disease. Mov Disord 20:271-282.

Alex KD, Pehek EA (2007) Pharmacologic mechanisms of serotonergic regulation of dopamine neurotransmission. Pharmacol Ther 113:296-320.

Allam MF, Del Castillo AS, Navajas RF (2002) Smoking and Parkinson's disease. Eur J Neurol 9:315-316.

Allam MF, Campbell MJ, Hofman A, Del Castillo AS, Fernandez-Crehuet Navajas R (2004) Smoking and Parkinson's disease: systematic review of prospective studies. Mov Disord 19:614-621.

Andersson KK, Cox DD, Que L, Jr., Flatmark T, Haavik J (1988) Resonance Raman studies on the blue-green-colored bovine adrenal tyrosine 3-monooxygenase (tyrosine hydroxylase). Evidence that the feedback inhibitors adrenaline and noradrenaline are coordinated to iron. J Biol Chem 263:18621-18626.

Anglade P, Vyas S, Javoy-Agid F, Herrero MT, Michel PP, Marquez J, Mouatt-Prigent A, Ruberg M, Hirsch EC, Agid Y (1997) Apoptosis and autophagy in nigral neurons of patients with Parkinson's disease. Histol Histopathol 12:25-31.

Annunziato L, Leblanc P, Kordon C, Weiner RI (1980) Differences in the kinetics of dopamine uptake in synaptosome preparations of the median eminence relative to other dopaminergically inervated brain regions. Neuroendocrinology 31:316-320.

Arbogast LA, Voogt JL (1991) Hyperprolactinemia increases and hypoprolactinemia decreases tyrosine hydroxylase messenger ribonucleic acid levels in the arcuate nuclei, but not the substantia nigra or zona incerta. Endocrinology 128:997-1005.

Arbogast LA, Voogt JL (1997) Prolactin (PRL) receptors are colocalized in dopaminergic neurons in fetal hypothalamic cell cultures: effect of PRL on tyrosine hydroxylase activity. Endocrinology 138:3016-3023.

Auluck PK, Chan HY, Trojanowski JQ, Lee VM, Bonini NM (2002) Chaperone suppression of alpha-synuclein toxicity in a Drosophila model for Parkinson's disease. Science 295:865-868.

Backman C, Perlmann T, Wallen A, Hoffer BJ, Morales M (1999) A selective group of dopaminergic neurons express Nurr1 in the adult mouse brain. Brain Res 851:125-132.

Bannon MJ (2005) The dopamine transporter: role in neurotoxicity and human disease. Toxicol Appl Pharmacol 204:355-360.

Beal MF (2005) Mitochondria take center stage in aging and neurodegeneration. Ann Neurol 58:495-505.

Beaucamp N, Harding TC, Geddes BJ, Williams J, Uney JB (1998) Overexpression of hsp70i facilitates reactivation of intracellular proteins in neurones and protects them from denaturing stress. FEBS Lett 441:215-219.

Beckman JS, Crow JP (1993) Pathological implications of nitric oxide, superoxide and peroxynitrite formation. Biochem Soc Trans 21:330-334.

Behrouz B, Drolet RE, Sayed ZA, Lookingland KJ, Goudreau JL (2007) Unique responses to mitochondrial complex I inhibition in tuberoinfundibular dopamine neurons may impart resistance to toxic insult. Neuroscience 147:592-598.

Bergman H, Feingold, A, Nini, A, Raz, A, Slovin, H, Abeles, M, Vaadia, E (1998) Physiological Aspects of Information Processing in the Basal Ganglia of Normal and Parkinsonism Primates. TINS 21:32.

Bernheimer H, Birkmayer W, Hornykiewicz O, Jellinger K, Seitelberger F (1973) Brain dopamine and the syndromes of Parkinson and Huntington. Clinical, morphological and neurochemical correlations. J Neurol Sci 20:415-455.

Betarbet R, Sherer TB, Greenamyre JT (2002) Animal models of Parkinson's disease. Bioessays 24:308-318.

Betarbet R, Sherer TB, MacKenzie G, Garcia-Osuna M, Panov AV, Greenamyre JT (2000) Chronic systemic pesticide exposure reproduces features of Parkinson's disease. Nat Neurosci 3:1301-1306.

Bezard E, Dovero S, Bioulac B, Gross C (1997) Effects of different schedules of MPTP administration on dopaminergic neurodegeneration in mice. Exp Neurol 148:288-292.

Bindoff LA, Birch-Machin M, Cartlidge NE, Parker WD, Jr., Turnbull DM (1989) Mitochondrial function in Parkinson's disease. Lancet 2:49.

Biskup S, Moore DJ, Rea A, Lorenz-Deperieux B, Coombes CE, Dawson VL, Dawson TM, West AB (2007) Dynamic and redundant regulation of LRRK2 and LRRK1 expression. BMC Neurosci 8:102.

Björklund A LO (1984) Dopamine-containing systems in the CNS. In: Handbook of Chemical Neuroanatomy. (Björklund A HT, eds., ed), pp 55-122: Elsevier.

Blum D, Torch S, Lambeng N, Nissou M, Benabid AL, Sadoul R, Verna JM (2001) Molecular pathways involved in the neurotoxicity of 6-OHDA, dopamine and MPTP: contribution to the apoptotic theory in Parkinson's disease. Prog Neurobiol 65:135-172.

Bonifati V, Rizzu P, Squitieri F, Krieger E, Vanacore N, van Swieten JC, Brice A, van Duijn CM, Oostra B, Meco G, Heutink P (2003a) DJ-1(PARK7), a novel gene for autosomal recessive, early onset parkinsonism. Neurol Sci 24:159-160.

Bonifati V, Rizzu P, van Baren MJ, Schaap O, Breedveld GJ, Krieger E, Dekker MC, Squitieri F, Ibanez P, Joosse M, van Dongen JW, Vanacore N, van Swieten JC, Brice A, Meco G, van Duijn CM, Oostra BA, Heutink P (2003b) Mutations in the DJ-1 gene associated with autosomal recessive early-onset parkinsonism. Science 299:256-259.

Braak H, Braak E (2000) Pathoanatomy of Parkinson's disease. J Neurol 247 Suppl 2:II3-10.

Braak H, Braak E, Yilmazer D, de Vos RA, Jansen EN, Bohl J (1996) Pattern of brain destruction in Parkinson's and Alzheimer's diseases. J Neural Transm 103:455-490.

Braak H, Bohl JR, Muller CM, Rub U, de Vos RA, Del Tredici K (2006a) Stanley Fahn Lecture 2005: The staging procedure for the inclusion body pathology associated with sporadic Parkinson's disease reconsidered. Mov Disord 21:2042-2051.

Braak H, Muller CM, Rub U, Ackermann H, Bratzke H, de Vos RA, Del Tredici K (2006b) Pathology associated with sporadic Parkinson's disease--where does it end? J Neural Transm Suppl:89-97.

Bucci M, Roviezzo F, Cicala C, Sessa WC, Cirino G (2000) Geldanamycin, an inhibitor of heat shock protein 90 (Hsp90) mediated signal transduction has anti-inflammatory effects and interacts with glucocorticoid receptor in vivo. Br J Pharmacol 131:13-16.

Buch PK, Bainbridge JW, Ali RR (2008) AAV-mediated gene therapy for retinal disorders: from mouse to man. Gene Ther 15:849-857.

Burke WJ, Li SW, Williams EA, Nonneman R, Zahm DS (2003) 3,4-Dihydroxyphenylacetaldehyde is the toxic dopamine metabolite in vivo: implications for Parkinson's disease pathogenesis. Brain Res 989:205-213.

Buzzard KA, Giaccia AJ, Killender M, Anderson RL (1998) Heat shock protein 72 modulates pathways of stress-induced apoptosis. J Biol Chem 273:17147-17153.

Bywood PT, Johnson SM (2003) Mitochondrial complex inhibitors preferentially damage substantia nigra dopamine neurons in rat brain slices. Exp Neurol 179:47-59.

Cabin DE, Shimazu K, Murphy D, Cole NB, Gottschalk W, McIlwain KL, Orrison B, Chen A, Ellis CE, Paylor R, Lu B, Nussbaum RL (2002) Synaptic vesicle depletion correlates with attenuated synaptic responses to prolonged repetitive stimulation in mice lacking alpha-synuclein. J Neurosci 22:8797-8807.

Carboni E, Tanda G, Di Chiara G (1992) Extracellular striatal concentrations of endogenous 3,4-dihydroxyphenylalanine in the absence of a decarboxylase inhibitor: a dynamic index of dopamine synthesis in vivo. J Neurochem 59:2230-2236.

Carlsson A (1975a) Monoamine-depleting drugs. Pharmacol Ther [B] 1:393-400.

Carlsson A (1975b) Drugs acting through dopamine release. Pharmacol Ther [B] 1:401-405.

Cha GH, Kim S, Park J, Lee E, Kim M, Lee SB, Kim JM, Chung J, Cho KS (2005) Parkin negatively regulates JNK pathway in the dopaminergic neurons of Drosophila. Proc Natl Acad Sci U S A 102:10345-10350.

Chan P, DeLanney LE, Irwin I, Langston JW, Di Monte D (1991) Rapid ATP loss caused by 1-methyl-4-phenyl-1,2,3,6-tetrahydropyridine in mouse brain. J Neurochem 57:348-351.

Chartier-Harlin MC, Kachergus J, Roumier C, Mouroux V, Douay X, Lincoln S, Levecque C, Larvor L, Andrieux J, Hulihan M, Waucquier N, Defebvre L, Amouyel P, Farrer M, Destee A (2004) Alpha-synuclein locus duplication as a cause of familial Parkinson's disease. Lancet 364:1167-1169.

Checkoway H, Powers K, Smith-Weller T, Franklin GM, Longstreth WT, Jr., Swanson PD (2002) Parkinson's disease risks associated with cigarette smoking, alcohol consumption, and caffeine intake. Am J Epidemiol 155:732-738.

Chen L, Cagniard B, Mathews T, Jones S, Koh HC, Ding Y, Carvey PM, Ling Z, Kang UJ, Zhuang X (2005) Age-dependent motor deficits and dopaminergic dysfunction in DJ-1 null mice. J Biol Chem 280:21418-21426.

Chiueh CC, Wu RM, Mohanakumar KP, Sternberger LM, Krishna G, Obata T, Murphy DL (1994) In vivo generation of hydroxyl radicals and MPTP-induced dopaminergic toxicity in the basal ganglia. Ann N Y Acad Sci 738:25-36.

Christiansen J, Squires RF (1974) Antagonistic effects of apomorphine and haloperidol on rat striatal synaptosomal tyrosine hydroxylase. J Pharm Pharmacol 26:367-369.

Chu Y, Le W, Kompoliti K, Jankovic J, Mufson EJ, Kordower JH (2006) Nurr1 in Parkinson's disease and related disorders. J Comp Neurol 494:495-514.

Clark IE, Dodson MW, Jiang C, Cao JH, Huh JR, Seol JH, Yoo SJ, Hay BA, Guo M (2006) Drosophila pink1 is required for mitochondrial function and interacts genetically with parkin. Nature 441:1162-1166.

Cookson MR (2005) Neurons inflict self-harm. Nat Med 11:1159-1161.

Cookson MR, Dauer W, Dawson T, Fon EA, Guo M, Shen J (2007) The roles of kinases in familial Parkinson's disease. J Neurosci 27:11865-11868.

Coppede F, Mancuso M, Siciliano G, Migliore L, Murri L (2006) Genes and the environment in neurodegeneration. Biosci Rep 26:341-367.

Cosi C, Marien M (1999) Implication of poly (ADP-ribose) polymerase (PARP) in neurodegeneration and brain energy metabolism. Decreases in mouse brain NAD+ and ATP caused by MPTP are prevented by the PARP inhibitor benzamide. Ann N Y Acad Sci 890:227-239.

D'Amelio M, Ragonese P, Morgante L, Reggio A, Callari G, Salemi G, Savettieri G (2006) Long-term survival of Parkinson's disease: a population-based study. J Neurol 253:33-37.

Dai M, Wang P, Boyd AD, Kostov G, Athey B, Jones EG, Bunney WE, Myers RM, Speed TP, Akil H, Watson SJ, Meng F (2005) Evolving gene/transcript definitions significantly alter the interpretation of GeneChip data. Nucleic Acids Res 33:e175.

Darios F, Corti O, Lucking CB, Hampe C, Muriel MP, Abbas N, Gu WJ, Hirsch EC, Rooney T, Ruberg M, Brice A (2003) Parkin prevents mitochondrial swelling and cytochrome c release in mitochondria-dependent cell death. Hum Mol Genet 12:517-526.

Dauer W, Przedborski S (2003) Parkinson's disease: mechanisms and models. Neuron 39:889-909.

Dauer W, Kholodilov N, Vila M, Trillat AC, Goodchild R, Larsen KE, Staal R, Tieu K, Schmitz Y, Yuan CA, Rocha M, Jackson-Lewis V, Hersch S, Sulzer D, Przedborski S, Burke R, Hen R (2002) Resistance of alpha -synuclein null mice to the parkinsonian neurotoxin MPTP. Proc Natl Acad Sci U S A 99:14524-14529.

De Deurwaerdere P, Spampinato U (1999) Role of serotonin(2A) and serotonin(2B/2C) receptor subtypes in the control of accumbal and striatal dopamine release elicited in vivo by dorsal raphe nucleus electrical stimulation. J Neurochem 73:1033-1042.

De Deurwaerdere P, Bonhomme N, Lucas G, Le Moal M, Spampinato U (1996) Serotonin enhances striatal dopamine outflow in vivo through dopamine uptake sites. J Neurochem 66:210-215.

Del Zompo M, Piccardi MP, Ruiu S, Quartu M, Gessa GL, Vaccari A (1993) Selective MPP+ uptake into synaptic dopamine vesicles: possible involvement in MPTP neurotoxicity. Br J Pharmacol 109:411-414.

Demarest KT, Moore KE (1979a) Lack of a high affinity transport system for dopamine in the median eminence and posterior pituitary. Brain Res 171:545-551.

Demarest KT, Moore KE (1979b) Comparison of dopamine synthesis regulation in the terminals of nigrostriatal, mesolimbic, tuberoinfundibular and tuberohypophyseal neurons. J Neural Transm 46:263-277.

DeMaria JE, Lerant AA, Freeman ME (1999) Prolactin activates all three populations of hypothalamic neuroendocrine dopaminergic neurons in ovariectomized rats. Brain Res 837:236-241.

Deng H, Dodson MW, Huang H, Guo M (2008) The Parkinson's disease genes pink1 and parkin promote mitochondrial fission and/or inhibit fusion in Drosophila. Proc Natl Acad Sci U S A 105:14503-14508.

Di Chiara G, Tanda G, Carboni E (1996) Estimation of in-vivo neurotransmitter release by brain microdialysis: the issue of validity. Behav Pharmacol 7:640-657.

Dringen R, Gutterer JM, Hirrlinger J (2000) Glutathione metabolism in brain metabolic interaction between astrocytes and neurons in the defense against reactive oxygen species. Eur J Biochem 267:4912-4916.

Drolet RE (2006) In: Neuroscience, p 284. East Lansing: Michigan State University.

Drolet RE, Behrouz B, Lookingland KJ, Goudreau JL (2004a) Mice lacking a-synuclein have an attenuated loss of striatal dopamine following prolonged chronic MPTP administration. Neurotoxicology 25:available online June 25, 2004.

Drolet RE, Behrouz B, Lookingland KJ, Goudreau JL (2004b) Mice lacking alpha-synuclein have an attenuated loss of striatal dopamine following prolonged chronic MPTP administration. Neurotoxicology 25:761-769.

Drolet RE, Behrouz B, Lookingland KJ, Goudreau JL (2006) Substrate-mediated enhancement of phosphorylated tyrosine hydroxylase in nigrostriatal dopamine neurons: evidence for a role of alpha-synuclein. J Neurochem 96:950-959.

Ebadi M, Sharma SK, Ghafourifar P, Brown-Borg H, El Refaey H (2005) Peroxynitrite in the pathogenesis of Parkinson's disease and the neuroprotective role of metallothioneins. Methods Enzymol 396:276-298.

Eisen MB, Spellman PT, Brown PO, Botstein D (1998) Cluster analysis and display of genome-wide expression patterns. Proc Natl Acad Sci U S A 95:14863-14868.

Eisler T, Thorner MO, MacLeod RM, Kaiser DL, Calne DB (1981) Prolactin secretion in Parkinson disease. Neurology 31:1356-1359.

Farrer MJ (2007) Lrrk2 in the limelight! Neurology 69:1732-1733.

Feany MB, Bender WW (2000) A Drosophila model of Parkinson's disease. Nature 404:394-398.

Fearnley JM, Lees AJ (1991) Ageing and Parkinson's disease: substantia nigra regional selectivity. Brain 114 (Pt 5):2283-2301.

Fernagut PO, Hutson CB, Fleming SM, Tetreaut NA, Salcedo J, Masliah E, Chesselet MF (2007) Behavioral and histopathological consequences of paraquat intoxication in mice: effects of alpha-synuclein over-expression. Synapse 61:991-1001.

Firestone JA, Smith-Weller T, Franklin G, Swanson P, Longstreth WT, Jr., Checkoway H (2005) Pesticides and risk of Parkinson disease: a population-based case-control study. Arch Neurol 62:91-95.

Fleming SM, Salcedo J, Fernagut PO, Rockenstein E, Masliah E, Levine MS, Chesselet MF (2004) Early and progressive sensorimotor anomalies in mice overexpressing wild-type human alpha-synuclein. J Neurosci 24:9434-9440.

Fornai F, Schluter OM, Lenzi P, Gesi M, Ruffoli R, Ferrucci M, Lazzeri G, Busceti CL, Pontarelli F, Battaglia G, Pellegrini A, Nicoletti F, Ruggieri S, Paparelli A, Sudhof TC (2005) Parkinson-like syndrome induced by continuous MPTP infusion: convergent roles of the ubiquitin-proteasome system and alpha-synuclein. Proc Natl Acad Sci U S A 102:3413-3418.

Franceschi M, Camerlingo M, Perego L, Bottacchi E, Truci G, Mamoli A (1988) Tuberoinfundibular dopaminergic function in Parkinson's disease. Eur Neurol 28:117-119.

Freed C, Revay R, Vaughan RA, Kriek E, Grant S, Uhl GR, Kuhar MJ (1995) Dopamine transporter immunoreactivity in rat brain. J Comp Neurol 359:340-349.

Gandhi S, Muqit MM, Stanyer L, Healy DG, Abou-Sleiman PM, Hargreaves I, Heales S, Ganguly M, Parsons L, Lees AJ, Latchman DS, Holton JL, Wood NW, Revesz T (2006) PINK1 protein in normal human brain and Parkinson's disease. Brain 129:1720-1731.

Gautier CA, Kitada T, Shen J (2008) Loss of PINK1 causes mitochondrial functional defects and increased sensitivity to oxidative stress. Proc Natl Acad Sci U S A 105:11364-11369.

George JM, Jin H, Woods WS, Clayton DF (1995) Characterization of a novel protein regulated during the critical period for song learning in the zebra finch. Neuron 15:361-372.

German DC, Manaye K, Smith WK, Woodward DJ, Saper CB (1989) Midbrain dopaminergic cell loss in Parkinson's disease: computer visualization. Ann Neurol 26:507-514.

Giasson BI, Duda JE, Quinn SM, Zhang B, Trojanowski JQ, Lee VM (2002) Neuronal alpha-synucleinopathy with severe movement disorder in mice expressing A53T human alpha-synuclein. Neuron 34:521-533.

Gispert S, Del Turco D, Garrett L, Chen A, Bernard DJ, Hamm-Clement J, Korf HW, Deller T, Braak H, Auburger G, Nussbaum RL (2003) Transgenic mice expressing mutant A53T human alpha-synuclein show neuronal dysfunction in the absence of aggregate formation. Mol Cell Neurosci 24:419-429.

Goldberg MS, Fleming SM, Palacino JJ, Cepeda C, Lam HA, Bhatnagar A, Meloni EG, Wu N, Ackerson LC, Klapstein GJ, Gajendiran M, Roth BL, Chesselet MF, Maidment NT, Levine MS, Shen J (2003) Parkin-deficient mice exhibit nigrostriatal deficits but not loss of dopaminergic neurons. J Biol Chem 278:43628-43635.

Golub TR, Slonim DK, Tamayo P, Huard C, Gaasenbeek M, Mesirov JP, Coller H, Loh ML, Downing JR, Caligiuri MA, Bloomfield CD, Lander ES (1999) Molecular classification of cancer: class discovery and class prediction by gene expression monitoring. Science 286:531-537.

Gomez-Isla T, Irizarry MC, Mariash A, Cheung B, Soto O, Schrump S, Sondel J, Kotilinek L, Day J, Schwarzschild MA, Cha JH, Newell K, Miller DW, Ueda K, Young AB, Hyman BT, Ashe KH (2003) Motor dysfunction and gliosis with preserved

dopaminergic markers in human alpha-synuclein A30P transgenic mice. Neurobiol Aging 24:245-258.

Gong B, Leznik E (2007) The role of ubiquitin C-terminal hydrolase L1 in neurodegenerative disorders. Drug News Perspect 20:365-370.

Graham DG (1978) Oxidative pathways for catecholamines in the genesis of neuromelanin and cytotoxic quinones. Mol Pharmacol 14:633-643.

Graham DG, Tiffany SM, Bell WR, Jr., Gutknecht WF (1978) Autoxidation versus covalent binding of quinones as the mechanism of toxicity of dopamine, 6-hydroxydopamine, and related compounds toward C1300 neuroblastoma cells in vitro. Mol Pharmacol 14:644-653.

Greenamyre JT, Sherer TB, Betarbet R, Panov AV (2001) Complex I and Parkinson's disease. IUBMB Life 52:135-141.

Greene JC, Whitworth AJ, Kuo I, Andrews LA, Feany MB, Pallanck LJ (2003) Mitochondrial pathology and apoptotic muscle degeneration in Drosophila parkin mutants. Proc Natl Acad Sci U S A 100:4078-4083.

Greene JG, Dingledine R, Greenamyre JT (2005) Gene expression profiling of rat midbrain dopamine neurons: implications for selective vulnerability in parkinsonism. Neurobiol Dis 18:19-31.

Gundersen HJ, Jensen EB (1987) The efficiency of systematic sampling in stereology and its prediction. J Microsc 147 (Pt 3):229-263.

Gunnet JW, Lookingland KJ, Lindley SE, Moore KE (1987) Effect of electrical stimulation of the arcuate nucleus on neurochemical estimates of tuberoinfundibular and tuberohypophysial dopaminergic neuronal activities. Brain Res 424:371-378.

Haavik J, Martinez A, Flatmark T (1990) pH-dependent release of catecholamines from tyrosine hydroxylase and the effect of phosphorylation of Ser-40. FEBS Lett 262:363-365.

Haber SN, Ryoo H, Cox C, Lu W (1995) Subsets of midbrain dopaminergic neurons in monkeys are distinguished by different levels of mRNA for the dopamine transporter: comparison with the mRNA for the D2 receptor, tyrosine hydroxylase and calbindin immunoreactivity. J Comp Neurol 362:400-410.

Halliwell B (1992) Reactive oxygen species and the central nervous system. J Neurochem 59:1609-1623.

Hampe C, Ardila-Osorio H, Fournier M, Brice A, Corti O (2006) Biochemical analysis of Parkinson's disease-causing variants of Parkin, an E3 ubiquitin-protein ligase with monoubiquitylation capacity. Hum Mol Genet 15:2059-2075.

Haque ME, Thomas KJ, D'Souza C, Callaghan S, Kitada T, Slack RS, Fraser P, Cookson MR, Tandon A, Park DS (2008) Cytoplasmic Pink1 activity protects neurons from dopaminergic neurotoxin MPTP. Proc Natl Acad Sci U S A 105:1716-1721.

Hartman ZC, Appledorn DM, Amalfitano A (2008) Adenovirus vector induced innate immune responses: impact upon efficacy and toxicity in gene therapy and vaccine applications. Virus Res 132:1-14.

Hashimoto M, Rockenstein E, Masliah E (2003) Transgenic models of alpha-synuclein pathology: past, present, and future. Ann N Y Acad Sci 991:171-188.

Haywood AF, Staveley BE (2004) Parkin counteracts symptoms in a Drosophila model of Parkinson's disease. BMC Neurosci 5:14.

Haywood AF, Staveley BE (2006) Mutant alpha-synuclein-induced degeneration is reduced by parkin in a fly model of Parkinson's disease. Genome 49:505-510.

Hershko A, Heller H, Elias S, Ciechanover A (1983) Components of ubiquitin-protein ligase system. Resolution, affinity purification, and role in protein breakdown. J Biol Chem 258:8206-8214.

Hicke L, Schubert HL, Hill CP (2005) Ubiquitin-binding domains. Nat Rev Mol Cell Biol 6:610-621.

Hirsch EC (1992) Why are nigral catecholaminergic neurons more vulnerable than other cells in Parkinson's disease? Ann Neurol 32 Suppl:S88-93.

Hirsch EC, Faucheux B, Damier P, Mouatt-Prigent A, Agid Y (1997) Neuronal vulnerability in Parkinson's disease. J Neural Transm Suppl 50:79-88.

Hofer A, Gasser T (2004) New aspects of genetic contributions to Parkinson's disease. J Mol Neurosci 24:417-424.

Hoglinger GU, Carrard G, Michel PP, Medja F, Lombes A, Ruberg M, Friguet B, Hirsch EC (2003a) Dysfunction of mitochondrial complex I and the proteasome: interactions between two biochemical deficits in a cellular model of Parkinson's disease. J Neurochem 86:1297-1307.

Hoglinger GU, Feger J, Prigent A, Michel PP, Parain K, Champy P, Ruberg M, Oertel WH, Hirsch EC (2003b) Chronic systemic complex I inhibition induces a hypokinetic multisystem degeneration in rats. J Neurochem 84:491-502.

Hokfelt T, Fuxe K (1972) Effects of prolactin and ergot alkaloids on the tubero-infundibular dopamine (DA) neurons. Neuroendocrinology 9:100-122.

Honig LS (2000) Relationship between caffeine intake and Parkinson disease. Jama 284:1378-1379.

Hung HC, Tao PL, Lee EH (1995) 1-Methyl-4-phenyl-pyridinium (MPP+) uptake does not explain the differential toxicity of MPP+ in the nigrostriatal and mesolimbic dopaminergic pathways. Neurosci Lett 196:93-96.

Hurd YL, Pristupa ZB, Herman MM, Niznik HB, Kleinman JE (1994) The dopamine transporter and dopamine D2 receptor messenger RNAs are differentially expressed in limbic- and motor-related subpopulations of human mesencephalic neurons. Neuroscience 63:357-362.

Hwang DY, Ardayfio P, Kang UJ, Semina EV, Kim KS (2003) Selective loss of dopaminergic neurons in the substantia nigra of Pitx3-deficient aphakia mice. Brain Res Mol Brain Res 114:123-131.

Hyun DH, Lee M, Halliwell B, Jenner P (2005) Effect of overexpression of wild-type or mutant parkin on the cellular response induced by toxic insults. J Neurosci Res 82:232-244.

Irwin I, DeLanney LE, Di Monte D, Langston JW (1989) The biodisposition of MPP+ in mouse brain. Neurosci Lett 101:83-88.

Jackson PK, Eldridge AG, Freed E, Furstenthal L, Hsu JY, Kaiser BK, Reimann JD (2000) The lore of the RINGs: substrate recognition and catalysis by ubiquitin ligases. Trends Cell Biol 10:429-439.

Jankovic J (2005) Searching for a relationship between manganese and welding and Parkinson's disease. Neurology 64:2021-2028.

Jeon BS, Jackson-Lewis V, Burke RE (1995) 6-Hydroxydopamine lesion of the rat substantia nigra: time course and morphology of cell death. Neurodegeneration 4:131-137.

Jiang H, Jiang Q, Feng J (2004a) Parkin increases dopamine uptake by enhancing the cell surface expression of dopamine transporter. J Biol Chem 279:54380-54386.

Jiang H, Ren Y, Zhao J, Feng J (2004b) Parkin protects human dopaminergic neuroblastoma cells against dopamine-induced apoptosis. Hum Mol Genet 13:1745-1754.

Jiang H, Jiang Q, Liu W, Feng J (2006) Parkin suppresses the expression of monoamine oxidases. J Biol Chem 281:8591-8599.

Kahle PJ, Neumann M, Ozmen L, Muller V, Jacobsen H, Schindzielorz A, Okochi M, Leimer U, van Der Putten H, Probst A, Kremmer E, Kretzschmar HA, Haass C (2000) Subcellular localization of wild-type and Parkinson's disease-associated mutant alpha -synuclein in human and transgenic mouse brain. J Neurosci 20:6365-6373.

Katunar MR, Saez T, Brusco A, Antonelli MC (2008) Immunocytochemical expression of dopamine-related transcription factors Pitx3 and Nurr1 in prenatally stressed adult rats. J Neurosci Res.

Kilbourn MR, Kuszpit K, Sherman P (2000) Rapid and differential losses of in vivo dopamine transporter (DAT) and vesicular monoamine transporter (VMAT2) radioligand binding in MPTP-treated mice. Synapse 35:250-255.

Kilty JE, Lorang D, Amara SG (1991) Cloning and expression of a cocaine-sensitive rat dopamine transporter. Science 254:578-579.

Kim RH, Smith PD, Aleyasin H, Hayley S, Mount MP, Pownall S, Wakeham A, You-Ten AJ, Kalia SK, Horne P, Westaway D, Lozano AM, Anisman H, Park DS, Mak TW (2005) Hypersensitivity of DJ-1-deficient mice to 1-methyl-4-phenyl-1,2,3,6-tetrahydropyrindine (MPTP) and oxidative stress. Proc Natl Acad Sci U S A 102:5215-5220.

Kirik D, Annett LE, Burger C, Muzyczka N, Mandel RJ, Bjorklund A (2003) Nigrostriatal alpha-synucleinopathy induced by viral vector-mediated overexpression of human alpha-synuclein: a new primate model of Parkinson's disease. Proc Natl Acad Sci U S A 100:2884-2889.

Kirik D, Rosenblad C, Burger C, Lundberg C, Johansen TE, Muzyczka N, Mandel RJ, Bjorklund A (2002) Parkinson-like neurodegeneration induced by targeted overexpression of alpha-synuclein in the nigrostriatal system. J Neurosci 22:2780-2791.

Kirkpatrick B, Tamminga CA (1988) The endocrinology of extrapyramidal system disorders. Endocrinol Metab Clin North Am 17:159-172.

Kitada T, Asakawa S, Hattori N, Matsumine H, Yamamura Y, Minoshima S, Yokochi M, Mizuno Y, Shimizu N (1998) Mutations in the parkin gene cause autosomal recessive juvenile parkinsonism. Nature 392:605-608.

Kitada T, Pisani A, Porter DR, Yamaguchi H, Tscherter A, Martella G, Bonsi P, Zhang C, Pothos EN, Shen J (2007) Impaired dopamine release and synaptic plasticity in the striatum of PINK1-deficient mice. Proc Natl Acad Sci U S A 104:11441-11446.

Klein RL, King MA, Hamby ME, Meyer EM (2002) Dopaminergic cell loss induced by human A30P alpha-synuclein gene transfer to the rat substantia nigra. Hum Gene Ther 13:605-612.

Krige D, Carroll MT, Cooper JM, Marsden CD, Schapira AH (1992) Platelet mitochondrial function in Parkinson's disease. The Royal Kings and Queens Parkinson Disease Research Group. Ann Neurol 32:782-788.

Kruger R, Kuhn W, Muller T, Woitalla D, Graeber M, Kosel S, Przuntek H, Epplen JT, Schols L, Riess O (1998) Ala30Pro mutation in the gene encoding alpha-synuclein in Parkinson's disease. Nat Genet 18:106-108.

Kuhn K, Wellen J, Link N, Maskri L, Lubbert H, Stichel CC (2003) The mouse MPTP model: gene expression changes in dopaminergic neurons. Eur J Neurosci 17:1-12.

Kumer SC, Vrana KE (1996) Intricate regulation of tyrosine hydroxylase activity and gene expression. J Neurochem 67:443-462.

Laihinen A, Rinne UK (1986) Function of dopamine receptors in Parkinson's disease: prolactin responses. Neurology 36:393-395.

Lamensdorf I, Eisenhofer G, Harvey-White J, Nechustan A, Kirk K, Kopin IJ (2000) 3,4-Dihydroxyphenylacetaldehyde potentiates the toxic effects of metabolic stress in PC12 cells. Brain Res 868:191-201.

Langston JW, Forno LS (1978) The hypothalamus in Parkinson disease. Ann Neurol 3:129-133.

Langston JW, Ballard PA, Jr. (1983) Parkinson's disease in a chemist working with 1-methyl-4-phenyl-1,2,5,6-tetrahydropyridine. N Engl J Med 309:310.

Langston JW, Irwin I (1986) MPTP: current concepts and controversies. Clin Neuropharmacol 9:485-507.

Langston JW, Ballard P, Tetrud JW, Irwin I (1983) Chronic Parkinsonism in humans due to a product of meperidine-analog synthesis. Science 219:979-980.

Lau YS, Trobough KL, Crampton JM, Wilson JA (1990) Effects of probenecid on striatal dopamine depletion in acute and long-term 1-methyl-4-phenyl-1,2,3,6-tetrahydropyridine (MPTP)-treated mice. Gen Pharmacol 21:181-187.

Lauwers E, Debyser Z, Van Dorpe J, De Strooper B, Nuttin B, Baekelandt V (2003) Neuropathology and neurodegeneration in rodent brain induced by lentiviral vector-mediated overexpression of alpha-synuclein. Brain Pathol 13:364-372.

Lavoie B, Parent A (1991) Dopaminergic neurons expressing calbindin in normal and parkinsonian monkeys. Neuroreport 2:601-604.

Lavoie B, Parent A, Bedard PJ (1991) Effects of dopamine denervation on striatal peptide expression in parkinsonian monkeys. Can J Neurol Sci 18:373-375.

LaVoie MJ, Hastings TG (1999a) Peroxynitrite- and nitrite-induced oxidation of dopamine: implications for nitric oxide in dopaminergic cell loss. J Neurochem 73:2546-2554.

LaVoie MJ, Hastings TG (1999b) Dopamine quinone formation and protein modification associated with the striatal neurotoxicity of methamphetamine: evidence against a role for extracellular dopamine. J Neurosci 19:1484-1491.

LaVoie MJ, Ostaszewski BL, Weihofen A, Schlossmacher MG, Selkoe DJ (2005) Dopamine covalently modifies and functionally inactivates parkin. Nat Med 11:1214-1221.

Lawton NF, MacDermot J (1980) Abnormal regulation of prolactin release in idiopathic Parkinson's disease. J Neurol Neurosurg Psychiatry 43:1012-1015.

Le W, Conneely OM, Zou L, He Y, Saucedo-Cardenas O, Jankovic J, Mosier DR, Appel SH (1999) Selective agenesis of mesencephalic dopaminergic neurons in Nurr1-deficient mice. Exp Neurol 159:451-458.

Lee HJ, Shin SY, Choi C, Lee YH, Lee SJ (2002a) Formation and removal of alpha-synuclein aggregates in cells exposed to mitochondrial inhibitors. J Biol Chem 277:5411-5417.

Lee MK, Stirling W, Xu Y, Xu X, Qui D, Mandir AS, Dawson TM, Copeland NG, Jenkins NA, Price DL (2002b) Human alpha-synuclein-harboring familial Parkinson's disease-linked Ala-53 --> Thr mutation causes neurodegenerative disease with alpha-synuclein aggregation in transgenic mice. Proc Natl Acad Sci U S A 99:8968-8973.

Lee VM, Trojanowski JQ (2006) Mechanisms of Parkinson's disease linked to pathological alpha-synuclein: new targets for drug discovery. Neuron 52:33-38.

Legros H, Dingeval MG, Janin F, Costentin J, Bonnet JJ (2004) Toxicity of a treatment associating dopamine and disulfiram for catecholaminergic neuroblastoma SH-SY5Y cells: relationships with 3,4-dihydroxyphenylacetaldehyde formation. Neurotoxicology 25:365-375.

Lerant A, Freeman ME (1998) Ovarian steroids differentially regulate the expression of PRL-R in neuroendocrine dopaminergic neuron populations: a double label confocal microscopic study. Brain Res 802:141-154.

Leroy E, Anastasopoulos D, Konitsiotis S, Lavedan C, Polymeropoulos MH (1998) Deletions in the Parkin gene and genetic heterogeneity in a Greek family with early onset Parkinson's disease. Hum Genet 103:424-427.

Levitt M, Spector S, Sjoerdsma A, Udenfriend S (1965) Elucidation Of The Rate-Limiting Step In Norepinephrine Biosynthesis In The Perfused Guinea-Pig Heart. J Pharmacol Exp Ther 148:1-8.

Lewis TB, Standaert DG (2008) Design of clinical trials of gene therapy in Parkinson disease. Exp Neurol 209:41-47.

Lim KL, Chew KC, Tan JM, Wang C, Chung KK, Zhang Y, Tanaka Y, Smith W, Engelender S, Ross CA, Dawson VL, Dawson TM (2005) Parkin mediates nonclassical, proteasomal-independent ubiquitination of synphilin-1: implications for Lewy body formation. J Neurosci 25:2002-2009.

Liu Y, Peter D, Roghani A, Schuldiner S, Prive GG, Eisenberg D, Brecha N, Edwards RH (1992) A cDNA that suppresses MPP+ toxicity encodes a vesicular amine transporter. Cell 70:539-551.

Lo Bianco C, Ridet JL, Schneider BL, Deglon N, Aebischer P (2002) alpha - Synucleinopathy and selective dopaminergic neuron loss in a rat lentiviral-based model of Parkinson's disease. Proc Natl Acad Sci U S A 99:10813-10818.

Lockhart PJ, O'Farrell CA, Farrer MJ (2004) It's a double knock-out! The quaking mouse is a spontaneous deletion of parkin and parkin co-regulated gene (PACRG). Mov Disord 19:101-104.

Lookingland KJ, Moore KE (1984) Dopamine receptor-mediated regulation of incertohypothalamic dopaminergic neurons in the male rat. Brain Res 304:329-338.

Lookingland KJ, Moore KE (2005) Functional neuroanatomy of hypothalamic dopaminergic neuroendocrine systems. In: Handbook of Chemical Neuroanatomy (Dunnett SB, Bentivoglio M, Björklund A, Hökfelt T, eds), pp 433-521. Amsterdam: Elsevier.

Lookingland KJ, Gunnet JW, Moore KE (1987a) Electrical stimulation of the arcuate nucleus increases the metabolism of dopamine in terminals of tuberoinfundibular neurons in the median eminence. Brain Res 436:161-164.

Lookingland KJ, Jarry HD, Moore KE (1987b) The metabolism of dopamine in the median eminence reflects the activity of tuberoinfundibular neurons. Brain Res 419:303-310.

Lorenzetti D, Antalffy B, Vogel H, Noveroske J, Armstrong D, Justice M (2004) The neurological mutant quaking(viable) is Parkin deficient. Mamm Genome 15:210-217.

Lotharius J, O'Malley KL (2000) The parkinsonism-inducing drug 1-methyl-4-phenylpyridinium triggers intracellular dopamine oxidation. A novel mechanism of toxicity. J Biol Chem 275:38581-38588.

Lotharius J, Brundin P (2002) Pathogenesis of Parkinson's disease: dopamine, vesicles and alpha-synuclein. Nat Rev Neurosci 3:932-942.

Lowry OH, Rosebrough NJ, Farr AL, Randall RJ (1951) Protein measurement with the Folin phenol reagent. J Biol Chem 193:265-275.

Luthman J, Fredriksson A, Sundstrom E, Jonsson G, Archer T (1989) Selective lesion of central dopamine or noradrenaline neuron systems in the neonatal rat: motor

behavior and monoamine alterations at adult stage. Behav Brain Res 33:267-277.

MacDonald ME (1999) Gadzooks! Nat Genet 23:10-11.

Manfredsson FP, Burger C, Sullivan LF, Muzyczka N, Lewin AS, Mandel RJ (2007) rAAV-mediated nigral human parkin over-expression partially ameliorates motor deficits via enhanced dopamine neurotransmission in a rat model of Parkinson's disease. Exp Neurol 207:289-301.

Mann VM, Cooper JM, Daniel SE, Srai K, Jenner P, Marsden CD, Schapira AH (1994) Complex I, iron, and ferritin in Parkinson's disease substantia nigra. Ann Neurol 36:876-881.

Manning-Bog AB, McCormack AL, Purisai MG, Bolin LM, Di Monte DA (2003) Alpha-synuclein overexpression protects against paraquat-induced neurodegeneration. J Neurosci 23:3095-3099.

Manning-Bog AB, McCormack AL, Li J, Uversky VN, Fink AL, Di Monte DA (2002) The herbicide paraquat causes up-regulation and aggregation of alpha-synuclein in mice: paraquat and alpha-synuclein. J Biol Chem 277:1641-1644.

Marks WJ, Jr., Ostrem JL, Verhagen L, Starr PA, Larson PS, Bakay RA, Taylor R, Cahn-Weiner DA, Stoessl AJ, Olanow CW, Bartus RT (2008) Safety and tolerability of intraputaminal delivery of CERE-120 (adeno-associated virus serotype 2-neurturin) to patients with idiopathic Parkinson's disease: an open-label, phase I trial. Lancet Neurol 7:400-408.

Martin LJ, Pan Y, Price AC, Sterling W, Copeland NG, Jenkins NA, Price DL, Lee MK (2006) Parkinson's disease alpha-synuclein transgenic mice develop neuronal mitochondrial degeneration and cell death. J Neurosci 26:41-50.

Masliah E, Rockenstein E, Veinbergs I, Sagara Y, Mallory M, Hashimoto M, Mucke L (2001) beta-amyloid peptides enhance alpha-synuclein accumulation and neuronal deficits in a transgenic mouse model linking Alzheimer's disease and Parkinson's disease. Proc Natl Acad Sci U S A 98:12245-12250.

Masliah E, Rockenstein E, Veinbergs I, Mallory M, Hashimoto M, Takeda A, Sagara Y, Sisk A, Mucke L (2000) Dopaminergic loss and inclusion body formation in alpha-synuclein mice: implications for neurodegenerative disorders. Science 287:1265-1269.

Matsuda N, Kitami T, Suzuki T, Mizuno Y, Hattori N, Tanaka K (2006) Diverse effects of pathogenic mutations of Parkin that catalyze multiple monoubiquitylation in vitro. J Biol Chem 281:3204-3209.

Matsuoka Y, Vila M, Lincoln S, McCormack A, Picciano M, LaFrancois J, Yu X, Dickson D, Langston WJ, McGowan E, Farrer M, Hardy J, Duff K, Przedborski S, Di Monte DA (2001) Lack of nigral pathology in transgenic mice expressing human alpha-synuclein driven by the tyrosine hydroxylase promoter. Neurobiol Dis 8:535-539.

Matzuk MM, Saper CB (1985) Preservation of hypothalamic dopaminergic neurons in Parkinson's disease. Ann Neurol 18:552-555.

McCormack AL, Atienza JG, Johnston LC, Andersen JK, Vu S, Di Monte DA (2005) Role of oxidative stress in paraquat-induced dopaminergic cell degeneration. J Neurochem 93:1030-1037.

McNaught KS, Jenner P (2001) Proteasomal function is impaired in substantia nigra in Parkinson's disease. Neurosci Lett 297:191-194.

McNaught KS, Olanow CW (2003) Proteolytic stress: a unifying concept for the etiopathogenesis of Parkinson's disease. Ann Neurol 53 Suppl 3:S73-84; discussion S84-76.

McNaught KS, Belizaire R, Isacson O, Jenner P, Olanow CW (2003) Altered proteasomal function in sporadic Parkinson's disease. Exp Neurol 179:38-46.

Meister B, Hokfelt T, Steinbusch HW, Skagerberg G, Lindvall O, Geffard M, Joh TH, Cuello AC, Goldstein M (1988) Do tyrosine hydroxylase-immunoreactive neurons in the ventrolateral arcuate nucleus produce dopamine or only L-dopa? J Chem Neuroanat 1:59-64.

Melamed E, Rosenthal J, Globus M, Cohen O, Frucht Y, Uzzan A (1985) Mesolimbic dopaminergic neurons are not spared by MPTP neurotoxicity in mice. Eur J Pharmacol 114:97-100.

Melrose HL, Kent CB, Taylor JP, Dachsel JC, Hinkle KM, Lincoln SJ, Mok SS, Culvenor JG, Masters CL, Tyndall GM, Bass DI, Ahmed Z, Andorfer CA, Ross OA, Wszolek ZK, Delldonne A, Dickson DW, Farrer MJ (2007) A comparative analysis of leucine-rich repeat kinase 2 (Lrrk2) expression in mouse brain and Lewy body disease. Neuroscience 147:1047-1058.

Mochizuki H, Goto K, Mori H, Mizuno Y (1996) Histochemical detection of apoptosis in Parkinson's disease. J Neurol Sci 137:120-123.

Mogi M, Harada M, Kojima K, Kiuchi K, Nagatsu T (1988) Effects of systemic administration of 1-methyl-4-phenyl-1,2,3,6-tetrahydropyridine to mice on tyrosine hydroxylase, L-3,4-dihydroxyphenylalanine decarboxylase, dopamine beta-hydroxylase, and monoamine oxidase activities in the striatum and hypothalamus. J Neurochem 50:1053-1056.

Monsma FJ, Jr., Mahan LC, McVittie LD, Gerfen CR, Sibley DR (1990) Molecular cloning and expression of a D1 dopamine receptor linked to adenylyl cyclase activation. Proc Natl Acad Sci U S A 87:6723-6727.

Moore DJ, West AB, Dikeman DA, Dawson VL, Dawson TM (2008) Parkin mediates the degradation-independent ubiquitination of Hsp70. J Neurochem 105:1806-1819.

Murphy DD, Rueter SM, Trojanowski JQ, Lee VM (2000) Synucleins are developmentally expressed, and alpha-synuclein regulates the size of the presynaptic vesicular pool in primary hippocampal neurons. J Neurosci 20:3214-3220.

Nagel F, Falkenburger BH, Tonges L, Kowsky S, Poppelmeyer C, Schulz JB, Bahr M, Dietz GP (2008) Tat-Hsp70 protects dopaminergic neurons in midbrain cultures and in the substantia nigra in models of Parkinson's disease. J Neurochem 105:853-864.

Neckers L (2002) Hsp90 inhibitors as novel cancer chemotherapeutic agents. Trends Mol Med 8:S55-61.

Nieto M, Gil-Bea FJ, Dalfo E, Cuadrado M, Cabodevilla F, Sanchez B, Catena S, Sesma T, Ribe E, Ferrer I, Ramirez MJ, Gomez-Isla T (2006) Increased sensitivity to MPTP in human alpha-synuclein A30P transgenic mice. Neurobiol Aging 27:848-856.

Norris EH, Uryu K, Leight S, Giasson BI, Trojanowski JQ, Lee VM (2007) Pesticide exposure exacerbates alpha-synucleinopathy in an A53T transgenic mouse model. Am J Pathol 170:658-666.

Noyes K, Liu H, Temkin-Greener H (2006) Cost of caring for Medicare beneficiaries with Parkinson's disease: impact of the CMS-HCC risk-adjustment model. Dis Manag 9:339-348.

Okuno S, Fujisawa H (1985) A new mechanism for regulation of tyrosine 3-monooxygenase by end product and cyclic AMP-dependent protein kinase. J Biol Chem 260:2633-2635.

Oldendorf WH, Szabo J (1976) Amino acid assignment to one of three blood-brain barrier amino acid carriers. Am J Physiol 230:94-98.

Olzmann JA, Chin LS (2008) Parkin-mediated K63-linked polyubiquitination: a signal for targeting misfolded proteins to the aggresome-autophagy pathway. Autophagy 4:85-87.

Onali P, Olianas MC, Gessa GL (1985) Characterization of dopamine receptors mediating inhibition of adenylate cyclase activity in rat striatum. Mol Pharmacol 28:138-145.

Oxender DL, Christensen HN (1963) Distinct Mediating Systems For The Transport Of Neutral Amino Acids By The Ehrlich Cell. J Biol Chem 238:3686-3699.

Palacin M, Estevez R, Bertran J, Zorzano A (1998) Molecular biology of mammalian plasma membrane amino acid transporters. Physiol Rev 78:969-1054.

Palkovits M (1973) Isolated removal of hypothalamic or other brain nuclei of the rat. Brain Res 59:449-450.

Palkovits M (1978) Neurochemical anatomy of the neuroendocrine hypothalamus. Neurochemical anatomy of the hypothalamus. Bull Schweiz Akad Med Wiss 34:113-130.

Parent A, Lavoie B (1993) The heterogeneity of the mesostriatal dopaminergic system as revealed in normal and parkinsonian monkeys. Adv Neurol 60:25-33.

Pasqualini C, Guibert B, Frain O, Leviel V (1994) Evidence for protein kinase C involvement in the short-term activation by prolactin of tyrosine hydroxylase in tuberoinfundibular dopaminergic neurons. J Neurochem 62:967-977.

Paterna JC, Leng A, Weber E, Feldon J, Bueler H (2007) DJ-1 and Parkin modulate dopamine-dependent behavior and inhibit MPTP-induced nigral dopamine neuron loss in mice. Mol Ther 15:698-704.

Perez FA, Palmiter RD (2005) Parkin-deficient mice are not a robust model of parkinsonism. Proc Natl Acad Sci U S A 102:2174-2179.

Perez FA, Curtis WR, Palmiter RD (2005) Parkin-deficient mice are not more sensitive to 6-hydroxydopamine or methamphetamine neurotoxicity. BMC Neurosci 6:71.

Periquet M, Corti O, Jacquier S, Brice A (2005) Proteomic analysis of parkin knockout mice: alterations in energy metabolism, protein handling and synaptic function. J Neurochem 95:1259-1276.

Perry TL, Yong VW, Jones K, Wall RA, Clavier RM, Foulks JG, Wright JM (1985) Effects of N-methyl-4-phenyl-1,2,3,6-tetrahydropyridine and its metabolite, N-methyl-4-phenylpyridinium ion, on dopaminergic nigrostriatal neurons in the mouse. Neurosci Lett 58:321-326.

Pesah Y, Pham T, Burgess H, Middlebrooks B, Verstreken P, Zhou Y, Harding M, Bellen H, Mardon G (2004) Drosophila parkin mutants have decreased mass and cell size and increased sensitivity to oxygen radical stress. Development 131:2183-2194.

Petroske E, Meredith GE, Callen S, Totterdell S, Lau YS (2001) Mouse model of Parkinsonism: a comparison between subacute MPTP and chronic MPTP/probenecid treatment. Neuroscience 106:589-601.

Petrucelli L, O'Farrell C, Lockhart PJ, Baptista M, Kehoe K, Vink L, Choi P, Wolozin B, Farrer M, Hardy J, Cookson MR (2002) Parkin protects against the toxicity associated with mutant alpha-synuclein: proteasome dysfunction selectively affects catecholaminergic neurons. Neuron 36:1007-1019.

Pileblad E, Carlsson A (1985) Catecholamine-uptake inhibitors prevent the neurotoxicity of 1-methyl-4-phenyl-1,2,3,6-tetrahydropyridine (MPTP) in mouse brain. Neuropharmacology 24:689-692.

Pileblad E, Nissbrandt H, Carlsson A (1984) Biochemical and functional evidence for a marked dopamine releasing action of N-methyl-4-phenyl-1,2,3,6-tetrahydropyridine (NMPTP) in mouse brain. J Neural Transm 60:199-203.

Pileblad E, Fornstedt B, Clark D, Carlsson A (1985) Acute effects of 1-methyl-4-phenyl-1,2,3,6-tetrahydropyridine on dopamine metabolism in mouse and rat striatum. J Pharm Pharmacol 37:707-711.

Polymeropoulos MH, Lavedan C, Leroy E, Ide SE, Dehejia A, Dutra A, Pike B, Root H, Rubenstein J, Boyer R, Stenroos ES, Chandrasekharappa S, Athanassiadou A, Papapetropoulos T, Johnson WG, Lazzarini AM, Duvoisin RC, Di Iorio G, Golbe LI, Nussbaum RL (1997) Mutation in the alpha-synuclein gene identified in families with Parkinson's disease. Science 276:2045-2047.

Poole AC, Thomas RE, Andrews LA, McBride HM, Whitworth AJ, Pallanck LJ (2008) The PINK1/Parkin pathway regulates mitochondrial morphology. Proc Natl Acad Sci U S A 105:1638-1643.

Priyadarshi A, Khuder SA, Schaub EA, Shrivastava S (2000) A meta-analysis of Parkinson's disease and exposure to pesticides. Neurotoxicology 21:435-440.

Priyadarshi A, Khuder SA, Schaub EA, Priyadarshi SS (2001) Environmental risk factors and Parkinson's disease: a metaanalysis. Environ Res 86:122-127.

Przedborski S, Ischiropoulos H (2005) Reactive oxygen and nitrogen species: weapons of neuronal destruction in models of Parkinson's disease. Antioxid Redox Signal 7:685-693.

Przedborski S, Jackson-Lewis V, Naini AB, Jakowec M, Petzinger G, Miller R, Akram M (2001) The parkinsonian toxin 1-methyl-4-phenyl-1,2,3,6-tetrahydropyridine (MPTP): a technical review of its utility and safety. J Neurochem 76:1265-1274.

Reinhard JF, Jr., Diliberto EJ, Jr., Viveros OH, Daniels AJ (1987) Subcellular compartmentalization of 1-methyl-4-phenylpyridinium with catecholamines in adrenal medullary chromaffin vesicles may explain the lack of toxicity to adrenal chromaffin cells. Proc Natl Acad Sci U S A 84:8160-8164.

Reveron ME, Savelieva KV, Tillerson JL, McCormack AL, Di Monte DA, Miller GW (2002) L-DOPA does not cause neurotoxicity in VMAT2 heterozygote knockout mice. Neurotoxicology 23:611-619.

Ribeiro MJ, Vidailhet M, Loc'h C, Dupel C, Nguyen JP, Ponchant M, Dolle F, Peschanski M, Hantraye P, Cesaro P, Samson Y, Remy P (2002) Dopaminergic function and dopamine transporter binding assessed with positron emission tomography in Parkinson disease. Arch Neurol 59:580-586.

Richfield EK, Thiruchelvam MJ, Cory-Slechta DA, Wuertzer C, Gainetdinov RR, Caron MG, Di Monte DA, Federoff HJ (2002) Behavioral and neurochemical effects of wild-type and mutated human alpha-synuclein in transgenic mice. Exp Neurol 175:35-48.

Rockenstein E, Mallory M, Hashimoto M, Song D, Shults CW, Lang I, Masliah E (2002) Differential neuropathological alterations in transgenic mice expressing alpha-synuclein from the platelet-derived growth factor and Thy-1 promoters. J Neurosci Res 68:568-578.

Roth RH (1975) Gamma-hydroxybutyrate and control of dopaminergic neurons. Psychopharmacol Bull 11:57-58.

Sakurai H, Kawabata K, Sakurai F, Nakagawa S, Mizuguchi H (2008) Innate immune response induced by gene delivery vectors. Int J Pharm 354:9-15.

Saporito MS, Thomas BA, Scott RW (2000) MPTP activates c-Jun NH(2)-terminal kinase (JNK) and its upstream regulatory kinase MKK4 in nigrostriatal neurons in vivo. J Neurochem 75:1200-1208.

Schapira AH (2008) Mitochondria in the aetiology and pathogenesis of Parkinson's disease. Lancet Neurol 7:97-109.

Schapira AH, Cooper JM, Dexter D, Jenner P, Clark JB, Marsden CD (1989) Mitochondrial complex I deficiency in Parkinson's disease. Lancet 1:1269.

Schenkman M, Wei Zhu C, Cutson TM, Whetten-Goldstein K (2001) Longitudinal evaluation of economic and physical impact of Parkinson's disease. Parkinsonism Relat Disord 8:41-50.

Schluter OM, Fornai F, Alessandri MG, Takamori S, Geppert M, Jahn R, Sudhof TC (2003) Role of alpha-synuclein in 1-methyl-4-phenyl-1,2,3,6-tetrahydropyridine-induced parkinsonism in mice. Neuroscience 118:985-1002.

Schmitz C (1997) Towards more readily comprehensible procedures in disector stereology. J Neurocytol 26:707-710.

Schmitz C, Hof PR (2000) Recommendations for straightforward and rigorous methods of counting neurons based on a computer simulation approach. J Chem Neuroanat 20:93-114.

Schmitz C, Hof PR (2005) Design-based stereology in neuroscience. Neuroscience 130:813-831.

Schober A (2004) Classic toxin-induced animal models of Parkinson's disease: 6-OHDA and MPTP. Cell Tissue Res 318:215-224.

Shen HY, He JC, Wang Y, Huang QY, Chen JF (2005) Geldanamycin induces heat shock protein 70 and protects against MPTP-induced dopaminergic neurotoxicity in mice. J Biol Chem 280:39962-39969.

Shimizu K, Matsubara K, Ohtaki K, Shiono H (2003) Paraquat leads to dopaminergic neural vulnerability in organotypic midbrain culture. Neurosci Res 46:523-532.

Shimizu K, Ohtaki K, Matsubara K, Aoyama K, Uezono T, Saito O, Suno M, Ogawa K, Hayase N, Kimura K, Shiono H (2001) Carrier-mediated processes in blood--brain barrier penetration and neural uptake of paraquat. Brain Res 906:135-142.

Singleton AB, Farrer M, Johnson J, Singleton A, Hague S, Kachergus J, Hulihan M, Peuralinna T, Dutra A, Nussbaum R, Lincoln S, Crawley A, Hanson M, Maraganore D, Adler C, Cookson MR, Muenter M, Baptista M, Miller D, Blancato J, Hardy J, Gwinn-Hardy K (2003) alpha-Synuclein locus triplication causes Parkinson's disease. Science 302:841.

Sittler A, Lurz R, Lueder G, Priller J, Lehrach H, Hayer-Hartl MK, Hartl FU, Wanker EE (2001) Geldanamycin activates a heat shock response and inhibits huntingtin aggregation in a cell culture model of Huntington's disease. Hum Mol Genet 10:1307-1315.

Smeyne RJ, Jackson-Lewis V (2005) The MPTP model of Parkinson's disease. Brain Res Mol Brain Res 134:57-66.

Sossi V, de La Fuente-Fernandez R, Holden JE, Doudet DJ, McKenzie J, Stoessl AJ, Ruth TJ (2002) Increase in dopamine turnover occurs early in Parkinson's disease: evidence from a new modeling approach to PET 18 F-fluorodopa data. J Cereb Blood Flow Metab 22:232-239.

Specht CG, Schoepfer R (2001) Deletion of the alpha-synuclein locus in a subpopulation of C57BL/6J inbred mice. BMC Neurosci 2:11.

Speciale SG, Liang CL, Sonsalla PK, Edwards RH, German DC (1998) The neurotoxin 1-methyl-4-phenylpyridinium is sequestered within neurons that contain the vesicular monoamine transporter. Neuroscience 84:1177-1185.

Spillantini MG, Schmidt ML, Lee VM, Trojanowski JQ, Jakes R, Goedert M (1997) Alpha-synuclein in Lewy bodies. Nature 388:839-840.

Squire LR, Barondes SH (1973) Memory impairment during prolonged training in mice given inhibitors of cerebral protein synthesis. Brain Res 56:215-225.

Squire LR, Barondes SH (1976) Amnesic effect of cycloheximide not due to depletion of a consitutive brain protein with short half-life. Brain Res 103:183-189.

Squire LR, Smith GA, Barondes SH (1973) Cycloheximide affects memory within minutes after the onset of training. Nature 242:201-202.

Sriram SR, Li X, Ko HS, Chung KK, Wong E, Lim KL, Dawson VL, Dawson TM (2005) Familial-associated mutations differentially disrupt the solubility, localization, binding and ubiquitination properties of parkin. Hum Mol Genet 14:2571-2586.

Staropoli JF (2008) Tumorigenesis and neurodegeneration: two sides of the same coin? Bioessays 30:719-727.

Staropoli JF, McDermott C, Martinat C, Schulman B, Demireva E, Abeliovich A (2003) Parkin is a component of an SCF-like ubiquitin ligase complex and protects postmitotic neurons from kainate excitotoxicity. Neuron 37:735-749.

Steidl JV, Gomez-Isla T, Mariash A, Ashe KH, Boland LM (2003) Altered short-term hippocampal synaptic plasticity in mutant alpha-synuclein transgenic mice. Neuroreport 14:219-223.

Sullivan PG, Dragicevic NB, Deng JH, Bai Y, Dimayuga E, Ding Q, Chen Q, Bruce-Keller AJ, Keller JN (2004) Proteasome inhibition alters neural mitochondrial homeostasis and mitochondria turnover. J Biol Chem 279:20699-20707.

Sundstrom E, Stromberg I, Tsutsumi T, Olson L, Jonsson G (1987) Studies on the effect of 1-methyl-4-phenyl-1,2,3,6-tetrahydropyridine (MPTP) on central catecholamine neurons in C57BL/6 mice. Comparison with three other strains of mice. Brain Res 405:26-38.

Takamidoh H, Naoi M, Nagatsu T (1987) Inhibition of type A monoamine oxidase by 1-methyl-4-phenylpyridine. Neurosci Lett 73:293-297.

Tatton NA, Kish SJ (1997) In situ detection of apoptotic nuclei in the substantia nigra compacta of 1-methyl-4-phenyl-1,2,3,6-tetrahydropyridine-treated mice using terminal deoxynucleotidyl transferase labelling and acridine orange staining. Neuroscience 77:1037-1048.

Thiffault C, Langston JW, Di Monte DA (2000) Increased striatal dopamine turnover following acute administration of rotenone to mice. Brain Res 885:283-288.

Thiruchelvam M, Brockel BJ, Richfield EK, Baggs RB, Cory-Slechta DA (2000) Potentiated and preferential effects of combined paraquat and maneb on nigrostriatal

dopamine systems: environmental risk factors for Parkinson's disease? Brain Res 873:225-234.

Thomas B, von Coelln R, Mandir AS, Trinkaus DB, Farah MH, Leong Lim K, Calingasan NY, Flint Beal M, Dawson VL, Dawson TM (2007a) MPTP and DSP-4 susceptibility of substantia nigra and locus coeruleus catecholaminergic neurons in mice is independent of parkin activity. Neurobiol Dis.

Thomas B, von Coelln R, Mandir AS, Trinkaus DB, Farah MH, Leong Lim K, Calingasan NY, Flint Beal M, Dawson VL, Dawson TM (2007b) MPTP and DSP-4 susceptibility of substantia nigra and locus coeruleus catecholaminergic neurons in mice is independent of parkin activity. Neurobiol Dis 26:312-322.

Thorner MO, Login IS (1981) Prolactin secretion as an index of brain dopaminergic function. Adv Biochem Psychopharmacol 28:503-520.

Turrens JF, Alexandre A, Lehninger AL (1985) Ubisemiquinone is the electron donor for superoxide formation by complex III of heart mitochondria. Arch Biochem Biophys 237:408-414.

Uhl GR (1998) Hypothesis: the role of dopaminergic transporters in selective vulnerability of cells in Parkinson's disease. Ann Neurol 43:555-560.

Ungerstedt U (1968) 6-Hydroxy-dopamine induced degeneration of central monoamine neurons. Eur J Pharmacol 5:107-110.

van den Munckhof P, Luk KC, Ste-Marie L, Montgomery J, Blanchet PJ, Sadikot AF, Drouin J (2003) Pitx3 is required for motor activity and for survival of a subset of midbrain dopaminergic neurons. Development 130:2535-2542.

Van den Pol AN, Herbst RS, Powell JF (1984) Tyrosine hydroxylase-immunoreactive neurons of the hypothalamus: a light and electron microscopic study. Neuroscience 13:1117-1156.

van der Brug MP, Blackinton J, Chandran J, Hao LY, Lal A, Mazan-Mamczarz K, Martindale J, Xie C, Ahmad R, Thomas KJ, Beilina A, Gibbs JR, Ding J, Myers AJ, Zhan M, Cai H, Bonini NM, Gorospe M, Cookson MR (2008) RNA binding activity

of the recessive parkinsonism protein DJ-1 supports involvement in multiple cellular pathways. Proc Natl Acad Sci U S A 105:10244-10249.

van der Putten H, Wiederhold KH, Probst A, Barbieri S, Mistl C, Danner S, Kauffmann S, Hofele K, Spooren WP, Ruegg MA, Lin S, Caroni P, Sommer B, Tolnay M, Bilbe G (2000) Neuropathology in mice expressing human alpha-synuclein. J Neurosci 20:6021-6029.

Van Gelder RN, von Zastrow ME, Yool A, Dement WC, Barchas JD, Eberwine JH (1990) Amplified RNA synthesized from limited quantities of heterogeneous cDNA. Proc Natl Acad Sci U S A 87:1663-1667.

Vercammen L, Van der Perren A, Vaudano E, Gijsbers R, Debyser Z, Van den Haute C, Baekelandt V (2006) Parkin protects against neurotoxicity in the 6-hydroxydopamine rat model for Parkinson's disease. Mol Ther 14:716-723.

Vergo S, Johansen JL, Leist M, Lotharius J (2007) Vesicular monoamine transporter 2 regulates the sensitivity of rat dopaminergic neurons to disturbed cytosolic dopamine levels. Brain Res 1185:18-32.

Vila M, Przedborski S (2003) Targeting programmed cell death in neurodegenerative diseases. Nat Rev Neurosci 4:365-375.

Vingerhoets FJ, Snow BJ, Tetrud JW, Langston JW, Schulzer M, Calne DB (1994) Positron emission tomographic evidence for progression of human MPTP-induced dopaminergic lesions. Ann Neurol 36:765-770.

Vogel HP, Ketsche R (1986) Effect of hypoglycaemia, TRH and levodopa on plasma growth hormone, prolactin, thyrotropin and cortisol in Parkinson's disease before and during therapy. J Neurol 233:149-152.

Wang P, Ding F, Chiang H, Thompson RC, Watson SJ, Meng F (2002) ProbeMatchDB--a web database for finding equivalent probes across microarray platforms and species. Bioinformatics 18:488-489.

Weiner DM, Levey AI, Sunahara RK, Niznik HB, O'Dowd BF, Seeman P, Brann MR (1991) D1 and D2 dopamine receptor mRNA in rat brain. Proc Natl Acad Sci U S A 88:1859-1863.

Wermuth L, Stenager EN, Stenager E, Boldsen J (1995) Mortality in patients with Parkinson's disease. Acta Neurol Scand 92:55-58.

West A, Farrer M, Petrucelli L, Cookson M, Lockhart P, Hardy J (2001) Identification and characterization of the human parkin gene promoter. J Neurochem 78:1146-1152.

West MJ, Slomianka L, Gundersen HJ (1991) Unbiased stereological estimation of the total number of neurons in thesubdivisions of the rat hippocampus using the optical fractionator. Anat Rec 231:482-497.

Westerink BH, Spaan SJ (1982) Simultaneous determination of the formation rate of dopamine and its metabolite 3,4-dihydroxyphenylacetic acid (DOPAC) in various rat brain areas. Brain Res 252:239-245.

Whetten-Goldstein K, Sloan F, Kulas E, Cutson T, Schenkman M (1997) The burden of Parkinson's disease on society, family, and the individual. J Am Geriatr Soc 45:844-849.

Willis GL, Donnan GA (1987) Histochemical, biochemical and behavioural consequences of MPTP treatment in C-57 black mice. Brain Res 402:269-274.

Wilson JM, Kalasinsky KS, Levey AI, Bergeron C, Reiber G, Anthony RM, Schmunk GA, Shannak K, Haycock JW, Kish SJ (1996) Striatal dopamine nerve terminal markers in human, chronic methamphetamine users. Nat Med 2:699-703.

Yamada M, Mizuno Y, Mochizuki H (2005) Parkin gene therapy for alpha-synucleinopathy: a rat model of Parkinson's disease. Hum Gene Ther 16:262-270.

Yamada M, Iwatsubo T, Mizuno Y, Mochizuki H (2004) Overexpression of alpha-synuclein in rat substantia nigra results in loss of dopaminergic neurons, phosphorylation of alpha-synuclein and activation of caspase-9: resemblance to pathogenetic changes in Parkinson's disease. J Neurochem 91:451-461.

Yamada T, McGeer PL, Baimbridge KG, McGeer EG (1990) Relative sparing in Parkinson's disease of substantia nigra dopamine neurons containing calbindin-D28K. Brain Res 526:303-307.

Yamamoto A, Friedlein A, Imai Y, Takahashi R, Kahle PJ, Haass C (2005) Parkin phosphorylation and modulation of its E3 ubiquitin ligase activity. J Biol Chem 280:3390-3399.

Yang Y, Gehrke S, Imai Y, Huang Z, Ouyang Y, Wang JW, Yang L, Beal MF, Vogel H, Lu B (2006) Mitochondrial pathology and muscle and dopaminergic neuron degeneration caused by inactivation of Drosophila Pink1 is rescued by Parkin. Proc Natl Acad Sci U S A 103:10793-10798.

Yu WH, Matsuoka Y, Sziraki I, Hashim A, Lafrancois J, Sershen H, Duff KE (2008) Increased dopaminergic neuron sensitivity to 1-methyl-4-phenyl-1,2,3,6-tetrahydropyridine (MPTP) in transgenic mice expressing mutant A53T alpha-synuclein. Neurochem Res 33:902-911.

Zang LY, Misra HP (1993) Generation of reactive oxygen species during the monoamine oxidase-catalyzed oxidation of the neurotoxicant, 1-methyl-4-phenyl-1,2,3,6-tetrahydropyridine. J Biol Chem 268:16504-16512.

Zarranz JJ, Alegre J, Gomez-Esteban JC, Lezcano E, Ros R, Ampuero I, Vidal L, Hoenicka J, Rodriguez O, Atares B, Llorens V, Gomez Tortosa E, del Ser T, Munoz DG, de Yebenes JG (2004) The new mutation, E46K, of alpha-synuclein causes Parkinson and Lewy body dementia. Ann Neurol 55:164-173.

Zhou H, Falkenburger BH, Schulz JB, Tieu K, Xu Z, Xia XG (2007) Silencing of the Pink1 gene expression by conditional RNAi does not induce dopaminergic neuron death in mice. Int J Biol Sci 3:242-250.

MICHIGAN STATE UNIVERSITY LIBRARIES
3 1293 03062 4831